The Relevance of Ribonuclease III in Pathogenic Bacteria

Ana Margarida Teixeira Saramago

Dissertation presented to obtain the Ph.D degree in Biology

Instituto de Tecnologia Química e Biológica
Universidade Nova de Lisboa

Oeiras, March, 2014

Financial Support from **Fundação para a Ciência e Tecnologia** (**FCT**) – Ph.D: grant - SFRH/BD/65607/2009

Work performed at:

Control of Gene Expression Laboratory

Instituto de Tecnologia Química e Biológica

Av. da República (EAN)

2781-901 Oeiras – Portugal

Tel: +351-21-4469548

Fax:+351-21-4469549

Supervisor :

Professora Doutora Cecília Maria Pais de Faria de Andrade Arraiano – Investigadora Coordenadora, Instituto de Tecnologia Química e Biológica, Universidade Nova de Lisboa.
(Head of the Laboratory of Control of Gene Expression, where the work of this Dissertation was performed)

Co-supervisor :

Doutora Susana Margarida Lopes Domingues – Investigadora Pós-Doutorada, Instituto de Tecnologia Química e Biológica, Universidade Nova de Lisboa.
(Post-doc Fellow in the Laboratory of Control of Gene Expression, where the work of this Dissertation was performed)

President of the Jury :

Doutor Carlos José Rodrigues Crispim Romão – Professor Catedrático Aposentado do Instituto de Tecnologia Química e Biológica da Universidade Nova de Lisboa, por delegação.

***Examiners*:**

Professora Doutora Mónica Amblar Esteban – Investigadora Principal do Instituto de Salud Carlos III, Madrid *(Principal Examiner).*

Professor Doutor Arsénio do Carmo Sales Mendes Fialho – Professor Associado com Agregação, Instituto Superior Técnico, Universidade Técnica de Lisboa *(Principal Examiner).*

Professor Doutor Miguel Agostinho Sousa Pinto Torres Fevereiro – Investigador Principal do Instituto Nacional de Investigação Agrária e Veterinária - INIAV

Professora Doutora Maria Teresa Ferreira de Oliveira Barreto Goulão Crespo – Investigadora Principal, IBET - Instituto de Biologia Experimental e Tecnológica

"A journey of a thousand miles begins with a single step."

-Anonymous

Acknowledgements

I want express my gratitude to all that supported me in the realization of my Ph.D. and dedicate to them several words:

- To **Instituto de Tecnologia Química e Biológica (ITQB)** for hosting me**, f**or providing good work conditions, and to give me the excellent opportunity to develop exceptional scientific projects, even with a surrounding environment of economic crisis. Once more, we proved that we (Portuguese people) are plastic and creative people who do not let themselves go down easily. I also would like to thank to the past and present ITQB directors, namely **Professor Doutor José Artur Martinho Simões, Professor Doutor Luís Paulo Rebelo**, **and currently Professor Doutor Cláudio Soares**.

- To **Fundação para a Ciência e Tecnologia (FCT)** for financial support that made my Ph.D. possible. for

- To my Supervisor **Professora Cecília Maria Arraiano** for supporting me during these past years, and for continuing to support me. I would like to thank you for encouraging my research and for allowing me to grow as a research scientist. I hope that I could be as energic and enthusiastic as Professor Cecília, and to someday be able to command an audience as well as she can. I am also thankful for the excellent example she has provided as a successful woman and professor.

- This thesis would not have been possible without the help and patience of my co-supervisor, good friend (and officemate) **Susana Domingues**. Thank you for being so supportive, to give me the freedom to pursue ideas without objection, to trust on my capacities, to share your knowledge, and for challenging my mind to bring me to another level. I also want to acknowledge for all the crazy and funny moments!! Laugh is the best medicine!!

- I also would like to thank to **Sandra Viegas**, my friend and officemate, for all the good advices, support and good friendship. She has been precious on both academic and at personal level, for which I am extremely grateful!!

- To **Inês Silva** and **Andreia Aires**, also my very good and special friends! I want to thank you for being wonderful persons, for sharing so many pleasant moments (never forgetting the professional side), and for being such good friends.

- To **Rute Matos** for the friendship and for giving me the pleasure to work with her! I hope that we continue to work together!

- To may labmate **Igor Ruiz de los Mozos** for being an exceptional friend and hard worker, and for all the fun and crazy times during my last year of Ph.D… and to **Nabila Haddad** for being an extremely nice and helpful person!! I will never forget you both!!

- To the members of the **CMA group** that have contributed greatly to my personal and professional time. The group has been a source of friendships as well as good advices, fun and team spirit. My greatest thanks to **Inês Silva**, **Sandra Viegas**, **Susana Domingues**, **Andreia Aires**, **Cátia Bárria**, **Susana Barahona**, **Patrícia Apura**, **Ricardo Moreira**, **Rute Matos**, **Teresa Pinto** (thank you for helping me to rescue my polyacrylamide gels), **Ricardo Santos**, **Raquel Santos**, **Lisete Galego**, **Clémentine Dressaire**, **Michal Malecki**, **Filipa Reis**, **Vânia Pobre**, **Zé Andrade**, **Patrick Freire** and **Ana Barbas**!

- To **Iñigo Lasa**, **Alejandro Toledo-Arana** and **Igor Ruiz de los Mozos** from Instituto de Agrobiotecnología, Pamplona, Spain, and to **Nabila Haddad** and **Hervé Prévost** from LUNAM Université, Nantes, France for their collaboration and precious help in this Doctoral work. I hope that we can continue our collaboration.

- I want to thank to **Professor Arsénio Fialho**, **Doutora Mónica Amblar**, **Doutora Teresa Crespo** and **Doutor Miguel Fevereiro** for letting my defense be an enjoyable moment, and for your brilliant comments and suggestions.

- I thank to my **good friends** and **Ph.D. colleagues** for all the fun, friendship, and for all the memorable moments altogether!
- I also want to express my greatest gratitude to my **biggest friends** who are always by my side (they know who they are) for their unconditional friendship, support and encouragement throughout all the important moments of my life.
- I also want to express my gratitude for my two lovely feline friends, **Pantufa** and **Lucky** for their unconditional love.
- Lastly, I would like to thank to my **mom** who raised me with an unconditional love, and supported me in all my pursuits. Without her continuous support and encouragement I never would have been able to achieve my goals! To my **dad** for all the motivation and also for being always by my side! And to **my family** for all the love and encouragement.

At the end of my thesis, it is a pleasant task to express my gratitude to all who contributed in many ways to the success of this study and made it an unforgettable experience for me. Thank you!!

Table of contents

Abstract

Ribonucleases (RNases) are key factors in the control of all biological processes, since they modulate the stability of RNA transcripts, allowing rapid changes in gene expression. Some RNases are up-regulated under stress situations and are involved in virulence processes in pathogenic microorganisms. RNases also control the levels of regulatory RNAs, which play very important roles in cell physiology.

In general, RNA degradation starts with an internal cleavage performed by an endoribonuclease. This is followed by degradation from one extremity by one or more exoribonucleases. RNase E has been considered the main enzyme that catalyses the initial cleavage event in Gram-negative bacteria. In Gram-positives, this degradation step has been attributed to its functional equivalents: RNase Y and RNases J1/2. However, the ubiquitous RNase III-like enzymes, which cleave the RNA molecule internally within double-stranded segments, are also emerging as important players in the control of bacterial mRNA stability.

The first objective of this doctoral work was to perform a functional and biochemical analysis of RNase III from *Campylobacter jejuni*. This microorganism is a foodborne pathogen for which there is little information regarding ribonucleases. However, there are hints that they can be instrumental in the virulence mechanisms of this bacterium. Namely, Polynucleotide phosphorylase (PNPase) was shown to allow survival of *C. jejuni* in cold conditions, and to have a role in bacterial swimming, cell adhesion, colonization and invasion. Since PNPase synthesis is auto-controlled in an RNase III-dependent mechanism, it was also relevant to study the role of RNase III in *C. jejuni*. Hence, we have cloned, overexpressed, purified and studied the activity of *C. jejuni* RNase III (*Cj*-RNase III) over a range of different conditions. Throughout this study, we showed that this enzyme is similarly active over a wide range of pH values and temperatures.

Plasticity of *Cj*-RNase III suggests that this enzyme may be important for all the environmental demands that *C. jejuni* must face during its lifestyle. The results also demonstrated that Mn^{2+} seems to be the preferred co-factor of the enzyme, contrarily to what was described for other RNase III orthologues. Therefore, *Cj*-RNase III may have an important role under a Mn^{2+}-rich environment, namely inside macrophages. We have also demonstrated that *Cj*-RNase III is able to complement an RNase III^- *Escherichia coli* strain in the maturation of 30S rRNA and in the regulation of PNPase production. Mutational analysis of residues involved in the catalytic activity of *Cj*-RNase III confirmed a conservation of the catalytic mechanism characteristic of this family. Altogether these results reinforce the notion that members of the RNase III family of enzymes from different species retain some conserved functions. This study brought relevant information regarding functionality and biochemical properties of *Cj*-RNase III. Despite the functional conservation, the peculiarities found in *Cj*-RNase III activity lead us to speculate that this enzyme might be also a main player in the survival of this pathogen to environmental demands.

The second goal of this dissertation was to examine the role of RNase III and other *Salmonella* Typhimurium ribonucleases in the control of antibiotic susceptibility and biofilm formation, two important factors in bacterial survival. *Salmonella* infections are a serious medical and veterinary problem worldwide and there is an increasing need for new strategies for prevention and control. This study showed that in particular, endoribonucleases E and III affect the susceptibility of *Salmonella* to ribosome-targeting antibiotics, and affect biofilm formation. We also studied *in vitro* the role of these two endoribonucleases in the degradation of the small non-coding RNA (sRNA) MicA, which has a role in biofilm development and in the control of outer membrane porins in *Enterobacteriaceae*. We found that *Salmonella* RNase III cleaves MicA only when the

latter is hybridized with its mRNA target. The target is also cleaved. This "gene silencing" mechanism resembles eukaryotic RNA interference process. By contrast, RNase E is only able to efficiently degrade free MicA sRNA. Our results allowed us to propose a model explaining the cooperation of both enzymes in the cell in order to achieve the fine-tuned control of the posttranscriptional regulator MicA.

In the third part of this work, we have studied the role of RNase III in *Staphylococcus aureus*, particularly in biofilm production. Biofilm development is a highly complex process, and constitutes one of the major medical concerns within *S. aureus* pathogenesis. *S. aureus icaR* encodes a key transcription regulator that represses the *ica* operon, which has a key role in biofilm production. It was demonstrated that the 3'untraslated region (3'-UTR) of *icaR* mRNA affects the expression level of the IcaR protein by modulating the stability of its own transcript. The modulation of *icaR* is performed through RNA base-pairing between the 3'-UTR and the 5'-UTR regions, which triggers the degradation by RNase III, leading to the destruction of the *icaR* transcript. So far the relevance of 3'-UTRs in the regulation of bacterial mRNA functionality has been disregarded. Our data illustrate that bacterial 3'-UTRs can provide strategies for fine-tuning control of gene expression.

From the previous work some questions remained unanswered, namely the influence of environmental signals in the modulation of IcaR levels. In the last stage of this doctoral work, we have collected evidences that a temperature shift may dictate the formation/destabilization of the 5'-3'-UTR duplex, adjusting IcaR levels according to the temperature sensed in the surrounding environment. We have also seen that a *S. aureus* strain lacking PNPase is not able to form biofilm, and this exoribonuclease could have a role in the control of IcaR levels. This

mechanism provides a rapid and efficient activation/inactivation of IcaR production in response to a sudden change in environmental conditions, and a fine-tuned adjustment of biofilm production in *S. aureus.*

In this work it was shown that RNase III seems to be important to the survival of *Campylobacte*r to different environments, with consequences for its pathogenicity. In *Salmonella*, RNase III contributes to antibiotic resistance, biofilm development and is involved in the control in the coupled-degradation of MicA sRNA and its targets. RNase III is also a major player in the control of biofilm production in *S. aureus*, and 3′ untranslated regions of prokaryotic mRNAs can regulate gene expression. Overall, the work developed during this Dissertation provided important results for a better understanding of the versatile contribution of RNase III to several relevant cellular mechanisms in different pathogenic microorganisms. This reinforces the importance of this endoribonuclease as a global regulator.

Resumo

As Ribonucleases (RNases) são factores chave no controlo de todos os processos biológicos, pois são responsáveis pela modulação da estabilidade dos transcriptos de RNA, permitindo assim rápidas mudanças na expressão génica. Algumas RNases são altamente expressas em situações de stress e estão envolvidas em processos de virulência em microrganismos patogénicos. As RNases são também responsáveis pelo controlo dos níveis de RNAs regulatórios que, por sua vez, também têm um papel igualmente importante para a fisiologia da célula.

Em geral, a degradação de RNA é iniciada por uma clivagem interna efectuada por uma endoribonuclease. Segue-se depois a degradação a partir de uma das extremidades levada a cabo por uma ou várias exoribonucleases. A RNase E tem sido considerada como a principal enzima que catalisa o evento de clivagem inicial, em bactérias Gram-negativas. Em bactérias Gram-positivas, este passo de degradação tem sido atribuído a outras RNases funcionalmente equivalentes: RNase Y e RNase J1/2. No entanto, a RNase III é uma enzima ubíqua, cuja família está a emergir como importantes intervenientes no controlo da estabilidade de RNA em bactérias. Estas enzimas têm a particularidade de serem específicas para o corte interno de segmentos de RNA em cadeia dupla.

O primeiro objectivo deste trabalho doutoral consistiu numa análise funcional e bioquímica da RNase III de *Campylobacter jejuni*. Este é um microrganismo responsável por provocar intoxicações alimentares, para o qual existe muito pouca informação relativamente a RNases. No entanto, existem pistas para o facto estas enzimas poderem ser instrumentais para os mecanismos de virulência nesta bactéria. Nomeadamente, a enzima polinucleotídeo fosforilase (PNPase) demonstrou ser necessária à sobrevivência de *C. jejuni* em condições de frio e contribuir para "swimming" bacteriano, adesão celular,

colonização e invasão. Tendo em conta que a síntese da PNPase é auto-controlada num mecanismo dependente da RNase III, pode-se inferir que esta última possa também ter um papel importante para *Campylobacter*. Como tal, procedeu-se à clonagem, sobreexpressão, purificação e estudo da actividade da RNase III de *C. jejuni* (*Cj*-RNase III) numa gama de diferentes condições. Com este estudo, foi possível demonstrar que esta enzima é activa numa larga gama de pHs e temperaturas. A plasticidade da *Cj*-RNase III é sugestiva de que esta enzima poderá ter um papel importante nos vários desafios ambientais que *C. jejuni* tem de enfrentar ao longo do seu ciclo de vida. Os resultados sugeriram que o ião divalente manganês (Mn^{2+}) é o co-factor preferencial desta enzima, contrariamente ao que foi previamente descrito para os outros ortólogos da RNase III. Estes dados levantam a hipótese de que a *Cj*-RNase III possa ter uma função relevante em ambientes ricos em manganês, nomeadamente dentro dos macrófagos. Neste trabalho também se demonstrou que *Cj*-RNase III é capaz de complementar uma estirpe de *Escherichia coli* RNase III^- na maturação do rRNA 30S e na regulação da síntese da PNPase, reforçando a ideia de que os membros desta família de enzimas provenientes de diferentes espécies possuem funções conservadas. Finalmente, uma análise mutacional dos resíduos envolvidos na actividade catalítica da *Cj*-RNase III confirmou a conservação do mecanismo catalítico que é característico dos membros já reportados desta família de enzimas. Em geral, este estudo revelou informação relevante relativamente à funcionalidade e propriedades bioquímicas da *Cj*-RNase III. Apesar da conservação funcional, as peculiaridades encontradas na actividade desta enzima levantam a hipótese de que este pode ser um interveniente com um papel importante na sobrevivência deste microrganismo patogénico aos diferentes desafios ambientais.

O segundo objectivo desta dissertação foi examinar o papel da RNase III, bem como de outras ribonucleases, no controlo da susceptibilidade a antibióticos e na formação de biofilme em *Salmonella* Typhimurium, dois factores importantes para a sobrevivência das bactérias. As infecções por *Salmonella* reflectem-se a nível mundial e têm graves repercussões na medicina humana e veterinária. Como tal, há uma necessidade crescente de novas estratégias de prevenção e controlo. Com este estudo demonstrou-se que, em particular, as endoribonucleases E e III afectam a susceptibilidade aos antibióticos que actuam ao nível do ribossoma em *Salmonella,* bem como a capacidade de formação de biofilmes. Também se estudou *in vitro*, o papel destas duas endoribonucleases na degradação de um pequeno RNA não codificante designado de MicA, que por sua vez está implicado na formação de biofilmes e que adicionalmente tem como função o controlo de porinas da membrana externa em *Enterobacteriaceae.* Os nossos resultados revelaram que a RNase III apenas é capaz de degradar o pequeno RNA MicA quando este se encontra hibridado com o seu RNA mensageiro alvo. Desta forma o alvo é também destruído. Este mecanismo de silenciamente génico assemelha-se, de certa forma, ao fenómeno de RNA de interferência que existe em células eucariótas. Contrariamente a este cenário, a RNase E é capaz de degradar o pequeno RNA quando este se encontra livre, ou seja, sem estar hibridado com nenhum dos seus alvos. Desta forma, pode-se concluir que a RNase III apenas cliva o pequeno RNA num mecanismo dependente do alvo, enquanto que a RNase E degrada o MicA quando este está desemparelhado. Os resultados obtidos permitiram propor um modelo que explica a cooperação de ambas as enzimas na obtenção de um controlo pós-transcricional preciso e minucioso na célula.

A terceira parte deste trabalho teve como objectivo estudar a função da RNase III na produção de biofilmes em *Staphylococcus aureus*. O desenvolvimento

de biofilmes é um processo altamente complexo e, no âmbito da patogénese de *S. aureus*, constitui uma das principais preocupações a nível médico. O gene *icaR* de *S. aureus* codifica para um regulador transcricional que reprime o operão *ica*, que por sua vez tem um papel na produção de biofilmes. Neste trabalho, demonstrou-se que a região não traduzida a 3′ (3′-UTR) do mRNA do *icaR* afecta o nível de expressão da proteína IcaR através da modulação da estabilidade deste próprio transcrito. A modulação do *icaR* é efectuada através de um emparelhamento entre as regiões 3′-UTR e 5′-UTR e, consequentemente, o duplex de RNA formado é clivado pela RNase III, levando à destruição do transcrito *icaR*. Até há bem pouco tempo a relevância de regiões 3′-UTR na regulação de RNAs mensageiros bacterianos foi negligenciada. Estes dados são ilustrativos de que as regiões 3′-UTR em bactérias também possuem a capacidade de controlar a expressão génica.

Este trabalho originou algumas questões, nomeadamente quais os sinais ambientais eventualmente responsáveis pela modulação da interacção 5′-3′-UTR do transcrito *icaR*. Na última fase deste trabalho doutoral, obtiveram-se evidências de que alterações de temperatura ditam a formação/destabilização do duplex 5′-3′-UTR, ajustando desta forma os níveis de IcaR de acordo com a temperatura sentida no ambiente circundante. Adicionalmente, o mutante da PNPase não é apto na formação de biofilmes. Os dados obtidos sugerem um provável papel desta enzima no controlo dos níveis de IcaR na célula. Este complexo mecanismo regulatório permite uma rápida e eficiente activação/inactivação da produção de IcaR em reposta a uma mudança ambiental repentina e assim um ajustamento fino na produção de biofilmes em *S. aureus*.

Nesta dissertação demonstrou-se que a enzima RNase III parece ser importante para a sobrevivência de *Campylobacter* a diferentes ambientes com consequências para a sua patogénese. No caso de *Salmonella*, a RNase III contribui

para a resistência a antibióticos, para o desenvolvimento de biofilmes e também está implicada no controlo de um pequeno RNA, em particular quando este está hibridado com os RNAs mensageiros-alvo. Neste trabalho, a RNase III revelou ser um interveniente global na produção de biofilmes em *Staphylococcus* e desmistificou-se a ideia de que as extremidades a 3′ dos RNAs mensageiros procarióticos não têm um papel regulatório. O trabalho desenvolvido ao longo deste doutoramento permitiu a obtenção de dados importantes para uma melhor compreensão da contribuição da versátil RNase III para vários mecanismos celulares relevantes em diferentes microrganismos patogénicos. Todos estes dados reforçam a importância desta endoribonuclease como um regulador global.

List of Publications

SARAMAGO M, Bárria C, Santos R, Silva IJ, Pobre V, Domingues S, Andrade J, Viegas SC and Arraiano CM **(2013)**. Ribonucleases and the regulation of small non-coding RNAs. **Accepted in Curr Opin Microbiol.**

SARAMAGO M, Domingues S, Viegas SC and Arraiano CM **(2013).** Biofilm formation and antibiotic resistance in *Salmonella* Typhimurium are affected by different ribonucleases. **J Microbiol Biotechnol**

Haddad N*, **SARAMAGO M***, Matos RG, Prévost H and Arraiano CM **(2013).** Characterization of the biochemical properties of *Campylobacter jejuni* RNase III. **Accepted in Bioscience Reports**. *These authors contributed equally to this work

de los Mozos IR, Vergara-Irigaray M, Segura V, Villanueva M, Bitarte N, **SARAMAGO M**, Domingues S, Arraiano CM, Fechter P, Romby P, Valle J, Solano C, Lasa I, Toledo-Arana A **(2013).** Base pairing interaction between 5'- and 3'UTRs controls *icaR* mRNA translation in *Staphylococcus aureus*. **Accepted in PLoS Genetics**

Santos R*, Barahona S*, Bárria C, Pinto T, Apura P, **SARAMAGO M**, Pobre V, Andrade JM, Moreira R, Domingues S, Matos RG, Silva IJ, Viegas SC, Arraiano CM. **(2013).** RNA Degradation Pathways. **Invited Review in Cellular and Molecular Life Sciences -CMLS Springer** *These authors contributed equally to this work

Silva IJ, **SARAMAGO M**, Dressaire C, Domingues S, Viegas SC, Arraiano CM **(2011).** Importance and key events of prokaryotic RNA decay: the ultimate fate of an RNA molecule. **WIREs RNA; 2(6):818-36**

Viegas SC*, Silva IJ*, **SARAMAGO M**, Domingues S, Arraiano CM **(2011).** Regulation of the small regulatory RNA MicA by ribonuclease III: a target-dependent pathway. **Nucleic Acids Research; 39(7):2918-30** *These authors contributed equally to this work

Arraiano CM, Andrade JM, Domingues S, Guinote IB, Malecki M, Matos RG, Moreira RN, Pobre V, Reis FP, **SARAMAGO M**, Silva IJ, Viegas SC. **(2010)**. The Critical Role of RNA Processing and Degradation in the Control of Gene Expression. **FEMS Microbiology Reviews, 34(5):883-923**

Dissertation Outline

This Dissertation is divided in six chapters.

Chapter one consists of a general introduction on the RNA degradation mechanisms, highlighting the main differences between the RNA degradation models for the two main Gram-negative and Gram-positive bacteria - *Escherichia coli* and *Bacillus subtilis*. This chapter describes the importance of ribonucleases and other factors such as regulatory RNAs during the decay process. Part of this section was published in the Journals *FEMS Microbiology Reviews, WIREs RNA* and *Current Opinion in Microbiology*. The author of this thesis is co-author of these publications, being second author in *WIREs RNA* and first author in *Current Opinion in Microbiology.*

Chapter two focuses on the functional and biochemical analysis of RNase III from *Campylobacter jejuni*. From this work resulted a publication in *Bioscience Reports* in which the author of this dissertation played a major contribution and is the first author.

Chapter three describes the investigation of the contribution of the endoribonucleases III and E in antibiotic resistance, biofilm formation and on the degradation of MicA sRNA, in *Salmonella* Typhimurium. This work resulted in two articles, one published in *Nucleic Acids Research*, and the other in *Journal of Microbiology and Biotechnology*. In both articles the author of this dissertation played a major contribution, as a second and first author, respectively.

Chapter four consists in the study of RNase III in *Staphylococcus aureus*, namely in the regulation of IcaR protein levels, a transcriptional regulator which is involved in biofilm production. This work contributed to unravel the unprecedented

mechanism of gene regulation by long 3′ untranslated regions in prokaryotes. The results reported in this chapter were published on *PlosGenetics* in which the author of this Dissertation is a co-author.

In chapter five, we have further addressed some questions regarding the existence of other players in the regulation of IcaR levels, and how the 5′-3′UTR interaction can be modulated by environmental signals. The results described in this chapter gave additional and important information that will be instrumental for future publications.

To finalize, chapter six consists of an integrated discussion of the global results obtained during this Dissertation, and includes future perspectives.

Abbreviations

A adenine

Amp ampicillin

A. aeolicus *Aquifex aeolicus*

ATP adenosine triphosphate

BHI brain heart infusion

bp base pair

B. subtillis *Bacillus subtillis*

°C degree Celsius

C cytosine

Ca^{2+} calcium

cDNA complementary DNA

CFU colony-forming unit

C. jejuni *Campylobacter jejuni*

Cm chloramphenicol

cpm counts per minute

CRISPR clustered regularly interspaced short palindromic repeats

Δ deletion

DEPC diethyl pyrocarbonate

DG Gibbs free energy

DSS disuccinimidyl suberate

DTT dithiothreitol

DNA deoxyribonucleic acid

DNase deoxyribonuclease

dsRBD double-stranded RNA binding domain

dsRNA double stranded RNA

E. coli *Escherichia coli*

EDTA ethylenediaminetetraacetic acid

Em erythromycin

G guanine

g relative centrifugal force

g grams

GMP deoxyguanosine monophosphate

h hour

His histidine

IgG immunoglobulin G

IPTG isoPropyl-β-D-thiogalactopyranoside

Kb kilobase

Kcal kilocalories

kDa kilodalton

L. lactis *Lactococcus lactis*

L. monocytogenes *Listeria monocytogenes*

LB luria-bertani broth

M molar/ molarity (mol/L)

Mg^{2+} magnesium

mg milligram

µg microgram

µl microliter

ml milliliter

min minute

mM milliMolar

Mn^{2+} manganese

mRNA messenger RNA

ng nanogram

nM nanomolar

nt nucleotide

OD optical density

Oligo oligonucleotide

OMP outer membrane protein

^{32}P phosphorus 32 radionucleotide

P p-value

PAA polyacrylamide

PAGE polyacrylamide gel electrophoresis

PAP I poly(A) polymerase I

PBS phosphate-buffered saline buffer

PCR polymerase chain reaction

PDB protein data bank

PIA-PNAG Poly-N-Acetyl-β-(1,6)-lucosamine

pmol picomol

PMSF phenylmethylsulfonyl fluoride

PNPase polynucleotide phosphorylase

Poly(A) polyadenylate

qRT-PCR quantitative real-time polymerase chain reaction

psi pressure unit

RACE rapid amplification of cDNA ends

RBS ribosome binding site

RNA ribonucleic acid

RNAi RNA interference

RNase ribonuclease

rpm rotations per minute

rRNA ribosomal RNA

RT-PCR reverse transcriptase polymerase chain reaction

SD Shine-Dalgarno

SDS sodium dodecyl sulphate

sec second

siRNA small interfering RNA

sRNA small RNA

SSC sodium chloride/sodium citrate

S. aureus *Staphylococcus aureus*

T thymine

TAE tris/acetic acid/EDTA

TAP tobacco acid pyrophosphatase

TBE tris/borate/EDTA

tmRNA transfer messenger RNA

Tris trishydroxymethylaminomethane (2-Amino-2-(hydroxymethyl)propane-1,3-diol**)**

tRNA transfer RNA

TSB-gluc Trypticase soy broth with glucose

TSS transcriptional start site

TTS transcriptional termination site

U uracil

U units

UTP uracil triphosphate

UTR untranslated region

UV ultraviolet radiation

V volt

v/v volume/volume

wt wild-type

w/v weight/volume

Zn^{2+} zinc

Chapter 1

INTRODUCTION

Part of this chapter was based on:

Saramago M, Bárria C, Santos R, Silva IJ, Pobre V, Domingues S, Andrade J, Viegas SC and Arraiano CM **(2013)**. Ribonucleases and the regulation of small non-coding RNAs. Accepted in Curr Opin Microbiol

Silva IJ, **Saramago M**, Dressaire C, Domingues S, Viegas SC, Arraiano CM. 2011. Importance and key events of prokaryotic RNA decay: the ultimate fate of an RNA molecule. WIREs RNA. 2(6):818-36

Arraiano CM, Andrade JM, Domingues S, Guinote IB, Malecki M, Matos RG, Moreira RN, Pobre V, Reis FP, **Saramago M**, Silva IJ, and Viegas SC. 2010. The critical role of RNA processing and degradation in the control of gene expression. FEMS Microbiol Rev. 34(5):883-923

INTRODUCTION

Many cellular mechanisms cannot be fully understood without a profound knowledge of the RNA metabolism. Protein production depends not only on the levels of mRNAs but also on other RNA species. The translation of mRNAs is mediated by tRNAs and rRNAs and functional RNAs also intervene in the regulation of gene expression. Regulation of bacterial mRNAs allows microorganisms to rapidly adapt to changing environments. Even though transcription is important to determine steady-state levels, the role of post-transcriptional control is also critical in the regulation of gene expression. Analyzing RNA degradation in prokaryotes has been particularly difficult due to the coupling of transcription, translation and mRNA degradation, and to a rapid exponential decay with an average of 1.3 min at 37°C. rRNAs and tRNAs are usually more stable, but in order to be functionally active, they have to be processed to the mature form. It has been shown that the levels of small non-coding RNAs (sRNAs) are also highly dependent on post-transcriptional events. The collected knowledge makes it clear how far our understanding of RNA degradation has come in the last few years and how much remains to be discovered about this important genetic regulatory process.

RNases are the enzymes that intervene in the processing, degradation and quality control of all types of RNAs. A limited number of RNases can exert a determinant control, monitoring and adapting RNA levels to the cell needs. Many of them are essential, but others exhibit a functional overlap and are interchangeable. RNases can act alone or they can cooperate in RNA degradation complexes. During RNA degradation, they do not only act as 'molecular killers' eliminating RNA species. RNases act according to the requirements of growth in adaptation to the environment. They play an extremely important role in

contributing to the recycling of ribonucleotides, and also carry out surveillance, destroying aberrant RNAs detrimental to the cell. Individual RNA species differ widely with respect to their stability. The rate of turnover has no relation to the length of the gene. The segments that decay more rapidly can be anywhere in the mRNA and the stability of the gene transcripts seems to be regulated by determinants localized in specific mRNA segments. Secondary structure features can also influence the degradation by RNases. Several factors can intervene in the decay mechanisms: the sequence/structure of RNAs can act as stabilizer or destabilizer elements to specific RNases; the presence of ribosomes during active translation can hide some RNA *loci* that are vulnerable to RNases; poly(A) stretches are the preferred substrate for several RNases – therefore, the addition of poly(A) tails can modulate the stability of full-length transcripts and degradation intermediates, and accelerate the decay of normally stable RNAs; *trans*-acting factors such as regulatory small non-coding RNAs (sRNAs) can bind to the RNAs and expose or hide RNA sites that are preferential targets for RNases; the host factor Hfq is known to bind sRNAs and affect their turnover; and other factors such as helicases can act in *trans* unwinding RNA structures and changing their accessibility to RNases.

In the Introduction chapter, a brief overview on the current knowledge on prokaryotic RNA degradation mechanisms is presented. We will start by giving a picture of the most known enzymes involved on RNA degradation and their specific role in the decay in Gram negative and Gram positive bacteria. Since this Dissertation is mostly focused on RNase III and RNase E, we decided to focus on the structural details of these endoribonucleases, and then describe their role on several regulatory RNAs.

BACTERIAL RNA DEGRADATION MECHANISMS

General model of RNA decay

Turnover of RNA molecules involves cleavage reactions that are carried out by RNases, a diverse collection of cellular enzymes, whose functions and properties have been mainly elucidated through the study of mutants (Arraiano *et al.*, 2010; Arraiano *et al.*, 1988). Although *E. coli* possesses a plethora of RNases only a few are devoted to the RNA degradation. The conventional model for RNA decay in this bacterium usually begins with an endonucleolytic cleavage at one or more internal sites on the RNA molecule (Figure 1A). Two endonucleases have been associated with the initial cleavage event: RNase III and RNase E. However, RNase E is believed to be the main endonuclease involved in the RNA turnover in *E. coli* (Arraiano *et al.*, 2010). In fact, in the absence of RNase E 60% of the annotated coding sequences were either increased or decreased in their steady-state levels (Stead *et al.*, 2011). In contrast, only 12% of the coding sequences were affected by the absence of RNase III (Stead *et al.*, 2011).

RNase E is an essential single-stranded endonuclease that exhibits a preference for A/U-rich regions in close proximity to stem-loops (Mackie, 1998; McDowall *et al.*, 1994). This characteristic is also shown by its paralogue, RNase G. This endonuclease, which has a strong resemblance with the amino-terminal portion of RNase E (McDowall *et al.*, 1993), is also involved in the degradation and processing of RNA (Carpousis *et al.*, 2009). Both enzymes display higher activity over substrates bearing a monophosphorylated than over substrates with a triphosphorylated 5'-end (Carpousis *et al.*, 2009). Nonetheless, some substrates are cleaved by RNase E regardless of the 5'-phosphorylation status. This occurs in molecules with multiple single-stranded sites that allow the direct entry of RNase

E through a different pathway, called 'bypass' or 'internal entry' (Baker and Mackie, 2003; Kime *et al.*, 2010).

RppH is an RNA pyrophosphohydrolase that removes the pyrophosphate from the 5'-termini and preferentially acts on single-stranded RNA. The discovery of this enzyme presented an alternative pathway in which the initial event is non-nucleolytic (Deana *et al.*, 2008). Conversion of 5'-triphosphate to 5'-monophosphate by RppH provides the ideal substrate for RNase E, and the preference of RppH for single-stranded RNA explains why 5'-stem-loops are mediators of stability. Ribosome loading is also known to mediate RNA stability. A poor ribosome binding site, possibly by increasing the distance between the actively translating ribosomes, exposes putative internal cleavage sites and may increase message instability.

The catalytic domain of RNase E is located in the N-terminal region, which is highly conserved and essential for cell viability (Kaberdin *et al.*, 1998). The C-terminus associate the enzyme with the cytoplasmic membrane (Liou *et al.*, 2001), and forms a scaffold for interactions with other proteins, which together form the degradosome, the main RNA degradative complex in *E. coli* (Liou *et al.*, 2001). The RNA degradosome can undergo changes in composition depending on the growth or stress conditions (Gao *et al.*, 2006; Prud'homme-Genereux *et al.*, 2004). For instance, two different RNA helicases are known to associate with RNase E depending on the temperature (Prud'homme-Genereux *et al.*, 2004; Py *et al.*, 1996). This remodelling of the degradosome strongly affects its RNA target spectrum (Gao *et al.*, 2006). In *E. coli* under normal growth conditions, the major components of the degradosome, in addition to RNase E, are the exonuclease PNPase, the helicase RhlB and the glycolytic enzyme enolase (Carpousis *et al.*, 1994; Py *et al.*, 1996). *Pseudomonas syringae*, on the other hand, has selected RNase R as a degradosome component, despite possessing polynucleotide phosphorylase (PNPase) (Purusharth *et al.*, 2005). This complex of enzymes

assures the coordination of the endo- and exonucleolytic degradation of an RNA molecule. After the initial endonucleolytic cleavage step the upstream fragment, lacking the 3'-terminal hairpin, can be readily digested by 3'-exonucleases. The activity of these enzymes is impaired by a 3'-stem-loop, which protects the majority of the primary transcripts (Andrade *et al.*, 2009). The downstream fragment generated after the initial endonucleolytic cleavage is usually more prone to degradation. It bears a monophosphorylated 5'-end and therefore may be the ideal substrate for an additional cleavage by RNase E. The turnover of *malEF* transcript illustrates how the endo- and exonucleolytic enzymes can act in a concerted way. PNPase degradation of *malEF* is only accomplished in the presence of RNase E and RhlB, indicating that the degradosome participates in its degradation (Stickney *et al.*, 2005). Even though RNase E has been considered the main enzyme in *E. coli* that catalyses the initial cleavage event, the RNase III family of enzymes has emerged as an important group of endonucleases in the control of RNA stability (Jaskiewicz and Filipowicz, 2008). RNase III deletion in *E. coli* causes a slow growth phenotype (Babitzke *et al.*, 1993). Its homologue in *B. subtilis* was first considered essential for viability (Herskovitz and Bechhofer, 2000). However, Durand *et al.* (Durand *et al.*, 2012b) showed that RNase III is not essential, but it is required for the protection of the cell against toxic molecules. A second *B. subtilis* RNase III-like enzyme (called Mini-III) was also described (Redko *et al.*, 2008). Both enzymes seem to act mostly in bacteriophage mRNA and rRNA processing (Bechhofer, 2009; Durand *et al.*, 2012b).

RNase III is specific for double-stranded RNA (dsRNA), and its role in RNA turnover has been associated with the removal of protective stem-loop structures that act as degradation barriers (Arraiano *et al.*, 2010) (Figure 1A). RNase III has also recently been implicated in the decay of sRNA/mRNA complexes, which constitute an optimal substrate for this enzyme (Viegas and

Arraiano, 2008; Viegas *et al.*, 2011). This phenomenon closely resembles siRNA–direct RNA cleavage in eukaryotes, a process that also involves enzymes of the RNase III family.

Three exonucleases are mainly involved in RNA decay in *E. coli*: PNPase, RNase R and RNase II (Figure 1A). All of these enzymes degrade RNA processively and non-specifically from the 3′-end. While PNPase is a phosphorolytic exonuclease yielding nucleoside diphosphates as reaction products, both RNase R and RNase II catalyse the hydrolysis of the RNA substrates, producing nucleoside monophosphates. Among the three, only RNase R is able to digest structured RNA by itself (Andrade *et al.*, 2009). The degrading activity of PNPase or RNase II is stalled by the presence of secondary structures (Spickler and Mackie, 2000). However, PNPase can also proceed through extensive folded RNA when acting in association with other proteins. Its association with the helicase RhlB or integration into the degradosome allows the unwinding of the RNA stem-loops (Liou *et al.*, 2002). Surprisingly, the PNPase homologue of *Thermus termophilus*, whose optimal temperature is 65°C, has been reported to completely degrade RNAs with stable intramolecular secondary structures without the aid of a helicase (Falaleeva *et al.*, 2008). Nonetheless, both PNPase and RNase R require a minimal 3′-overhang of 7–10 unpaired nucleotides in order to be able to bind and initiate digestion of an RNA molecule (Vincent and Deutscher, 2006). By providing a single-stranded platform for the initiation of the exonucleolytic attack, the degradation of RNA molecules containing 3′-stem-loops is stimulated by the addition of poly(A) tails to the 3′-end of the RNA molecules. These poly(A) tails constitute the preferred substrate for PNPase and RNase II (Lisitsky and Schuster, 1999; Marujo *et al.*, 2000). Paradoxically, RNase II can protect mRNAs from degradation by removing the poly(A) tails that can act as a substrate to other RNases {Marujo, 2000 #1237}.

None of the three 3′-exonucleases seems to be indispensable for *E. coli* growth at optimal temperature. However the combined absence of both PNPase and RNase II or PNPase and RNase R is lethal for the cell, indicating some overlapping role between these exonucleases (Cheng and Deutscher, 2003). For instance, both RNase R and PNPase are involved in the degradation of rRNA fragments, whose accumulation was proposed to lead to cell death (Cheng and Deutscher, 2003). A transcriptome analysis revealed that, although RNase II accounts for 90% of exonuclease activity in the cell, PNPase probably plays a greater role in mRNA degradation than previously thought (Deutscher and Reuven, 1991; Mohanty and Kushner, 2003). RNase II is the major exonuclease involved in *E. coli* RNA decay and other enterobacteriaceae but, this enzyme is absent in several other bacterial species, such as *B. subtilis*, *Legionella pneumophila* and *Streptococcus pneumoniae*, in which RNase R is the only hydrolytic 3′–5′ exonuclease (Charpentier *et al.*, 2008; Domingues *et al.*, 2009). In *B. subtilis* the RNA decay is primarily phosphorolytic and this major activity is attributed to PNPase (Arraiano *et al.*, 2010). Regarding the main exonucleases, PNPase is the only one found in *Streptomyces*, thus constituting an essential protein in these organisms (Bralley *et al.*, 2006). Conversely, the unique exonuclease in *Mycoplasma genitalium* is RNase R, and therefore it is essential (Hutchison *et al.*, 1999).

The degradative action of the ribonucleases described above releases RNA fragments of 2-5 nucleotides, and their accumulation may be deleterious to the cell (Ghosh and Deutscher, 1999). *E. coli* possesses another exonuclease, termed oligoribonuclease, which acts as a scavenger of these short oligoribonucleotides (Niyogi and Datta, 1975) (see Figure 1A). This essential enzyme processively hydrolyses RNA in the 3′-5′ direction. Overall, oligoribonuclease is a finishing enzyme in RNA metabolism, and the presence of

proteins with analogous functions seems to be widespread. Two homologues, NrnA and NrnB, have been recently described in *B. subtilis* (Fang *et al.*, 2009).

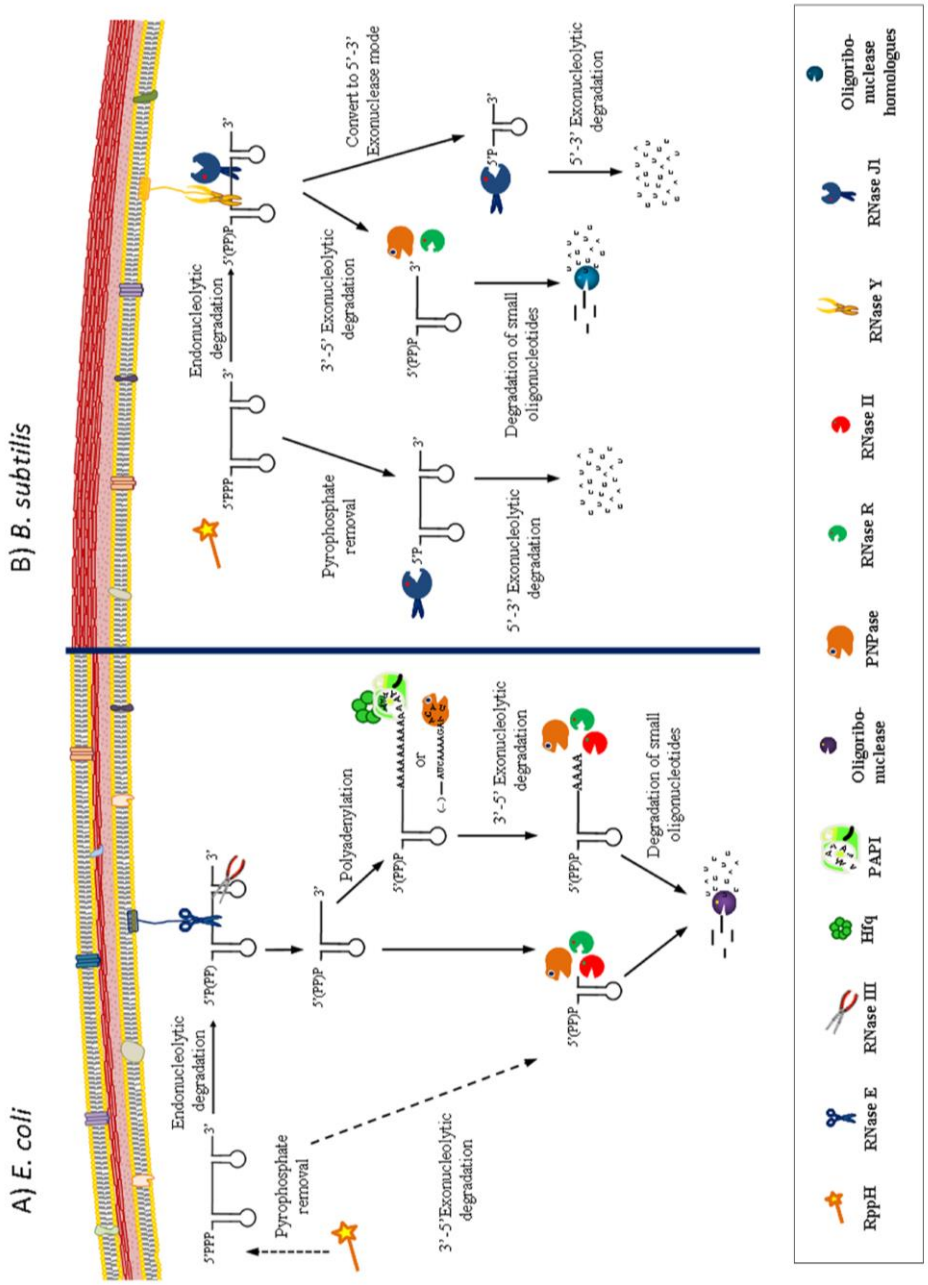

Figure 1 - Mechanisms of RNA decay in the *Gram*-negative and *Gram*-positive bacterial models. (A) In *E. coli* the decay of the majority of transcripts starts with an endonucleolytic cleavage by RNase E. The enzyme has a preference for 5′-monophosphorylated substrates. A possible pathway for RNase E cleavage involves a primary cleavage by the RNA pyrophosphohydrolase RppH, which converts the 5′-triphosphorylated terminus of primary transcripts to monophosphate. However, some substrates are cleaved by RNase E regardless of the 5′-phosphorylation status, through an alternative pathway called 'bypass' or 'internal entry', which involves the direct entry of RNase E at single-stranded sites. RNase III is double-stranded specific and can also initiate the decay of structured RNAs. After endonucleolytic cleavage, breakdown products are ready for exonucleolytic digestion by any of the three main exonucleases in this bacterium. Unlike RNase R, both RNase II and PNPase are sensitive to secondary structures. Exonucleolytic activity is promoted by the 3′-polyadenylation of substrates. The activity of PAP I, the main polyadenylating enzyme in *E. coli*, is modulated by the RNA-chaperone Hfq. PNPase can synthesize heteropolymeric tails that also facilitate degradation. Cycles of polyadenylation and exonucleolytic degradation have been proposed as one way to overcome secondary structures. A minor alternative pathway in the cell is the direct exonucleolytic degradation of full length transcripts (represented by a dashed arrow). Exonucleolytic degradation releases short fragments which are subsequently degraded to mononucleotides by oligoribonuclease. **(B)** In *B. subtilis*, transcripts can be degraded from the 5′-end through the 5′–3′ exonuclease activity of RNase J1, or they can be first endonucleolytically cleaved. Since the 5′–3′ exonuclease activity of RNase J1 is blocked by 5′-PPP, before this cleavage the recently discovered BsRppH removes the pyrophosphate. The endonucleolytic cleavage can be either performed by RNase J1/RNase J2 or RNase Y. The breakdown products can be then further degraded by the 3′–5′ exonucleases, PNPase and RNase R (unprotected 3′-ends), or by the 5′–3′ exonuclease activity of RNase J1 (newly generated monophosphorylated 5′-ends). RNase J1 is able to fully degrade its RNA substrates to mononucleotides. The final products released by RNase R and PNPase are further degraded by the oligoribonuclease homologues in *B. subtilis*. Here we represent ribonucleases acting independently. However some of these enzymes can act together in degradation complexes. For instance in *E. coli* the degradosome (RNase E, PNPase, RhlB and enolase) and in *B. subtilis* the putative complex formed by RNase J1/J2, RNase Y, PNPase, the RNA helicase CshA and two glycolytic enzymes {Silva, 2011 #8}.

RNA decay involving different endonucleases

Despite its essential role in *E. coli* RNA turnover, RNase E homologues are absent in numerous bacterial species. This is the case of the model organism *B. subtilis* and is a common characteristic of the low G/C content *Gram*-positive bacteria. For quite some time, a good candidate that could have the analogous

role of RNase E was not found, leaving no clue for the process of *B. subtilis* RNA degradation. One answer came from the discovery of two different ribonucleases, the paralogous RNase J1 and J2, which are present in almost all bacteria lacking RNase E (Even *et al.*, 2005). Curiously, both RNase E and RNase J1 orthologs have been found in *Sinorhizobium meliloti* (Madhugiri and Evguenieva-Hackenberg, 2009). Although there is no sequence homology, the RNase J enzymes share a similar architecture with RNase E (Li de la Sierra-Gallay *et al.*, 2008) and exhibit equivalent endonucleolytic activity. RNase J1, which is essential for cell viability, is involved in RNA turnover (Mader *et al.*, 2008) (Figure 1B). Surprisingly, this enzyme is also able to catalyse the exonucleolytic degradation of RNA in the 5'-3' direction (Mathy *et al.*, 2007). To date this is the only 5'-exonuclease known in prokaryotes and its discovery has had important implications in the RNA decay model. The exonucleolytic decay from the 5'-end may explain the stabilizing effect conferred by 5'-stem-loops, 5'-protein binding, 5'-ribosome stalling and the presence of a 5'-triphosphate in *B. subtilis* (Bechhofer, 2009). It has been suggested that this dual-function enzyme (alone or in complex with RNase J2) catalyses not only the endonucleolytic cleavage of an RNA substrate but also continues the degradation of the generated 5'-end by switching to the 5'-exonucleolytic mode (Li de la Sierra-Gallay *et al.*, 2008). In fact, global analysis of RNase J-depleted *B. subtilis* strains showed an altered abundance for a large number of mRNA transcripts, indicating that this ribonuclease affects gene expression on a global scale (Durand *et al.*, 2012a; Mader *et al.*, 2008). Interestingly, only the exonucleolytic activity of RNase J1 is dependent on the 5'-end phosphorylation status, as it is blocked by triphosphorylated RNA (Li de la Sierra-Gallay *et al.*, 2008). The complex formed by RNase J1 and J2 changes their individual cleavage activities and specificities (Mathy *et al.*, 2010).

Another insight into the RNA degradation mechanism of *B. subtilis* was the recent discovery of RNase Y, an essential single-stranded endonuclease

(Figure 1B), that shares extensive functional homologies with RNase E. In fact, several reports suggest that the predominant activity of RNase J1 is the 5′-3′ exonucleolytic activity (Condon, 2010; Durand *et al.*, 2012a; Lehnik-Habrink *et al.*, 2012; Newman *et al.*, 2011), while RNase Y has an effect on the global mRNA half-life in *B. subtilis* comparable to that of RNase E in *E. coli*. There are several studies reporting an increase of the bulk mRNA half-life in *B. subtilis* upon RNase Y deletion (Durand *et al.*, 2012a; Lehnik-Habrink *et al.*, 2011; Shahbabian *et al.*, 2009). Like RNase E, RNase Y is sensitive to the phosphorylation state of the 5′-end, exhibiting a marked preference for monophosphorylated RNA. Hence, two essential enzymes in *B. subtilis* RNA decay are dependent on a monophosphorylated 5′-end. Indeed, it was recently discovered the existence of an RNA pyrophosphohydrolase in *B. subtilis* (BsRppH) (Richards *et al.*, 2011). BsRppH was shown to remove the γ and β phosphates from the 5′-end of the RNA as orthophosphate (Richards *et al.*, 2011), whereas the corresponding from *E. coli* releases them mainly as a pyrophosphate (Deana *et al.*, 2008). Interestingly, the results obtained with *rppH* deletion mutant suggested the existence of other(s) RNA pyrophosphohydrolase(s) in *B. subtilis* (Richards *et al.*, 2011).

Based on the amino acid sequence, RNase Y seems to comprise at least four domains: a short N-terminal *trans*-membrane domain; a coiled-coil domain seemingly important for oligomerization (Lehnik-Habrink *et al.*, 2011); a KH domain required for RNA binding; and an HD domain that contains the catalytic site (Condon, 2003). The presence of an N-terminal *trans*-membrane domain in RNase Y suggests membrane localization further extending the analogy to RNase E (Shahbabian *et al.*, 2009) (Figure 1B). In fact, the proper membrane localization of RNase Y is essential for *B. subtilis* (Lehnik-Habrink *et al.*, 2011).

Evidence for the presence of a complex involving RNase Y, RNase J1/J2, PNPase, the RNA helicase CshA and two glycolytic enzymes, enolase and

phosphofructokinase, has been reported (Commichau *et al.*, 2009). This complex brings together some of the degrading activities necessary to achieve full degradation of an RNA molecule. The RNA fragments released by the RNase Y endonucleolytic cleavage could be good substrates for the 3'-exonucleolytic activity of PNPase and for the 5'-exonucleolytic degradation by RNase J1/J2 (Bechhofer, 2009). This putative degradosome-like complex indicates that the presence of such an RNA degradative machine may be a common feature in prokaryotes, even those that lack an RNase E homologue. Nonetheless, the existence of this complex in *B. subtilis* is still controversial. The presence of a degradosome-like complex in this organism has been challenged by the failure of isolating it as a complex in its native state and by the absence of detection of degradosome interactions in yeast two- and three-hybrid screens (Mathy *et al.*, 2010). However, these screens failed to detect also the established self-interactions of the RNase J1 and J2 (Commichau *et al.*, 2009; Li de la Sierra-Gallay *et al.*, 2008; Newman *et al.*, 2011). Further studies are still required to definitely establish the presence or absence of an RNA degradosome in this bacterium.

FUNCTIONAL AND STRUCTURAL DETERMINANTS OF RNA DEGRADING ENZYMES

Ribonuclease E

RNase E was first identified by temperature-sensitive mutations on *rne* (initially called *ams* for altered message stability) (Apirion and Lassar, 1978; Arraiano *et al.*, 1988; Babitzke and Kushner, 1991; Melefors and von Gabain, 1991; Misra and Apirion, 1979; Mudd *et al.*, 1990; Taraseviciene *et al.*, 1991). This important endonuclease is essential for cell growth, and the inactivation of temperature-sensitive mutants impedes processing and prolongs the lifetime of

bulk mRNA (Apirion and Lassar, 1978; Arraiano *et al.*, 1988; Babitzke and Kushner, 1991; Melefors and von Gabain, 1991; Mudd *et al.*, 1990; Ono and Kuwano, 1979; Taraseviciene *et al.*, 1991). It has been reported that RNase E plays a central role in the processing of precursors of the 5S rRNA (Apirion and Lassar, 1978; Misra and Apirion, 1979), the 16S rRNA gene (Li *et al.*, 1999), tRNAs (Ow and Kushner, 2002), transfer-messenger RNA (tmRNA) (Lin-Chao *et al.*, 1999) and the M1 RNA component of the RNase P ribozyme (Ko *et al.*, 2008; Lundberg and Altman, 1995). Homologues of RNase E have been identified in 450 bacteria, archaea and plants (Lee and Cohen, 2003).

E. coli RNase E is a 1061-residue enzyme composed of two distinct functional regions. The amino terminal half forms the catalytic domain (residues 1-529), which is organized as a dimer of dimers in a final homotetramer quaternary structure (Callaghan *et al.*, 2005) (Figure 2). Each protomer contains the following structural domains: S1, RNase H, DNase I and a small domain that is responsible for dimer–dimer interaction. The arrangement of the domains within each dimer resembles the blades and handles of an open pair of scissors. The crystal structure explains some features of the enzyme and suggests a mechanism for RNA recognition and cleavage (Koslover *et al.*, 2008). The influence of 5′-phosphorylation is a consequence of the pocket formed between the S1 and the RNase H subdomains, which binds 5′-monophosphorylated RNA and promotes downstream degradation. A 5′-monophosphate in substrate RNAs serves as an allosteric activator of RNase E activity (Jiang and Belasco, 2004; Mackie, 1998). After binding, a conformational change induced by the movement of the RNA-binding domains clamps the substrate down and organizes the active site (Koslover *et al.*, 2008). The catalytic site contains conserved residues of the DNase I domain and a single metal-binding site that coordinates an Mg^{2+} ion implicated in catalysis. The internal flexibility within the quaternary structure

may be related to the deformation required to accommodate structured RNA for processing by internal entry. An amphipathic segment (called segment A) at the C-terminal region of RNase E (residues 530-1061) directs the enzyme to the inner membrane (Khemici *et al.*, 2008). The existence of a second RNase E-membrane binding involving the catalytic domain of the enzyme was also reported (Murashko *et al.*, 2012). The N-terminal RNase E membrane binding alters its enzymatic activity by increasing the substrate affinity, and affects the secondary structure of the catalytic domain stabilizing the folding state of the protein (Murashko *et al.*, 2012). Membrane localization of this enzyme could be determinant for spatial discrimination of the RNA substrates (Khemici *et al.*, 2008; Liou *et al.*, 2001; Taghbalout and Rothfield, 2008). The efficiency of RNase E cleavage also depends on the structure of the substrates and the accessibility of putative cleavage sites.

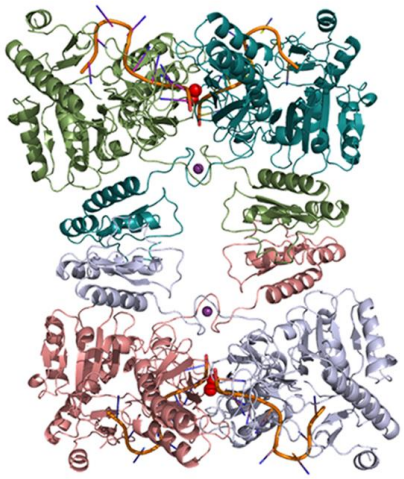

Figure 2 - Structure of RNase E in complex with RNA substrate. Crystal structure of the catalytic domain of *E. coli* RNase E, PDB ID 2C4R. RNA substrate in complex with the enzyme is coloured in orange and the metal ions that assist catalysis are shown as red spheres. Purple spheres denote the Zn^{2+} ions important for maintenance of the principal dimers in the RNase E quaternary structure. Structure was drawn using PyMOL (http://pymol.sourceforge.net).

Interactions of mRNA targets with the RNA chaperone Hfq and sRNAs play an important role in the cleavage of certain mRNAs by RNase E (Wagner and Flardh, 2002). The activity of RNase E is also globally affected by protein inhibitors, namely the L4 ribosomal protein, RraA and RraB (the regulator of

RNase activity A and B, respectively) that interact with RNase E and inhibit RNase E endonucleolytic cleavages of a selective group of transcripts (Gao *et al.*, 2006; Lee and Cohen, 2003).

The cellular level and activity of RNase E are subject to complex regulation. The enzyme concentration in the cell is regulated by a feedback loop in which RNase E modulates the decay of its own mRNA, maintaining the level of the enzyme within a narrow range (Diwa *et al.*, 2000; Jain and Belasco, 1995; Mudd and Higgins, 1993; Ow *et al.*, 2002; Sousa *et al.*, 2001).

Ribonuclease III

RNase III was originally identified by Robertson *et al.* (Robertson *et al.*, 1968) in extracts of *E. coli* as the first dsRNA specific endoribonuclease. Members of the RNase III family are widely distributed among prokaryotic and eukaryotic organisms, sharing structural and functional features (Lamontagne *et al.*, 2001). However, until now, homologues of RNase III have not been found in the genomes of archaea (Condon and Putzer, 2002; Marchfelder *et al.*, 2012). All enzymes of this family are hydrolytic and have specificity for dsRNAs, generating 5'-monophosphate and 3'-hydroxyl termini with a two-base overhang at the 3'end (Meng and Nicholson, 2008). The RNase III family comprises four classes, according to their polypeptide structure. The class I is the simplest, containing an endonuclease domain (NucD), characterized in several bacteria by the presence of a highly conserved amino acid stretch NERLEFLGDS, and a dsRNA-binding domain (dsRBD) (Blaszczyk *et al.*, 2001). The class II is exemplified by the *Drosophila melanogaster* Drosha protein, which contains a long N-terminal extension, followed by two NucD and a single dsRBD. The class III is represented by Dicer, which has an N-terminal helicase/ATPase domain, followed by a domain of unknown function (DUF283), a centrally positioned Piwi

Argonaute Zwille (PAZ) domain and a C-terminal configuration like Drosha, consisting of two NucD and one dsRBD (Drider and Condon, 2004; MacRae and Doudna, 2007). Finally, the class IV is only represented, to date, by the Mini-RNase III of *B. subtilis*, which is constituted by a single NucD domain (Redko *et al.*, 2008). The class I members of the RNase III family are ubiquitously found in bacteria, bacteriophages and some fungi (MacRae and Doudna, 2007). *Escherichia coli* RNase III has served as the prototypical member of the family. In this model microorganism, RNase III is encoded by the *rnc* gene, and is active as a 52 kDa homodimer (Li and Nicholson, 1996) (Figure 3). Each monomer contains a C-terminal dsRBD, located in the last 74 amino acids, which is responsible for substrate recognition and adopts a tertiary fold with the characteristic α1-β1-β2-β3-α2 structure that is conserved throughout the RNase III family (Blaszczyk *et al.*, 2001). Additionally, each monomer contains an N-terminal NucD. When the two monomers are combined (RNase III homodimer), they form a single processing center in the subunit interface, in which each monomer contributes to the hydrolysis of one RNA strand of the duplex substrate. Ji and co-workers (Blaszczyk *et al.*, 2004; Gan *et al.*, 2006) resolved the structure of the hyperthermophilic bacteria *Aquifex aeolicus* RNase III and the data have revealed two functional forms of dsRNA binding by RNase III: a catalytic form, functioning as a dsRNA-processing enzyme, cleaving both natural and synthetic dsRNA, and a noncatalytic form, in which RNase III plays the role of a dsRNA-binding protein (without cleaving). The latter activity is in agreement with previous studies in which this enzyme binds certain substrates in order to influence gene expression (Calin-Jageman and Nicholson, 2003; Dasgupta *et al.*, 1998; Oppenheim *et al.*, 1993). Magnesium (Mg^{2+}) is the preferred cofactor. It was reported that each active site contains two divalent cations during substrate hydrolysis (Meng and Nicholson, 2008).

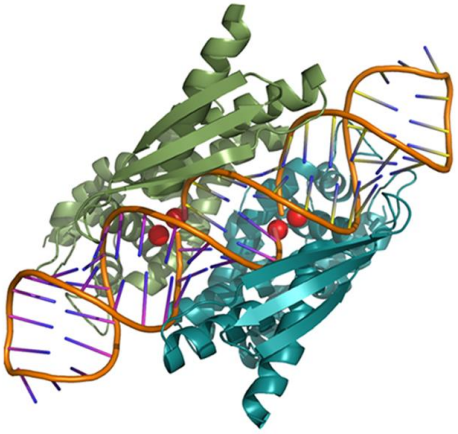

Figure 3 - Structures of RNase III in complex with RNA substrate. Crystal structure of *A. aeolicus* RNase III, PDB ID 2NUF. RNA substrate in complex with the enzyme is coloured in orange and the metal ions that assist catalysis are shown as red spheres. Structures were drawn using PyMOL (http://pymol.sourceforge.net).

The RNase III substrate selection consists of a combination of structural determinants and sequence elements referred to as reactivity epitopes, such as the helix length, the strength of base-pairing or the occurrence of specific nucleotide pairs (termed proximal and distal boxes) located at defined positions related to the cleavage site. In addition, there are two classes of double-helical elements that can function as negative determinants, which can either inhibit the recognition of this endoribonuclease or suppress the cleavage (without affecting recognition) (Pertzev and Nicholson, 2006; Zhang and Nicholson, 1997).

Regarding the maturation of rRNA, RNase III is involved in the processing of 16S and 23S rRNAs (Babitzke *et al.*, 1993). In *Salmonella* and other members of Alphaproteobacteria, the enzyme is also responsible for the cleavage of the intervening sequences (IVS) found in their 23S rRNA gene (Evguenieva-Hackenberg and Klug, 2000), and in the decay of several mRNA species. For example, in *E. coli*, RNase III participates in the first step of the decay of *pnp* mRNA (Regnier and Portier, 1986), the gene encoding the exoribonuclease PNPase, downregulating its synthesis (Jarrige *et al.*, 2001; Regnier and Grunberg-Manago, 1990; Robert-Le Meur and Portier, 1992). Interestingly, this

endoribonuclease also has the ability to regulate its own synthesis with a specific cleavage near the 5'end of its own mRNA that removes a stem loop, which acts as a degradation barrier (Bardwell *et al.*, 1989; Matsunaga *et al.*, 1996). A genome-wide study in *E. coli* revealed a broad function of RNase III in gene regulation (Stead *et al.*, 2011). Indeed, some studies have reported the involvement of RNase III in the control of steady-state levels of genes involved in cellular adaptation to stress (Freire *et al.*, 2006; Santos *et al.*, 1997; Sim *et al.*, 2010). Additionally, this double-stranded enzyme is implicated in the decay of sRNA/mRNA complexes upon translational silencing {Viegas, 2008 #79}.

Bs-RNase III is a homologue of *E. coli* RNase III in *B. subtilis*. It is a 28-kDa protein (Mitra and Bechhofer, 1994), encoded by the *rncS* gene (Herskovitz and Bechhofer, 2000; Mitra and Bechhofer, 1994). Although the local environment of the site of *Bs*-RNase III cleavage appears to be very similar to that of *E. coli* RNase III, there are important differences in their substrate specificity (Mitra and Bechhofer, 1994; Wang and Bechhofer, 1997). More recently, the *B. subtilis* Mini-III was reported to be involved in 23S rRNA gene maturation (Redko *et al.*, 2008). Interestingly, like *Bs*-RNaseIII, Mini-III does not seem to have endogenous mRNA substrates (Bechhofer, 2009). In *Lactococcus lactis*, RNase III plays a determinant role in the control of the stability of *citQRP* mRNA, which encodes for an operon involved in citrate metabolism (Drider *et al.*, 1999; Drider *et al.*, 1998). Complementation assays performed in *E. coli* showed that *L. lactis* RNase III can process *E. coli* rRNAs and regulate the levels of PNPase mRNA, substituting the endogenous RNase III (Amblar *et al.*, 2004). The role of RNase III was even more strengthened in a recent study that showed that this enzyme in *S. aureus* is involved in the processing of hybridized sense/antisense RNA (Lasa *et al.*, 2011).

Taken together, the functional and evolutionary conservation of the RNase III family in bacteria and higher organisms is indicative of their biological relevance in RNA maturation and degradation. Despite the fact that RNase E is

considered the major RNase that catalyzes the initial rate determining cleavage of several transcripts, the RNase III family of enzymes has emerged as one of the most important groups of endoribonucleases in the control of RNA stability (Jaskiewicz and Filipowicz, 2008).

REGULATORY RNAS

The universality of regulatory RNAs playing a role in gene regulation in bacteria, primarily at the posttranscriptional level, is now well established. These elements are responsible to influence the translation and/or stability of mRNAs using several modes of action. There are many RNA regulatory elements (Waters and Storz, 2009). sRNAs mostly exert their regulatory functions by interacting with proteins or by pairing with mRNA targets. Besides sRNAs, a variety of large mRNA leaders sense environmental cues or intracellular concentrations of small metabolites to adopt structures that prevent/activate their extended transcription or translation. These RNA elements are the so-called riboswitches and thermosensors. Finally, the CRISPR RNAs are central to the defense against foreign DNA in many bacteria and archaea.

In order to understand the action of the regulatory RNAs, it is fundamental to study the processing and turnover of these molecules. Here we will give some details about the contribution of RNase E and RNase III, which are the main focus of this dissertation, into the regulatory role of some of these RNA elements.

RNase E, RNase III and small RNAs

All sRNAs participate in regulatory circuits involved in metabolism, stress adaptation and virulence. Due to bioinformatic approaches and genome-wide identification, the number of sRNAs identified in bacteria has considerably increased. The mechanisms by which sRNAs modulate gene expression are diverse, but two general modes of action have been established. sRNAs can act by interaction with a protein to modify its activity, but the most common are the antisense sRNAs that act by base-pairing with one or more targets. These antisense RNAs can be located in the complementary strand to the mRNA they regulate (*cis*-encoded sRNAs), containing perfect complementarity, and/or can be localised in a different genomic region apart from the target (*trans*-encoded sRNAs), thus they exhibit limited base-pairing. Such *trans*-encoded sRNAs typically require the bacterial RNA chaperone, Hfq, both for target interaction and for intracellular stability. It is generally assumed that Hfq binds both the regulator and the target RNA, favoring their interaction (Waters and Storz, 2009).

Most commonly, base-pairing between sRNA and the mRNA targets can cause the inhibition or activation of mRNA translation, mRNA stabilization or mRNA degradation (Lalaouna *et al.*, 2013; Storz *et al.*, 2005; Waters and Storz, 2009).

The majority of sRNAs reported in the literature are known to block translation by hybridization with the ribosome binding site (RBS) in the 5'untranslated region (UTR) region of the target mRNAs. This interaction prevents the 30S ribosome loading and sometimes can also trigger RNA degradation. In fact, a physiological role for sRNAs-mediated degradation may be to render the gene silencing irreversible. An innovative example of sRNA-mediated degradation is the case of ChiX sRNA. This sRNA was discovered during the study of the *Salmonella* ChiP outer membrane protein. This porin is necessary for the uptake of the chitin-derived oligosaccharides when

chitooligosaccharides are the only source of both carbon and nitrogen available (Figueroa-Bossi *et al.*, 2009). When ChiP is no longer needed, ChiX sRNA represses its synthesis by pairing with a sequence in the 5′-UTR of *chiP* mRNA. This pairing destabilizes *chiP* mRNA and promotes its degradation by RNase E. This silencing is relieved in the presence of chitooligosaccharides due to the accumulation of an RNA, anti-ChiX, that base-pairs with ChiX sRNA triggering its nucleolytic degradation (Figueroa-Bossi *et al.*, 2009). The anti-ChiX RNA is located in an intercistronic region of the *chb* operon, which contain genes for chitooligosaccharide metabolism. Transcription of the *chb* operon is activated in the presence of these sugars, and processing of *chb* transcript by RNase E releases the anti-ChiX RNA (Figueroa-Bossi *et al.*, 2009). This ultimately activates ChiP porin production. Thereby, RNase E acts in two distinct steps of this regulatory mechanism.

Besides RNase E, there are other RNases involved in the sRNA-mediated mRNA degradation. RNase III for instance acts over RNAIII from *S. aureus*, which encodes for hemolysin delta (Novick and Jiang, 2003), but also acts as a sRNA. The large 3′-UTR from RNAIII represses the synthesis of several surface and secreted proteins (Boisset *et al.*, 2007) by forming RNAIII-mRNA duplexes. These duplexes induce degradation by RNase III, causing an irreversible repression of the virulent factors synthesis (Boisset *et al.*, 2007; Chevalier *et al.*, 2010; Geisinger *et al.*, 2006; Huntzinger *et al.*, 2005).

In contrast to this scenario, some sRNAs are devoted to activate translation by binding to the 5′-UTR of the target mRNA. Normally, these target mRNAs contain a secondary structure in the 5′-UTR region that inhibits ribosome loading. Thus, upon sRNA hybridization with the inhibitory sequence in the 5′-UTR, the RBS becomes available, allowing initiation of translation. The RNA base-paring can be combined with endoribonucleolytic cleavage or can lead to

protection from RNases (Obana *et al.*, 2010; Papenfort *et al.*, 2013; Ramirez-Pena *et al.*, 2010).

We decided to go deeper in the example of RpoS, a known example of activation of translation by mRNA stabilization. RpoS is a sigma factor highly expressed during stationary phase and in response to multiple stresses in order to activate transcription of many genes required to cope with such demands. Hence, its expression is tightly regulated at several levels, namely at the posttranscriptional level. The sRNAs DsrA and RprA are known to positively regulate the expression of RpoS, and thus their respective levels also respond to environmental stimuli (Madhugiri *et al.*, 2010). The *rpoS* stimulation of translation is performed through base-pairing with the 5'-UTR region (Majdalani *et al.*, 1998; McCullen *et al.*, 2010). RNase E was shown to have a central role in the degradation of *rpoS* transcript. Thus, binding of DsrA sRNA leads to *rpoS* accumulation by protecting this mRNA from RNase E-dependent degradation (McCullen *et al.*, 2010). RNase E was also found to be involved in the turnover of the sRNAs RprA and DsrA (Madhugiri *et al.*, 2010; Moll *et al.*, 2003). However, Hfq binding to these sRNAs impacts the RNase E cleavage ability, probably by inducing structural changes in the sRNAs (Henderson *et al.*, 2013; Madhugiri *et al.*, 2010).

RNase III was also reported to promote mRNA stability. GadY is a *cis*-encoded antisense RNA encoded in the bacterial chromosome, within the intergenic region of *gadX-gadW* mRNA. These genes are part of a complex regulatory circuit controlling the *E. coli* response to acid stress (Opdyke *et al.*, 2004). GadY sRNA positively regulates *gadX* through a perfectly complementary sequence in the 3'-UTR of *gadX* mRNA. Base-pairing of GadY with the intergenic region of the *gadX-gadW* mRNA results in the processing of the bicistronic message and involves RNase III. This processing event stabilizes each of the transcripts (Opdyke *et al.*, 2011).

RNases are also responsible for the maturation of some RNAs. In the case of sRNAs, the initial processing may facilitate further degradation of the sRNA or generate mature sRNA species with higher regulatory activity as a consequence of either increased stability or increased affinity for the target mRNA. The sRNA DicF of *E. coli* was shown to be processed to an active form by a mechanism mediated by RNase E and RNase III (Faubladier *et al.*, 1990). This sRNA is responsible for the translation inhibition of its target *ftsZ* mRNA and for this reason it is associated with the blocking of the cell division in *E. coli* (Tetart and Bouche, 1992). RNase III processing in the 5′ end of the transcript generates a 190 nts precursor which is further processed by RNase E to generate the functional 53 nts DicF asRNA (Faubladier *et al.*, 1990).

RNases, Riboswitches and RNA thermometers

Riboswitches are RNA structures located within the 5′-UTR of mRNAs that fold into complex structures whose conformation change upon binding of intracellular metabolites (e.g. amino acids, vitamins, etc.). These regulatory RNAs are also targets of RNase-mediated decay (Bastet *et al.*, 2011). For instance, a riboswitch called *lysC* was shown to control both translation initiation and mRNA decay. It senses the amino acid lysine and adopts an OFF conformation. This conformation blocks translation and induces RNase E-based degradosome degradation (Caron *et al.*, 2012). Thus, RNase E together with the other degradosome components are involved in lysine-dependent degradation of *lysC* mRNA. This mechanism was called nucleolytic repression (Caron *et al.*, 2012).

Like riboswicthes, known RNA thermometers are located in the 5′-UTR region of mRNAs. Despite few exceptions, these RNA elements control translation initiation of several genes by forming a secondary structure that traps the ribosome binding site. An increase of temperature destabilizes the structure,

liberates the RBS leading to the formation of the translation initiation complex (Kortmann and Narberhaus, 2012). The study of the involvement of RNases on the regulation of RNA thermosensors is rather poor. A known example is the *ibpAB* operon that encodes two small heat-shock proteins, inclusion-body-binding IbpA and IbpB, in *E. coli* (Gaubig *et al.*, 2011). Heat-induced transcription of the bicistronic operon is followed by processing events performed by RNase E, resulting in monocistronic *ibpA* and *ibpB* transcrips. Upon a down-shift of the temperature to 30°C, the ribosome access for *ibpA* and *ibpB* Shine-Dalgarno sites is blocked, hindering the expression of the respective downstream ORFs. This triggers the RNase E degradation of the untranslatable *ibpAB* mRNA (Gaubig *et al.*, 2011). However, in this case the function of the RNA thermosensor is not dependent on the action of RNase E. In fact, there is only one example of a bacterial RNA thermometer known to require the action of an RNase for its function, though the precise role of the RNase needs further clarification (Altuvia *et al.*, 1989; Altuvia *et al.*, 1987).

Overall, bacteria have evolved a panoply of intricate mechanisms to control gene expression. There are many examples reported in the literature representative of different modes of action that involve regulatory RNAs in cooperation with RNases. All these examples contain peculiar details that make them unique. Due to this fact in the Introduction section we have detailed some illustrative examples that only show a small fraction of the immensity of RNA regulatory mechanisms in bacteria. By looking at this variety, we imagine that much more could still be discovered.

AIM OF THIS DISSERTATION

This Dissertation is mainly focused on the contribution of RNase III endoribonuclease to the mechanisms of posttranscriptional regulation of gene expression in three different pathogenic microorganisms: *C. jejuni*, *S.* Typhimurium and *S. aureus*.

There is little information regarding ribonucleases in *C. jejuni*. To our knowledge there is only one published report about the importance of polynucleotide phosphorylase (PNPase) for *C. jejuni* survival and pathogenicity. This exoribonuclease was shown to facilitate *Campylobacter* swimming, cell adhesion, colonization and invasion, plus to allow survival in refrigerated temperatures {Haddad, 2009 #740;Haddad, 2012 #741}. Compelling evidences suggest that RNases are involved in virulence. Among these, RNase III has been shown to be implicated in the expression of virulence related genes in several pathogens. In the first part of this doctoral work, we intended to perform a functional and biochemical analysis of RNase III from *C. jejuni* (*Cj*-RNase III).

Salmonella infections are a serious medical and veterinary problem worldwide and there is an increasing need for new strategies for prevention and control. The second objective of this dissertation was to examine antibiotic susceptibility on *Salmonella* ribonucleases mutant strains and their ability in forming biofilm. We also intended to study *in vitro* the role of endoribonuclease E and III in the degradation of MicA. This sRNA down-regulates the levels of outer membrane porins in *Enterobacteriaceae*, and was shown to have a role in biofilm production.

The role of RNase III was further study in *S. aureus* biofilm production. Biofilm production is a main factor of *S. aureus* virulence, being critical for the progression of infections caused by this bacterium. Expression of the main

exopolysaccharidic compound of the *S. aureus* biofilm matrix is repressed by IcaR. Through a combination of *in vivo* and *in vitro* experiments we studied the involvement of RNase III in the posttranscriptional control of IcaR. Other players that may be involved in the posttranscriptional regulation of IcaR were also evaluated.

In summary, the work developed in this Doctoral work was mainly focused on studying endoribonucleases. We unveiled additional information about the function of these endoribonucleases, especially RNase III, on different posttranscriptional mechanisms, and highlighted the importance of this enzyme as a global regulator.

REFERENCES

Afonyushkin, T., B. Vecerek, I. Moll, U. Blasi, and V.R. Kaberdin. 2005. Both RNase E and RNase III control the stability of sodB mRNA upon translational inhibition by the small regulatory RNA RyhB. *Nucleic Acids Res*. 33:1678-1689.

Agrawal, N., P.V. Dasaradhi, A. Mohmmed, P. Malhotra, R.K. Bhatnagar, and S.K. Mukherjee. 2003. RNA interference: biology, mechanism, and applications. *Microbiol Mol Biol Rev*. 67:657-685.

Altuvia, S., D. Kornitzer, D. Teff, and A.B. Oppenheim. 1989. Alternative mRNA structures of the cIII gene of bacteriophage lambda determine the rate of its translation initiation. *J Mol Biol*. 210:265-280.

Altuvia, S., H. Locker-Giladi, S. Koby, O. Ben-Nun, and A.B. Oppenheim. 1987. RNase III stimulates the translation of the cIII gene of bacteriophage lambda. *Proc Natl Acad Sci U S A*. 84:6511-6515.

Amblar, M., S.C. Viegas, P. Lopez, and C.M. Arraiano. 2004. Homologous and heterologous expression of RNase III from Lactococcus lactis. *Biochem Biophys Res Commun*. 323:884-890.

Andrade, J.M., V. Pobre, I.J. Silva, S. Domingues, and C.M. Arraiano. 2009. The role of 3'-5' exoribonucleases in RNA degradation. *Prog Mol Biol Transl Sci*. 85:187-229.

Apirion, D., and A.B. Lassar. 1978. A conditional lethal mutant of Escherichia coli which affects the processing of ribosomal RNA. *J Biol Chem*. 253:1738-1742.

Arraiano, C.M., J.M. Andrade, S. Domingues, I.B. Guinote, M. Malecki, R.G. Matos, R.N. Moreira, V. Pobre, F.P. Reis, M. Saramago, I.J. Silva, and S.C. Viegas. 2010. The critical role of RNA processing and degradation in the control of gene expression. *FEMS Microbiol Rev*. 34:883-923.

Arraiano, C.M., S.D. Yancey, and S.R. Kushner. 1988. Stabilization of discrete mRNA breakdown products in ams pnp rnb multiple mutants of Escherichia coli K-12. *J Bacteriol*. 170:4625-4633.

Babitzke, P., L. Granger, J. Olszewski, and S.R. Kushner. 1993. Analysis of mRNA decay and rRNA processing in Escherichia coli multiple mutants carrying a deletion in RNase III. *J Bacteriol*. 175:229-239.

Babitzke, P., and S.R. Kushner. 1991. The Ams (altered mRNA stability) protein and ribonuclease E are encoded by the same structural gene of Escherichia coli. *Proc Natl Acad Sci U S A*. 88:1-5.

Baker, K.E., and G.A. Mackie. 2003. Ectopic RNase E sites promote bypass of 5'-end-dependent mRNA decay in Escherichia coli. *Mol Microbiol*. 47:75-88.

Bardwell, J.C., P. Regnier, S.M. Chen, Y. Nakamura, M. Grunberg-Manago, and D.L. Court. 1989. Autoregulation of RNase III operon by mRNA processing. *EMBO J*. 8:3401-3407.

Bastet, L., A. Dube, E. Masse, and D.A. Lafontaine. 2011. New insights into riboswitch regulation mechanisms. *Mol Microbiol*. 80:1148-1154.

Bechhofer, D.H. 2009. Messenger RNA decay and maturation in Bacillus subtilis. *Prog Mol Biol Transl Sci*. 85:231-273.

Blaszczyk, J., J. Gan, J.E. Tropea, D.L. Court, D.S. Waugh, and X. Ji. 2004. Noncatalytic assembly of ribonuclease III with double-stranded RNA. *Structure*. 12:457-466.

Blaszczyk, J., J.E. Tropea, M. Bubunenko, K.M. Routzahn, D.S. Waugh, D.L. Court, and X. Ji. 2001. Crystallographic and modeling studies of RNase III suggest a mechanism for double-stranded RNA cleavage. *Structure*. 9:1225-1236.

Boisset, S., T. Geissmann, E. Huntzinger, P. Fechter, N. Bendridi, M. Possedko, C. Chevalier, A.C. Helfer, Y. Benito, A. Jacquier, C. Gaspin, F. Vandenesch, and P. Romby. 2007. Staphylococcus aureus RNAIII coordinately represses the synthesis of virulence factors and the transcription regulator Rot by an antisense mechanism. *Genes Dev*. 21:1353-1366.

Bralley, P., B. Gust, S. Chang, K.F. Chater, and G.H. Jones. 2006. RNA 3'-tail synthesis in Streptomyces: in vitro and in vivo activities of RNase PH, the SCO3896 gene product and polynucleotide phosphorylase. *Microbiology*. 152:627-636.

Calin-Jageman, I., and A.W. Nicholson. 2003. RNA structure-dependent uncoupling of substrate recognition and cleavage by Escherichia coli ribonuclease III. *Nucleic Acids Res*. 31:2381-2392.

Callaghan, A.J., M.J. Marcaida, J.A. Stead, K.J. McDowall, W.G. Scott, and B.F. Luisi. 2005. Structure of Escherichia coli RNase E catalytic domain and implications for RNA turnover. *Nature*. 437:1187-1191.

Caron, M.P., L. Bastet, A. Lussier, M. Simoneau-Roy, E. Masse, and D.A. Lafontaine. 2012. Dual-acting riboswitch control of translation initiation and mRNA decay. *Proc Natl Acad Sci U S A*. 109:E3444-3453.

Carpousis, A.J., B.F. Luisi, and K.J. McDowall. 2009. Endonucleolytic initiation of mRNA decay in Escherichia coli. *Prog Mol Biol Transl Sci*. 85:91-135.

Carpousis, A.J., G. Van Houwe, C. Ehretsmann, and H.M. Krisch. 1994. Copurification of E. coli RNAase E and PNPase: evidence for a specific association between two enzymes important in RNA processing and degradation. *Cell*. 76:889-900.

Charpentier, X., S.P. Faucher, S. Kalachikov, and H.A. Shuman. 2008. Loss of RNase R induces competence development in Legionella pneumophila. *J Bacteriol*. 190:8126-8136.

Cheng, Z.F., and M.P. Deutscher. 2003. Quality control of ribosomal RNA mediated by polynucleotide phosphorylase and RNase R. *Proc Natl Acad Sci U S A*. 100:6388-6393.

Chevalier, C., S. Boisset, C. Romilly, B. Masquida, P. Fechter, T. Geissmann, F. Vandenesch, and P. Romby. 2010. Staphylococcus aureus RNAIII binds to two distant regions of coa mRNA to arrest translation and promote mRNA degradation. *PLoS Pathog*. 6:e1000809.

Commichau, F.M., F.M. Rothe, C. Herzberg, E. Wagner, D. Hellwig, M. Lehnik-Habrink, E. Hammer, U. Volker, and J. Stulke. 2009. Novel activities of glycolytic enzymes in Bacillus subtilis: interactions with essential proteins involved in mRNA processing. *Mol Cell Proteomics*. 8:1350-1360.

Condon, C. 2003. RNA processing and degradation in Bacillus subtilis. *Microbiol Mol Biol Rev*. 67:157-174, table of contents.

Condon, C. 2010. What is the role of RNase J in mRNA turnover? *RNA Biol*. 7:316-321.

Condon, C., and H. Putzer. 2002. The phylogenetic distribution of bacterial ribonucleases. *Nucleic Acids Res*. 30:5339-5346.

Dasgupta, S., L. Fernandez, L. Kameyama, T. Inada, Y. Nakamura, A. Pappas, and D.L. Court. 1998. Genetic uncoupling of the dsRNA-binding and RNA cleavage activities of the Escherichia coli endoribonuclease RNase III--the effect of dsRNA binding on gene expression. *Mol Microbiol*. 28:629-640.

Deana, A., H. Celesnik, and J.G. Belasco. 2008. The bacterial enzyme RppH triggers messenger RNA degradation by 5' pyrophosphate removal. *Nature*. 451:355-358.

Deutscher, M.P., and N.B. Reuven. 1991. Enzymatic basis for hydrolytic versus phosphorolytic mRNA degradation in Escherichia coli and Bacillus subtilis. *Proc Natl Acad Sci U S A*. 88:3277-3280.

Diwa, A., A.L. Bricker, C. Jain, and J.G. Belasco. 2000. An evolutionarily conserved RNA stem-loop functions as a sensor that directs feedback regulation of RNase E gene expression. *Genes Dev*. 14:1249-1260.

Domingues, S., R.G. Matos, F.P. Reis, A.M. Fialho, A. Barbas, and C.M. Arraiano. 2009. Biochemical characterization of the RNase II family of exoribonucleases from the human pathogens Salmonella typhimurium and Streptococcus pneumoniae. *Biochemistry*. 48:11848-11857.

Drider, D., and C. Condon. 2004. The continuing story of endoribonuclease III. *J Mol Microbiol Biotechnol*. 8:195-200.

Drider, D., N. Garcia-Quintans, J.M. Santos, C.M. Arraiano, and P. Lopez. 1999. A comparative analysis of the citrate permease P mRNA stability in Lactococcus lactis biovar diacetylactis and Escherichia coli. *FEMS Microbiol Lett*. 172:115-122.

Drider, D., J.M. Santos, C.M. Arraiano, and P. Lopez. 1998. RNA processing is involved in the post-transcriptional control of the citQRP operon from Lactococcus lactis biovar diacetylactis. *Mol Gen Genet*. 258:9-15.

Durand, S., L. Gilet, P. Bessieres, P. Nicolas, and C. Condon. 2012a. Three essential ribonucleases-RNase Y, J1, and III-control the abundance of a majority of Bacillus subtilis mRNAs. *PLoS Genet*. 8:e1002520.

Durand, S., L. Gilet, and C. Condon. 2012b. The essential function of B. subtilis RNase III is to silence foreign toxin genes. *PLoS Genet*. 8:e1003181.

Even, S., O. Pellegrini, L. Zig, V. Labas, J. Vinh, D. Brechemmier-Baey, and H. Putzer. 2005. Ribonucleases J1 and J2: two novel endoribonucleases in B.subtilis with functional homology to E.coli RNase E. *Nucleic Acids Res*. 33:2141-2152.

Evguenieva-Hackenberg, E., and G. Klug. 2000. RNase III processing of intervening sequences found in helix 9 of 23S rRNA in the alpha subclass of Proteobacteria. *J Bacteriol*. 182:4719-4729.

Falaleeva, M.V., H.V. Chetverina, V.I. Ugarov, E.A. Uzlova, and A.B. Chetverin. 2008. Factors influencing RNA degradation by Thermus thermophilus polynucleotide phosphorylase. *FEBS J*. 275:2214-2226.

Fang, M., W.M. Zeisberg, C. Condon, V. Ogryzko, A. Danchin, and U. Mechold. 2009. Degradation of nanoRNA is performed by multiple redundant RNases in Bacillus subtilis. *Nucleic Acids Res*. 37:5114-5125.

Faubladier, M., K. Cam, and J.P. Bouche. 1990. Escherichia coli cell division inhibitor DicF-RNA of the dicB operon. Evidence for its generation in vivo by transcription termination and by RNase III and RNase E-dependent processing. *J Mol Biol*. 212:461-471.

Figueroa-Bossi, N., M. Valentini, L. Malleret, F. Fiorini, and L. Bossi. 2009. Caught at its own game: regulatory small RNA inactivated by an inducible transcript mimicking its target. *Genes Dev*. 23:2004-2015.

Freire, P., J.D. Amaral, J.M. Santos, and C.M. Arraiano. 2006. Adaptation to carbon starvation: RNase III ensures normal expression levels of bolA1p mRNA and sigma(S). *Biochimie*. 88:341-346.

Gan, J., J.E. Tropea, B.P. Austin, D.L. Court, D.S. Waugh, and X. Ji. 2006. Structural insight into the mechanism of double-stranded RNA processing by ribonuclease III. *Cell*. 124:355-366.

Gao, J., K. Lee, M. Zhao, J. Qiu, X. Zhan, A. Saxena, C.J. Moore, S.N. Cohen, and G. Georgiou. 2006. Differential modulation of E. coli mRNA abundance by inhibitory proteins that alter the composition of the degradosome. *Mol Microbiol*. 61:394-406.

Gaubig, L.C., T. Waldminghaus, and F. Narberhaus. 2011. Multiple layers of control govern expression of the Escherichia coli ibpAB heat-shock operon. *Microbiology*. 157:66-76.

Geisinger, E., R.P. Adhikari, R. Jin, H.F. Ross, and R.P. Novick. 2006. Inhibition of rot translation by RNAIII, a key feature of agr function. *Mol Microbiol*. 61:1038-1048.

Ghosh, S., and M.P. Deutscher. 1999. Oligoribonuclease is an essential component of the mRNA decay pathway. *Proc Natl Acad Sci U S A*. 96:4372-4377.

Henderson, C.A., H.A. Vincent, C.M. Stone, J.O. Phillips, P.D. Cary, D.M. Gowers, and A.J. Callaghan. 2013. Characterization of MicA interactions suggests a potential novel means of gene regulation by small non-coding RNAs. *Nucleic Acids Res*. 41:3386-3397.

Herskovitz, M.A., and D.H. Bechhofer. 2000. Endoribonuclease RNase III is essential in Bacillus subtilis. *Mol Microbiol*. 38:1027-1033.

Huntzinger, E., S. Boisset, C. Saveanu, Y. Benito, T. Geissmann, A. Namane, G. Lina, J. Etienne, B. Ehresmann, C. Ehresmann, A. Jacquier, F. Vandenesch, and P. Romby. 2005. Staphylococcus aureus RNAIII and the endoribonuclease III coordinately regulate spa gene expression. *EMBO J*. 24:824-835.

Hutchison, C.A., S.N. Peterson, S.R. Gill, R.T. Cline, O. White, C.M. Fraser, H.O. Smith, and J.C. Venter. 1999. Global transposon mutagenesis and a minimal Mycoplasma genome. *Science*. 286:2165-2169.

Jagannath, A., and M. Wood. 2007. RNA interference based gene therapy for neurological disease. *Brief Funct Genomic Proteomic*. 6:40-49.

Jain, C., and J.G. Belasco. 1995. Autoregulation of RNase E synthesis in Escherichia coli. *Nucleic Acids Symp Ser*:85-88.

Jarrige, A.C., N. Mathy, and C. Portier. 2001. PNPase autocontrols its expression by degrading a double-stranded structure in the pnp mRNA leader. *EMBO J*. 20:6845-6855.

Jaskiewicz, L., and W. Filipowicz. 2008. Role of Dicer in posttranscriptional RNA silencing. *Curr Top Microbiol Immunol*. 320:77-97.

Jiang, X., and J.G. Belasco. 2004. Catalytic activation of multimeric RNase E and RNase G by 5'-monophosphorylated RNA. *Proc Natl Acad Sci U S A*. 101:9211-9216.

Jinek, M., and J.A. Doudna. 2009. A three-dimensional view of the molecular machinery of RNA interference. *Nature*. 457:405-412.

Kaberdin, V.R., and U. Blasi. 2006. Translation initiation and the fate of bacterial mRNAs. *FEMS Microbiol Rev*. 30:967-979.

Kaberdin, V.R., A. Miczak, J.S. Jakobsen, S. Lin-Chao, K.J. McDowall, and A. von Gabain. 1998. The endoribonucleolytic N-terminal half of Escherichia coli RNase E is evolutionarily conserved in Synechocystis sp. and other bacteria but not the C-terminal half, which is sufficient for degradosome assembly. *Proc Natl Acad Sci U S A*. 95:11637-11642.

Khemici, V., L. Poljak, B.F. Luisi, and A.J. Carpousis. 2008. The RNase E of Escherichia coli is a membrane-binding protein. *Mol Microbiol*. 70:799-813.

Kime, L., S.S. Jourdan, J.A. Stead, A. Hidalgo-Sastre, and K.J. McDowall. 2010. Rapid cleavage of RNA by RNase E in the absence of 5' monophosphate stimulation. *Mol Microbiol*. 76:590-604.

Ko, J.H., K. Han, Y. Kim, S. Sim, K.S. Kim, S.J. Lee, B. Cho, K. Lee, and Y. Lee. 2008. Dual function of RNase E for control of M1 RNA biosynthesis in Escherichia coli. *Biochemistry*. 47:762-770.

Kortmann, J., and F. Narberhaus. 2012. Bacterial RNA thermometers: molecular zippers and switches. *Nat Rev Microbiol*. 10:255-265.

Koslover, D.J., A.J. Callaghan, M.J. Marcaida, E.F. Garman, M. Martick, W.G. Scott, and B.F. Luisi. 2008. The crystal structure of the Escherichia coli RNase E apoprotein and a mechanism for RNA degradation. *Structure*. 16:1238-1244.

Lalaouna, D., M. Simoneau-Roy, D. Lafontaine, and E. Masse. 2013. Regulatory RNAs and target mRNA decay in prokaryotes. *Biochim Biophys Acta*. 1829:742-747.

Lamontagne, B., S. Larose, J. Boulanger, and S.A. Elela. 2001. The RNase III family: a conserved structure and expanding functions in eukaryotic dsRNA metabolism. *Curr Issues Mol Biol*. 3:71-78.

Lasa, I., A. Toledo-Arana, A. Dobin, M. Villanueva, I.R. de los Mozos, M. Vergara-Irigaray, V. Segura, D. Fagegaltier, J.R. Penades, J. Valle, C. Solano, and T.R. Gingeras. 2011. Genome-wide antisense transcription drives mRNA processing in bacteria. *Proc Natl Acad Sci U S A*. 108:20172-20177.

Lee, K., and S.N. Cohen. 2003. A Streptomyces coelicolor functional orthologue of Escherichia coli RNase E shows shuffling of catalytic and PNPase-binding domains. *Mol Microbiol*. 48:349-360.

Lehnik-Habrink, M., R.J. Lewis, U. Mader, and J. Stulke. 2012. RNA degradation in Bacillus subtilis: an interplay of essential endo- and exoribonucleases. *Mol Microbiol*. 84:1005-1017.

Lehnik-Habrink, M., M. Schaffer, U. Mader, C. Diethmaier, C. Herzberg, and J. Stulke. 2011. RNA processing in Bacillus subtilis: identification of targets of the essential RNase Y. *Mol Microbiol*. 81:1459-1473.

Li de la Sierra-Gallay, I., L. Zig, A. Jamalli, and H. Putzer. 2008. Structural insights into the dual activity of RNase J. *Nat Struct Mol Biol*. 15:206-212.

Li, H., and A.W. Nicholson. 1996. Defining the enzyme binding domain of a ribonuclease III processing signal. Ethylation interference and hydroxyl radical footprinting using catalytically inactive RNase III mutants. *EMBO J*. 15:1421-1433.

Li, Z., S. Pandit, and M.P. Deutscher. 1999. RNase G (CafA protein) and RNase E are both required for the 5' maturation of 16S ribosomal RNA. *EMBO J*. 18:2878-2885.

Lin-Chao, S., C.L. Wei, and Y.T. Lin. 1999. RNase E is required for the maturation of ssrA RNA and normal ssrA RNA peptide-tagging activity. *Proc Natl Acad Sci U S A*. 96:12406-12411.

Liou, G.G., H.Y. Chang, C.S. Lin, and S. Lin-Chao. 2002. DEAD box RhlB RNA helicase physically associates with exoribonuclease PNPase to degrade double-stranded RNA independent of the degradosome-assembling region of RNase E. *J Biol Chem*. 277:41157-41162.

Liou, G.G., W.N. Jane, S.N. Cohen, N.S. Lin, and S. Lin-Chao. 2001. RNA degradosomes exist in vivo in Escherichia coli as multicomponent complexes associated with the cytoplasmic membrane via the N-terminal region of ribonuclease E. *Proc Natl Acad Sci U S A*. 98:63-68.

Lisitsky, I., and G. Schuster. 1999. Preferential degradation of polyadenylated and polyuridinylated RNAs by the bacterial exoribonuclease polynucleotide phosphorylase. *Eur J Biochem*. 261:468-474.

Lundberg, U., and S. Altman. 1995. Processing of the precursor to the catalytic RNA subunit of RNase P from Escherichia coli. *RNA*. 1:327-334.

Ma, Y., C.Y. Chan, and M.L. He. 2007. RNA interference and antiviral therapy. *World J Gastroenterol*. 13:5169-5179.

Mackie, G.A. 1998. Ribonuclease E is a 5'-end-dependent endonuclease. *Nature*. 395:720-723.

MacRae, I.J., and J.A. Doudna. 2007. Ribonuclease revisited: structural insights into ribonuclease III family enzymes. *Curr Opin Struct Biol*. 17:138-145.

Mader, U., L. Zig, J. Kretschmer, G. Homuth, and H. Putzer. 2008. mRNA processing by RNases J1 and J2 affects Bacillus subtilis gene expression on a global scale. *Mol Microbiol*. 70:183-196.

Madhugiri, R., S.R. Basineni, and G. Klug. 2010. Turn-over of the small non-coding RNA RprA in E. coli is influenced by osmolarity. *Mol Genet Genomics*. 284:307-318.

Madhugiri, R., and E. Evguenieva-Hackenberg. 2009. RNase J is involved in the 5'-end maturation of 16S rRNA and 23S rRNA in Sinorhizobium meliloti. *FEBS Lett*. 583:2339-2342.

Majdalani, N., C. Cunning, D. Sledjeski, T. Elliott, and S. Gottesman. 1998. DsrA RNA regulates translation of RpoS message by an anti-antisense mechanism, independent of its action as an antisilencer of transcription. *Proc Natl Acad Sci U S A*. 95:12462-12467.

Manasherob, R., C. Miller, K.S. Kim, and S.N. Cohen. 2012. Ribonuclease E modulation of the bacterial SOS response. *PLoS One*. 7:e38426.

Marchfelder, A., S. Fischer, J. Brendel, B. Stoll, L.K. Maier, D. Jager, D. Prasse, A. Plagens, R.A. Schmitz, and L. Randau. 2012. Small RNAs for defence and regulation in archaea. *Extremophiles*. 16:685-696.

Marujo, P.E., E. Hajnsdorf, J. Le Derout, R. Andrade, C.M. Arraiano, and P. Regnier. 2000. RNase II removes the oligo(A) tails that destabilize the rpsO mRNA of Escherichia coli. *RNA*. 6:1185-1193.

Mathy, N., L. Benard, O. Pellegrini, R. Daou, T. Wen, and C. Condon. 2007. 5'-to-3' exoribonuclease activity in bacteria: role of RNase J1 in rRNA maturation and 5' stability of mRNA. *Cell*. 129:681-692.

Mathy, N., A. Hebert, P. Mervelet, L. Benard, A. Dorleans, I. Li de la Sierra-Gallay, P. Noirot, H. Putzer, and C. Condon. 2010. Bacillus subtilis ribonucleases J1 and J2 form a complex with altered enzyme behaviour. *Mol Microbiol*. 75:489-498.

Matsunaga, J., E.L. Simons, and R.W. Simons. 1996. RNase III autoregulation: structure and function of rncO, the posttranscriptional "operator". *RNA*. 2:1228-1240.

McCullen, C.A., J.N. Benhammou, N. Majdalani, and S. Gottesman. 2010. Mechanism of positive regulation by DsrA and RprA small noncoding RNAs: pairing increases translation and protects rpoS mRNA from degradation. *J Bacteriol*. 192:5559-5571.

McDowall, K.J., R.G. Hernandez, S. Lin-Chao, and S.N. Cohen. 1993. The ams-1 and rne-3071 temperature-sensitive mutations in the ams gene are in close proximity to each other and cause substitutions within a domain that resembles a product of the Escherichia coli mre locus. *J Bacteriol*. 175:4245-4249.

McDowall, K.J., S. Lin-Chao, and S.N. Cohen. 1994. A+U content rather than a particular nucleotide order determines the specificity of RNase E cleavage. *J Biol Chem*. 269:10790-10796.

Melefors, O., and A. von Gabain. 1991. Genetic studies of cleavage-initiated mRNA decay and processing of ribosomal 9S RNA show that the Escherichia coli ams and rne loci are the same. *Mol Microbiol*. 5:857-864.

Meng, W., and A.W. Nicholson. 2008. Heterodimer-based analysis of subunit and domain contributions to double-stranded RNA processing by Escherichia coli RNase III in vitro. *Biochem J*. 410:39-48.

Misra, T.K., and D. Apirion. 1979. RNase E, an RNA processing enzyme from Escherichia coli. *J Biol Chem*. 254:11154-11159.

Mitra, S., and D.H. Bechhofer. 1994. Substrate specificity of an RNase III-like activity from Bacillus subtilis. *J Biol Chem*. 269:31450-31456.

Mohanty, B.K., and S.R. Kushner. 2003. Genomic analysis in Escherichia coli demonstrates differential roles for polynucleotide phosphorylase and RNase II in mRNA abundance and decay. *Mol Microbiol*. 50:645-658.

Moll, I., T. Afonyushkin, O. Vytvytska, V.R. Kaberdin, and U. Blasi. 2003. Coincident Hfq binding and RNase E cleavage sites on mRNA and small regulatory RNAs. *RNA*. 9:1308-1314.

Mudd, E.A., and C.F. Higgins. 1993. Escherichia coli endoribonuclease RNase E: autoregulation of expression and site-specific cleavage of mRNA. *Mol Microbiol*. 9:557-568.

Mudd, E.A., H.M. Krisch, and C.F. Higgins. 1990. RNase E, an endoribonuclease, has a general role in the chemical decay of Escherichia coli mRNA: evidence that rne and ams are the same genetic locus. *Mol Microbiol*. 4:2127-2135.

Murashko, O.N., V.R. Kaberdin, and S. Lin-Chao. 2012. Membrane binding of Escherichia coli RNase E catalytic domain stabilizes protein structure and increases RNA substrate affinity. *Proc Natl Acad Sci U S A*. 109:7019-7024.

Newman, J.A., L. Hewitt, C. Rodrigues, A. Solovyova, C.R. Harwood, and R.J. Lewis. 2011. Unusual, dual endo- and exonuclease activity in the degradosome explained by crystal structure analysis of RNase J1. *Structure*. 19:1241-1251.

Niyogi, S.K., and A.K. Datta. 1975. A novel oligoribonuclease of Escherichia coli. I. Isolation and properties. *J Biol Chem*. 250:7307-7312.

Novick, R.P., and D. Jiang. 2003. The staphylococcal saeRS system coordinates environmental signals with agr quorum sensing. *Microbiology*. 149:2709-2717.

Obana, N., Y. Shirahama, K. Abe, and K. Nakamura. 2010. Stabilization of Clostridium perfringens collagenase mRNA by VR-RNA-dependent cleavage in 5' leader sequence. *Mol Microbiol*. 77:1416-1428.

Oguro, A., H. Kakeshita, K. Nakamura, K. Yamane, W. Wang, and D.H. Bechhofer. 1998. Bacillus subtilis RNase III cleaves both 5'- and 3'-sites of the small cytoplasmic RNA precursor. *J Biol Chem*. 273:19542-19547.

Ono, M., and M. Kuwano. 1979. A conditional lethal mutation in an Escherichia coli strain with a longer chemical lifetime of messenger RNA. *J Mol Biol*. 129:343-357.

Opdyke, J.A., E.M. Fozo, M.R. Hemm, and G. Storz. 2011. RNase III participates in GadY-dependent cleavage of the gadX-gadW mRNA. *J Mol Biol*. 406:29-43.

Opdyke, J.A., J.G. Kang, and G. Storz. 2004. GadY, a small-RNA regulator of acid response genes in Escherichia coli. *J Bacteriol*. 186:6698-6705.

Oppenheim, A.B., D. Kornitzer, S. Altuvia, and D.L. Court. 1993. Posttranscriptional control of the lysogenic pathway in bacteriophage lambda. *Prog Nucleic Acid Res Mol Biol*. 46:37-49.

Ow, M.C., and S.R. Kushner. 2002. Initiation of tRNA maturation by RNase E is essential for cell viability in E. coli. *Genes Dev*. 16:1102-1115.

Ow, M.C., Q. Liu, B.K. Mohanty, M.E. Andrew, V.F. Maples, and S.R. Kushner. 2002. RNase E levels in Escherichia coli are controlled by a complex regulatory system that involves transcription of the rne gene from three promoters. *Mol Microbiol*. 43:159-171.

Papenfort, K., Y. Sun, M. Miyakoshi, C.K. Vanderpool, and J. Vogel. 2013. Small RNA-mediated activation of sugar phosphatase mRNA regulates glucose homeostasis. *Cell*. 153:426-437.

Pertzev, A.V., and A.W. Nicholson. 2006. Characterization of RNA sequence determinants and antideterminants of processing reactivity for a minimal substrate of Escherichia coli ribonuclease III. *Nucleic Acids Res*. 34:3708-3721.

Prud'homme-Genereux, A., R.K. Beran, I. Iost, C.S. Ramey, G.A. Mackie, and R.W. Simons. 2004. Physical and functional interactions among RNase E, polynucleotide phosphorylase and the cold-shock protein, CsdA: evidence for a 'cold shock degradosome'. *Mol Microbiol*. 54:1409-1421.

Purusharth, R.I., F. Klein, S. Sulthana, S. Jager, M.V. Jagannadham, E. Evguenieva-Hackenberg, M.K. Ray, and G. Klug. 2005. Exoribonuclease R interacts with endoribonuclease E and an RNA helicase in the psychrotrophic bacterium Pseudomonas syringae Lz4W. *J Biol Chem*. 280:14572-14578.

Py, B., C.F. Higgins, H.M. Krisch, and A.J. Carpousis. 1996. A DEAD-box RNA helicase in the Escherichia coli RNA degradosome. *Nature*. 381:169-172.

Ramirez-Pena, E., J. Trevino, Z. Liu, N. Perez, and P. Sumby. 2010. The group A Streptococcus small regulatory RNA FasX enhances streptokinase activity by increasing the stability of the ska mRNA transcript. *Mol Microbiol*. 78:1332-1347.

Redko, Y., D.H. Bechhofer, and C. Condon. 2008. Mini-III, an unusual member of the RNase III family of enzymes, catalyses 23S ribosomal RNA maturation in B. subtilis. *Mol Microbiol*. 68:1096-1106.

Regnier, P., and M. Grunberg-Manago. 1990. RNase III cleavages in non-coding leaders of Escherichia coli transcripts control mRNA stability and genetic expression. *Biochimie*. 72:825-834.

Regnier, P., and C. Portier. 1986. Initiation, attenuation and RNase III processing of transcripts from the Escherichia coli operon encoding ribosomal protein S15 and polynucleotide phosphorylase. *J Mol Biol*. 187:23-32.

Richards, J., Q. Liu, O. Pellegrini, H. Celesnik, S. Yao, D.H. Bechhofer, C. Condon, and J.G. Belasco. 2011. An RNA pyrophosphohydrolase triggers 5'-exonucleolytic degradation of mRNA in Bacillus subtilis. *Mol Cell*. 43:940-949.

Robert-Le Meur, M., and C. Portier. 1992. E.coli polynucleotide phosphorylase expression is autoregulated through an RNase III-dependent mechanism. *EMBO J*. 11:2633-2641.

Robertson, H.D., R.E. Webster, and N.D. Zinder. 1968. Purification and properties of ribonuclease III from Escherichia coli. *J Biol Chem*. 243:82-91.

Santos, J.M., D. Drider, P.E. Marujo, P. Lopez, and C.M. Arraiano. 1997. Determinant role of E. coli RNase III in the decay of both specific and heterologous mRNAs. *FEMS Microbiol Lett*. 157:31-38.

Shahbabian, K., A. Jamalli, L. Zig, and H. Putzer. 2009. RNase Y, a novel endoribonuclease, initiates riboswitch turnover in Bacillus subtilis. *EMBO J*. 28:3523-3533.

Sim, S.H., J.H. Yeom, C. Shin, W.S. Song, E. Shin, H.M. Kim, C.J. Cha, S.H. Han, N.C. Ha, S.W. Kim, Y. Hahn, J. Bae, and K. Lee. 2010. Escherichia coli ribonuclease III activity is downregulated by osmotic stress: consequences for the degradation of bdm mRNA in biofilm formation. *Mol Microbiol*. 75:413-425.

Sousa, S., I. Marchand, and M. Dreyfus. 2001. Autoregulation allows Escherichia coli RNase E to adjust continuously its synthesis to that of its substrates. *Mol Microbiol*. 42:867-878.

Spickler, C., and G.A. Mackie. 2000. Action of RNase II and polynucleotide phosphorylase against RNAs containing stem-loops of defined structure. *J Bacteriol*. 182:2422-2427.

Stead, M.B., S. Marshburn, B.K. Mohanty, J. Mitra, L. Pena Castillo, D. Ray, H. van Bakel, T.R. Hughes, and S.R. Kushner. 2011. Analysis of Escherichia coli RNase E and RNase III activity in vivo using tiling microarrays. *Nucleic Acids Res*. 39:3188-3203.

Stickney, L.M., J.S. Hankins, X. Miao, and G.A. Mackie. 2005. Function of the conserved S1 and KH domains in polynucleotide phosphorylase. *J Bacteriol*. 187:7214-7221.

Storz, G., S. Altuvia, and K.M. Wassarman. 2005. An abundance of RNA regulators. *Annu Rev Biochem*. 74:199-217.

Taghbalout, A., and L. Rothfield. 2008. New insights into the cellular organization of the RNA processing and degradation machinery of Escherichia coli. *Mol Microbiol*. 70:780-782.

Taraseviciene, L., A. Miczak, and D. Apirion. 1991. The gene specifying RNase E (rne) and a gene affecting mRNA stability (ams) are the same gene. *Mol Microbiol*. 5:851-855.

Tetart, F., and J.P. Bouche. 1992. Regulation of the expression of the cell-cycle gene ftsZ by DicF antisense RNA. Division does not require a fixed number of FtsZ molecules. *Mol Microbiol*. 6:615-620.

Viegas, S.C., and C.M. Arraiano. 2008. Regulating the regulators: How ribonucleases dictate the rules in the control of small non-coding RNAs. *RNA Biol*. 5:230-243.

Viegas, S.C., I.J. Silva, M. Saramago, S. Domingues, and C.M. Arraiano. 2011. Regulation of the small regulatory RNA MicA by ribonuclease III: a target-dependent pathway. *Nucleic Acids Res*. 39:2918-2930.

Vincent, H.A., and M.P. Deutscher. 2006. Substrate recognition and catalysis by the exoribonuclease RNase R. *J Biol Chem*. 281:29769-29775.

Vogel, J., L. Argaman, E.G. Wagner, and S. Altuvia. 2004. The small RNA IstR inhibits synthesis of an SOS-induced toxic peptide. *Curr Biol*. 14:2271-2276.

Wagner, E.G., and K. Flardh. 2002. Antisense RNAs everywhere? *Trends Genet*. 18:223-226.

Wang, W., and D.H. Bechhofer. 1997. Bacillus subtilis RNase III gene: cloning, function of the gene in Escherichia coli, and construction of Bacillus subtilis strains with altered rnc loci. *J Bacteriol*. 179:7379-7385.

Waters, L.S., and G. Storz. 2009. Regulatory RNAs in bacteria. *Cell*. 136:615-628.

Yao, S., J.B. Blaustein, and D.H. Bechhofer. 2007. Processing of Bacillus subtilis small cytoplasmic RNA: evidence for an additional endonuclease cleavage site. *Nucleic Acids Res*. 35:4464-4473.

Zhang, K., and A.W. Nicholson. 1997. Regulation of ribonuclease III processing by double-helical sequence antideterminants. *Proc Natl Acad Sci U S A*. 94:13437-13441.

Chapter 2

CHARACTERIZATION OF THE BIOCHEMICAL PROPERTIES OF CAMPYLOBACTER JEJUNI RNASE III

This chapter contains data published in:

Haddad N*, **Saramago M***, Matos RG, Prévost H and Arraiano CM (2013). Characterization of the biochemical properties of *Campylobacter jejuni* RNase III. Accepted in Bioscience Reports.

*These authors contributed equally to this work

The author of this Dissertation had a major contribution in the work described in this chapter, both in the planning of the experimental work and in the performance of the experiments.

ABSTRACT

Campylobacter jejuni is a foodborne bacterial pathogen, which is now considered as a leading cause of human bacterial gastroenteritis. The information regarding ribonucleases in *C. jejuni* is very scarce but there are hints that they can be instrumental in virulence mechanisms. Namely, polynucleotide phosphorylase (PNPase) was shown to allow survival of *C. jejuni* in refrigerated conditions, to facilitate bacterial swimming, cell adhesion, colonization and invasion. In several microorganisms PNPase synthesis is auto controlled in an RNase III-dependent mechanism. Thereby, we have cloned, overexpressed, purified and characterize *C. jejuni* RNase III (*Cj*-RNase III). We have demonstrated that *Cj*-RNase III is able to complement an *Escherichia coli rnc* deficient strain in 30S rRNA processing and PNPase regulation. *Cj*-RNase III was shown to be active in an unexpectedly large range of conditions, and Mn^{2+} seems to be its preferred co-factor, contrarily to what was described for other RNase III orthologues. The results lead us to speculate that *Cj*-RNase III may have an important role under a Mn^{2+}-rich environment. Mutational analysis strengthened the function of some residues in the catalytic mechanism of action of RNase III, which was shown to be conserved.

Keywords: RNase III, *C. jejuni*, manganese, ribonuclease, catalytic activity

INTRODUCTION

Bacteria are able to rapidly adjust their physiology in order to survive in response to environmental demands. This adaptation is accompanied by a fast adjustment of the RNA levels. The cellular concentration of a given RNA is the result of the balance between its synthesis and degradation. RNA degradation involves the concerted action of ribonucleases. Changes in RNA turnover facilitate stress responses, growth phase transitions, and production of virulence factors (Saramago, 2013; Silva *et al.*, 2011; Viegas *et al.*, 2013).

Ribonuclease III (RNase III) family of enzymes is a highly conserved group of double-stranded (ds) RNA-specific endoribonucleases widely distributed among prokaryotic and eukaryotic organisms. In bacteria, RNase III has the ability to regulate its own synthesis with a specific cleavage near the 5'end of its mRNA. Moreover, it is also responsible for rRNA operon maturation, processing of cellular, phage, and plasmid RNAs, and decay of sRNA/mRNA complexes upon translational silencing (Arraiano *et al.*, 2010; Arraiano *et al.*, 2013; Silva *et al.*, 2011).

Bacterial RNase III is the simplest member of the family, containing an endonuclease domain (NucD), characterized by the presence of a set of highly conserved carboxylic acid residues essential for catalytic activity, and a dsRNA binding domain (dsRBD) (Figure 1C). In *E. coli*, this enzyme is encoded by the *rnc* gene and it is active as a 52 kDa homodimer (Arraiano *et al.*, 2010).

Important insights on structural features and mechanism of action of RNase III have been provided by crystallographic studies. Structural analysis of *Aquifex aeolicus* RNase III revealed a symmetric positioning of the two catalytic domains that form the dimer through hydrophobic interactions, and

demonstrated a positional mobility of the dsRBD (Blaszczyk *et al.*, 2001). A divalent metal ion is required for RNase III activity, with magnesium (Mg^{2+}) as the preferred co-factor. This homodimer uses a two metal mechanism of catalysis, with each active site containing two divalent cations during substrate hydrolysis (Meng and Nicholson, 2008). The structure of *Thermotoga maritime* together with the one from *A. aeolicus* provided the basis for a proposed pathway of dsRNA recognition and cleavage by the bacterial RNase III members (Gan *et al.*, 2008). Accordingly, RNase III can affect gene expression in two different ways. When the dsRNA is not bound to the catalytic valley, RNase III binds it without cleaving (Blaszczyk *et al.*, 2004). In this form RNase III can affect RNA structures and modulates gene expression (Dasgupta *et al.*, 1998; Oppenheim *et al.*, 1993). In addition, it can also function as a dsRNA-processing enzyme, cleaving both natural and synthetic dsRNA (Blaszczyk *et al.*, 2001). The RNase III cleavage originates 5′ phosphate and 3′ hydroxyl termini with a two base overhang at the 3′end (Blaszczyk *et al.*, 2001). In eukaryotes, homologues of this enzyme have a key role in RNA interference phenomenon that starts with a dsRNA cleavage (Arraiano *et al.*, 2010).

Campylobacter jejuni is a Gram negative microorganism, which remains as one of the major causes of human gastroenteritis worldwide (Ruiz-Palacios, 2007). The main reservoir of *C. jejuni* is the guts of avian species with up to 10^9 CFU/g in feces (Newell and Fearnley, 2003). Due to the spillage of intestinal content that contains a large number of the pathogen, *C. jejuni* can contaminate cooling water, knives and poultry meat during slaughter. Thus, the consumption of contaminated poultry is the major cause of campylobacteriosis, however, a diverse range of environmental sources are also all recognized causes of infection (Taylor *et al.*, 2013). Despite specific microaerobic growth requirements, *C. jejuni* is ubiquitous in the aerobic environment and is capable to face different stresses during transmission, including temperature changes, starvation, hypo- and

hyper-osmotic stress, and desiccation. Additionally, during human infection, *C. jejuni* has to withstand a further range of stresses, including changes in pH and the host innate immune response (Murphy *et al*., 2006). Although major advances have been made in the understanding of *C. jejuni* pathobiology and physiology, many unanswered questions remain. A more complete understanding of the regulation of *C. jejuni* response mechanisms is required to facilitate appropriate intervention strategies in order to reduce *C. jejuni*-associated diseases (Pittman *et al*., 2007).

It was demonstrated by Haddad *et al*. (Haddad *et al*., 2009; Haddad *et al*., 2012) that the exoribonuclease polynucleotide phosphorylase (PNPase) is involved in low-temperature survival of *C. jejuni*, and that the lack of PNPase induces swimming limitation, chick colonization delay and decrease of cell adhesion/invasion ability. However, little is known regarding RNases in this pathogen. In *E. coli*, PNPase synthesis is autocontrolled at a post-transcriptional level in an RNase III-dependent mechanism (Jarrige *et al*., 2001; Robert-Le Meur and Portier, 1992). The functional and evolutionary conservation of the RNase III family in bacteria and higher organisms is indicative of their biological relevance.

We present here relevant information regarding functionality and biochemical properties of *C. jejuni* RNase III (*Cj*-RNase III). We show that this endoribonuclease is able to replace *E. coli* RNase III (*Ec*-RNase III) in the 30S processing and in the regulation of PNPase levels. We also demonstrate the dependence of *Cj*-RNase III catalytic activity on divalent metal ions, and its ability to cleave at different temperatures and pH values that mimic different physiological environments that *C. jejuni* may face. Finally, a biochemical analysis was assessed on *Cj*-RNase III mutants with substitutions on two conserved acidic residues in the nuclease domain.

EXPERIMENTAL PROCEDURES

Bacterial strains and culture conditions

The strains used in this study are listed in Table 1. *Campylobacter jejuni* 81-176 was routinely cultured on Karmali agar plates (Oxoid, Basingstoke Hampshire, England) or in brain heart infusion (BHI) broth (Merck, Molsheim, France). Cultures on plates and broth were incubated at 42°C for 48h and 24h, respectively, under a microaerophilic atmosphere in jars flushed with a gas mixture of 10% CO_2, 5% O_2, and 85% N_2. *E. coli* strains were cultivated overnight at 37°C in Luria-Bertani medium (Sigma, Steinheim, Germany). Growth medium was supplemented with ampicillin (100 μg/ml) when appropriate.

Construction of the plasmids expressing RNase III from C. jejuni

The *C. jejuni* 81-176 RNase III gene (*rnc*) (GenBank accession no. YP_001001278) was amplified from genomic DNA using the primers MO608 (5′-AATTCATATGCAAGGGAAAATGATGAAAAA-3′) and MO612 (5′-GTAGGATCCAATTTCAATCTCGTACCAAAGGTAT-3′) (Table 3) (NdeI and BamHI sites, respectively, are underlined). For *rnc* amplification by PCR, 1U of Phusion High-Fidelity DNA Polymerase (BioLabs, Evry, France) was used. The purified PCR product (734 pb) was cloned into the pGEM-T plasmid (Promega, Charbonnieres, France) to generate pGEMT-*rnc*. To overexpress the *Cj*-RNase III protein, the *rnc* gene double digested with NdeI and BamHI was subcloned from pGEMT-*rnc* into the pET19b expression vector previously digested with the same enzymes (Novagen, Merck). Plasmids and primers used are presented in Tables 2 and 3, respectively. The resultant pET19b-*rnc* was confirmed by DNA sequencing (Beckman Coulter Genomics).

Table 1- Strains used in this study

Strain	Antibiotic resistance	Reference	Genetic
E. coli DH5α	-	Invitrogen	*rec*A1 *end*A1
BL21(DE3) *rec*A*rnc*105	chloramphenicol	(Amarasinghe *et al.*, 2001)	*rec*A::Tn9Δ*rnc*105
E. coli MG1693	-	(Bachmann and Low, 1980)	thyA715
E. coli SK7622	kanamycin	(Babitzke *et al.*, 1993)	thyA715 Δ*rnc*
C. jejuni 81-176	-	(Korlath *et al.*, 1985)	-

Table 2- Plasmids used in this study

Plasmid	Antibiotic resistance	Reference	Comments
pGEM-T	ampicillin	Promega	Commercial vector
pET19b	ampicillin	Novagen	Commercial expression vector
pGEMT-*rnc*	ampicillin	this study	Encodes Cj-RNC
pET19b-*rnc*	ampicillin	this study	Encodes his-Cj-RNC
pET19b-*rnc*_D44A	ampicillin	this study	Encodes his-Cj-RNC_D44A mutant
pET19b-*rnc*_E116Q	ampicillin	this study	Encodes his-Cj-RNC_E116Q mutant
pET19b-*rnc*_E116D	ampicillin	this study	Encodes his-Cj-RNC_E116D mutant

Table 3- Primers used in this study

Primers	Sequence (5′ – 3′)	Restriction site
MO608	AATTCATATGCAAGGGAAAATGATGAAAAA	NdeI
MO612	GTAGGATCCAATTTCAATCTCGTACCAAAGGTAT	BamHI
Cjej_9	CATCACAGCAGCGGC	
Cjej_10	GCAGCCGGATCCTAT	
D44A_1	GGTgcaGCTGTGCTTG	Introduction of D44A mutation and PvuII site
D44A_2	CAAGCACAGCtgcACC	
E116Q_1	CAGAcGCGTTAGAtGCCAT	Introduction of E116Q mutation and MluI site
E116Q_2	ATGGCaTCTAACGCgTCTG	
E116D_1	CAGAcGCGTTAcAAGCCAT	Introduction of E116D mutation and MluI site
E116D_2	ATGGCTTgTAACGCgTCTG	

Construction of RNase III Mutants by Overlapping PCR

The point mutations D44A, E116Q and E116D were introduced into pET19b-*rnc* by overlapping PCR (Higuchi, 1990). The primers used are listed in Table 3 and base changes are indicated in small letters. All mutant constructs were confirmed by DNA sequencing at STAB Vida, Portugal.

Overexpressing and purification of recombinant wild-type RNase III and mutants from C. jejuni

The plasmids harbouring the histidine-tagged *Cj*-RNase III wild-type protein (pET19b-*rnc*) and the mutants (pET19b-*rnc*_D44A, pET19b-*rnc*_E116Q, pET19b-*rnc*_E116D) were transformed into *E. coli* BL21(DE3) *rec*A*rnc*105 strain ((Amarasinghe *et al.*, 2001), kindly provided by Prof. A. Nicholson) to allow the expression of the recombinant proteins. This derivative strain of BL21(DE3), carrying an RNase III mutation, was used since it blocks the regulation of *Cj*-RNase III by the endogenous *E. coli* homologue, resulting in a higher yield of the enzyme upon overexpression. Cells were grown at 37ºC in 100 ml LB medium supplemented with 100 μg/ml ampicillin to an optical density of 0.5 at 600 nm. At this point, protein expression was induced by addition of 0.5 mM IPTG and left to grow for 2h. Cells were pelleted by centrifugation and stored at -80ºC. Purification was performed by histidine affinity chromatography using HiTrap Chelating HP columns (GE Healthcare) and AKTA FPLC system (GE Healthcare) following a protocol previously described (Viegas *et al.*, 2011). The purity of the proteins was verified in a 12% SDS-PAGE gel followed by Coomassie blue staining. Proteins were quantified using the Bradford Method (Bradford, 1976) and 50% (v/v) glycerol was added to the final fractions prior storage at -20ºC.

Cross-linking of Cj-RNase III wild-type and mutants

In order to verify if RNase III wild-type and mutants are able to dimerize, the purified proteins were incubated with increasing concentrations of DSS (disuccinimidyl suberate). Cross-linking reaction was performed in a final volume of 10 μl, including 0.5 μg of purified protein, 10 mM Hepes pH 7.4, 250 mM NaCl, 0.1 mM EDTA, 0.1 mM DTT and increasing concentrations of DSS (1 to 20 μg). The reaction was performed at room temperature for 30 minutes and quenched by adding 1 μl of Tris-HCl 1M pH 7.5 and SDS loading buffer. The samples were boiled during five minutes and then analysed in a 12% SDS-PAGE gel.

In vitro transcription

A canonical substrate for RNase III, called R1.1, was constructed using a synthetic DNA template and a promoter oligonucleotide obtained by commercial source (StabVida) for *in vitro* transcription, using the method described by (Milligan *et al.*, 1987). Briefly, the DNA synthetic template (0.5 μM) and the promoter oligonucleotide (0.6 μM) were annealed in 10 mM of Tris-HCl pH 8.0 by heating for 5 min at 70ºC, following by incubation for 30 min, at 37ºC. *In vitro* transcription was carried out using 'Riboprobe *in vitro* Transcription System' (Promega) and T7 RNA polymerase with a molar excess of [^{32}P]-α-UTP over nonradioactive UTP. In order to remove DNA template, 1U of DNase (Promega) was added and incubated 30 min at 37°C. R1.1 transcript was purified by electrophoresis on an 8.3M urea/10% polyacrylamide gel. The gel slice was crushed and the RNA was eluted overnight at room temperature with elution buffer [3M ammonium acetate pH 5.2, 1mM EDTA, 2.5% (v/v) phenol pH 4.3]. The RNA was ethanol precipitated and resuspended in RNase free water. The yield of the labeled substrates (cpm/μl) was determined by scintillation counting.

RNase III activity assays

The activity assays were performed in a final volume of 50 µl containing the RNase III activity buffer (30 mM Tris-HCl pH 8, 160 mM NaCl, 10 mM $MgCl_2$ or $MnCl_2$, 0.1 mM DTT) and 100 000 cpm of substrate. As a control, prior to the beginning of each assay an aliquot was taken and was incubated until the end of the assay (without the enzyme). The reactions were started by the addition of the enzyme, and further incubated at the indicated temperature. Aliquots of 5 µl were withdrawn at the time-points indicated in the respective figures, and the reactions were stopped by the addition of formamide containing dye supplemented with 10 mM EDTA. RNase activity assays were carried out at various pH values (pH 5.2, 5.4, 6.1, and 7.3), at different temperatures (4°C, 30°C, 37°C and 42°C), and at different Mg^{2+} and Mn^{2+} concentrations (0.1, 1, 10, 50 and 100 mM). Reaction products were resolved in a 7M urea/15% polyacrylamide gel as indicated in the respective figure legends. Signals were visualized by PhosphorImaging and analyzed using ImageQuant software (Molecular Dynamics).

Analysis of rRNA pattern on agarose gels

E. coli MG1693 (wt) and SK7622 (Δ*rnc*) alone or carrying the plasmids pGEMT and pGEMT:*rnc* were grown at 37ºC in Luria-Bertani medium to an optical density of 0.5 at 600 nm. Cells were pelleted and stored at -80ºC. Total RNA was extracted following the protocol described in Stead *et al.* (Stead *et al.*, 2011). RNA was quantified on a Nanodrop 1000 machine (NanoDrop Technologies), and 15 µg of total RNA were visualized in a 1.5% agarose gel.

Western Blot

E. coli MG1693 (wt) and SK7622 (Δ*rnc*) alone or carrying the plasmids pGEMT and pGEMT:*rnc* were grown at 37ºC in Luria-Bertani medium to an

optical density of 0.5 at 600 nm. Cells were pelleted and lysed by addition of 200 µl of Bug Buster reagent (Merck Millipore). After 10 min of centrifugation at maximum speed, the soluble fraction was transferred to a new tube and protein concentration was measured. 30 ng of soluble protein were separated by SDS-PAGE and transferred to a nitrocellulose membrane (Hybond ECL, GE Healthcare) by electroblotting using the Trans-Blot SD semidry electrophoretic system (Bio-Rad). Membranes were probed with a 1:10000 dilution of anti-PNPase or anti-RNase R antibodies. ECL anti-rabbit IgG-conjugated horseradish peroxidase was used as the secondary reagent in a 1:10000 dilution. Immunodetection was conducted via a chemiluminescence reaction using Amersham ECL Western Blotting Detection Reagents (GE Healthcare).

Sequence alignment and construction of the phylogenetic tree

RNase III sequences of *Escherichia coli*, *Salmonella enterica*, *Pseudomonas aeruginosa*, *Coxiella burnetii*, *Rhodobacter capsulatus*, *Lactococcus lactis*, *Staphylococcus aureus*, *Streptomyces coelicolor*, *Campylobacter jejuni* and *Helicobacter pylori* were aligned using Clustal W2 (http://www.ebi.ac.uk/Tools/msa/clustalw2/) (Larkin *et al.*, 2007). The phylogenetic tree was built using Phylogeny.fr (www.phylogeny.fr) (Dereeper *et al.*, 2010).

RESULTS AND DISCUSSION

Analysis of C. jejuni RNase III features

RNase III is a specific double-stranded RNA endoribonuclease widely conserved in prokaryotes and eukaryotes. The amino acid alignment of the putative *Cj*-RNase III with 9 different RNase III orthologs from Gram negative and Gram positive microorganisms reveals high conservation (Figure 1A). Indeed, *Cj*-RNase III exhibits the highly conserved amino acid stretch (NERLEFLGDS) in the catalytic domain like in all RNase III members already documented (Figure 1A, C) (Arraiano *et al.*, 2010). Furthermore, in Figure 1B, the phylogenetic tree demonstrates that the sequences can be divided into two groups, which reflects well the phylogenetic relationships of RNase III between the corresponding bacteria. *Cj*-RNase III is located in a different group than *E. coli* and *S. enterica* RNase III. Among the 9 microorganisms analyzed, the highest similarity is observed with the *H. pylori* counterpart (48% identity).

A
B
C
D
Escherichia coli
Salmonella enterica
Pseudomonas aeruginosa
Coxiella burnetii
Rhodobacter capsulatus
Lactococcus lactis
Staphylococcus aureus
Streptomyces coelicolor
Campylobacter jejuni
Helicobacter pylori
0.96
0.67
0.89
0.84
0.85
0.84
0.16
0.97
N-terminal
NucD
dsRBD
C-terminal
1
152 (151)
226 (224)
HNERLEFLGDS
M 0 1µg 5µg 10µg 20µg DSS
50 KDa
25 KDa

Figure 1- *C. jejuni* RNase III protein features (a) Sequence alignment of RNase III from *E. coli*, *S. enterica*, *P. aeruginosa*, *C. burnetii*, *R. capsulatus*, *S. coelicolor*, *C. jejuni*, *H. pylori*, *S. aureus and L. lactis*. Fully conserved residues are in bold, and the signature sequence of these proteins is highlighted. **(b)** Phylogenetic tree of RNase III from the species considered in (a). **(c)** Schematic representation of the domain organization of RNase III, showing the catalytic domain (NucD) (residues 1 to 151 in *E. coli* protein and 1 to 150 in *C. jejuni* protein) and the dsRNA binding domain (residues 152 to 226 in *E. coli* protein and 151 to 224 in *C. jejuni* protein). The signature sequence present in the catalytic domain is emphasized. **(d)** Cross-linking of RNase III from *C. jejuni* using DSS. 0.5 μg of protein was incubated with increasing concentrations of DSS as indicated in the figure. Proteins were visualized by Coomassie blue staining.

Cj-RNase III is a dimeric protein

In order to characterize the activity of *Cj*-RNase III, we cloned the *rnc* gene in an expression vector and overexpressed the protein in an *E. coli* BL21(DE3) *rec*A*rnc*105 strain. *Ec*-RNase III is able to regulate its own synthesis by cleaving near the 5'end of its own message (Matsunaga *et al.*, 1996). The *rnc*105 mutation changes the highly conserved Gly44 residue in the catalytic domain to aspartic acid abolishing RNase III activity, whereas the *rec*A inactivation increases the stability of the recombinant plasmid. Thus, the *E. coli* BL21(DE3) *rec*A*rnc*105 strain allowed us to have higher levels of *Cj*-RNase III expression when compared to the wild-type strain, by preventing the cleavage of the overexpressed RNase III.

RNase III family members function as a homodimer (Li and Nicholson, 1996). To examine whether *Cj*-RNase III acts like a homodimer we performed a cross-linking assay using the cross-linker disuccinimidyl suberate (DSS). The protein was incubated with different amounts of DSS and the reaction was observed in a 12% SDS page gel. DSS reacts with primary amino groups forming stable amide bonds. This will "fix" the protein interactions, allowing their identification. In figure 1D is possible to see the formation of a DSS-dependent specie which has two times the size of the monomeric form (~50 kDa). The result

is consistent with the formation of a dimer, which led us to conclude that *Cj*-RNase III also undergoes dimerization.

Functional complementation of Cj-RNase III in E. coli

RNase III is involved in the processing of 30S ribosomal RNA (rRNA). In the *E. coli* strain SK7622 that has a deletion in the *rnc* gene, is possible to detect the unprocessed 30S rRNA due to RNase III absence (Babitzke *et al.*, 1993) (Figure 2A). To see whether the *Cj*-RNase III was able to complement the loss of endogenous RNase III in *E. coli*, we have transformed the SK7622 (Δ*rnc*) strain with the plasmid pGEMT:*rnc* that carries the *rnc* gene from *C. jejuni* and analyzed the rRNA pattern. SK7622 does not express T7 RNA polymerase, and the expression of the *Cj*-RNase III is this strain is derived from the weak expression of the plasmid. The results obtained revealed that in the presence of pGEMT:*rnc* the 30S rRNA species is no longer observed (Figure 2A). We can then conclude that *Cj*-RNase III is able to functionally replace *E. coli* RNase III in the 30S processing and that this may be also its role in *C. jejuni*.

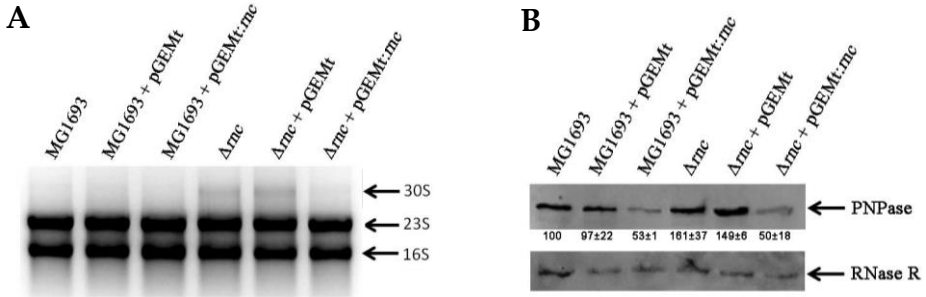

Figure 2- *E. coli* complementation by *Cj*-RNase III. (a) Processing of 30S rRNA. Total RNA was extracted from *E. coli* MG1693 (wt) and SK7622 (Δ*rnc*) empty or containing pGEMt and pGEMt:*rnc* plasmids, and analyzed in a 1.5% agarose gel. Bands were visualized by staining with ethidium bromide. The RNA species are indicated in the figure. This experiment was performed in quadruplicate. **(b)** PNPase regulation. Total soluble proteins were extracted from *E. coli* MG1693 (wt) and SK7622 (Δ*rnc*) empty or containing pGEMt and pGEMt:*rnc* plasmids, and 30ng of protein were applied in a SDS-Page gel. A Western blot was performed using anti-PNPase and anti-RNase R antibodies.

This experiment was performed in quadruplicate. PNPase levels were quantified and the values are indicated in the figure.

It is also known that RNase III is involved in the posttranscriptional control of *pnp* message, which codes for the exoribonuclease PNPase. Strains deficient in RNase III present higher levels of PNPase when compared to the wild-type (Portier *et al.*, 1987; Zilhao *et al.*, 1996). Since we showed that *Cj*-RNase III is able to complement an *E. coli* mutant at the level of 30S processing, we checked if the same is valid for PNPase regulation. For that purpose, we extracted total soluble proteins and performed a Western blot using anti-PNPase antibodies. By comparing the *E. coli* parental and mutant strains, we can see that the PNPase levels are ~1.5-fold higher in Δ*rnc* and Δ*rnc*+pGEMt strains (Figure 2B). The presence of pGEMT:*rnc* plasmid that harbors *Cj*-RNase III in both parental and mutant strains, causes a substantial decrease in PNPase levels due to the presence of higher levels of this protein (Figure 2B). As a control, we used antibodies against another ribonuclease, RNase R, which regulation does not involve RNase III. We can see that for RNase R there are no changes at the protein level (Figure 2B), indicating that the modifications observed for PNPase are specific. These complementation assays indicate that *Cj*-RNase III is efficient in the processing of *E. coli* rRNA and in the cleavage of *pnp* message, demonstrating that this enzyme is able to substitute its *E. coli* counterpart in rRNA processing and in the control of mRNA levels. This is an interesting result considering the phylogenetic distance between RNase III from *C. jejuni* and *E. coli* (Figure 1B). Similar results were previously obtained for the *Lactococcus lactis* RNase III (Amblar *et al.*, 2004), strengthening the high conservation of this family of enzymes.

Divalent metal ion dependence of Cj-RNase III catalytic activity

R1.1 RNA is a well-known 60 nucleotides (nt) substrate for *E. coli* RNase III, which contains a single primary cleavage site (Figure 3A, (a)) that is recognized *in vivo* and *in vitro*, and a secondary site (Figure 3A, (b)) that is cleaved only under specific conditions (Gross and Dunn, 1987). This canonical substrate was used to check the activity of *Cj*-RNase III purified in this work. It is known that the cleavage of dsRNA by RNase III is dependent of divalent cations (Gan *et al.*, 2008). *E. coli* RNase III (*Ec*-RNase III) can use different divalent ions with Mg^{2+} as the preferred co-factor (Li *et al.*, 1993). A cleavage assay using Mg^{2+} is shown in Figure 3B, which reveals that *Cj*-RNase III is catalytically active and cleaves R1.1.

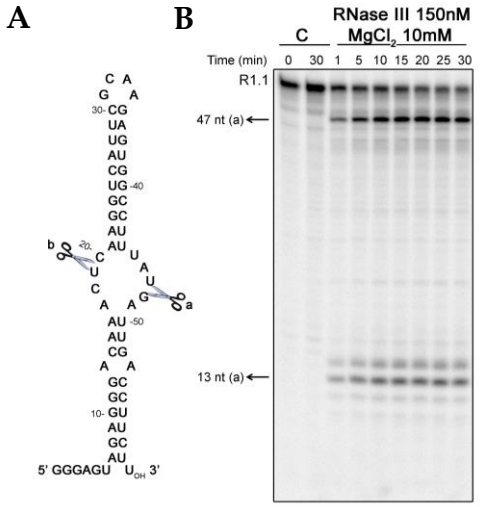

Figure 3- Substrate cleavage *in vitro* by *Cj*-RNase III (a) Sequence and secondary structure of R1.1 RNA substrate. The cleavage sites are indicated. **(b)** *In vitro* cleavage of R1.1 RNA by RNase III from *C. jejuni*. The activity assay was performed at 37ºC as described in Experimental section using Mg^{2+} as co-factor. Protein concentration is indicated in the figure. Samples were taken during the reaction at the time points indicated and reaction products were analyzed in a 15% polyacrylamide/7M urea gel. Control reactions with no enzyme added were incubated at the maximum reaction time. Length of substrates and degradation products are indicated. These experiments were performed at least in triplicate.

We also tested the activity of *Cj*-RNase III in the presence of other two divalent ions, manganese (Mn^{2+}), and calcium (Ca^{2+}). It was described that Mn^{2+} is also able to support catalysis, while Ca^{2+} functions as an inhibitor (Li and Nicholson, 1996; Li *et al.*, 1993). As expected, Ca^{2+} at 10 mM does not support *Cj*-RNase III catalysis, but Mn^{2+} does (Figure 4A). However, the RNA cleavage pattern is different according to the divalent ion used. With Mg^{2+}, RNase III cleaves R1.1 into two major products (47 nt and 13 nt) resulting from cleavage in the primary site (a) (Figure 3A), and a fraction of the substrate is not digested (Figures 3 and 4). When higher amount of enzyme is used (1200 nM) and the reaction occurs for longer periods of time (2h), we can observe that cleavage at the secondary site (b) can also occur (data not shown). However, in the presence of 10 mM of Mn^{2+} it is possible to observe immediately the formation of the four degradation products (47 nt, 28 nt, 19 nt and 13 nt), which results from cleavage at both sites (a and b) (Figure 4A).

We have quantified the amount of substrate present at each time point of the reaction with Mg^{2+} and Mn^{2+} at the same concentration and using the same amount of protein. The graphic in Figure 4B shows that, after one minute of reaction, *Cj*-RNase III degraded > 95% of the substrate in the presence of 10 mM of Mn^{2+}, while only ~35% is degraded in the presence of 10 mM of Mg^{2+}. Moreover, in those conditions, the degradation obtained in the presence of Mg^{2+} did not reach more than 70% during the 30 minutes of reaction (Figure 4B). We also quantified the degradation products of the reaction in both conditions. In the presence of Mg^{2+} we can observe the formation of the 47 nt and 13 nt fragments resulting of cleavage in (a) site (Figure 4C). In the presence of Mn^{2+}, we see a decreased in the 47 nt fragment and an increased in the 28 nt, which results at cleavage at (b) site, while the 13 nt remains constant (Figure 4D). These results

support the conclusion that cleavage at (b) site is only promoted in the presence of Mn^{2+}.

A

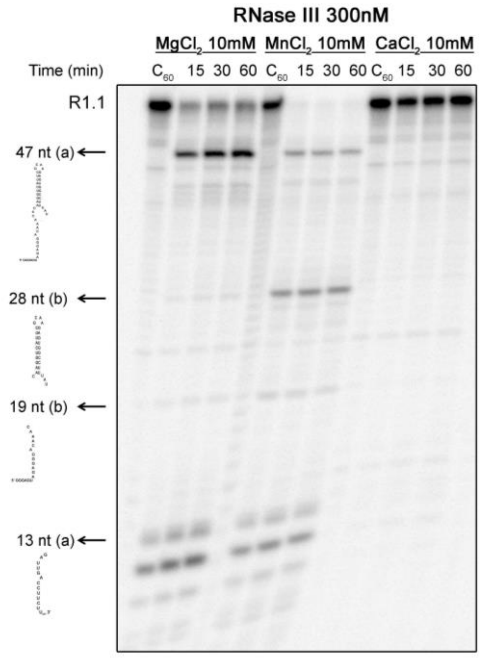

B

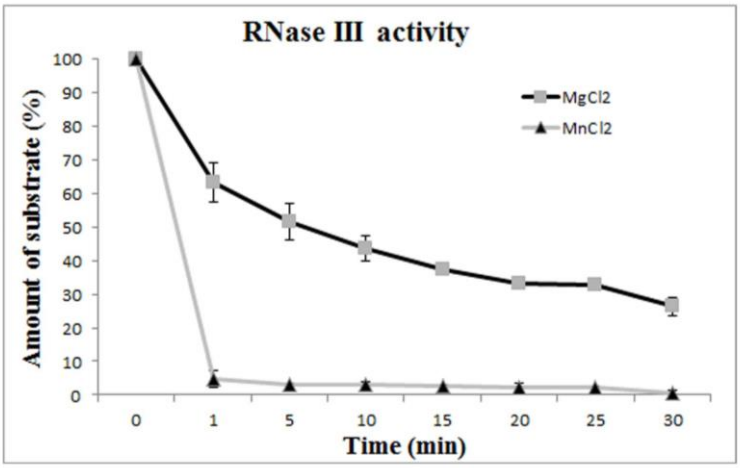

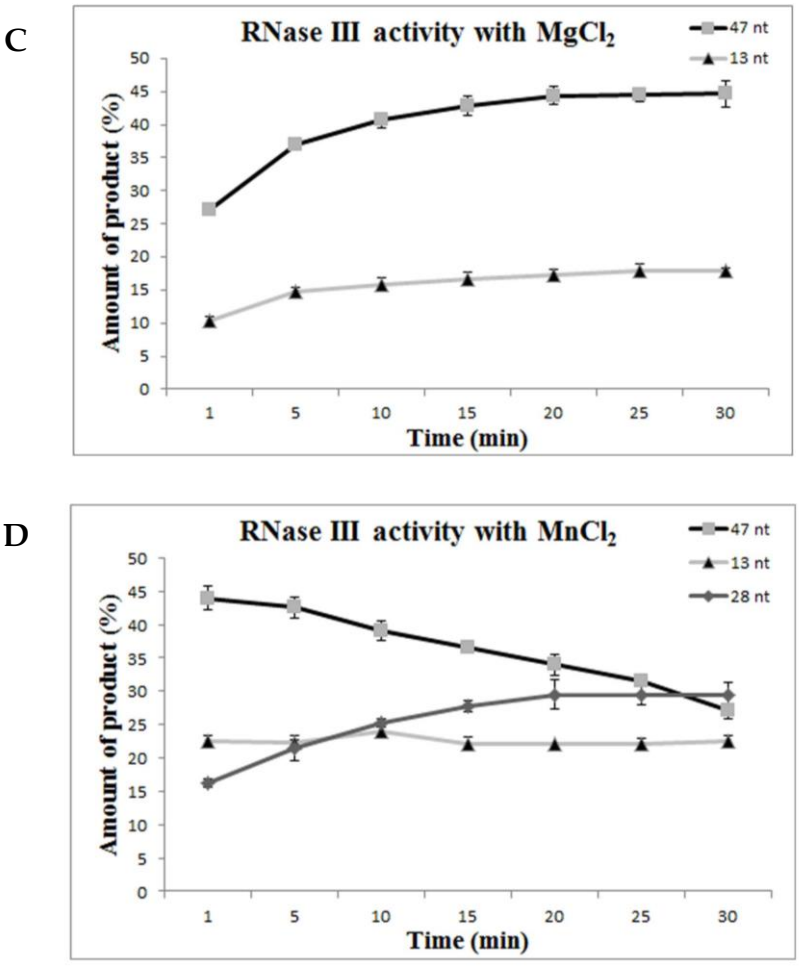

Figure 4- *Cj*-RNase III activity with different divalent ions. (a) 300 nM of recombinant protein were incubated with 10000 cpm of R1.1 substrate at 37ºC in a reaction buffer with $MgCl_2$, $MnCl_2$, and $CaCl_2$. This experiment was performed at least in triplicate. **(b)** Determination of the amount of substrate degraded in the presence of 300 nM of *Cj*-RNase III with $MgCl_2$ and $MnCl_2$. **(c)** Determination of the amount of degradation products (47 nt and 13 nt) in the presence of $MgCl_2$. **(d)** Determination of the amount of degradation products (47 nt, 28 nt and 13 nt) in the presence of $MnCl_2$.

In *E. coli*, it is known that Mn^{2+} can support catalysis when used in a concentration range of 0.1-1 mM. For higher concentrations (> 5mM), Mn^{2+} was shown to have an inhibitory effect (Li *et al.*, 1993). In addition, *Ec*-RNase III cleaves R1.1 substrate with the same efficiency at the optimal concentrations of Mg^{2+} and Mn^{2+} (Sun *et al.*, 2001). Thus, we decided to test the activity of *Cj*-RNase III in a broad range of Mg^{2+} and Mn^{2+} concentrations from 0.1 mM to 100 mM. The results presented in Figure 5 indicate that this protein is active over a wide range of Mg^{2+} concentrations. However, it seems to prefer values in the order of 10 to 50 mM (Figure 5A) since we can observe higher consumption of the substrate. Moreover, in the presence of Mn^{2+} the protein is most active between 1 and 10 mM (Figure 5B). When higher concentrations are used (above 20 mM), the reaction is inhibited. Overall, our experiments show that in contrary to what was reported for *E. coli* RNase III, the Mn^{2+} seems to be the preferred co-factor of *Cj*-RNase III. Also, Mn^{2+} shows to have an inhibitory effect when increased concentrations are used, however the enzyme supports a higher concentration of this metal ion when compared to *E. coli* counterpart.

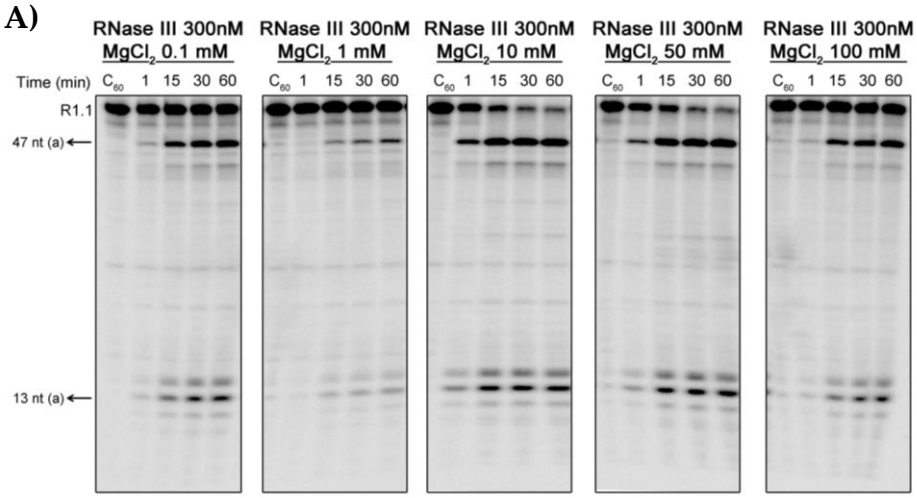

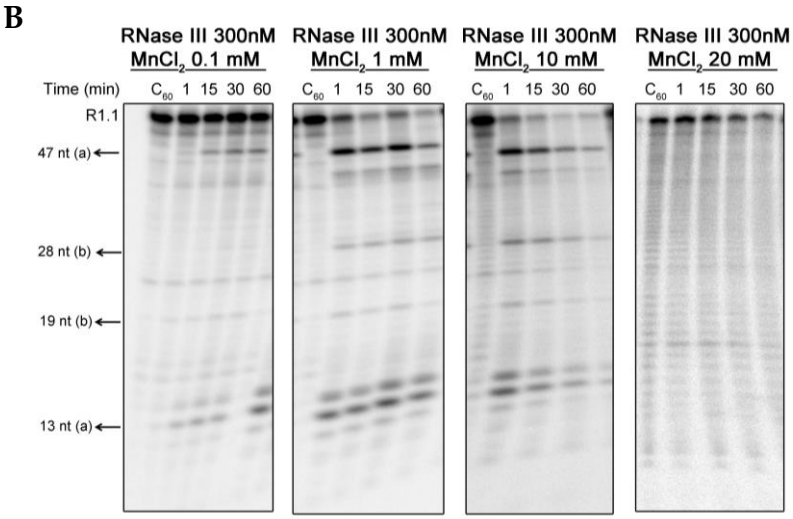

Figure 5- *Cj*-RNase III activity with different concentrations of divalent ions. 300 nM of recombinant protein were incubated with 10000 cpm of R1.1 substrate at 37ºC in a reaction buffer with different $MgCl_2$ **(a)** or $MnCl_2$ **(b)** concentrations, ranging from 0.1 to 100 mM. These experiments were performed at least in triplicate.

Our study strengthen the idea that Mn^{2+} and Mg^{2+} ions are responsible to control or adapt ribonuclease activity. Very interestingly, a recent study suggests that RNase HII from *Pyrococcus furiosus* digests dsRNA in the presence of Mn^{2+} ions, whereas there is no dsRNA digestion activity using Mg^{2+} in the reaction (Kitamura *et al.*, 2010).

The maintenance of metal homeostasis is essential for proper functioning of the cell, and has significant implications for microbial adaptations in changing environments. Bacteria have evolved several mechanisms to acquire metals and to sustain growth in environments with limited amounts of free trace metals (Kovacs-Simon *et al.*, 2011). Manganese is an example of a cofactor that could replace the role of Mg^{2+} in certain proteins that has emerged as a very important metal in virulence (Papp-Wallace and Maguire, 2006). It is known that macrophages have a poor magnesium, acidic, and low oxygen environment

(Papp-Wallace and Maguire, 2006). Curiously, divalent manganese is thermodynamically favored in acidic environments and in the absence of oxygen. *Campylobacter* is able to survive within macrophages for a period of 24h to 30h. It is within the macrophages that Mn^{2+} homeostasis is thought to be important for *C. jejuni*, however the specific cellular role of this metal is not yet established (Pogacar *et al*., 2010). It raises the question if a possible shift of the metal cofactor could be related with an adaptation of the enzyme activities to new conditions. The results obtained in this work lead us to speculate that *Cj*-RNase III may have an important role under a Mn^{2+}-rich environment, namely during invasion and infection.

pH dependence and thermostability of Cj-RNase III catalytic activity

C. jejuni faces different pH values during the infection process, and is able to survive during the passage from food or water source into the host gastrointestinal tract. Thus, this pathogen is prepared to sense and respond to a rapid decrease of pH (normally below the threshold for growth) (Reid *et al*., 2008). It is known that the pH of a human stomach depends on physiological variables. Following transit through the stomach, bacteria encounter a variety of environments within the intestine, ranging from mildly acidic (pH 5.5) to moderately alkaline (pH 7.4) (Holzer, 2007; Rao *et al*., 2004). Taking this into account, we have tested the activity of *Cj*-RNase III at different pH values between 5.2 and 7.3, in the presence of 10 mM Mg^{2+} or Mn^{2+}. As showed in Figures 6, *Cj*-RNase III is active in all pH tested, and it seems that the protein was efficient in cleaving R1.1 RNA even in the mildly acidic comparing with the standard conditions (Figure 3).

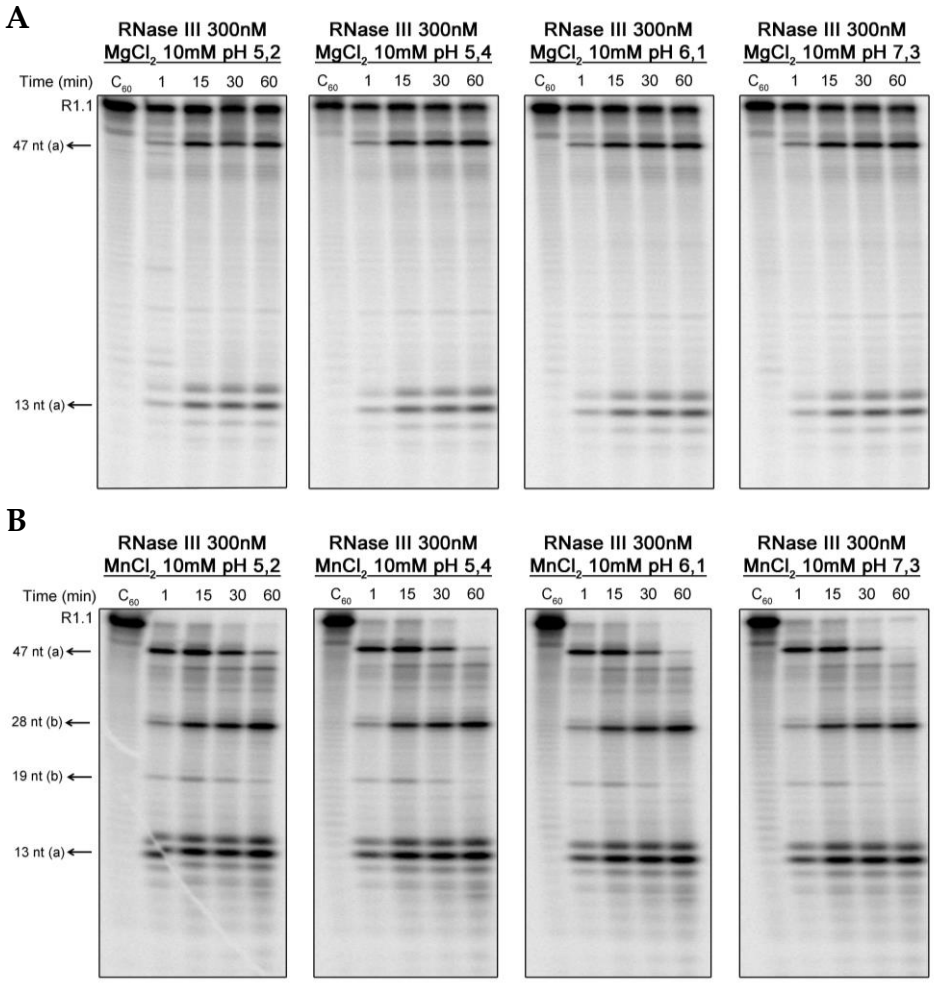

Figure 6- *Cj*-RNase III activity using different pH values. 300 nM of recombinant protein were incubated with 10000 cpm of R1.1 substrate at 37ºC in a reaction buffer with $MgCl_2$ **(a)** or $MnCl_2$ **(b)** and different pH, ranging from 5.2 to 7.3. These experiments were performed at least in triplicate.

Differences of temperature constitute another key factor during *C. jejuni* survival. Although this microorganism is able to grow at 37ºC, its optimal temperature is around 42ºC, the avian body temperature (Lee *et al.*, 1998). Moreover, it has the potential to survive under refrigerated temperatures (Chan *et al.*, 2001). The ability of *C. jejuni* to survive refrigeration is of major interest to

food safety and public health, since it is a typically intervention used in the control of bacterial growth in food. For this reason, we decided to analyze the activity of *Cj*-RNase III at different temperatures: 4ºC, 30ºC, 37ºC and 42ºC. The results obtained show that *Cj*-RNase III is active in an unexpectedly large range of temperatures from 4ºC to 42ºC (Figure 7).

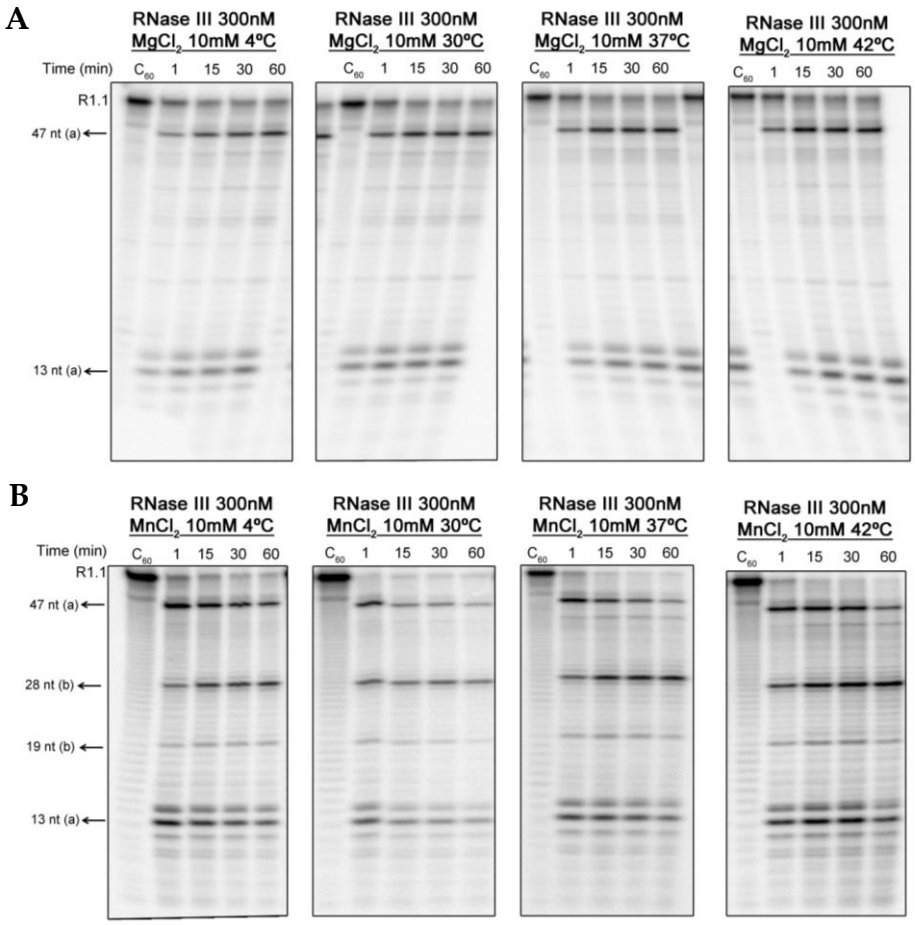

Figure 7- *Cj*-RNase III activity at different temperatures. 300 nM of recombinant protein were incubated with 10000 cpm of R1.1 substrate at 4, 30, 37 and 42 ºC in a reaction buffer with $MgCl_2$ **(a)** or $MnCl_2$ **(b)**. These experiments were performed at least in triplicate.

Altogether, these experiments showed that *Cj*-RNase III is active in a wide range of conditions. The pH tolerance of *Cj*-RNase III and its capability to cleave over different temperatures, including 4ºC could be indicative of a possible role of RNase III during the acid shock and temperature response of *Campylobacter* during the infection process.

Analysis of the effect of point mutations in the activity of Cj-RNase III in the presence of Mg^{2+} and Mn^{2+}

Structural advances combined with directed mutagenesis provide powerful tools to uncover important issues of RNase III catalytic activity. RNase III orthologues have eight highly conserved aspartate (D) and glutamate (E) residues in the catalytic domain (E38, E41, D45, E65, E100, D114, E117 and D126 in *E. coli*), which were suggested to have an important role in activity. In *E. coli* the metal binding is coordinated by four of these residues: E41 and D45 that belong to the signature box (NERLEFLGDS), and D114 and E117 (Blaszczyk *et al.*, 2001). Substitution of D45 for an alanine (*Ec*-D45A) had a severe impact on the catalytic function of *Ec*-RNase III both *in vitro* (Sun *et al.*, 2004) and *in vivo* (Blaszczyk *et al.*, 2001). The replacement of E117 by an alanine or lysine also blocked the phosphodiester hydrolysis, and was also reported to suppress RNase III activity *in vivo* (Li and Nicholson, 1996). Additionally, two other substitutions of E117 residue were performed, in which this amino acid was substituted for an aspartic acid (*Ec*-E117D) and for a glutamine (*Ec*-E117Q) (Sun *et al.*, 2001). The introduction of these mutations in *Ec*-RNase III induced minimal structural changes but affected the activity of the enzyme in the presence of Mg^{2+}. Curiously, the presence of Mn^{2+} in the reaction rescued the activity of the *Ec*-D45A and *Ec*-E117D mutant (Sun *et al.*, 2001; Sun *et al.*, 2004). Considering the importance that Mn^{2+} plays in the activity of *Cj*-RNase III, we decided to alter the equivalent E117 in *C. jejuni* protein (*Cj*-E116) for aspartic acid and glutamine and see the effect of

these mutations in the activity of the enzyme. We also substituted the equivalent residue D45 (*Cj*-D44) for an alanine and checked its effect on catalysis.

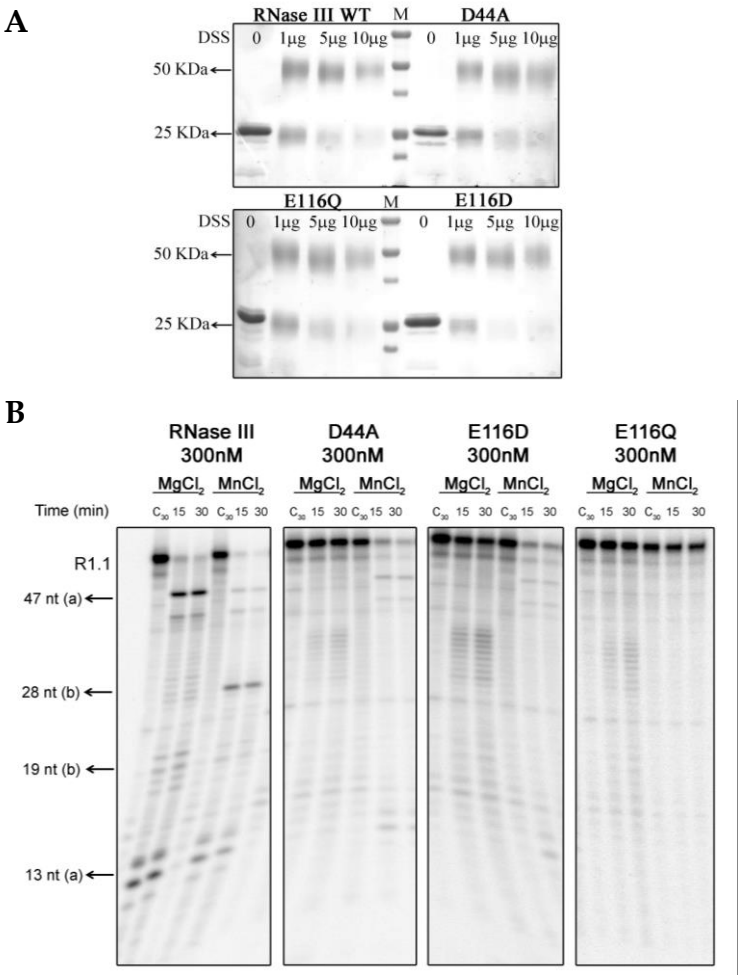

Figure 8. Characterization of *Cj*-RNase III mutants. **(a)** Cross-linking of RNase III mutants from *C. jejuni* using DSS. 0.5 µg of protein was incubated with increasing concentrations of DSS as indicated in the figure. Proteins were visualized by Coomassie blue staining. **(b)** *Cj*-RNase III mutants activity in the presence of Mg^{2+} and Mn^{2+}. 300 nM of protein were incubated with 10000 cpm of R1.1 substrate at 37ºC in a reaction buffer with $MgCl_2$ or $MnCl_2$. These experiments were performed at least in triplicate.

As already mentioned, in order to be active, the nuclease domains of RNase III undergoes dimerization. After purification of the mutant proteins, their

ability to form dimers was tested by incubation the DSS cross-linker. The mutants exhibited normal homodimeric behavior, comparable to the wild-type protein (Figure 8A).

We also analyzed the capacity of the mutant proteins to support catalysis. For this purpose, we tested the activity of the enzymes in the conditions where the wt *Cj*-RNase III carries out efficient degradation of the RNA substrate, in the presence of Mg^{2+} or Mn^{2+}. Using Mg^{2+} as cofactor, the results reveal that the mutants do not cleave efficiently R1.1 RNA (Figure 8B). However, for the three mutants, it is possible to observe a residual activity. The same was verified for the equivalent mutants in *E. coli* when extended reaction times and high enzyme concentrations were used (Sun *et al.*, 2001; Sun *et al.*, 2004). These data suggest a conservation of the role of these residues in the catalytic mechanism of action of RNase III.

Regarding the use of Mn^{2+} in the reactions, we have shown that this metal ion was able to rescue the activity of *Cj*-D44A and *Cj*-E116D mutants. As previously discussed, in the presence of Mn^{2+}, the wt *Cj*-RNase III is able to recognize the secondary site (b) of R1.1 RNA (Figures 3 and 4). Nevertheless, *Cj*-D44A and *Cj*-E116D mutants are no longer able to cleave at this site (Figure 8B), even when higher amounts of protein are used (data not shown). When dsRNA is cleaved, two hydrolysis events occur at each active center of RNase III. Moreover, it is known that the residues D44 and E110 in *A. aeolicus* (D45 and E116 in *C. jejuni*, respectively) are responsible for a second RNA-cutting site (Blaszczyk *et al.*, 2001). This is in good agreement with the lost of *Cj*-D44A and *Cj*-E116D mutants to recognize and cleave the R1.1 substrate at the secondary site.

Regarding the *Cj*-E116Q mutant, we demonstrated that Mn^{2+} was not able to restore its catalytic activity (Figure 8B). Our findings are consistent with the weak affinity of the carboxamide group for divalent metal ions as previously

discussed by Sun and Nicholson, which explains the inability of Mg^{2+} and Mn^{2+} ions to restore the activity of this mutant (Sun *et al.*, 2001).

Overall, these results show that D44 and E116 residues are important for the catalytic activity of *Cj*-RNase III by providing a metal binding site, which is recognized by Mg^{2+} and Mn^{2+}. The mutants are not able to cleave in the presence of Mg^{2+}, but a different behavior is seen in the presence of Mn^{2+}. Moreover, our data strengthen that in fact RNase III family of enzymes contains a conserved mechanism of action.

In this paper we have undertaken a functional and biochemical analysis of *Cj*-RNase III. We demonstrated that *Cj*-RNase III is able to complement an *E. coli rnc* deficient strain in 30S rRNA processing and in regulation of PNPase levels. These observations reinforce the conservation of these functions in bacteria, since similar results were previously obtained for other microorganisms (Amblar *et al.*, 2004). We were also able to show that *Cj*-RNase III is active in a wide range of conditions. Such plasticity may be important for the adaptation of this pathogen to different conditions during infection. The data obtained lead us to speculate that *Cj*-RNase III may have an important role under a Mn^{2+}-rich environment, contrarily to the consensus that Mg^{2+} is the physiologic relevant cofactor for RNase III orthologues.

PNPase has an impact on cell biology of *C. jejuni*, namely in survival at refrigerated conditions, bacterial swimming, colonization, cell adhesion and invasion. Moreover, its levels are controlled in an RNase III-dependent manner. Taking these into account, RNase III might be also a main player in the adaptation of this pathogen to environmental demands. Hence, it is crucial to better understand the mechanism of action of this endoribonuclease.

ACKNOWLEDGEMENTS

We want to thank Prof. Allen W. Nicholson for providing BL21 (DE3) *rnc*105 *rec*A strain. We also thank Andreia Aires for technical support in the lab.

FUNDING

RNA research in UMR1014 SECALIM was funded by the *Région* Pays de la Loire through the program grant GENICAMP. N. Haddad was supported by GENICAMP program and a PhD scholarship awarded by the Institut National de la Recherche Agronomique and Région des Pays de la Loire. Work at ITQB was supported by grants from Fundação para a Ciência e Tecnologia (FCT), including grant PEst-OE/EQB/LA0004/2011. M. Saramago was a recipient of Doctoral fellowship (SFRH/BD/65607/2009) and R.G. Matos was a recipient of a Post-Doctoral fellowship (SFRH/BPD/75887/2011), both funded by FCT.

REFERENCES

Amarasinghe, A.K., I. Calin-Jageman, A. Harmouch, W. Sun, and A.W. Nicholson. 2001. Escherichia coli ribonuclease III: affinity purification of hexahistidine-tagged enzyme and assays for substrate binding and cleavage. *Methods Enzymol*. 342:143-158.

Amblar, M., S.C. Viegas, P. Lopez, and C.M. Arraiano. 2004. Homologous and heterologous expression of RNase III from Lactococcus lactis. *Biochem Biophys Res Commun*. 323:884-890.

Arraiano, C.M., J.M. Andrade, S. Domingues, I.B. Guinote, M. Malecki, R.G. Matos, R.N. Moreira, V. Pobre, F.P. Reis, M. Saramago, I.J. Silva, and S.C. Viegas. 2010. The critical role of RNA processing and degradation in the control of gene expression. *FEMS Microbiol Rev*. 34:883-923.

Arraiano, C.M., F. Mauxion, S.C. Viegas, R.G. Matos, and B. Seraphin. 2013. Intracellular ribonucleases involved in transcript processing and decay: Precision tools for RNA. *Biochim Biophys Acta*.

Babitzke, P., L. Granger, J. Olszewski, and S.R. Kushner. 1993. Analysis of mRNA decay and rRNA processing in Escherichia coli multiple mutants carrying a deletion in RNase III. *J Bacteriol*. 175:229-239.

Bachmann, B.J., and K.B. Low. 1980. Linkage map of Escherichia coli K-12, edition 6. *Microbiol Rev*. 44:1-56.

Blaszczyk, J., J. Gan, J.E. Tropea, D.L. Court, D.S. Waugh, and X. Ji. 2004. Noncatalytic assembly of ribonuclease III with double-stranded RNA. *Structure*. 12:457-466.

Blaszczyk, J., J.E. Tropea, M. Bubunenko, K.M. Routzahn, D.S. Waugh, D.L. Court, and X. Ji. 2001. Crystallographic and modeling studies of RNase III suggest a mechanism for double-stranded RNA cleavage. *Structure*. 9:1225-1236.

Bradford, M.M. 1976. A rapid and sensitive method for the quantitation of microgram quantities of protein utilizing the principle of protein-dye binding. *Anal Biochem*. 72:248-254.

Chan, K.F., H. Le Tran, R.Y. Kanenaka, and S. Kathariou. 2001. Survival of clinical and poultry-derived isolates of Campylobacter jejuni at a low temperature (4 degrees C). *Appl Environ Microbiol*. 67:4186-4191.

Dasgupta, S., L. Fernandez, L. Kameyama, T. Inada, Y. Nakamura, A. Pappas, and D.L. Court. 1998. Genetic uncoupling of the dsRNA-binding and RNA cleavage activities of the Escherichia coli endoribonuclease RNase III--the effect of dsRNA binding on gene expression. *Mol Microbiol*. 28:629-640.

Dereeper, A., S. Audic, J.M. Claverie, and G. Blanc. 2010. BLAST-EXPLORER helps you building datasets for phylogenetic analysis. *BMC Evol Biol*. 10:8.

Gan, J., G. Shaw, J.E. Tropea, D.S. Waugh, D.L. Court, and X. Ji. 2008. A stepwise model for double-stranded RNA processing by ribonuclease III. *Mol Microbiol*. 67:143-154.

Gross, G., and J.J. Dunn. 1987. Structure of secondary cleavage sites of E. coli RNAaseIII in A3t RNA from bacteriophage T7. *Nucleic Acids Res*. 15:431-442.

Haddad, N., C.M. Burns, J.M. Bolla, H. Prevost, M. Federighi, D. Drider, and J.M. Cappelier. 2009. Long-term survival of Campylobacter jejuni at low temperatures is dependent on polynucleotide phosphorylase activity. *Appl Environ Microbiol*. 75:7310-7318.

Haddad, N., O. Tresse, K. Rivoal, D. Chevret, Q. Nonglaton, C.M. Burns, H. Prevost, and J.M. Cappelier. 2012. Polynucleotide phosphorylase has an impact on cell biology of Campylobacter jejuni. *Front Cell Infect Microbiol*. 2:30.

Higuchi, R. 1990. Recombinant PCR. . *In* PCR protocols: A guide to methods and applications. M.A. Innis, D.H. Gelfand, J.J. Sninsky, and T.J. White, editors. Academic Press, San Diego. 171–183.

Holzer, P. 2007. Taste receptors in the gastrointestinal tract. V. Acid sensing in the gastrointestinal tract. *Am J Physiol Gastrointest Liver Physiol*. 292:G699-705.

Jarrige, A.C., N. Mathy, and C. Portier. 2001. PNPase autocontrols its expression by degrading a double-stranded structure in the pnp mRNA leader. *EMBO J*. 20:6845-6855.

Kitamura, S., K. Fujishima, A. Sato, D. Tsuchiya, M. Tomita, and A. Kanai. 2010. Characterization of RNase HII substrate recognition using RNase HII-argonaute chimaeric enzymes from Pyrococcus furiosus. *Biochem J*. 426:337-344.

Korlath, J.A., M.T. Osterholm, L.A. Judy, J.C. Forfang, and R.A. Robinson. 1985. A point-source outbreak of campylobacteriosis associated with consumption of raw milk. *J Infect Dis*. 152:592-596.

Kovacs-Simon, A., R.W. Titball, and S.L. Michell. 2011. Lipoproteins of bacterial pathogens. *Infect Immun*. 79:548-561.

Larkin, M.A., G. Blackshields, N.P. Brown, R. Chenna, P.A. McGettigan, H. McWilliam, F. Valentin, I.M. Wallace, A. Wilm, R. Lopez, J.D. Thompson, T.J. Gibson, and D.G. Higgins. 2007. Clustal W and Clustal X version 2.0. *Bioinformatics*. 23:2947-2948.

Lee, A., S.C. Smith, and P.J. Coloe. 1998. Survival and growth of Campylobacter jejuni after artificial inoculation onto chicken skin as a function of temperature and packaging conditions. *J Food Prot*. 61:1609-1614.

Li, H., and A.W. Nicholson. 1996. Defining the enzyme binding domain of a ribonuclease III processing signal. Ethylation interference and hydroxyl radical footprinting using catalytically inactive RNase III mutants. *EMBO J*. 15:1421-1433.

Li, H.L., B.S. Chelladurai, K. Zhang, and A.W. Nicholson. 1993. Ribonuclease III cleavage of a bacteriophage T7 processing signal. Divalent cation specificity, and specific anion effects. *Nucleic Acids Res*. 21:1919-1925.

Matsunaga, J., E.L. Simons, and R.W. Simons. 1996. RNase III autoregulation: structure and function of rncO, the posttranscriptional "operator". *RNA*. 2:1228-1240.

Meng, W., and A.W. Nicholson. 2008. Heterodimer-based analysis of subunit and domain contributions to double-stranded RNA processing by Escherichia coli RNase III in vitro. *Biochem J*. 410:39-48.

Milligan, J.F., D.R. Groebe, G.W. Witherell, and O.C. Uhlenbeck. 1987. Oligoribonucleotide synthesis using T7 RNA polymerase and synthetic DNA templates. *Nucleic Acids Res*. 15:8783-8798.

Murphy, C., C. Carroll, and K.N. Jordan. 2006. Environmental survival mechanisms of the foodborne pathogen Campylobacter jejuni. *J Appl Microbiol*. 100:623-632.

Newell, D.G., and C. Fearnley. 2003. Sources of Campylobacter colonization in broiler chickens. *Appl Environ Microbiol*. 69:4343-4351.

Oppenheim, A.B., D. Kornitzer, S. Altuvia, and D.L. Court. 1993. Posttranscriptional control of the lysogenic pathway in bacteriophage lambda. *Prog Nucleic Acid Res Mol Biol*. 46:37-49.

Papp-Wallace, K.M., and M.E. Maguire. 2006. Manganese transport and the role of manganese in virulence. *Annu Rev Microbiol*. 60:187-209.

Pittman, M.S., K.T. Elvers, L. Lee, M.A. Jones, R.K. Poole, S.F. Park, and D.J. Kelly. 2007. Growth of Campylobacter jejuni on nitrate and nitrite: electron transport to NapA and NrfA via NrfH and distinct roles for NrfA and the globin Cgb in protection against nitrosative stress. *Mol Microbiol*. 63:575-590.

Pogacar, M.S., A. Klancnik, S.S. Mozina, and A. Cencic. 2010. Attachment, invasion, and translocation of Campylobacter jejuni in pig small-intestinal epithelial cells. *Foodborne Pathog Dis*. 7:589-595.

Portier, C., L. Dondon, M. Grunberg-Manago, and P. Regnier. 1987. The first step in the functional inactivation of the Escherichia coli polynucleotide phosphorylase messenger is a ribonuclease III processing at the 5' end. *EMBO J*. 6:2165-2170.

Rao, K.A., E. Yazaki, D.F. Evans, and R. Carbon. 2004. Objective evaluation of small bowel and colonic transit time using pH telemetry in athletes with gastrointestinal symptoms. *Br J Sports Med*. 38:482-487.

Reid, A.N., R. Pandey, K. Palyada, H. Naikare, and A. Stintzi. 2008. Identification of Campylobacter jejuni genes involved in the response to acidic pH and stomach transit. *Appl Environ Microbiol*. 74:1583-1597.

Robert-Le Meur, M., and C. Portier. 1992. E.coli polynucleotide phosphorylase expression is autoregulated through an RNase III-dependent mechanism. *EMBO J*. 11:2633-2641.

Ruiz-Palacios, G.M. 2007. The health burden of Campylobacter infection and the impact of antimicrobial resistance: playing chicken. *Clin Infect Dis*. 44:701-703.

Saramago, M., Domingues, S., Viegas, SC and Arraiano C.M. 2013. Ribonucleases promote biofilm formation and antibiotic resistance in Salmonella Typhimurium. *Submitted in Appl Environ Microbiol*

Silva, I.J., M. Saramago, C. Dressaire, S. Domingues, S.C. Viegas, and C.M. Arraiano. 2011. Importance and key events of prokaryotic RNA decay: the ultimate fate of an RNA molecule. *Wiley Interdiscip Rev RNA*. 2:818-836.

Stead, M.B., S. Marshburn, B.K. Mohanty, J. Mitra, L. Pena Castillo, D. Ray, H. van Bakel, T.R. Hughes, and S.R. Kushner. 2011. Analysis of Escherichia coli RNase E and RNase III activity in vivo using tiling microarrays. *Nucleic Acids Res*. 39:3188-3203.

Sun, W., E. Jun, and A.W. Nicholson. 2001. Intrinsic double-stranded-RNA processing activity of Escherichia coli ribonuclease III lacking the dsRNA-binding domain. *Biochemistry*. 40:14976-14984.

Sun, W., G. Li, and A.W. Nicholson. 2004. Mutational analysis of the nuclease domain of Escherichia coli ribonuclease III. Identification of conserved acidic residues that are important for catalytic function in vitro. *Biochemistry*. 43:13054-13062.

Taylor, E.V., K.M. Herman, E.C. Ailes, C. Fitzgerald, J.S. Yoder, B.E. Mahon, and R.V. Tauxe. 2013. Common source outbreaks of Campylobacter infection in the USA, 1997-2008. *Epidemiol Infect*. 141:987-996.

Viegas, S.C., D. Mil-Homens, A.M. Fialho, and C.M. Arraiano. 2013. The Virulence of Salmonella enterica Serovar Typhimurium in the Insect Model Galleria mellonella Is Impaired by Mutations in RNase E and RNase III. *Appl Environ Microbiol*. 79:6124-6133.

Viegas, S.C., I.J. Silva, M. Saramago, S. Domingues, and C.M. Arraiano. 2011. Regulation of the small regulatory RNA MicA by ribonuclease III: a target-dependent pathway. *Nucleic Acids Res*. 39:2918-2930.

Zilhao, R., F. Cairrao, P. Regnier, and C.M. Arraiano. 1996. PNPase modulates RNase II expression in Escherichia coli: implications for mRNA decay and cell metabolism. *Mol Microbiol*. 20:1033-1042.

Chapter 3

THE IMPORTANCE OF ENDORIBONUCLEASES E AND III IN DIFFERENT CELLULAR PROCESSES IN SALMONELLA TYPHIMURIUM

This chapter contains data from:

Saramago M, Domingues S, Viegas SC and Arraiano CM. 2013. Biofilm formation and antibiotic resistance in *Salmonella* Typhimurium are affected by different ribonucleases. Accepted in J Microbiol Biotechnol.

Viegas SC*, Silva IJ*, **Saramago M**, Domingues S and Arraiano CM. 2011. Regulation of the small regulatory RNA MicA by ribonuclease III: a target-dependent pathway. Nucleic Acids Research: 39(7):2918-30.
*These authors contributed equally to this work

The author of this Dissertation had a major contribution on the work described in this chapter, both in the planning of the experimental work and in the performance of the experiments.

ABSTRACT

Salmonella infections are a serious medical and veterinary problem worldwide and there is an increasing need for new strategies for prevention and control. Additionally, there is increasing evidence that ribonucleases (RNases) have an important role on virulence mechanisms and in the adaptation of bacteria to environmental cues. Antibiotic resistance and biofilm formation are important determinants for bacterial pathogenicity. In this work, we have studied the influence of *Salmonella* ribonucleases on these two processes. Our data shows that endoribonucleases E and III affect susceptibility against ribosome-targeting antibiotics and biofilm development in *Salmonella*.

Small non-coding RNAs (sRNAs) also play very important roles in post-transcriptional control of gene expression. Through the control of the cellular levels of sRNAs, RNases ultimately control their functions. It was previously reported a large impact of *Salmonella* RNase E and RNase III mutant strains for on the levels and stability of a sRNA denoted MicA, which is known to control biofilm formation and the expression of outer membrane porins (OMPs). We intended to study more deeply the contribution of both endoribonucleases in the degradation of this sRNA. For this purpose we have purified *Salmonella* RNase III and RNase E and have demonstrated that *in vitro* RNase III is only active over MicA when in complex with its mRNA targets. On the other hand, RNase E is able to cleave unpaired MicA and does not show a marked dependence on its 5′ phosphorylation state. Our results demonstrate the existence of two independent pathways for MicA turnover. Each pathway involves a distinct endoribonuclease with a different role in the context of the fine-tuned regulation of porin levels. Cleavage of MicA by RNase III in a target-dependent fashion, with the concomitant decay of the mRNA target, strongly resembles the eukaryotic RNAi system, where RNase III-like enzymes play a pivotal role.

Overall, the data collected in this Chapter strengthen the importance of these two endoribonucleases on different cellular mechanisms of the pathogenic bacterium *Salmonella* Typhimurium.

INTRODUCTION

RNases, the enzymes that degrade RNA, are key factors in the control of important cellular processes since they determine the final levels of every transcript. Endoribonucleases cleave RNA internally, while exoribonucleases degrade the RNA molecule from one extremity. In *Escherichia coli* and *Salmonella*, the main endoribonucleases are RNase E and RNase III (Arraiano *et al.*, 2013; Silva *et al.*, 2011). RNase E is an essential endoribonuclease, which cleaves single stranded RNA. The C-terminus of RNase E includes binding sites for other proteins forming the degradosome, a multiprotein complex involved in RNA degradation. RNase III is an ubiquitous enzyme specific for double-stranded RNA. The main exoribonucleases are PNPase, RNase R and RNase II, which degrade RNA from the 3'-extremity (Arraiano *et al.*, 2010; Domingues *et al.*, 2009; Silva *et al.*, 2011). Some RNases are up-regulated under stress situations and have been reported to be involved in virulence processes in pathogenic organisms (reviewed in (Arraiano *et al.*, 2010; Arraiano *et al.*, 2013; Lawal *et al.*, 2011; Silva *et al.*, 2011)).

Salmonella infections constitute an important food safety problem throughout the world (Majowicz *et al.*, 2010). Development of bacterial resistance to antimicrobial drugs is an ever-increasing clinical problem and RNases could be potential novel targets for therapeutic intervention. As a response to environmental pressure bacteria can aggregate on abiotic and biotic surfaces forming biofilm. Biofilm development and antibiotic resistance are intimately connected, since the biofilm matrix can delay the penetration of antimicrobial agents (Heeb *et al.*, 2011; Mah and O'Toole, 2001; Stewart, 2002; Wei *et al.*, 2011). Biofilm formation is a highly regulated process that includes an array of key regulators including small non-coding RNAs (sRNAs) and RNases (Carzaniga *et al.*, 2012; Jorgensen *et al.*, 2012; Sim *et al.*, 2010; Viegas *et al.*, 2013). In this work,

Salmonella deficient in the main ribonucleases were tested against a panoply of antimicrobial agents representative of different antibiotic classes. We have also investigated wether ribonucleases affect biofilm properties. We showed that in particular, endoribonucleases E and III have an influence on the susceptibility against ribosome-targeting antibiotics and biofilm formation in *Salmonella*.

sRNAs also play very important roles in post-transcriptional control of gene expression. An extensive network of *trans*-antisense sRNAs have been shown to down-regulate the expression of several outer membrande porins (OMPs). OMPs are embedded within the outer membrane, which together with the peptidoglycan layer and the inner membrane form the bacterial cell envelope, the first barrier of defence against external aggressions. Coordination in the expression of *omp* genes seems critical for proper envelope assembly, and accounts for the existence of many sRNAs to regulate OMP mRNAs. MicA is a sRNA expressed at stationary phase, and functions in the control of OMPs synthesis. In this work, we also intended to study the decay of the sRNA MicA. Besides the role of this sRNA on the control of OMPs levels, it was shown that MicA levels needs to be fine-tuned for proper biofilm formation in *S.* Typhimurium (Kint *et al.*, 2010). Viegas *et al.* (Viegas *et al.*, 2007) have studied the specific contribution of several *Salmonella* ribonucleases on the turnover of different sRNAs, namely on MicA sRNA. MicA turnover was seen to be significantly dependent on the activity of the degradosome complex. It was also seen that in the absence of the double stranded-specific RNase III this sRNA is extremely stable. We hypothesized that MicA regulation by RNase III could involve the interaction with its target, since MicA forms an extended RNA duplex when binding to its known mRNA targets. Hence, in this work we have purified *Salmonella* RNase III and RNase E and have demonstrated that both endoribonucleases are responsible for the control of MicA sRNA levels. The role of the endoribonuclease III over MicA is dependent on previous hybridization

with the target. By contrast, the single stranded-specific endoribonuclease E is able to efficiently degrade free MicA sRNA. A model is proposed to explain the cooperation of both enzymes in the cell in order to achieve the fine-tuned control of the post-transcriptional regulator MicA.

EXPERIMENTAL PROCEDURES

Oligonucleotides

All nucleotides used in this study are listed in the Supplementary Table S1 and were synthesized by STAB Vida, Portugal.

Bacterial strains

All bacterial strains and plasmids used in this study are listed in Table 1 and 2, respectively. All *Salmonella* strains used are isogenic derivatives of the wild-type *Salmonella enterica* serovar Typhimurium strain SL1344. The RNase II and RNase R mutants were constructed following the lambda-red recombinase method as before (Viegas *et al.*, 2007), and using primer pairs pSCV-001/002 and pSCV-005/006, respectively. All mutations were moved to a fresh SL1344 background by P22 HT105/1 int-201 transduction (Schmieger, 1971).

For the construction of p*rnc* plasmid (pSVA-7), the pSVDA-01 plasmid expressing His-tag RNase III (see section "Construction of recombinant proteins") was digested with BamHI and XbaI to obtain the *rnc* fragment that was ligated with pWSK29 plasmid digested with the same enzymes. To construct *prne* (pSVA-8), *prnb* (pSVA-9) and p*rnr* (pSVA-10) plasmids, the *rne*, *rnb* and *rnr* genes were amplified from the SL1344 chromossomal DNA using primer pairs pSCV-009/010, pSCV-003/004 and pSCV-007/008, respectively. Each fragment was cloned into the XbaI and EcoRI sites of the pSE420 plasmid (Invitrogen). Competent *E. coli* DH5α

cells were used for cloning procedures during plasmid construction. The selected clones were sequenced to confirm the presence of the correct gene sequence, and transferred to the respective SL1344 derivative strain.

TABLE 1 - List of strains used in this work.

Strain	Relevant Markers	Reference
S. Typhimurium SL1344	Str^R*hisGrpsLxyl*	(Hoiseth and Stocker, 1981)
CMA-537 (*rne537*)	SL1344 *rne-537* (Δ*rne*::Cm^R)	(Viegas *et al.*, 2007)
CMA-539 (Δ*pnp*)	SL1344 *pnp-539* (Δ*pnp*::Cm^R)	(Viegas *et al.*, 2007)
CMA-551 (Δ*rnc*)	SL1344 *rnc-14*::ΔTn*10* (Tc^R)	(Viegas *et al.*, 2011)
CMA-700 (Δ*rnb*)	SL1344 *rnb* (Δ*rnb*::Cm^R)	(Saramago, 2013)
CMA-701 (Δ*rnr*)	SL1344 *rnr* (Δ*rnr*::Cm^R)	(Saramago, 2013)
E. coli DH5α	*rec*A1 *end*A1 *gyr*A96 thi-*hsd*R17 *sup*E44 *rel*A1 _*lac*ZYA-*arg*FU169 f80dLacZDM15	New England Biolabs
E. coli BL21 (DE3)	F$^-$ *omp*T *hsd* S$_B$ (*rb- mb-*) gal dcm (DE3)	(Studier and Moffatt, 1986)
E. coli BL21 (DE3) *rec*A *rnc*105	F$^-$ *omp*T *hsd* S$_B$ (*rb- mb-*) gal dcm (DE3) *rec*A *rnc*105	(Amarasinghe *et al.*, 2001)

Minimum Inhibitory Concentrations

The Minimum Inhibitory Concentration (MIC) was determined by the microdilution method as described (Andrews, 2001). Briefly, antibiotics were diluted and 75 μl of each concentration to be tested was dispensed into 96-well microtiter tray wells. In addition, 75 μl of Iso-Sensitest medium (Oxoid) were also added to each microtiter tray. All wells except the negative control were inoculated with 75 μl of actively growing cultures previously adjusted to the 0.5 McFarland standart. Microdilution trays were then incubated for 18-20h at 37ºC.

The lowest concentration of antibiotic that showed growth inhibition was interpreted as the MIC.

Biofilm assays

Curli fimbriae and cellulose biosynthesis were monitored by assessing growth and morphology of the different *Salmonella* strains on Congo Red Luria agar plates, as previously described (Hamilton *et al.*, 2009; Romling, 2005; Romling *et al.*, 1998). 5 μl of each overnight cultures were spotted onto Congo red agar plates (1% Bacto tryptone, 0.5% yeast extract, 40 μg/ml Congo red dye, 1.5% agar) and incubated at 28°C for 24 h.

The expression of cellulose was also evaluated by fluorescence analysis on Calcofluor agar plates (Solano *et al.*, 2002). 5 μl of each overnight culture were spotted onto LB plates containing 0.02% Calcofluor. The plates were incubated for 24h at 28ºC. The fluorescence of a spot under UV light revealed the binding of Calcofluor, indicating cellulose production.

Biofilm formation was evaluated in polystyrene microtiter plates, as previously described (Merritt *et al.*, 2005). Briefly, cells were allowed to grow in Iso-Sensitest medium (Oxoid) for 72h in 96-well polystyrene microtiter dishes. Unattached bacteria existing in the culture medium were removed, and the biofilm was stained with 0.2% crystal violet for 15 min (this dye stains the cells but not the polystyrene). The excess crystal violet dye was washed out, and the samples were washed three times with bidistilled water. 200 μl of ethanol were added to the wells to release the dye, and the optical density at 600 nm was measured in order to estimate the amount of biofilm formed.

TABLE 2 - List of plasmids used in this work.

Plasmid	Comments	Reference
pWSK29	Low copy plasmid (Amp^R)	(Wang and Kushner, 1991)
pSE420	IPTG inducible plasmid (Amp^R)	Invitrogen
pSVA-5 (p*pnp*)	pSE-420 expressing PNPase	(Viegas *et al.*, 2007)
pSVA-7 (p*rnc*)	pWSK29 expressing RNase III	(Viegas *et al.*, 2013)
pSVA-8 (p*rne*)	pSE-420 expressing RNase E	(Viegas *et al.*, 2013)
pSVA-9 (p*rnb*)	pSE-420 expressing RNase II	(Saramago, 2013)
pSVA-10 (p*rnr*)	pSE-420 expressing RNase R	(Saramago, 2013)
pET-15b	Inducible expression vector, N terminal HisTag (Amp^R)	Novagen
pSVDA-01	pET-15b encoding His-RNase III (Amp^R)	(Viegas *et al.*, 2011)
pSVDA-02	pET-15b encoding His-RNase E (Amp^R)	(Viegas *et al.*, 2011)

Construction of recombinant proteins

To overexpress *Salmonella* RNase E and RNase III proteins, the *rne* and *rnc* coding regions were amplified with primer pairs pSV-124/pSV-125 and pSV-129/pSV-130, respectively. In *E. coli*, the N-terminal half of RNase E (residues 1–498) was reported to be sufficient for the ribonuclease activity (McDowall and Cohen, 1996). We have thus amplified the N-terminal genomic region comprising residues 1–522, corresponding to the catalytic domain of *Salmonella* RNase E. The purified PCR products were double digested with BamHI and NdeI and ligated to the pET-15b vector previously digested with the same enzymes, yielding plasmids pSVDA-01 (*rnc*) and pSVDA-02 (*rne*). These plasmids were first cloned into *E. coli* DH5*α* and were subsequently transformed into BL21(DE3) strain in the case of pSVDA-02, and BL21(DE3) *rnc*105 *rec*A (Amarasinghe *et al.*, 2001) in the case of pSVDA-01 construction. In this derivative strain of BL21(DE3), which

carries an RNase III mutation, the auto-regulation of *Salmonella* RNase III by the endogenous *E. coli* homologue is blocked, resulting in a higher yield of the enzyme upon overexpression. All constructs were confirmed by DNA sequencing.

Overexpression and purification of Salmonella RNase E and RNase III proteins

The BL21(DE3) strain and derivative, containing the recombinant plasmids of interest, were grown in 100 ml of LB medium supplemented with ampicillin (150 μg/ml) to an OD_{600} of 0.5. At this point, protein expression was induced by addition of 1 mM of IPTG for 3 h at 37ºC. Cells were then harvested by centrifugation and the pellets stored at -80ºC. The culture pellets expressing RNase III or RNase E were resuspended in 3 ml of Buffer A (20 mM Tris-HCl pH 8, 500 mM NaCl, 20 mM imidazole pH 8). Suspensions were lysed using a French Press at 900 psi in the presence of 0.1 mM of PMSF. After lysis, the crude extracts were treated with 125 U of Benzonase (*Sigma*) to degrade the nucleic acids and clarified by a 30 min centrifugation at 10000g, 4ºC. The histidine-tagged recombinant proteins were purified by affinity chromatography, using the ÄKTA FPLC™ System (*GE Healthcare*). The clarified extracts were loaded onto a HisTrap HP Sepharose 1 ml column equilibrated in Buffer A. Protein elution was achieved in Buffer A with a linear imidazole gradient (from 20 to 500 mM). The fractions containing mostly the protein of interest, free of contaminants, were pooled. Eluted proteins were buffer exchanged with Desalting Buffer [10 mM Tris-HCl (pH 8), 3 mM $MgCl_2$, 100 mM NaCl, 1 mM DTT] and concentrated by centrifugation at 4ºC with Amicon Ultra Centrifugal Filter Devices (*Millipore*), with a molecular mass cut-off of 10 kDa (RNase III) or 50 kDa (RNase E). Proteins were quantified using the Bradford Method (Bradford, 1976) and stored at -20ºC in Desalting Buffer containing 50% (v/v) glycerol. The purity of the enzymes was

analysed by sodium dodecyl sulphate-polyacrylamide gel electrophoresis (SDS–PAGE) and revealed >90% homogeneity.

In vitro transcription and activity assays

DNA templates for the *in vitro* transcription were generated by PCR using chromosomal DNA from *S.* Typhimurium SL1344 strain. The phage T7 RNA polymerase promoter sequence was included in the forward primer sequences. *micA* was amplified with the primer pair pSV-116/pSV-117, *ompA* with pSV-122/pSV-123 and *lamB* with pSV-120/pSV-121. For the synthesis of the internally labelled 5′ triphosphate MicA, *in vitro* transcription was carried out using the purified PCR product as template in the presence of an excess of [^{32}P]-α –UTP over unlabelled UTP with 'Riboprobe *in vitro* Transcription System' (*Promega*) and T7 RNA polymerase. MicA substrate bearing 5′ monophosphate was obtained by adding an 8-fold excess of GMP over the other ribonucleotides to the *in vitro* transcription reaction (Condon *et al.*, 2008). Non-radioactive molecules were transcribed in the same conditions but using equimolar concentrations of all four ribonucleotides. MicA transcripts were purified by electrophoresis on an 8.3 M urea / 10% polyacrylamide gel. The gel slice was crushed and the RNA eluted with elution buffer [3 M ammonium acetate pH 5.2, 1 mM EDTA, 2.5% (v/v) phenol pH 4.3], overnight at room temperature. The RNA was ethanol precipitated and resuspended in RNase free water. For the synthesis of the 5′-end-labelled MicA or *ompA*, *in vitro* transcription was carried out using the corresponding PCR product as template. MicA and *ompA* transcripts were run on a 10 or 6% polyacrylamide gel, respectively, identified by ethidium bromide (EtBr) staining and cut out from the gel. The RNA was eluted from the gel slice as described above. The RNA substrates were end-labelled with [^{32}P]-γ-ATP at 37ºC for 1 h, with 10 units of T4 Polynucleotide Kinase (*Fermentas*) using the supplier

exchange buffer and again purified from gel as above. The yield of the labelled substrates (cpm/μl) was determined by scintillation counting.

The hybridization between labelled and unlabelled substrates was always performed in the Tris component of the activity buffer by incubation for 10 min at 80ºC, followed by 45 min at 37ºC. The activity assays were done in a final volume of 50 μl containing the activity buffer {for RNase III [30 mM Tris-HCl pH 8, 160 mM NaCl and 0.1 mM DTT] and for RNase E [25 mM Tris-HCl pH 7.5, 5 mM $MgCl_2$, 60 mM KCl, 100 mM NH_4Cl, 0.1 mM DTT and 5% (v/v) glycerol]} and ~10000 cpm of substrate. In the case of the activity assays with RNase III, 10 mM of $MgCl_2$ was added to the reaction mixture. As a control, prior to each assay an aliquot was taken and incubated under the same conditions of the other samples until the end of the assay (without the enzyme). The reactions were started by the addition of the enzyme at a concentration of 500 nM, and further incubated at 37ºC in the case of RNase III and 30ºC for RNase E (Chelladurai *et al.*, 1991; Jiang *et al.*, 2000). Samples were withdrawn at the time-points indicated in the respective figures, and the reactions were stopped by the addition of formamide-containing dye supplemented with 10 mM EDTA. Reaction products were resolved in a 7 M urea/15% or 8% polyacrylamide gel as indicated in the respective figure legends. Signals were visualized by PhosphorImaging and analyzed using ImageQuant software (*Molecular Dynamics*).

RESULTS AND DISCUSSION

RNases affect susceptibility against ribosome-targeting antibiotics

RNA degradation is a fundamental process in the regulation of the proper expression of the genetic information, and ribonucleases are key factors in the maintenance of the right amount of each transcript in the cell. Indeed these

enzymes have been shown to play important roles in several crucial cellular processes, and are known to modulate the expression of genes involved in resistance to stress and virulence. Thus, we hypothezised that ribonucleases by controlling the fate of RNA molecules and final protein levels, would have an important role on antibiotic susceptibility. *S.* Typhimurium SL1344 isogenic mutants deficient in the main ribonucleases (Table 1) were tested against a panoply of antimicrobial agents representatives of different antibiotic classes (Table 3). Our results showed that among the diverse classes of antibiotics tested, the susceptibility of the RNase mutant strains was only affected by ribosome-targeting agents (Table 3). Notably the RNase III mutant strain (Δ*rnc)* was more susceptible to kanamycin, spectinomycin, tobramycin and chloramphenicol. The first three are broad-spectrum antibiotics that belong to the aminoglycoside class. This class of antibiotics interferes with protein synthesis by selectively binding to the bacterial ribosome (Magnet and Blanchard, 2005). Chloramphenicol also inhibits protein synthesis and affects the assembly of ribosomal subunits (Siibak *et al.*, 2009). RNase III is involved in the primary processing of rRNA (reviewed in (Arraiano *et al.*, 2010)) and it was reported to copurify with ribosomes (Allas *et al.*, 2003). Such interaction was suggested to facilitate ribosomal biogenesis (Allas *et al.*, 2003). These observations provide a possible explanation to answer why antibiotics that affect ribosome assembly are more efficient in the absence of RNase III. Furthermore, neomycin and paromomycin, two other aminoglycosides, were recently reported to promote a reduction in the 30S and 50S ribosomal subunit amounts in an *E. coli* RNase III mutant (Frazier and Champney, 2012).

RNase R mutant also showed higher susceptibility to spectinomycin, an antibiotic that inhibits the elongation cycle of translation (Bilgin *et al.*, 1990; Noah *et al.*, 1999) (Table 3). *Trans*-translation releases stalled ribosomes from non-stop mRNAs and RNase R is known to be involved in the decay of these defective

transcripts (Richards *et al.*, 2006). In agreement with our results, deficiencies in *trans*-translation were seen to increase susceptibility to protein synthesis inhibitors in *Salmonella* (de la Cruz and Vioque, 2001; Luidalepp *et al.*, 2005; Vioque and de la Cruz, 2003).

TABLE 3 - MIC ranges of antibiotics (μg/ml).

The values presented are the result from at least three independent experiments. It is important to note that the growth pattern of the mutant strains is very similar to that of the wild-type (Viegas *et al.*, 2013), which excludes any influence of the growth rate in the observed MICs.

Strains	Aminoglycosides			Phenicol	Macrolide	Fluorquinolone		Quinolone	β-lactam
	KAN	SPT	TOB	CHL	ERY	NOR	OFL	NAL	AMP
wt	4	64	4	8	128	1	0.5	8	2
rne537	4	32	4	8	256	1	0.5	8	2
Δrnc	2	32	2	4	128	1	0.5	8	2
Δrnb	4	64	4	8	128	1	0.5	8	2
Δrnr	4	32	4	8	128	1	0.5	8	2
Δpnp	4	64	4	8	128	1	0.5	8	2

KAN, kanamycin; SPT, spectinomycin; TOB, tobramycin; CHL, chloramphenicol; ERI, erythromycin; NOR, norfloxacin; OFL, ofloxacin; NAL, nalidixic acid; AMP, ampicillin.

RNase E is essential and therefore we have used a viable mutant in which the protein is missing the C-terminus and cannot form the degradosome (the mutant was called *rne537*) (Viegas *et al.*, 2007). This mutant also showed a higher sensitivity to spectinomycin. The significant contribution of RNase E and the degradosome to the ribosome biogenesis and quality control may be a plausible explanation (Cheng and Deutscher, 2003; Ghora and Apirion, 1978; Misra and Apirion, 1979). Surprisingly the RNase E mutant had a higher resistance to erythromycin. Erythromycin is a macrolide that affects protein synthesis and inhibits 50S subunit formation (Siibak *et al.*, 2009; Usary and Champney, 2001). The absence of the degradosome somehow contributes to stabilize one or more transcripts involved in conferring erythromycin resistance.

The different susceptibilities of the ribonuclease mutants are indicative that they can act on disctint cellular targets, and strengthen the idea of the specificity of RNA degradation pathways that are not fully equivalent.

RNases influence biofilm formation

The capacity of biofilms to act as a diffusion barrier often slows down the infiltration of antimicrobial agents, and several antibiotics have reduced penetration throughout biofilms (Xu *et al.*, 2000). The extracellular matrix of biofilms is composed of curli fimbriae, cellulose plus other polysaccharides, and proteins. We have monitored curli fimbriae and cellulose biosynthesis by assessing the growth and morphology of the same *Salmonella* mutants on Congo Red Luria agar plates. PNPase mutant had previously been reported to display a different colony morphotype compared to the wild-type strain on these plates (Rouf *et al.*, 2011), and was used as a control. The expression of cellulose was also evaluated by fluorescence analysis on Calcofluor agar plates (Solano *et al.*, 2002).

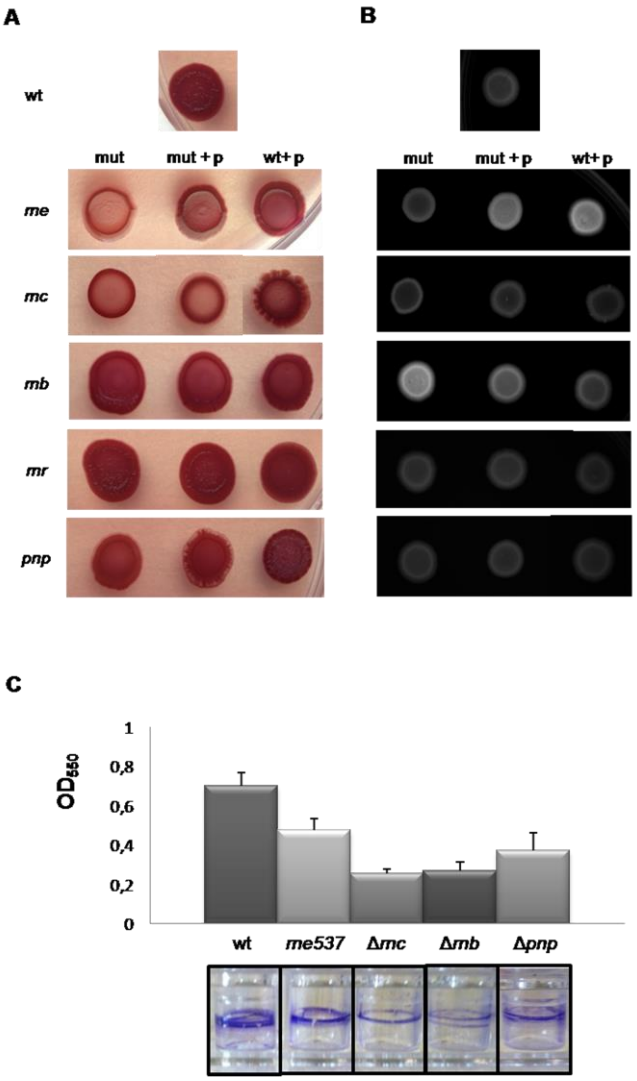

Figure 1 - Biofilm properties of different *Salmonella* strains on (**A**) LB plates without NaCl containing Congo red or (**B**) LB plates with calcofluor. Strains are indicated on the top of each spot and "mut" represents the different ribonuclease mutant strains; "mut+p" the complemented mutant and "wt+p" the overexpressing strain (**C**) Effect of the lack of some ribonucleases on biofilm development in microtiter plates in Iso-Sensitest medium (Oxoid). The thickness of biofilms in cultures of different strains was measured by determining optical density at 550 nm (OD_{550}) after staining with crystal violet. Error bars represent standard deviations.

Among the strains analyzed, the endoribonuclease mutants showed the major differences in colony morphotype (Figure 1). The wild-type strain presented colonies dark red and rough as previously reported for this strain (Hamilton *et al.*, 2009). On the other hand, Δ*rnc* mutant gave rise to smooth and pale colonies surrounded by a red circle around (Figure 1A). It is known that SL1344 strain produces a low amount of cellulose (Hamilton *et al.*, 2009). However, in the Calcofluor agar plates the Δ*rnc* mutant fluoresced with even less intensity than the wild-type (Figure 1B), which may indicate that cellulose biosynthesis is compromised. Deficiencies in the production of curli fimbriae can neither be ruled out. Complementation of the mutant with RNase III *in trans* partially restored the wild-type morphotype. Furthermore, the overexpressing strain also exhibited a morphotype distinct from that of the wild-type, indicating that RNase III has an important role on biofilm development. The ability to bind Congo Red dye seems to be also compromised in the *rne537* mutant (Figure 1A), revealing that expression of the extracellular matrix components (cellulose and/or curli fimbriae) might also be affected. The brighter fluorescence displayed in Calcofluor plates by the overexpression strain (Figure 1B), indicates a possible role of RNase E in modulating the amount of cellulose in the cell. Concerning exoribonucleases, the lack of RNase II seems to raise the cellular production of cellulose (Figure 1B), indicating that this enzyme may also modulate the levels of genes involved in cellulose production. As expected the PNPase mutant showed an altered morphotype on Congo Red plates (Figure 1A). CsgD, a master activator of biofilm development (Zakikhany *et al.*, 2010), was reported to be substantially reduced in the absence of PNPase in *Salmonella* (Rouf *et al.*, 2011).

The mutant strains that showed higher deviations on Congo Red and Calcofluor tests were further analyzed regarding biofilm formation in polystyrene microtiter plates, as previously described (Merritt *et al.*, 2005). This assay

measures the ability of bacteria to attach to the wells of a microtiter dish in the interface between the air and the liquid medium. In agreement, all the mutants tested showed a reduced ability to form biofilm but Δ*rnc* and Δ*rnb* were the mutants in which less biofilm was formed (Figure 1C). The deficiency on biofilm formation observed in Δ*rnb* was somehow surprising when considering the higher levels of cellulose produced by this strain. However, it has been shown in *E. coli* that cellulose overproduction negatively affects curli-mediated surface adhesion and cell aggregation, thus acting as a negative determinant for biofilm formation (Gualdi *et al.*, 2008). Consistent with this, in the RNase II mutant we observed an increased cellulose production, and consequently a decrease in adhesion and thus biofilm formation.

This study underlines the importance of RNases in antibiotic susceptibility and biofilm formation, two important factors in bacterial survival. Endoribonucleases E and III, in particular, seem to have an impact on these important functions. The involvement of these two ribonucleases in ribosomal biogenesis can be the basis of the higher sensitivity to ribosome-targeting antibiotics observed in the respective mutant strains. Mutants on these RNases are also known to exhibit a reduced motility, and a strong variation of CsgD mRNA levels (Viegas *et al.*, 2013), which may explain the deficiency in biofilm production. The simultaneous contribution of RNase III to biofilm development and antibiotic susceptibility reinforces the view that this enzyme is an important global regulator (Arraiano *et al.*, 2013). The evolutionary conservation of this ribonuclease in bacteria confirms its biological importance.

It was recently proposed that RNases could be attractive novel therapeutic targets (Eidem *et al.*, 2012). Further investigation on their mode of action may be applied in the design of new strategies to combat pathogenic bacteria.

Biofilm development is a multifactorial mechanism also controlled by sRNAs, like MicA (Jorgensen *et al.*, 2012; Kint *et al.*, 2010). This sRNA is mostly known by its role as a porin down-regulator whose transcription is σ^E-dependent (Figueroa-Bossi *et al.*, 2006; Johansen *et al.*, 2006; Papenfort *et al.*, 2006). Under stress conditions there is an unbalance of OMP levels leading to the activation of the σ^E response, which is a complex set of changes normally devoted to protect the cell envelope from environmental challenges (Rowley *et al.*, 2006). Thereby, the transcription factor σ^E triggers the synthesis of the sRNAs that control OMP levels (Johansen *et al.*, 2006; Papenfort *et al.*, 2006). Upon down-regulation of OMPs and after the relief of membrane stress, the high sRNA levels have to be brought back to normal amounts. Under this context, we were interested in studying this complex regulation of MicA cellular levels.

Contribution of endoribonucleases in the control of MicA levels

MicA cleavage by RNase III is facilitated by base-pairing with its mRNA target(s)

MicA was previously found to be highly stabilized in cells lacking a functional RNase III, with the concomitant accumulation of a degradation intermediate that is absent on the wild-type (Viegas *et al.*, 2007). Furthermore, we have obtained evidences that this smaller intermediate is a remnant of MicA-target mRNA paired species (Viegas *et al.*, 2011). Taking this into account, together with the fact that RNase III is a double-stranded-specific endoribonuclease, we wanted to compare *in vitro* the activity of the enzyme both over MicA transcript alone or in complex with its mRNA targets. Two main targets for this sRNA have been described in *Salmonella*, *ompA* and *lamB* mRNAs. MicA was reported to act over the translation initiation region of both molecules (Bossi and Figueroa-Bossi, 2007; Rasmussen *et al.*, 2005; Udekwu *et al.*, 2005). In

order to study the activity of *Salmonella* RNase III over MicA, we have cloned and purified the *Salmonella* enzyme as described in the "Experimental Procedures" section. An SDS-PAGE gel with the purified *Salmonella* RNase III is shown in Figure 2.

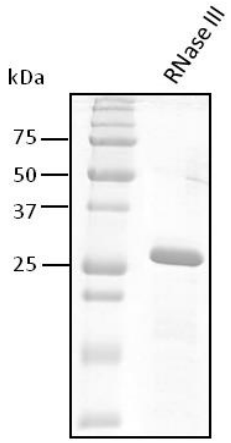

Figure 2 – SDS-PAGE analysis of the purified RNase III protein. Protein sample was visualized by Coomassie Brilliant Blue Staining. Molecular weight marker (Precision Plus Protein Pre-stained Standards – *Bio-Rad*) is shown on the left side of each image. Purified recombinant *Salmonella* RNase III (~27.5 kDa) was separated on a 15% polyacrylamide gel.

Activity assays were performed by incubating the purified *Salmonella* RNase III with internally labelled MicA molecule alone or in combination with the unlabelled 5'-UTR of *ompA* or *lamB* mRNAs. It has been shown that MicA is able to bind *ompA* mRNA without the help of the bacterial RNA chaperone Hfq that binds both the regulator and the target RNA, favouring their interaction (Udekwu *et al.*, 2005). Thus, this protein was not included in the activity assays. MicA alone was found to be resistant to RNase III cleavage (Figure 3A). By contrast, in conditions favouring the hybridization of the sRNA transcript with each one of the target molecules, we could see the increasing accumulation of specific reaction products simultaneously with the disappearance of the substrate. This indicates that the formation of the sRNA-target mRNA complex promotes the RNase III cleavage of MicA.

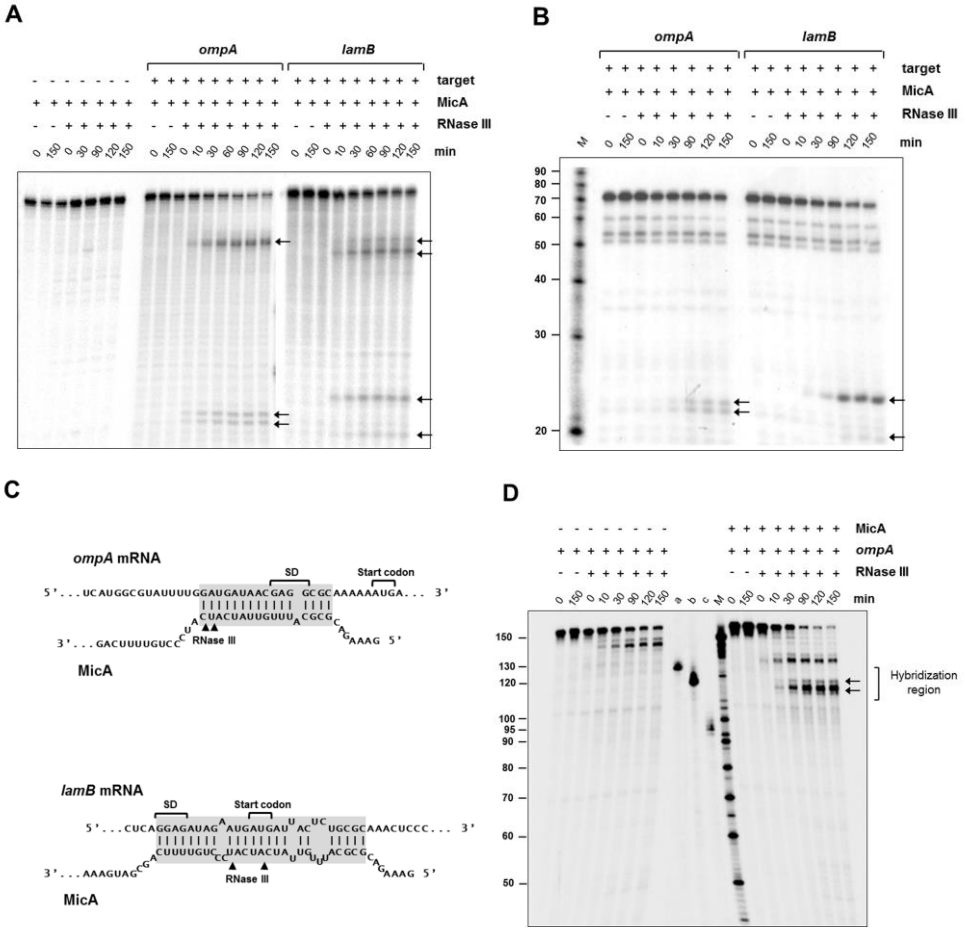

Figure 3 - *In vitro* cleavage of sRNA MicA or *ompA* 5′-UTR by RNase III. The radioactively labelled substrate was incubated with 500 nM of *Salmonella* RNase III. Aliquots withdrawn at the time-points indicated above each lane were analyzed on a 7 M urea / 15% or 8% PAA gel for MicA or *ompA*, respectively. The first two lanes of each reaction correspond to the controls without the protein at time zero (0) and at the end of the reaction time (150). The radiolabelled Decade Marker RNA (*Ambion*) is indicated by 'M'. The arrows in the figure indicate specific degradation products. **(A)** Assays performed with internally labelled MicA in the absence (-) (left panel) or in the presence (+) of a molar excess of *ompA* (middle panel) or *lamB* (right panel) unlabelled transcripts (5′-UTR sequence). **(B)** Assays performed with 5′-end-labeled MicA in the presence (+) of a molar excess of *ompA* (left panel) or *lamB* (right panel) unlabelled transcripts (5′-UTR sequence). The bands that are already observed in the absence of the enzyme (control reactions) arise due to the radiolysis of the substrate. **(C)** Proposed interaction regions of *ompA* and *lamB* mRNAs with MicA [adapted from (Bossi and Figueroa-Bossi, 2007)]. The Shine–Dalgarno regions of *ompA* and *lamB* are indicated. The arrows indicate the RNase III cleavage sites on MicA as determined on A and B. **(D)** Assays performed with 5′-end-labelled *ompA* in

the absence (-) (on the left) or in the presence (+) (right panel) of a molar excess of unlabelled MicA. On the left side of the marker (M) radiolabelled transcripts of known sizes were included (a) 130 nt; (b) 120 nt and (c) 95 nt. The arrows in the figure indicate the degradation products located inside the hybridization region.

The extension and location of MicA interaction with *ompA* or *lamB* mRNAs has been predicted to be slightly different (Bossi and Figueroa-Bossi, 2007; Udekwu *et al.*, 2005). Since RNase III cleaves dsRNA, the different interaction between MicA and the two targets could be in the origin of the distinct cleavage pattern induced by *ompA* or *lamB*. In order to identify the cleavage points generated by RNase III on the MicA-*ompA* and MicA-*lamB* hybrids, *in vitro* assays were performed as described above, but using 5′-end-labelled MicA in combination either with the unlabelled 5′-UTR of *ompA* or *lamB*. Since in this experiment MicA was 5′-end-labelled, the size of these fragments indicates the distance from the cleavage point to the 5′-end of MicA. The results are shown in Figure 3B. RNase III cleavage generates two main fragments of 22 and 23 nt on MicA-*ompA* hybrid, and 21 and 25 nt on MicA-*lamB*. The higher molecular weight bands, observed only when MicA was internally labelled (Figure 3A), correspond to 3′-end fragments, since they are not detected in the cleavage of 5′-end-labelled MicA. A representation of the hybridization regions showing the RNase III cleavage positions in MicA sequence is presented in Figure 3C. All the cleavage positions are located inside the predicted region of interaction with each target, strongly supporting our hypothesis that RNase III is responsible for the coupled MicA-target degradation.

According to our proposal, cleavage of MicA is coupled with the mRNA target cleavage. In this sense the same kind of activity assays were carried out in order to check the direct activity of RNase III over the corresponding region of *ompA* mRNA. For this, the purified *Salmonella* RNase III was incubated with the 5′-end-labelled UTR of *ompA* (172 nt) alone or in combination with unlabelled

MicA. As shown in Figure 3D although RNase III is able to cleave free *ompA*, a faster disappearance of the substrate when the hybrid *ompA*-MicA was used indicates that it is cleaved more efficiently. Moreover, the cleavage event gives rise to specific degradation products that were not observed after incubation with *ompA* alone (Figure 3D). Among these products, we could observe the accumulation of fragments in the range of 113–130 nt, which is the expected size of fragments generated by cleavage inside the hybridization region with MicA (Figure 3C). The other products with a higher molecular weight probably arise due to alterations in the secondary structure of *ompA* after the duplex formation, which could generate a new dsRNA region suitable for RNase III.

Taken together, our results indicate that MicA decay is dependent on RNase III and its cleavage by this enzyme *in vitro* is triggered upon base-pairing with its target mRNAs. The RNase III pathway has the advantage of simultaneously controlling the levels of the sRNA, whose function after the repression of the target will no longer be necessary in the cell. In addition RNase III cleavage makes the repression irreversible.

RNase E cleaves 'free MicA' sRNA in vitro

We have demonstrated that the sRNA MicA degradation is influenced by RNase III. However, this seems to happen only in the presence of the target mRNA. As we have shown *in vitro*, the enzyme was not able to cleave MicA alone. Thus, the question of how is free MicA degraded remains to be answered. *In vivo* experiments have shown a large impact of an RNase E mutant on the levels and stability of MicA. However, these results concern studies undertaken with the *rne-537* mutant derivative (Viegas *et al*., 2007). Since this mutant only prevents degradosome formation, without totally abolishing the enzyme activity, we were also interested in clarifying the role of the catalytic activity of RNase E on the decay of MicA. Moreover, it has been shown that -A/U rich sequences

together with adjacent stem-loop structures can comprise recognition sites for RNase E (Kaberdin *et al.*, 2000; Mackie, 1998). The sequence of the sRNA MicA matches these characteristics. Therefore, we have analyzed the ability of this endoribonuclease to cleave MicA sRNA transcript, *in vitro*. For this purpose we have cloned and purified the amino-terminal region of *Salmonella* RNase E. The homologous region in *E. coli* RNase E is known to be responsible for the catalytic activity of the enzyme (McDowall and Cohen, 1996). The results of the purification of the N-terminal segment of *Salmonella* RNase E are shown in Figure 4A.

In vitro assays with the purified protein were performed over uniformly labelled MicA transcript. It was seen before that RNase E preferentially cleaves RNAs with a 5′ monophosphate group over those endowed with a 5′ triphosphate (Celesnik *et al.*, 2007; Lin-Chao and Cohen, 1991; Mackie, 2000). Thus, in the activity assays we have used as substrates both the monophosphate and the triphosphate MicA transcripts. Our results show that RNase E is able to cleave both substrates *in vitro* (Figure 4B), though the efficiency of cleavage was superior over monophosphorylated MicA. This is in agreement with the recent report that *E. coli* RNase E is also active over some triphosphate substrates (Kime *et al.*, 2010).

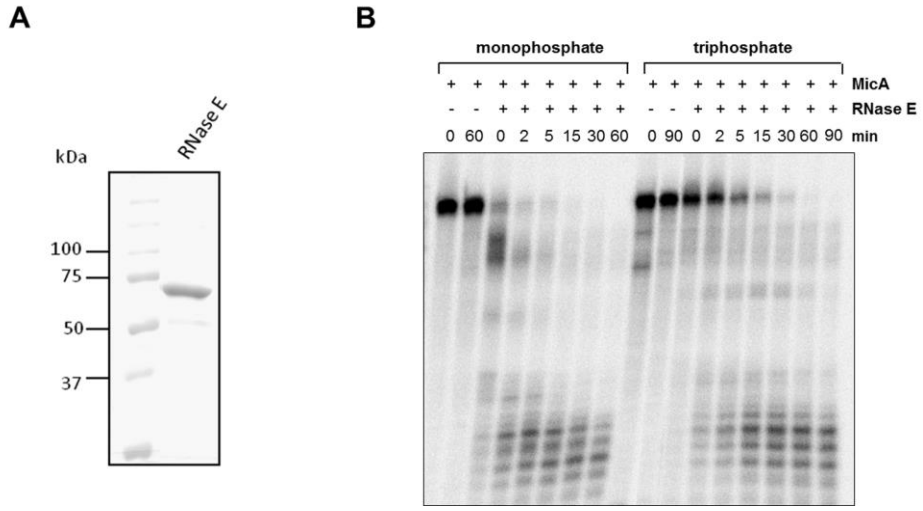

Figure 4 – *In vitro* study of MicA sRNA cleavage by RNase E. (A) SDS-PAGE analysis of the purified proteins. Protein sample was visualized by Coomassie Brilliant Blue Staining. Molecular weight marker (Precision Plus Protein Pre-stained Standards – *Bio-Rad*) is shown on the left side. Purified N-terminal region of *Salmonella* RNase E (~64 kDa) was separated on a 10% polyacrylamide gel. **(B)** α-^{32}P-labelled MicA transcript, 5′ monophosphate (left panel) or 5′ triphosphate (right panel), was incubated with 500 nM of purified *Salmonella* RNase E (residues 1–522) at 30ºC. Aliquots withdrawn at the time-points indicated above each lane were analyzed on a 15% PAA / 7 M urea gel. The two first lanes of each reaction correspond to the controls without the protein withdrawn at time zero and at the end of the reaction time, respectively.

For each sRNA the characterization of its turnover has to be analyzed from two different perspectives: the independent, and the dependent of target interaction. The later can be similar or not, whether the sRNA decay is influenced or not by the respective target(s). The results presented in this study indicate the existence of two different pathways for MicA sRNA turnover, each one involving a specific endoribonuclease. According to the model proposed in Figure 5, when MicA is free, RNase E seems to take the control by efficiently degrading the sRNA.

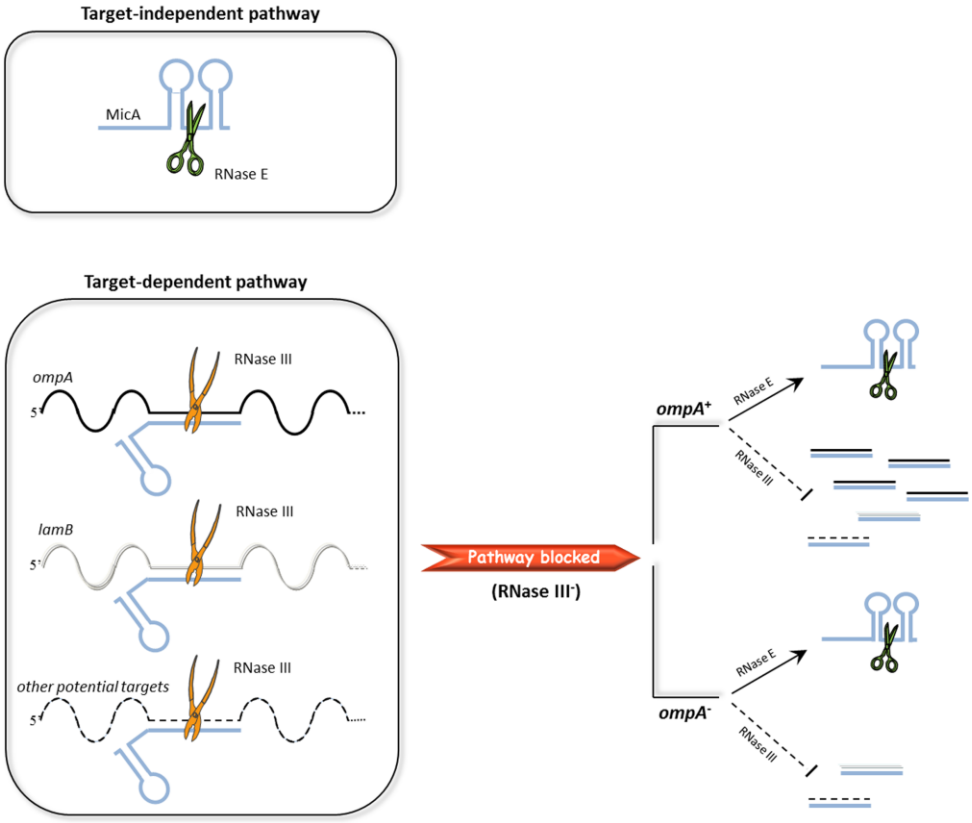

Figure 5 - Schematic representation of the two degradation pathways followed by MicA. RNase E and RNase III are represented by scissors and pliers, respectively. The two different pathways for MicA degradation are shown on the left side. The possible associations of MicA with its targets are also depicted. In the wild-type, MicA and the targets should be fully degraded as a result of both degradation pathways in cooperation with the exoribonucleolytic activity. In the RNase III$^-$ mutant, the MicA-target dependent degradation by RNase III is blocked. As a result, some degradation intermediates are stabilized and can be detected, namely the target and MicA strands that have interacted but could not be cleaved by RNase III. *ompA* being the main target of MicA, its species are over-represented. When additionally the *ompA* target mRNA is absent, the respective degradation intermediate is no longer present in the cell and, as a consequence, there is a reduced level of transcripts detected with probes complementary to MicA-targets.

However, if MicA is interacting with the targets the target-dependent pathway of degradation predominates. This mechanism involves a double stranded endoribonuclease that is able to degrade both the target and the sRNA simultaneously. From a physiological point of view, the existence of two distinct

pathways may enhance the cell response in stress conditions allowing a fine-tuned balance of OmpA levels needed to keep the envelop integrity. Moreover by having two alternative degradation pathways the cell warrants the metabolism of molecules no longer needed. This may be crucial in stationary phase, which is characterized by limited resources.

Interestingly, the cleavage by RNase III within the sRNA–mRNA duplex and the subsequent decay of the mRNA intermediate by the cell machinery could rather resemble the RNAi scenario in eukaryotic organisms. RNase III-like enzymes are known to have a pivotal role in eukaryotic small noncoding RNA function and biogenesis (Viegas and Arraiano, 2008). Hence, it is not surprising that RNase III would also be a main player in the control of prokaryotic sRNA expression and function, broadening the enzyme's role in the regulation of gene expression.

In this Chapter we have demonstrated that RNase E and RNase III are involved in antibiotic susceptibility, biofilm formation and in the control of the levels of MicA small RNA. Overall, this data highlights the specific contribution of these endoribonucleases on different cellular processes in *Salmonella*.

ACKNOWLEGMENTS

The authors want to thank Prof. Allen W. Nicholson for providing BL21(DE3) *rnc*105 *rec*A strain. This work was supported by Fundação para a Ciência e Tecnologia (FCT, Portugal) including grant #PEst-OE/EQB/LA0004/2011 and grant from European Commission FP7-KBBE-2011-1-289326. FCT Doctoral Fellowship (SFRH/BD/65607/2009 to M.S.).

REFERENCES

Allas, U., A. Liiv, and J. Remme. 2003. Functional interaction between RNase III and the Escherichia coli ribosome. *BMC Mol Biol*. 4:8.

Amarasinghe, A.K., I. Calin-Jageman, A. Harmouch, W. Sun, and A.W. Nicholson. 2001. Escherichia coli ribonuclease III: affinity purification of hexahistidine-tagged enzyme and assays for substrate binding and cleavage. *Methods Enzymol*. 342:143-158.

Amblar, M., S.C. Viegas, P. Lopez, and C.M. Arraiano. 2004. Homologous and heterologous expression of RNase III from Lactococcus lactis. *Biochem Biophys Res Commun*. 323:884-890.

Andrews, J.M. 2001. Determination of minimum inhibitory concentrations. *J Antimicrob Chemother*. 48 Suppl 1:5-16.

Arraiano, C.M., J.M. Andrade, S. Domingues, I.B. Guinote, M. Malecki, R.G. Matos, R.N. Moreira, V. Pobre, F.P. Reis, M. Saramago, I.J. Silva, and S.C. Viegas. 2010. The critical role of RNA processing and degradation in the control of gene expression. *FEMS Microbiol Rev*. 34:883-923.

Arraiano, C.M., F. Mauxion, S.C. Viegas, R.G. Matos, and B. Seraphin. 2013. Intracellular ribonucleases involved in transcript processing and decay: Precision tools for RNA. *Biochim Biophys Acta*.

Babitzke, P., L. Granger, J. Olszewski, and S.R. Kushner. 1993. Analysis of mRNA decay and rRNA processing in Escherichia coli multiple mutants carrying a deletion in RNase III. *J Bacteriol*. 175:229-239.

Bilgin, N., A.A. Richter, M. Ehrenberg, A.E. Dahlberg, and C.G. Kurland. 1990. Ribosomal RNA and protein mutants resistant to spectinomycin. *Embo J*. 9:735-739.

Blaszczyk, J., J.E. Tropea, M. Bubunenko, K.M. Routzahn, D.S. Waugh, D.L. Court, and X. Ji. 2001. Crystallographic and modeling studies of RNase III suggest a mechanism for double-stranded RNA cleavage. *Structure*. 9:1225-1236.

Bossi, L., and N. Figueroa-Bossi. 2007. A small RNA downregulates LamB maltoporin in Salmonella. *Mol Microbiol*. 65:799-810.

Bradford, M.M. 1976. A rapid and sensitive method for the quantitation of microgram quantities of protein utilizing the principle of protein-dye binding. *Anal Biochem*. 72:248-254.

Carzaniga, T., D. Antoniani, G. Deho, F. Briani, and P. Landini. 2012. The RNA processing enzyme polynucleotide phosphorylase negatively controls biofilm formation by repressing poly-N-acetylglucosamine (PNAG) production in Escherichia coli C. *BMC Microbiol*. 12:270.

Celesnik, H., A. Deana, and J.G. Belasco. 2007. Initiation of RNA decay in Escherichia coli by 5' pyrophosphate removal. *Mol Cell*. 27:79-90.

Chan, K.F., H. Le Tran, R.Y. Kanenaka, and S. Kathariou. 2001. Survival of clinical and poultry-derived isolates of Campylobacter jejuni at a low temperature (4 degrees C). *Appl Environ Microbiol*. 67:4186-4191.

Chelladurai, B.S., H. Li, and A.W. Nicholson. 1991. A conserved sequence element in ribonuclease III processing signals is not required for accurate in vitro enzymatic cleavage. *Nucleic Acids Res*. 19:1759-1766.

Cheng, Z.F., and M.P. Deutscher. 2003. Quality control of ribosomal RNA mediated by polynucleotide phosphorylase and RNase R. *Proc Natl Acad Sci U S A*. 100:6388-6393.

Condon, C., O. Pellegrini, N. Mathy, L. Benard, Y. Redko, I.A. Oussenko, G. Deikus, and D.H. Bechhofer. 2008. Assay of Bacillus subtilis ribonucleases in vitro. *Methods Enzymol*. 447:277-308.

de la Cruz, J., and A. Vioque. 2001. Increased sensitivity to protein synthesis inhibitors in cells lacking tmRNA. *Rna*. 7:1708-1716.

Dereeper, A., S. Audic, J.M. Claverie, and G. Blanc. 2010. BLAST-EXPLORER helps you building datasets for phylogenetic analysis. *BMC Evol Biol*. 10:8.

Domingues, S., R.G. Matos, F.P. Reis, A.M. Fialho, A. Barbas, and C.M. Arraiano. 2009. Biochemical characterization of the RNase II family of exoribonucleases from the human pathogens Salmonella typhimurium and Streptococcus pneumoniae. *Biochemistry*. 48:11848-11857.

Eidem, T.M., C.M. Roux, and P.M. Dunman. 2012. RNA decay: a novel therapeutic target in bacteria. *Wiley Interdiscip Rev RNA*. 3:443-454.

Figueroa-Bossi, N., S. Lemire, D. Maloriol, R. Balbontin, J. Casadesus, and L. Bossi. 2006. Loss of Hfq activates the sigmaE-dependent envelope stress response in Salmonella enterica. *Mol Microbiol*. 62:838-852.

Frazier, A.D., and W.S. Champney. 2012. Impairment of ribosomal subunit synthesis in aminoglycoside-treated ribonuclease mutants of Escherichia coli. *Arch Microbiol*. 194:1033-1041.

Gan, J., G. Shaw, J.E. Tropea, D.S. Waugh, D.L. Court, and X. Ji. 2008. A stepwise model for double-stranded RNA processing by ribonuclease III. *Mol Microbiol*. 67:143-154.

Ghora, B.K., and D. Apirion. 1978. Structural analysis and in vitro processing to p5 rRNA of a 9S RNA molecule isolated from an rne mutant of E. coli. *Cell*. 15:1055-1066.

Gross, G., and J.J. Dunn. 1987. Structure of secondary cleavage sites of E. coli RNAaseIII in A3t RNA from bacteriophage T7. *Nucleic Acids Res*. 15:431-442.

Gualdi, L., L. Tagliabue, S. Bertagnoli, T. Ierano, C. De Castro, and P. Landini. 2008. Cellulose modulates biofilm formation by counteracting curli-

mediated colonization of solid surfaces in Escherichia coli. *Microbiology*. 154:2017-2024.

Hamilton, S., R.J. Bongaerts, F. Mulholland, B. Cochrane, J. Porter, S. Lucchini, H.M. Lappin-Scott, and J.C. Hinton. 2009. The transcriptional programme of Salmonella enterica serovar Typhimurium reveals a key role for tryptophan metabolism in biofilms. *BMC Genomics*. 10:599.

Heeb, S., M.P. Fletcher, S.R. Chhabra, S.P. Diggle, P. Williams, and M. Camara. 2011. Quinolones: from antibiotics to autoinducers. *FEMS Microbiol Rev*. 35:247-274.

Hoiseth, S.K., and B.A. Stocker. 1981. Aromatic-dependent Salmonella typhimurium are non-virulent and effective as live vaccines. *Nature*. 291:238-239.

Holzer, P. 2007. Taste receptors in the gastrointestinal tract. V. Acid sensing in the gastrointestinal tract. *Am J Physiol Gastrointest Liver Physiol*. 292:G699-705.

Jiang, X., A. Diwa, and J.G. Belasco. 2000. Regions of RNase E important for 5'-end-dependent RNA cleavage and autoregulated synthesis. *J Bacteriol*. 182:2468-2475.

Johansen, J., A.A. Rasmussen, M. Overgaard, and P. Valentin-Hansen. 2006. Conserved small non-coding RNAs that belong to the sigmaE regulon: role in down-regulation of outer membrane proteins. *J Mol Biol*. 364:1-8.

Jorgensen, M.G., J.S. Nielsen, A. Boysen, T. Franch, J. Moller-Jensen, and P. Valentin-Hansen. 2012. Small regulatory RNAs control the multi-cellular adhesive lifestyle of Escherichia coli. *Mol Microbiol*. 84:36-50.

Kaberdin, V.R., A.P. Walsh, T. Jakobsen, K.J. McDowall, and A. von Gabain. 2000. Enhanced cleavage of RNA mediated by an interaction between substrates and the arginine-rich domain of E. coli ribonuclease E. *J Mol Biol*. 301:257-264.

Kime, L., S.S. Jourdan, J.A. Stead, A. Hidalgo-Sastre, and K.J. McDowall. 2010. Rapid cleavage of RNA by RNase E in the absence of 5' monophosphate stimulation. *Mol Microbiol*. 76:590-604.

Kint, G., D. De Coster, K. Marchal, J. Vanderleyden, and S.C. De Keersmaecker. 2010. The small regulatory RNA molecule MicA is involved in Salmonella enterica serovar Typhimurium biofilm formation. *BMC Microbiol*. 10:276.

Kitamura, S., K. Fujishima, A. Sato, D. Tsuchiya, M. Tomita, and A. Kanai. 2010. Characterization of RNase HII substrate recognition using RNase HII-argonaute chimaeric enzymes from Pyrococcus furiosus. *Biochem J*. 426:337-344.

Kovacs-Simon, A., R.W. Titball, and S.L. Michell. 2011. Lipoproteins of bacterial pathogens. *Infect Immun*. 79:548-561.

Larkin, M.A., G. Blackshields, N.P. Brown, R. Chenna, P.A. McGettigan, H. McWilliam, F. Valentin, I.M. Wallace, A. Wilm, R. Lopez, J.D. Thompson,

T.J. Gibson, and D.G. Higgins. 2007. Clustal W and Clustal X version 2.0. *Bioinformatics*. 23:2947-2948.

Lawal, A., O. Jejelowo, A.K. Chopra, and J.A. Rosenzweig. 2011. Ribonucleases and bacterial virulence. *Microb Biotechnol*. 4:558-571.

Lee, A., S.C. Smith, and P.J. Coloe. 1998. Survival and growth of Campylobacter jejuni after artificial inoculation onto chicken skin as a function of temperature and packaging conditions. *J Food Prot*. 61:1609-1614.

Li, H., and A.W. Nicholson. 1996. Defining the enzyme binding domain of a ribonuclease III processing signal. Ethylation interference and hydroxyl radical footprinting using catalytically inactive RNase III mutants. *EMBO J*. 15:1421-1433.

Li, H.L., B.S. Chelladurai, K. Zhang, and A.W. Nicholson. 1993. Ribonuclease III cleavage of a bacteriophage T7 processing signal. Divalent cation specificity, and specific anion effects. *Nucleic Acids Res*. 21:1919-1925.

Lin-Chao, S., and S.N. Cohen. 1991. The rate of processing and degradation of antisense RNAI regulates the replication of ColE1-type plasmids in vivo. *Cell*. 65:1233-1242.

Luidalepp, H., M. Hallier, B. Felden, and T. Tenson. 2005. tmRNA decreases the bactericidal activity of aminoglycosides and the susceptibility to inhibitors of cell wall synthesis. *RNA Biol*. 2:70-74.

Mackie, G.A. 1998. Ribonuclease E is a 5'-end-dependent endonuclease. *Nature*. 395:720-723.

Mackie, G.A. 2000. Stabilization of circular rpsT mRNA demonstrates the 5'-end dependence of RNase E action in vivo. *J Biol Chem*. 275:25069-25072.

Magnet, S., and J.S. Blanchard. 2005. Molecular insights into aminoglycoside action and resistance. *Chem Rev*. 105:477-498.

Mah, T.F., and G.A. O'Toole. 2001. Mechanisms of biofilm resistance to antimicrobial agents. *Trends Microbiol*. 9:34-39.

Majowicz, S.E., J. Musto, E. Scallan, F.J. Angulo, M. Kirk, S.J. O'Brien, T.F. Jones, A. Fazil, and R.M. Hoekstra. 2010. The global burden of nontyphoidal Salmonella gastroenteritis. *Clin Infect Dis*. 50:882-889.

Matsunaga, J., E.L. Simons, and R.W. Simons. 1996. RNase III autoregulation: structure and function of rncO, the posttranscriptional "operator". *RNA*. 2:1228-1240.

McDowall, K.J., and S.N. Cohen. 1996. The N-terminal domain of the rne gene product has RNase E activity and is non-overlapping with the arginine-rich RNA-binding site. *J Mol Biol*. 255:349-355.

Merritt, J.H., D.E. Kadouri, and G.A. O'Toole. 2005. Growing and analyzing static biofilms. *Curr Protoc Microbiol*. Chapter 1:Unit 1B 1.

Milligan, J.F., D.R. Groebe, G.W. Witherell, and O.C. Uhlenbeck. 1987. Oligoribonucleotide synthesis using T7 RNA polymerase and synthetic DNA templates. *Nucleic Acids Res*. 15:8783-8798.

Misra, T.K., and D. Apirion. 1979. RNase E, an RNA processing enzyme from Escherichia coli. *J Biol Chem*. 254:11154-11159.

Noah, J.W., M.A. Dolan, P. Babin, and P. Wollenzien. 1999. Effects of tetracycline and spectinomycin on the tertiary structure of ribosomal RNA in the Escherichia coli 30 S ribosomal subunit. *J Biol Chem*. 274:16576-16581.

Papenfort, K., V. Pfeiffer, F. Mika, S. Lucchini, J.C. Hinton, and J. Vogel. 2006. SigmaE-dependent small RNAs of Salmonella respond to membrane stress by accelerating global omp mRNA decay. *Mol Microbiol*. 62:1674-1688.

Papp-Wallace, K.M., and M.E. Maguire. 2006. Manganese transport and the role of manganese in virulence. *Annu Rev Microbiol*. 60:187-209.

Pogacar, M.S., A. Klancnik, S.S. Mozina, and A. Cencic. 2010. Attachment, invasion, and translocation of Campylobacter jejuni in pig small-intestinal epithelial cells. *Foodborne Pathog Dis*. 7:589-595.

Portier, C., L. Dondon, M. Grunberg-Manago, and P. Regnier. 1987. The first step in the functional inactivation of the Escherichia coli polynucleotide phosphorylase messenger is a ribonuclease III processing at the 5' end. *EMBO J*. 6:2165-2170.

Rao, K.A., E. Yazaki, D.F. Evans, and R. Carbon. 2004. Objective evaluation of small bowel and colonic transit time using pH telemetry in athletes with gastrointestinal symptoms. *Br J Sports Med*. 38:482-487.

Rasmussen, A.A., M. Eriksen, K. Gilany, C. Udesen, T. Franch, C. Petersen, and P. Valentin-Hansen. 2005. Regulation of ompA mRNA stability: the role of a small regulatory RNA in growth phase-dependent control. *Mol Microbiol*. 58:1421-1429.

Reid, A.N., R. Pandey, K. Palyada, H. Naikare, and A. Stintzi. 2008. Identification of Campylobacter jejuni genes involved in the response to acidic pH and stomach transit. *Appl Environ Microbiol*. 74:1583-1597.

Richards, J., P. Mehta, and A.W. Karzai. 2006. RNase R degrades non-stop mRNAs selectively in an SmpB-tmRNA-dependent manner. *Mol Microbiol*. 62:1700-1712.

Romling, U. 2005. Characterization of the rdar morphotype, a multicellular behaviour in Enterobacteriaceae. *Cell Mol Life Sci*. 62:1234-1246.

Romling, U., Z. Bian, M. Hammar, W.D. Sierralta, and S. Normark. 1998. Curli fibers are highly conserved between Salmonella typhimurium and Escherichia coli with respect to operon structure and regulation. *J Bacteriol*. 180:722-731.

Rouf, S.F., I. Ahmad, N. Anwar, S.K. Vodnala, A. Kader, U. Romling, and M. Rhen. 2011. Opposing contributions of polynucleotide phosphorylase and the membrane protein NlpI to biofilm formation by Salmonella enterica serovar Typhimurium. *J Bacteriol*. 193:580-582.

Rowley, G., M. Spector, J. Kormanec, and M. Roberts. 2006. Pushing the envelope: extracytoplasmic stress responses in bacterial pathogens. *Nat Rev Microbiol*. 4:383-394.

Saramago, M., Domingues, S., Viegas, SC and Arraiano C.M. 2013. Ribonucleases promote biofilm formation and antibiotic resistance in Salmonella Typhimurium. *Submitted in Appl Environ Microbiol*

Schmieger, H. 1971. The fate of the bacterial chromosome in P22-infected cells of Salmonella typhimurium. *Mol Gen Genet*. 110:238-244.

Siibak, T., L. Peil, L. Xiong, A. Mankin, J. Remme, and T. Tenson. 2009. Erythromycin- and chloramphenicol-induced ribosomal assembly defects are secondary effects of protein synthesis inhibition. *Antimicrob Agents Chemother*. 53:563-571.

Silva, I.J., M. Saramago, C. Dressaire, S. Domingues, S.C. Viegas, and C.M. Arraiano. 2011. Importance and key events of prokaryotic RNA decay: the ultimate fate of an RNA molecule. *Wiley Interdiscip Rev RNA*. 2:818-836.

Sim, S.H., J.H. Yeom, C. Shin, W.S. Song, E. Shin, H.M. Kim, C.J. Cha, S.H. Han, N.C. Ha, S.W. Kim, Y. Hahn, J. Bae, and K. Lee. 2010. Escherichia coli ribonuclease III activity is downregulated by osmotic stress: consequences for the degradation of bdm mRNA in biofilm formation. *Mol Microbiol*. 75:413-425.

Solano, C., B. Garcia, J. Valle, C. Berasain, J.M. Ghigo, C. Gamazo, and I. Lasa. 2002. Genetic analysis of Salmonella enteritidis biofilm formation: critical role of cellulose. *Mol Microbiol*. 43:793-808.

Stead, M.B., S. Marshburn, B.K. Mohanty, J. Mitra, L. Pena Castillo, D. Ray, H. van Bakel, T.R. Hughes, and S.R. Kushner. 2011. Analysis of Escherichia coli RNase E and RNase III activity in vivo using tiling microarrays. *Nucleic Acids Res*. 39:3188-3203.

Stewart, P.S. 2002. Mechanisms of antibiotic resistance in bacterial biofilms. *Int J Med Microbiol*. 292:107-113.

Studier, F.W., and B.A. Moffatt. 1986. Use of bacteriophage T7 RNA polymerase to direct selective high-level expression of cloned genes. *J Mol Biol*. 189:113-130.

Sun, W., E. Jun, and A.W. Nicholson. 2001. Intrinsic double-stranded-RNA processing activity of Escherichia coli ribonuclease III lacking the dsRNA-binding domain. *Biochemistry*. 40:14976-14984.

Sun, W., G. Li, and A.W. Nicholson. 2004. Mutational analysis of the nuclease domain of Escherichia coli ribonuclease III. Identification of conserved acidic residues that are important for catalytic function in vitro. *Biochemistry*. 43:13054-13062.

Udekwu, K.I., F. Darfeuille, J. Vogel, J. Reimegard, E. Holmqvist, and E.G. Wagner. 2005. Hfq-dependent regulation of OmpA synthesis is mediated by an antisense RNA. *Genes Dev*. 19:2355-2366.

Usary, J., and W.S. Champney. 2001. Erythromycin inhibition of 50S ribosomal subunit formation in Escherichia coli cells. *Mol Microbiol*. 40:951-962.

Viegas, S.C., and C.M. Arraiano. 2008. Regulating the regulators: How ribonucleases dictate the rules in the control of small non-coding RNAs. *RNA Biol*. 5:230-243.

Viegas, S.C., D. Mil-Homens, A.M. Fialho, and C.M. Arraiano. 2013. The Virulence of Salmonella enterica Serovar Typhimurium in the Insect Model Galleria mellonella Is Impaired by Mutations in RNase E and RNase III. *Appl Environ Microbiol*. 79:6124-6133.

Viegas, S.C., V. Pfeiffer, A. Sittka, I.J. Silva, J. Vogel, and C.M. Arraiano. 2007. Characterization of the role of ribonucleases in Salmonella small RNA decay. *Nucleic Acids Res*. 35:7651-7664.

Viegas, S.C., I.J. Silva, M. Saramago, S. Domingues, and C.M. Arraiano. 2011. Regulation of the small regulatory RNA MicA by ribonuclease III: a target-dependent pathway. *Nucleic Acids Res*. 39:2918-2930.

Vioque, A., and J. de la Cruz. 2003. Trans-translation and protein synthesis inhibitors. *FEMS Microbiol Lett*. 218:9-14.

Wang, R.F., and S.R. Kushner. 1991. Construction of versatile low-copy-number vectors for cloning, sequencing and gene expression in Escherichia coli. *Gene*. 100:195-199.

Wei, Q., S. Tarighi, A. Dotsch, S. Haussler, M. Musken, V.J. Wright, M. Camara, P. Williams, S. Haenen, B. Boerjan, A. Bogaerts, E. Vierstraete, P. Verleyen, L. Schoofs, R. Willaert, V.N. De Groote, J. Michiels, K. Vercammen, A. Crabbe, and P. Cornelis. 2011. Phenotypic and genome-wide analysis of an antibiotic-resistant small colony variant (SCV) of Pseudomonas aeruginosa. *PLoS One*. 6:e29276.

Xu, K.D., G.A. McFeters, and P.S. Stewart. 2000. Biofilm resistance to antimicrobial agents. *Microbiology*. 146 (Pt 3):547-549.

Zakikhany, K., C.R. Harrington, M. Nimtz, J.C. Hinton, and U. Romling. 2010. Unphosphorylated CsgD controls biofilm formation in Salmonella enterica serovar Typhimurium. *Mol Microbiol*. 77:771-786.

Zilhao, R., F. Cairrao, P. Regnier, and C.M. Arraiano. 1996. PNPase modulates RNase II expression in Escherichia coli: implications for mRNA decay and cell metabolism. *Mol Microbiol*. 20:1033-1042.

SUPPLEMENTARY INFORMATION

Table S1 – List of oligonucleaotides used in this work. The restriction and T7 sequences in the primers used for cloning procedures and for riboprobe synthesis, respectively, are shown in bold and underlined.

Oligo	Sequence 5' to 3'*
pSCV-001	GAGTTTCATCGGAGCAGGCCATTAATATGTTAGGCTGGTGCGGCGTGTGCGTGTAGGCTGGAGCTGCTTC
pSCV-002	CGGGTTTCCATGCGAACTTCCGCAATAGTGACATCAATGACATCCGTGGTCCATATGAATATCCTCCTTAG
pSCV-003	TTGGCTACGAGAATTCACGAATATGT
pSCV-004	CCGTTGAGTGATCTAGACGTGGTTACGCT
pSCV-005	CAACTGGTCTTTACCCGCCGCCAGTGCTATGCGCTGCCGGAACGCCTCGACGTGTAGGCTGGAGCTGCTTC
pSCV-006	GCCCGTTTCTGTGGTGTTGCCCTTGTTCCCTTGCTCTTTCGCCAGCAGGTAGGTCCATATGAATATCCTCCTTAG
pSCV-007	GAGATGACAATGGAGGAATTCCAATGTCACAAGATCC
pSCV-008	CTTCTGTTTCTAGAGGGGTATTGCTCACTC
pSCV-009	GTATCAGCATCTAGATCATTCTACCGGCT
pSCV-010	TCGTCAACGTAAGAATTCTGAGTAAGTTA
pSCV-116	GAAAT**TAATACGACTCACTATAGG**AAAGACGCGCATTTGTTAT
pSCV-117	AAAAAGGCCACTCACGGAGTG
pSCV-120	CCGTGGAAATCGACAGCCATTGCCTGAGCGGACATTAC
pSCV-121	GGGCC**TAATACGACTCACTATAG**CTCAGGAGATAGAATGATGATTACTCTGC
pSCV-122	GG**TAATACGACTCACTATAGG**CCAGGGGTGCTCGGCATAA
pSCV-123	GCCAGTGCCACTGCAATCGCGATA
pSV-124	**GGAATTCCATATG**AAAAGAATGTTAATCAACGCG
pSV-125	**CGCGGATCC**CTACGTGGCGACGCTAACCG
pSV-129	**GGAATTCCATATG**AACCCCATCGTAATTAATC
pSV-130	**CGCGGATCC**TCATTCCAACTCCAGTTTTTTC

Chapter 4

BASE-PAIRING INTERACTION BETWEEN 5′- AND 3′-UTRS CONTROLS ICAR MRNA TRANSLATION IN STAPHYLOCOCCUS AUREUS

This chapter contains data published in:

de los Mozos IR, Vergara-Irigaray M, Segura V, Villanueva M, Bitarte N, **Saramago M**, Domingues S, Arraiano CM, Fetcher P, Romby P, Uzqueda M, Corrales FJ, Valle J, Solano C, Lasa I, and Toledo-Arana A. 2013. Base-Pairing Interaction Between 5′- and 3′-UTRs Controls *icaR* mRNA Translation in *Staphylococcus aureus*. Accepted in PlosGenet

The contribution of the author for this publication was in the *in vitro* experiments, namely in the overexpression and purification of RNase III protein. Moreover, the author was responsible for RNA substrates synthesis, for developing and optimizing the gel shift experiments and *in vitro* cleavage assays (together with S. Domingues and IR de los Mozos).

ABSTRACT

The presence of regulatory sequences in the 3′ untranslated region (3′-UTR) of eukaryotic mRNAs controlling RNA stability and translation efficiency is widely recognized. In contrast, the relevance of 3′-UTRs in the regulation of bacterial mRNA functionality has been disregarded. Here, we report evidences showing that around one-third of the mapped mRNAs of the major human pathogen *Staphylococcus aureus* carry 3′-UTRs longer than 100-nt and thus, potential regulatory functions. We selected the long 3′-UTR of *icaR,* which codes for the repressor of the main exopolysaccharidic compound of the *S. aureus* biofilm matrix, to evaluate the role that 3′-UTRs may play in regulating mRNA expression. We showed that base-pairing between the 3′-UTR and the Shine-Dalgarno (SD) region of *icaR* mRNA interferes with the translation initiation complex and generates a double-stranded substrate for RNase III. Deletion or substitution of the motif (UCCCCUG) within *icaR* 3′-UTR was sufficient to abolish this interaction and resulted in the accumulation of IcaR repressor and inhibition of biofilm development. Our findings provide a singular example of a novel post-transcriptional regulatory mechanism to modulate bacterial gene expression through the interaction of a 3′-UTR with the 5′-UTR of the same mRNA.

INTRODUCTION

Regulation of translation is used to modulate gene expression in a wide range of biological situations in all living organisms. Compared to transcriptional regulation, mRNA translational control provides several advantages such as a more rapid response, reversibility, fine-tuning of protein amount, coordinated regulation of protein families, potential for spatial control and efficacy in systems lacking transcriptional control mechanisms (Mazumder *et al.*, 2003). In eukaryotes, translational control is largely conferred through specific *cis*-acting sequences located in mRNA 3′ untranslated regions (3′-UTR) that serve as binding sites for associated *trans*-acting factors. These localized 3′-UTR *cis*-acting sequences include microRNAs (miRNAs) specific binding sites, denoted as "seed sequences" that usually cause gene silencing by destabilization of target RNAs. miRNAs can also affect the translation process (Brodersen and Voinnet, 2009). In addition, the poly(A) tail acts as a binding site for a class of regulatory factors required for some mRNAs to be exported from the nucleus, promotes translation initiation and termination and recycling of ribosomes and enhances stability of mRNA (Garneau *et al.*, 2007; Mangus *et al.*, 2003). Furthermore, specific sequence or structure elements are also recognized by RNA-binding proteins or non-coding RNAs, that can either upregulate or downregulate gene expression (for review see (Matoulkova *et al.*, 2012)). Remarkably, several of these *cis*-acting sequences and *trans*-acting factors have been involved in end-to-end interactions of mRNA ("closed-loop" or "circular" mRNA structure) by which translation can be controlled (Mazumder *et al.*, 2003).

In contrast, as regards bacterial translational control, it is mainly modulated through the mRNA 5′-UTR which includes the Shine and Dalgarno (SD) sequence most probably because translation is coupled to transcription (Nakamoto, 2009). Bacterial 5′-UTRs also carry secondary structures, binding sites

for small regulatory RNAs (sRNAs) or RNA binding proteins that modify mRNA stability or protein translation (Agaisse and Lereclus, 1996; Babitzke *et al.*, 2009; Beuzon *et al.*, 1999; Chen *et al.*, 1991; Geissmann *et al.*, 2009b; Waters and Storz, 2009). In addition, thermosensors and riboswitches control protein expression through conformational changes upon a temperature shift or ligand binding, respectively (Kortmann and Narberhaus, 2012; Narberhaus, 2010; Serganov and Nudler, 2013; Winkler, 2005). Unlike the 5′-UTR, the only known regulatory element of bacterial 3′-UTRs is the intrinsic transcriptional terminator sequence which folds in a stem loop secondary structure that prevents exonucleases access to the 3′-end of the transcript (Arraiano *et al.*, 2010; Belasco, 2010). However, recent studies suggest that bacterial 3′-UTRs might have other regulatory roles (Gripenland *et al.*, 2010; Lasa *et al.*, 2011; Lasa *et al.*, 2012; Rasmussen *et al.*, 2009; Toledo-Arana *et al.*, 2009). For example, the existence of a conserved 3′-UTR in nine membrane-associated genes with conserved long 3′-UTRs in *Bacillus subtilis* suggested a functional role for these 3′-UTRs (Rasmussen *et al.*, 2009). In *Listeria monocytogenes* and *Staphylococcus aureus*, long 3′-UTRs that overlap adjacent convergent transcripts encoded at the opposite DNA strand have been described (Gripenland *et al.*, 2010; Lasa *et al.*, 2011; Toledo-Arana *et al.*, 2009). These overlapping 3′-UTRs may modulate the expression of neighbouring genes by a *cis*-acting antisense RNA mechanism (Gripenland *et al.*, 2010; Lasa *et al.*, 2011; Lasa *et al.*, 2012; Toledo-Arana *et al.*, 2009). In addition, 3′-UTRs could act as reservoirs of small regulatory RNAs either by processing the long 3′-UTR or by de novo transcription from an internal promoter (Chao *et al.*, 2012; Kawano *et al.*, 2005). Finally, co-immunoprecipitation experiments have shown a high affinity of *Salmonella typhimurium* Hfq and *S. aureus* RNase III proteins for mRNA 3′-UTRs suggesting that this region may provide a regulatory function (Lioliou *et al.*, 2012; Sittka *et al.*, 2008).

In this study, we mapped the 3′ boundaries of the *S. aureus* transcriptome combining custom-tiling microarrays and directional RNA-deep sequencing data. Results uncovered that at least one third of the *S. aureus* transcripts carry 3′-UTRs longer than 100 nucleotides (nt). Since this 3′-UTR length provides significant potential for transcript-specific regulation, we examined the putative role of bacterial 3′-UTRs in gene regulation using the long 3′-UTR of *icaR* transcript as a model. We chose *icaR* because of its involvement in the regulation of biofilm formation. This process is the main cause of nosocomial infections in patients with indwelling medical devices (Arciola *et al.*, 2012). Bacteria in a biofilm are surrounded by a self-produced extracellular matrix that contains exopolysaccharides, proteins and sometimes DNA. In the case of *S. aureus*, the main biofilm exopolysaccharide is a polymer of poly-β-1,6-*N*-acetylglucosamine (PIA-PNAG), whose synthesis depends on the enzymes encoded by the *icaADBC* operon (Cramton *et al.*, 1999; Gotz, 2002). One of the regulators that controls *icaADBC* expression is IcaR, a member of the TetR family of transcriptional regulatory proteins. IcaR is encoded at the *ica* locus but is divergently transcribed from the *icaADBC* operon. Binding of IcaR to the *icaADBC* promoter inhibits *icaADBC* expression (Jefferson *et al.*, 2003). However, how IcaR levels are adjusted to allow the rapid switch from a planktonic to a sessile lifestyle remains poorly understood.

Here, we first showed that deletion of the 3′-UTR of *icaR* caused a stabilization of *icaR* mRNA and consequently an increase in IcaR protein levels, indicating that *icaR* 3′-UTR regulates mRNA half-life. Then, *icaR* mRNA secondary structure prediction showed that a UCCCCUG motif located at the 3′-UTR paired the Shine-Dalgarno (SD) region at the 5′-UTR. *In vitro* experiments indicated that this interaction promotes mRNA decay and inhibits ribosome loading. Lastly, *in vivo* analysis of bacteria expressing *icaR* mRNA variants demonstrated that deletion or substitution of the UCCCCUG motif strongly

decreased the 3′-UTR/Shine-Dalgarno interaction facilitating IcaR expression. As a consequence, PIA-PNAG synthesis and biofilm formation was impaired demonstrating the biological relevance of this regulatory mechanism. This study illustrates that bacterial 3′-UTRs can provide strategies for post-transcriptional regulation through an interaction with the SD region at the 5′-UTR. In this case, it is worth noting that base-pairing is occurring between the 3′-UTR and the 5′-UTR contained in the same mRNA.

EXPERIMENTAL PROCEDURES

Oligonucleotides, plasmids, bacterial strains and culture conditions

Bacterial strains, plasmids and oligonucleotides used in this study are listed in Table S1, Table S2 and Table S3 respectively. *Staphylococcus aureus* strains were grown in trypticase soy broth supplemented with 0.25% glucose (TSB-gluc) (Pronadisa). *Escherichia coli* was grown in LB broth (Pronadisa). When required for selective growth, medium was supplemented with appropriated antibiotics at the following concentrations: erythromycin (Em), 1.5 μg/ml and 20 μg/ml; ampicillin (Amp), 100 μg/ml.

RNA extractions

Bacteria were grown in 20 ml of TSB-gluc at 37°C under shaking conditions (200 rpm) until the culture reached an OD_{600nm} of 0.8. Cultures were centrifuged, the pellets were frozen in liquid nitrogen and stored at −80°C until needed. Total RNA from bacterial pellets was extracted using the TRIzol reagent method as described (Toledo-Arana *et al.*, 2009). Briefly, bacterial pellets were resuspended into 400 μl of solution A (glucose 10%, Tris 12.5 mM, pH 7.6, EDTA

10 mM) and mixed with 60 µl of 0.5 M EDTA. Resuspended cells were transferred into Lysing Matrix B tubes (MP Biomedicals) containing 500 µl of acid phenol pH 4.5 (Ambion) and mixed. Bacteria were mechanically lysed with a Fastprep apparatus (BIO101) at speed 6.0 during 45 s at 4°C. After lysis, tubes were centrifuged for 10 min at 17,900 g at 4 °C. The aqueous phase was transferred to 2-ml tubes containing 1 ml of TRIzol (Invitrogen), mixed, and incubated for 5 min at room temperature. 100 µl of chloroform were added, mixed gently, and incubated for 3 min at room temperature. Tubes were centrifuged for 10 min at 17,900 g at 4°C. The aqueous phase was transferred into a 2-mL tube containing 200 µl of chloroform, mixed, and incubated for 5 min at room temperature. Tubes were centrifuged for 5 min at 17,900 g at 4°C. RNA contained in the aqueous phase was precipitated by addition of 500 µl of isopropanol and incubated for 15 min at room temperature. Tubes were centrifuged for 15 min at 17,900 g at 4°C. RNA pellets were washed with 75% ethanol. Dried RNA pellets were resuspended in DEPC-treated water. RNA concentrations were quantified, and RNA qualities were determined by using Agilent RNA Nano LabChips (Agilent Technologies). RNAs were stored at −80°C until needed.

cDNA synthesis, fragmentation, labelling and tiling array hybridization

Before cDNA synthesis, RNA integrity from each sample was confirmed on Agilent RNA Nano LabChips (Agilent Technologies). 10 µg of total RNA were reverse transcribed using SuperScript II reverse transcriptase (Invitrogen Life Technologies) and processed following the protocol of the Affymetrix GeneChip Expression Analysis Technical Manual (P/N 702232 Rev. 2) in the presence of 6 ng/ml Actinomycin D to avoid spurious second-strand cDNA synthesis during reverse transcription reaction (Perocchi *et al.*, 2007). Sense RNA corresponding to *B. subtilis* poly-A *lys*, *phe*, *thr*, *trp*, *dap* genes were spiked into sample RNA as

control for labeling and hybridization steps. cDNA was digested by DNase I (PIERCE) in 10X DNAse I buffer (USB-Affymetrix) and the size of digestion products was analyzed in the Agilent Bioanalyser 2100 using RNA Nano LabChips to ensure that the fragmentation resulted in a majority of products in the range of 50 to 200 base-pairs. The fragmented cDNA was then biotinylated using terminal deoxynucleotidyl transferase (Promega) and the GeneChip DNA labeling reagent (Affymetrix) following the manufacturer's recommendations. Biotinylated cDNA (5 microgram per array) was hybridized on custom *S. aureus* tiling microarrays designed as described (Segura *et al.*, 2012). Hybridization was carried out during 16 h according to the Affymetrix protocol in a total volume of 200 µl per hybridization chamber. Following incubation, the arrays were washed and stained in the Fluidics station 450 (Affymetrix) using the protocol n°FS450_0005. Scanning of the arrays was then performed using the GeneChip scanner 3000 (Affymetrix). A first scan of the chip was carried out with gene expression sub-array parameters followed by a second scan with tiling sub-array parameters. Intensity signals of each probe cells were computed by the GeneChip operating software (GCOS) and stored in cell intensity files (.CEL extension) before preprocessing and analysis.

Microarray data analysis

Data analysis of the tiling sub-array was performed using the Tiling Analysis Software (TAS) from Affymetrix (http://www.affymetrix.com). Output bar files containing probe signal values were converted in graphic type files (.gr extension file) to be loaded at the *Staphylococcus aureus* transcriptome browser (http://staph.unavarra.es/).

Construction of cDNA libraries for dRNA-seq, read mapping and statistics analysis

Deep sequencing of RNAs from *S. aureus* 15981 strain was performed as previously described (Lasa *et al.*, 2011). Mapped reads were included in .wig files to be loaded at the *Staphylococcus aureus* transcriptome browser (http://staph.unavarra.es/).

Simultaneous mapping of 5′- and 3′-ends of RNA molecules

The simultaneous mapping of 5′- and 3′-ends of the entire *icaR* mRNA molecule and the processing sites was performed by RACE (Rapid Amplification of cDNA Ends) using circularized RNAs as previously described (Britton *et al.*, 2007), with the following modifications. Specifically, reactions were performed on RNAs extracted from bacteria grown in TSB-gluc until an OD_{600nm} = 0.8 was reached. Six μg of RNA were treated with TURBO DNase I (Ambion). After phenol extraction to inactivate DNase I, the RNA was divided into two aliquots. Both aliquots were incubated for 45 min at 37°C with the corresponding buffer, in the presence or absence of Tobacco Acid Pyrophosphatase, (TAP) (Epicentre biotechnologies) respectively. This step allows discriminating a 5′-end generated by transcription initiation from a 5′-end provided by RNA processing. The TAP treatment step was avoided when processing sites wanted to be determined. After incubation, acid-phenol and chloroform extractions and ethanol precipitation was performed. Serial dilutions (from 500 ng to 0.5 ng) of the TAP+ and TAP- treated RNAs were prepared. Each dilution was ligated with 40 U of T4 RNA ligase I (New England Biolabs) in the presence of 1X RNA ligase Buffer, 8% DMSO, 10 U of RNase Inhibitor, 1 U of DNase I and RNase-free water in a total volume of 25 μl at 17°C overnight. After acid-phenol and chloroform extractions and ethanol precipitation, the ligated RNAs were resuspended in 10 μl of RNase-free water. RT-PCR reactions were performed using specific outward primers

(Table S3) and the SuperScript One-Step RTPCR kit (Invitrogen). RT-PCR products were run on 3% TAE-agarose gels. For mapping of the entire size of the molecule, bands only present in the TAP+ reactions were purified by Gel Extraction kit (QIAGEN) and cloned using TOPO TA Cloning kit (Invitrogen). For mapping of processing sites, all bands observed in the gel were purified and cloned. Eight transformants per cloned band were analysed by PCR using M13 forward and reverse primers. Plasmids containing the expected insert size were sent to sequencing. To determine the localization of the 5'- and 3'-ends, sequences were compared with *icaR* region from the *S. aureus* 132 genome sequence (Vergara-Irigaray *et al.*, 2009).

Riboprobes synthesis

Strand-specific riboprobes to detect *icaR* mRNA were synthesized from a PCR product containing a T7 phage promoter sequence (see Table S3 for oligonucleotides). One microgram of these PCR products was used as a matrix template for *in vitro* transcription reaction with phage T7 RNA polymerase, 0.5 mM each ATP, GTP, CTP, and 50 mCi of [α-32P] UTP using the Maxiscript kit (Ambion). The riboprobes were then treated with TURBO DNase I at 37°C for 30 min, and reactions were stopped by addition of 1µl of 0.5M EDTA. The riboprobes were purified on Bio-Spin 30 columns following the manufacturer's recommendations (Bio-Rad) and were immediately used.

Northern blots

Northern blots were performed as described (Toledo-Arana *et al.*, 2009). Briefly, 8-15 µg of total RNA were separated in precast 1.25% agarose gels (Sigma) by using 1X NorthernMax MOPS as running buffer (Ambion). After electrophoresis, gels were stained with ethidium bromide and photographed to verify equal loading of RNA samples. Then, RNAs were transferred onto Nytran

membranes (0.2 μm pore size) (Sigma) by using NorthernMax One Hour Transfer buffer reagent as described in the manufacturer's protocol (Ambion). RNA was UV cross-linked to the membrane by using the UV Stratalinker 1800 (Stratagene). Membranes were prehybridized for at least 30 min in ULTRAhyb solution (Ambion) at 65°C, followed by addition of labelled strand-specific riboprobe and overnight hybridization at 65 °C. Membranes were then washed twice with 2X SSC-0.1% SDS for 5 min at 65 °C. The size of the transcripts was estimated by comparison with RNA Millenium molecular weight standards (Ambion). Autoradiography images were registered at different exposition times according to each experiment.

Chromosomal allelic exchange

To generate the *icaR* 3′-UTR and *dpbA* deletions, we amplified by PCR two fragments of approximately 500 bp that flanked the left (primers A and B, Table S3) and right sequences (primers C and D, Table S3) of the region targeted for deletion. The PCR products were amplified with Phusion® High-Fidelity DNA Polymerase (Fermentas-Thermo Scientific), purified and cloned separately in pCR®-Blunt II TOPO vector (Invitrogen). Fragments were then fused by ligation into the shuttle vector pMAD (Arnaud *et al.*, 2004). The resulting plasmid was transformed into *S. aureus* 15981 or 132 strains by electroporation. Homologous recombination experiments were performed as described (Valle *et al.*, 2003). Erythromycin sensitive white colonies, which no longer contained the pMAD plasmid, were tested by PCR using primers E and F and DNA sequencing.

Plasmids constructions

All PCR fragments were amplified from *S. aureus* 132 chromosomal DNA using Phusion® High-Fidelity DNA Polymerase (Fermentas-Thermo Scientific) using the appropriate oligonucleotides. PCR fragments were purified and cloned

into pCR®-Blunt II TOPO vector (Invitrogen). DNA fragments were excised from this vector with appropriate restriction enzymes and then subcloned into the shuttle vectors pSA14 (Joanne *et al.*, 2009) or pCN40 (Charpentier *et al.*, 2004). pSA14 plasmid is a pMK4 derivative carrying promoterless *E. coli lacZ* gene for constructing transcriptional fusions while pCN40 plasmid allows the expression of the gene of interest from the constitutive P_{blaZ} promoter. To construct pSA14-Pica plasmid, a 422 bp DNA fragment, which includes the *ica* operon promoter, was amplified with icaA-pSA14-Fw and icaA-pSA14-Rv oligonucleotides. pCN40 plasmid derivatives which expressed different *icaR* mRNA versions from the constitutive P*blaZ* promoter were constructed as follows. pIcaRm plasmid was constructed by amplifying a PCR fragment of 1,079 nt with IcaR+1 and IcaR-Term oligonucleotides and cloning into the BamHI/EcoRI site of pCN40. pIcaRmΔ3'-UTR plasmid was constructed by amplifying a PCR fragment of 748 nt with IcaR+1 and IcaR-Term oligonucleotides using *S. aureus* 132 Δ3'-UTR chromosomal DNA as template and cloning into BamHI/EcoRI sites of pCN40. To construct p^{FLAG}IcaRm_WT, p^{FLAG}IcaRmΔ3'-UTR, pIcaRmΔanti-SD, pIcaRm_SUBST, p^{FLAG}IcaRmΔanti-SD, p^{FLAG}IcaRm_SUBST and pIcaRm-Compensatory plasmids, overlapping PCR was used with oligonucleotides shown in Table S3. All constructed plasmids were confirmed by sequencing.

Quantitative reverse transcription PCR

Total RNA from bacterial cells grown until OD_{600nm} of 0.8 was extracted as described above. Each RNA sample was subjected to TURBO DNase I (Ambion) treatment for 30 min at 37°C. The enzyme was inactivated by phenol-chloroform extractions. RNA quality was assessed with an Agilent 2100 Bioanalyzer. Twenty µl of random primers (50 ng/µl; Invitrogen) and 20 µl of deoxynucleoside triphosphates (dNTPs) (10 mM mix; Invitrogen) were added to the samples containing 8 to 10 µg of RNA in a volume of 100 µl of diethyl pyrocarbonate

(DEPC) water. After 5 min of incubation at 65°C, samples were chilled on ice at least during 1 min, and a reverse transcription (RT) mix containing 44 µl of 5X first-strand buffer (Invitrogen), 22 µl of dithiothreitol (DTT) (0.1 M; Invitrogen), 2 µl of SuperScript III Retrotranscriptase (200U/µl; Invitrogen) and 1 µl of RNase Out (40U/µl; Invitrogen) was added to each preparation. cDNA was obtained after a cycle of 10 min at 25°C, 50 min at 50°C, and 5 min at 85°C. RNA was eliminated by the addition of 1 µl of RNase H (10 U/µl; Invitrogen) and incubation for 20 min at 37°C. cDNA samples were purified with CentriSep spin columns (Princeton separations). cDNA concentration was adjusted to 100 ng/µl. One µl of the cDNA samples was used for real-time quantitative PCR using SYBR green PCR master mix (Applied Biosystems) and the ABI Prism 7900 HT instrument (Applied Biosystems). The PCR was performed under the following conditions: 95°C for 20 s, 40 cycles of 95°C for 1 s and 60°C for 20 s, and a final step at 95°C for 15 s, 60°C for 15 s, and 95°C for 15 s. *icaR* and *gyrB* mRNA levels were quantified by cDNA amplification using oligonucleotides described in Table S3 and values were normalized to those of the housekeeping *gyrB* gene.

Western blot analysis

Overnight cultures of the strains tested were diluted 1:100 in TSB-gluc, and 20 ml of this cell suspension were grown in 125 ml flasks until OD_{600nm} reached 0.8. Ten ml of bacterial cultures were centrifuged and pellets were resuspended in 100 µl PBS. Then, 2 µl of Lysostaphin 1 mg/ml (Sigma) and 3 µl of DNase I 1mg/ml (Sigma) were added. After 2 h of incubation at 37°C cell lysates were centrifuged and supernatants were collected. Protein concentration was determined with the Bio-Rad protein assay (Bio-Rad). Samples were adjusted to 5-10 µg/µl of total protein and one volume of Laemmli buffer was added. Total protein extracts were denatured by boiling at 100°C for 5 min. Proteins were separated on 12% SDS-polyacrylamide gels and stained with 0.25% Coomassie

brilliant blue R250 (Sigma) as loading controls. For Western blotting, proteins were transferred onto Hybond-ECL nitrocellulose membranes (Amersham Biosciences) by semi-dry electroblotting. Membranes were blocked overnight with 5% skimmed milk in phosphate-buffered saline (PBS) with 0.1% Tween 20, and incubated with anti-FLAG antibodies labelled with phosphatase alkaline (Sigma) diluted 1:500 for 2 h at room temperature. 3XFLAG labelled IcaR protein was detected with the SuperSignal West Pico Chemiluminescent Substrate (Thermo Scientific).

mRNA stability assays

Overnight cultures were diluted 1:100 in TSB-gluc, and 150 ml of these cell suspensions were grown in 500 ml flasks until OD_{600nm}=0.8 was reached. Twelve ml of cultures were transferred to six sterile 15 ml falcon tubes containing 300 μg/ml Rifampicin. The tube corresponding to time 0 min also contained 2.5 mL STOP solution (5% phenol equilibrated at pH 7 and 95% of ethanol). After addition of the culture, the time "0 min" tube was immediately centrifuged at 4,500 rpm during 3 min, the supernatant discarded and the pellet frozen in liquid nitrogen. The rest of the tubes were incubated at 37°C and 2.5 ml of STOP solution were added at times 2, 4, 8, 15 and 30 min respectively after rifampicin addition. Then, each tube was centrifuged at 4,500 rpm during 3 min. Supernatants were discarded and pellets were frozen in liquid nitrogen and stored at -80°C until needed. RNA extractions and Northern blots were performed as described above.

Visualization of icaR mRNA dimers on agarose gel electrophoresis

The full-length *icaR* mRNA was produced by *in vitro* transcription using T7 RNA polymerase. To visualize the monomeric form of the mRNA, *icaR* mRNA (0.25 μg) was denatured 3 min at 90°C in 10 μl of sterile bi-distillated water or of a

buffer containing Tris-HCl 20 mM pH 7.5, 1 mM EDTA, chilled on ice for 1 min followed by an incubation at 37°C for 15 min. To visualize alternative conformations of *icaR* mRNA, the mRNA (0.25 µg) was first denatured in 8 µl of sterile bi-distillated water for 3 min at 90°C, chilled on ice, and renatured at 37°C for 15 min by adding 2 µl of a 5 x concentrated buffer containing Tris-HCl 100 mM pH 7.5, 250 mM KCl in the absence or in the presence of 50 mM $MgCl_2$. All samples were then mixed with 2 µl of loading buffer (48% glycerol, 0.01% bromophenol blue) and electrophoresed on 1% agarose gel in 0.5X TBE buffer. The RNA was then visualized after ethidium bromide staining.

Gel shift assays

5′-UTR and 3′-UTR wild-type PCR fragments (117 and 120 nt respectively) used as templates for T7 *in vitro* transcription were amplified using chromosomal DNA from *S. aur*eus 132 strain, while 5′-UTR-compensatory and 3′-UTR-subsituted fragments were amplified from the corresponding plasmids using oligonucleotides shown in Table S3. RNA molecules used as substrates in gel shift assays were synthesized by *in vitro* T7 transcription using Riboprobe in vitro Transcription System (Promega). When needed 50 mCi of [α-32P] UTP was used for radiolabelling. RNA fragments were purified by electrophoresis on an 8.3 M urea/6% polyacrylamide gel. The bands were excised from the gel and RNA was eluted with elution buffer (3 M ammonium acetate pH 5.2, 1mM EDTA, 2.5% (v/v) phenol pH 4.3) overnight at room temperature. Then, RNA was ethanol precipitated, resuspended in RNase free water and quantified using the Biophotometer Plus (Eppendorf). The yield of the labelled substrates (cpm/µl) was determined by scintillation counting.

Binding assays were performed in 1X TMN buffer (20 mM Tris acetate pH7.6, 100 mM sodium acetate, 5 mM magnesium acetate) as previously described (Udekwu *et al.*, 2005). Briefly, labelled RNA molecules (0.025 pmol of

5'-UTR-wt or 5'-UTR-compensatory) were incubated with increasing concentrations of unlabelled RNA fragments (3'-UTR WT or 3'-UTR-substituted) in a total volume of 10 μl, at 37°C for 30 min. Binding reactions were then mixed with 2 μl of loading buffer (48% glycerol, 0.01% bromophenol blue) and electrophoresed on native 5% polyacrylamide gels in 0.5X TBE buffer at 200 V in a cold room for 3h. Gels were analyzed using a PhosphorImager (Molecular Dynamics).

Purification of recombinant S. aureus RNase III

S. aureus RNase III coding sequence (*rnc*) was amplified with primer pairs RNAse III Fw (NdeI) and RNAse III Rv (BamHI). The purified PCR fragment was double digested with BamHI and NdeI and ligated into the pET-15b vector (Promega), generating plasmid pET-15b RNAse III. This plasmid was transformed in *E. coli* BL21(DE3) *rnc*105 *recA*. This strain is slow growing but allows overproduction of His_6-RNase III (Amarasinghe *et al.*, 2001). The BL21(DE3) *rnc*105 *recA* strain carrying the pET-15b RNAse III plasmid was grown in 200 ml of LB medium supplemented with ampicillin (100 μg/ml) to an OD_{600nm} of 1.5. At this point, protein expression was induced by addition of 1 mM IPTG and the culture was further incubated overnight at 15°C. Cells were then harvested by centrifugation, the pellet was washed with 12 ml of cold buffer (25 mM Tris-HCl pH 8.0, 8% ammonium sulphate, 0.1 mM EDTA) and resuspended in 6 ml of the same buffer. Cells were lysed using a French Press at 900 psi in the presence of 0.1 mM of PMSF. After lysis, the crude extracts were treated with 125 U of Benzonase (Sigma). The protein extract was then clarified by centrifugation for 30 min, 27.000 g at 4°C. The histidine tagged recombinant RNase III was purified by affinity chromatography, using the ÄKTA FPLCTM System (GE Healthcare). The clarified extracts were loaded into a HisTrap HP Sepharose 1 ml column. Protein elution was achieved with a linear imidazole gradient (from 0

mM to 300 mM) in buffer B (25 mM Tris-HCl pH 8.0, 1M NH_4Cl, 300 mM imidazole). Fractions containing the protein of interest, free of contaminants, were pooled and buffer exchanged by dialysis against Desalting Buffer (25 mM Tris-HCl pH 8.0, 500 mM KCl, 0,1 mM DTT, 50 % glycerol) using a Slide-A-Lyzer Dialysis Cassette (Thermo Scientific) with a molecular mass cut-off of 10 kDa. Protein samples were quantified using the Bio-Rad protein assay (Bio-Rad) and stored at -20°C. The purity of the enzyme was analysed by SDS-PAGE.

RNase III activity assays

RNA substrates were prepared as described in the Gel shift assays section. The activity of purified RNase III was tested over [^{32}P]-α-UTP labelled 5′-UTR-WT fragment in the presence or absence of 3′-UTR-WT or 3′-UTR-substituted fragments. Hybridization between labelled and unlabelled substrates was performed in a 1:50 molar ratio in the Tris component of the activity buffer by incubation for 10 minutes at 80°C, followed by 45 minutes at 37°C. The same treatment was applied to free 5′-UTR-WT. Activity assays were carried out in a final volume of 40 µl containing the activity buffer (30 mM Tris-HCl pH 8, 160 mM NaCl and 0.1 mM DTT) and approximately 0.14 pmol of substrate. 10 mM $MgCl_2$ were added to the reaction mixture. As a control, prior to the beginning of each assay, an aliquot (without the enzyme) was taken and incubated in the same conditions until the end of the assay. Reactions were started by the addition of the enzyme at a concentration of 500 nM and were incubated at 37°C (Chelladurai *et al.*, 1991). Samples were withdrawn at different times and reactions were stopped by the addition of formamide-containing dye supplemented with 10 mM EDTA. Reaction products were run in a 7M urea/10% polyacrylamide gel, visualized by PhosphorImaging and analyzed using ImageQuant software (Molecular Dynamics).

Toeprinting assays

Full length *icaR* mRNA or its variants were cloned (Serganov *et al.*, 1997) into StuI and BamHI restriction sites of pUT7 plasmid for *in vitro* transcription. The whole 5′-UTR including 72-nt of the ORF and the 3′-UTR (186 nt) were transcribed from PCR products obtained with oligos T7 5′-UTR and IcaR 5′ rev, and T7 3′-UTR and IcaR 3′ rev, respectively (Table S3). *S. aureus* 30S ribosomal subunits were prepared as described (Fechter *et al.*, 2009). The formation of a simplified translation initiation complex with mRNAs and the extension conditions were as described (Fechter *et al.*, 2009). Standard conditions contained 5 nM *icaR* mRNA or *icaR* 5′-UTR annealed to a 5′-end labeled oligonucleotide (IcaR 5′ rev), 500 nM *S. aureus* 30S ribosomal subunits, and 0.5 to 10 μM of *icaR* 3′-UTR in 10 μl of buffer containing 20 mM Tris-acetate pH 7.5, 60 mM NH_4Cl, 8.5 mM magnesium acetate and 1 mM DTT. The 30S subunits were renatured for 10 min at 37°C before incubation with the mRNAs. After 10 min of incubation at 37°C, the initiator tRNA (1μM) was added, and the reaction was further incubated for 5 min at 37°C. Reverse transcription was conducted with one unit of AMV reverse transcriptase for 15 min at 15°C. Toeprint was run on 8% polyacrylamide gels and visualized by autoradiography.

PIA-PNAG quantification

Cell surface PIA/PNAG exopolysaccharide levels were quantified as previously described (Cramton *et al.*, 1999). Briefly, overnight cultures of the strains tested were diluted 1:40 in the appropriate medium and 2 ml of this cell suspension were used to inoculate sterile 24-well polystyrene microtiter plates (Sarstedt). After 24 h of static incubation at 37°C, the same number of cells of each strain was resuspended in 50 μl of 0.5 M EDTA (pH 8.0). Then, cells were incubated for 5 min at 100°C and centrifuged 17,000 g for 5 min. Each supernatant (40 μl) was incubated with 10 μl of proteinase K (20 mg ml^{-1}) (Sigma) for 30 min at

37°C. After the addition of 10 µl of Tris-buffered saline (20 mM Tris-HCl, 150 mM NaCl [pH 7.4]) containing 0.01% bromophenol blue, 5 µl were spotted on a nitrocellulose membrane using a Bio-Dot microfiltration apparatus (Bio-Rad). The membrane was blocked overnight with 5% skimmed milk in phosphate-buffered saline (PBS) with 0.1% Tween 20, and incubated for 2 h with specific anti-PNAG antibodies diluted 1:10,000 (Maira-Litran *et al.*, 2005). Bound antibodies were detected with peroxidase-conjugated goat anti-rabbit immunoglobulin G antibodies (Jackson ImmunoResearch Laboratories, Inc., Westgrove, PA) diluted 1:10,000 and developed using the SuperSignal West Pico Chemiluminescent Substrate (Thermo Scientific).

Biofilm formation assay

To analyze biofilm formation under flow conditions, we used 60-ml microfermentors (Ghigo, 2001) (Pasteur Institute; www.pasteur.fr/recherche/unites/Ggb/biofilmfermenter.html) with a continuous flow of 40 ml of TSB/h and constant aeration with sterile pressed air as previously described (Valle *et al.*, 2003). Submerged Pyrex slides served as the growth substratum. 10^8 bacteria from an overnight preculture grown in TSB-gluc of each strain were used to inoculate microfermenters and were cultivated 8 h at 37°C. Biofilm development was recorded with a digital camera.

RESULTS

Identification of long 3′-UTRs in the S. aureus transcriptome

Finding the 5′ boundaries of mRNAs is a critical step for transcriptional promoter recognition. Thus, in general, bacterial transcriptome analyses have been focused on the identification of mRNA 5′-ends while mRNA 3′ ends

mapping has been mostly disregarded, limiting our knowledge about the molecular features inside this mRNA region. To overcome this limitation, we have examined genome wide the 3′ boundaries of the *S. aureus* transcriptome by combining RNA-seq data obtained in a previous study (Lasa *et al.*, 2011) with tiling array hybridization data of four genetically unrelated *S. aureus* strains. The normalized tiling arrays signals and the mapped reads were integrated in a web repository that enables the visualization of the transcriptome information (*Staphylococcus aureus* Transcriptome Browser, http://staph.unavarra.es/). We calculated the 3′-UTR length of each mRNA as the distance between the annotated translational stop codon of the corresponding ORF and the last position of RNA reads downstream. Only 3′-UTRs that were present in the four strains analysed by tiling were considered in the analysis and, whenever possible, the position of the predicted intrinsic Rho-independent transcriptional terminator was calculated according to the TransTermHP v2.07 program (Kingsford *et al.*, 2007). As a result, we identified 1055 mRNAs carrying bona *fide* 3′-UTRs, that is, transcripts ending at an intrinsic TT (Figure 1 and Figure S1). Remarkably, 34.8% of these mRNAs contained 3′-UTRs longer than 100 nt. Also, we found that transcription of about one third of the mRNAs carrying *bona fide* 3′-UTRs may continue downstream the predicted TTs, thus generating a long terminating-read-through-dependent 3′-UTR (Figure 1 and Figure S1). These 3′-UTRs showed the longest size and usually overlapped with the mRNAs encoded at the opposite DNA strand. This antisense regulation is subsequently followed by RNA degradation induced by the endoribonuclease III (RNase III) (Lasa *et al.*, 2011). Confirming our previous findings in *L. monocytogenes* (Toledo-Arana *et al.*, 2009), we found 24 riboswitch-dependent 3′-UTRs, all of them presenting a length higher than 100 nt (Figure 1 and Figure S1). In this type of 3′-UTRs, the TT generated when the riboswitch is in an OFF conformation also acts as the TT of the gene encoded upstream of the riboswitch. As a consequence, the 3′-UTR

includes the riboswitch sequence. Taken together, these findings indicate that the presence of long 3′UTRs is very frequent in the *S. aureus* transcriptome and can generate diverse regulatory mechanisms.

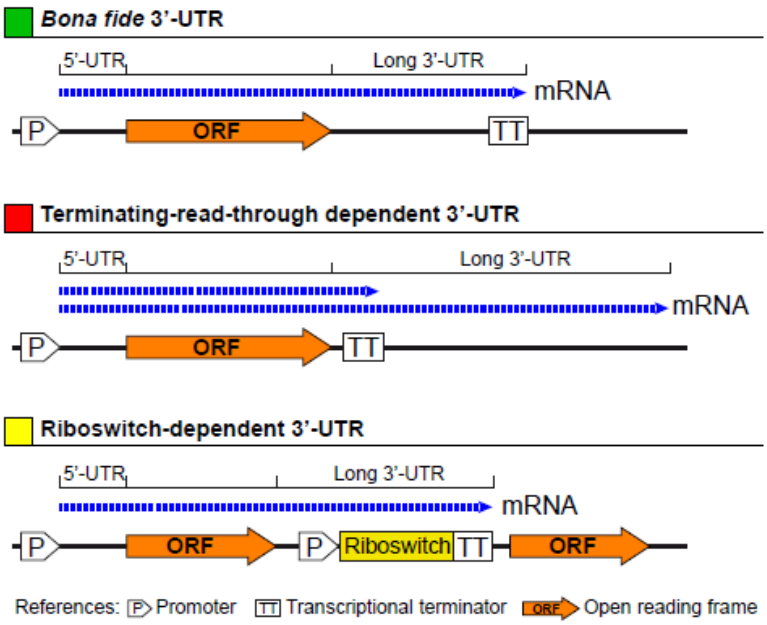

Figure 1 - Schematic representation of how long bacterial 3′-UTRs can be generated. A transcript ending in a transcriptional terminator located far away from the corresponding protein stop codon generates a *bona fide* long 3′-UTR. In other cases, despite the presence of a transcriptional terminator (TT) close to the end of the protein stop codon, transcription may continue downstream the predicted TT, generating a terminating-read-through-dependent long 3′-UTR. In addition, several transcripts end at a TT that is part of the expression platform of a riboswitch. In this case the long 3′-UTRs will be generated only when the riboswitch is in an OFF configuration. Otherwise, if the riboswitch is in an ON configuration, a polycistronic transcript is generated.

The icaR mRNA contains a highly conserved long 3′-UTR

To evaluate whether long 3′-UTRs have a regulatory role in *S. aureus*, we focused on *bona fide* long 3′-UTRs and exclusively concentrated on non-overlapping long 3′-UTRs in order to avoid possible effects due to antisense

regulation. Due to the relevance of biofilm formation during *S. aureus* infection, we chose the *bona fide* long 3'-UTR of *icaR* transcript (Figure S2), that encodes for a repressor of biofilm formation, as a model to examine whether long 3'-UTRs play a role in regulating the fate of the mRNA and/or its translation process. We first validated the *icaR* mRNA boundaries using a specialized mRACE protocol that uses circularized RNAs (Toledo-Arana *et al*., 2009). mRACE experiments located *icaR* mRNA 5' transcriptional start site (TSS) 72-nt upstream from the start codon and the transcriptional termination site (TTS) 390-nt after the stop codon, immediately downstream of the predicted Rho-independent transcriptional terminator (Figure 2A). Northern blot analysis using either a probe complementary to the 3'-UTR region or to the coding region, confirmed the presence of a band of ~1 Kb that is consistent with the 1023-nt mRNA molecule mapped by mRACE (Figure 2B). We next excluded that the 3'-UTR codes for a peptide using Glimmer v3.02 at the NCBI web page. From these experiments we concluded that *icaR* mRNA contains a long *bona fide* 3'-UTR that accounts for 38% of the complete mRNA molecule (Figure 2A).

Sequence conservation between intergenic regions of different bacterial species has been traditionally used to identify regulatory non-coding RNAs (Wassarman *et al*., 2001). Indeed, non-coding regions are more permissive to nucleotide substitutions than protein-coding regions, unless the sequence of the "non-coding" region plays a functional role. We compared sequence conservation of the coding sequence and also of the 3'-UTR inside *icaR* mRNA in the 173 *S. aureus* genomes available at the Microbes database from NCBI. Nucleotide variation analysis showed that 19 nt out of the 561 nt corresponding to *icaR* ORF were variable (3.4%). In the case of the 390 nt 3'-UTR, an accumulation of 26 nt changes occurred, which accounts for a 6.6% of this region. In contrast, the region comprised between the TTS of *icaR* mRNA and the TSS of the neighbour *capA* gene transcript showed a variation of 18.8% (Figure S3A). A similar analysis was

carried out with the RNAIII molecule, which is a multifunctional regulatory RNA that encodes δ-hemolysin, and that also contains a long 3′-UTR of 352 nt acting as an antisense RNA to repress the translation of target mRNAs (Felden *et al.*, 2011). Results again showed a very little nt variation inside both the coding region and the 3′-UTR when compared to the number of changes occurring downstream RNAIII (Figure S3B). Overall, the high degree of conservation present in the 3′-UTR of *icaR* transcript strengthened our hypothesis that this region might play a functional role in *S. aureus*.

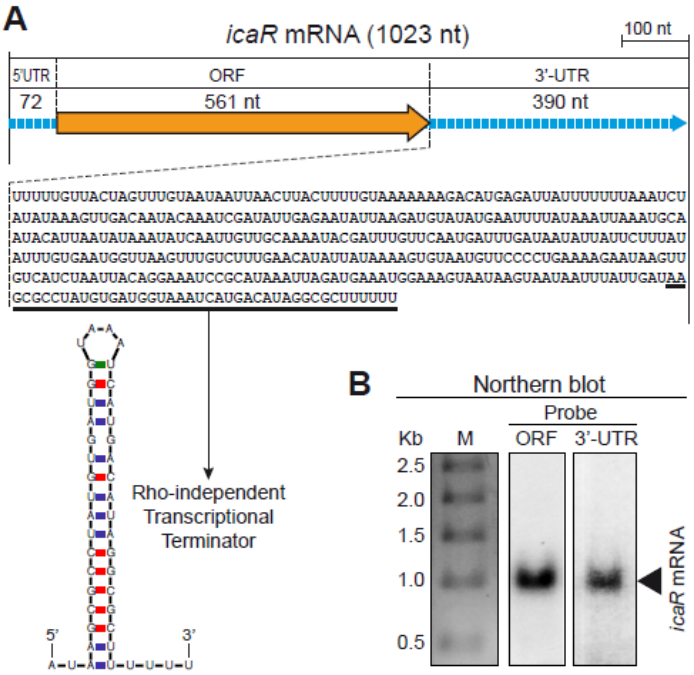

Figure 2 - *icaR* mRNA contains a conserved long 3′-UTR. (A) Schematic representation of the *icaR* mRNA molecule, mapped by RACE, showing the length of the 5′-UTR, ORF and 3′-UTR. The nucleotide sequence of the 3′-UTR is shown. The sequence of the transcriptional terminator is underlined and its secondary structure, predicted by Mfold, is shown. **(B)** Northern blots carried out with two different riboprobes, one targeting the *icaR* ORF region and the other, the *icaR* mRNA 3′-UTR.

The icaR mRNA contains a highly conserved long 3′-UTR

We then sought to determine whether the long 3′-UTR of *icaR* mRNA modulates the expression of the IcaR protein. We generated an isogenic mutant carrying a 330-bp chromosomal deletion that removes most of the 3′-UTR of *icaR* but preserves the intrinsic TT integrity in the *S. aureus* 15981 strain (Figure 3A). We then measured *icaR* mRNA levels of wild-type and mutant cells grown until exponential phase (OD_{600nm}=0.8) by qRT-PCR. Results showed that deletion of the 3′-UTR induced a ~3-fold increase in *icaR* mRNA levels (P=0.0286) (Figure 3B). This increase was also observed by Northern blot (Figure 3C). Note that the presence of a band corresponding to the expected ~0,7 kb in the Northern-blot implies that the deletion of the 3′-UTR did not affect transcription termination of the mutated *icaR* mRNA (Figure 3C). Next, we asked whether the increase in the amount of *icaR* mRNA correlated with higher levels of IcaR protein. We tagged the chromosomal copy of *icaR* gene with the 3XFLAG sequence in both the wild-type and Δ3′-UTR mutant strains. Results showed that Δ3′-UTR mutant strain produced significantly higher levels of IcaR protein compared to the wild-type strain (Figure 3D).

The increase in the amount of *icaR* mRNA/IcaR protein in the absence of the 3′-UTR could be explained either by the existence of higher transcriptional rates from the *icaR* promoter or by an increased stability of *icaR* mRNA or even by a combination of both processes. To distinguish between these possibilities, we uncoupled transcriptional and post-transcriptional regulatory mechanisms by ectopically expressing either the entire *icaR* mRNA or the *icaR* mRNA lacking the 3′-UTR under the control of a constitutive promoter. In both cases, IcaR was tagged with a 3XFLAG epitope at the N-terminal generating plasmids p^{FLAG}IcaRm_WT and p^{FLAG}IcaRmΔ3′-UTR (Figure 3E). Western blot analysis revealed that IcaR protein was produced in higher levels (~4 fold) in the strain harbouring p^{FLAG}IcaRmΔ3′-UTR compared to the strain harbouring

p^{FLAG}IcaRm_WT (Figure 3F). This result suggests that the 3′-UTR mediated regulation occurs at the post-transcriptional level.

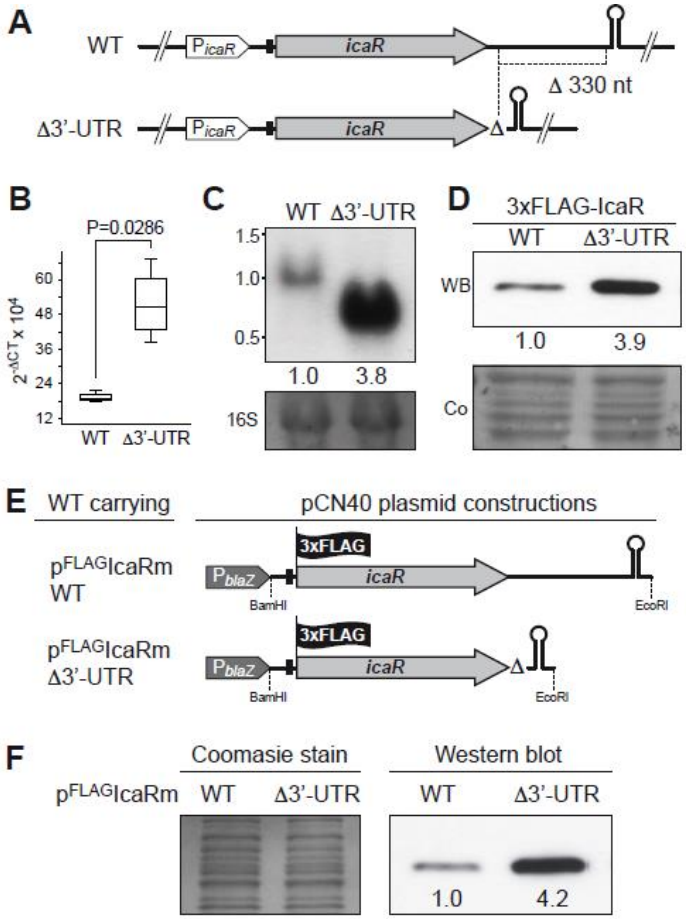

Figure 3 - *icaR* 3′-UTR post-transcriptionally regulates IcaR expression. (A) Schematic representation of chromosomal 3′-UTR deletion. Note that the transcriptional terminator is not affected by the deletion. **(B)** qRT-PCR analysis of *icaR* mRNA levels in *S. aureus* 15981 wild-type and Δ3′-UTR strains grown in TSB-gluc at 37°C until exponential phase (OD_{600nm}=0.8). The *gyrB* transcript was used as an endogenous control, and the results were expressed as the n-fold difference relative to the control gene ($2^{-\Delta Ct}$, where ΔCt represents the difference in threshold cycle between the target and control genes). **(C)** A representative Northern blot showing *icaR* mRNA of wild-type and Δ3′-UTR strains grown in TSB-gluc at 37°C until exponential phase (OD_{600nm}=0.8). Lower panel shows 16S ribosome band stained with ethidium bromide as loading control. **(D)** A representative Western blot showing IcaR protein levels expressed from strains shown in panel A. The 3XFLAG tagged IcaR protein was detected with commercial anti-3XFLAG antibodies.

Numbers below the image show relative band quantification according to densitometry analysis performed with ImageJ (http://rsbweb.nih.gov/ij/). A Coomasie stained gel portion is shown as loading control. **(E)** Schematic representation of plasmid constructions constitutively expressing the 3XFLAG tagged IcaR protein from the whole *icaR* mRNA or the mRNA carrying the 3'-UTR deletion. **(F)** A representative Western blot showing IcaR protein levels of strains shown in panel E. The 3XFLAG tagged IcaR protein was detected with commercial anti-3XFLAG antibodies. Densitometry analysis is also shown. On the left, a Coomasie stained gel portion is shown as loading control.

We then explored the possibility that the 3'-UTR may reduce mRNA stability. A comparison of *icaR* mRNA stability revealed that *icaR* mRNA half-life increased from 2.1 min in the wild-type to more than 10 min in the Δ3'-UTR strain (Figure 4A and B). Degradation of mRNA can follow several pathways involving a combination of exo- and endoribonucleases and RNA-binding proteins (Arraiano *et al.*, 2010; Belasco, 2010). In order to determine the proteins involved in *icaR* mRNA decay, we compared the relative abundance of IcaR protein in the wild-type 15981 *S. aureus* strain and isogenic deletion mutants in proteins that might affect mRNA stability such as PNPase, RNase III, RNA helicases and Hfq. Our reasoning was that the IcaR protein should accumulate in the mutants coding for proteins that might be required for *icaR* mRNA decay. The results revealed that only deletion of *rnc*, which encodes RNase III, an endoribonuclease able to degrade double stranded RNA, caused a significant increase in IcaR levels (Figure 4C). Accordingly, *icaR* mRNA half-life increased from 2.1 min in the wild-type to 7.5 min in the *rnc* mutant (Figure 4A and B). Taken together, these results provide compelling evidence that the 3'-UTR is involved in regulating *icaR* mRNA decay in a process that is dependent, at least in part, on RNase III activity.

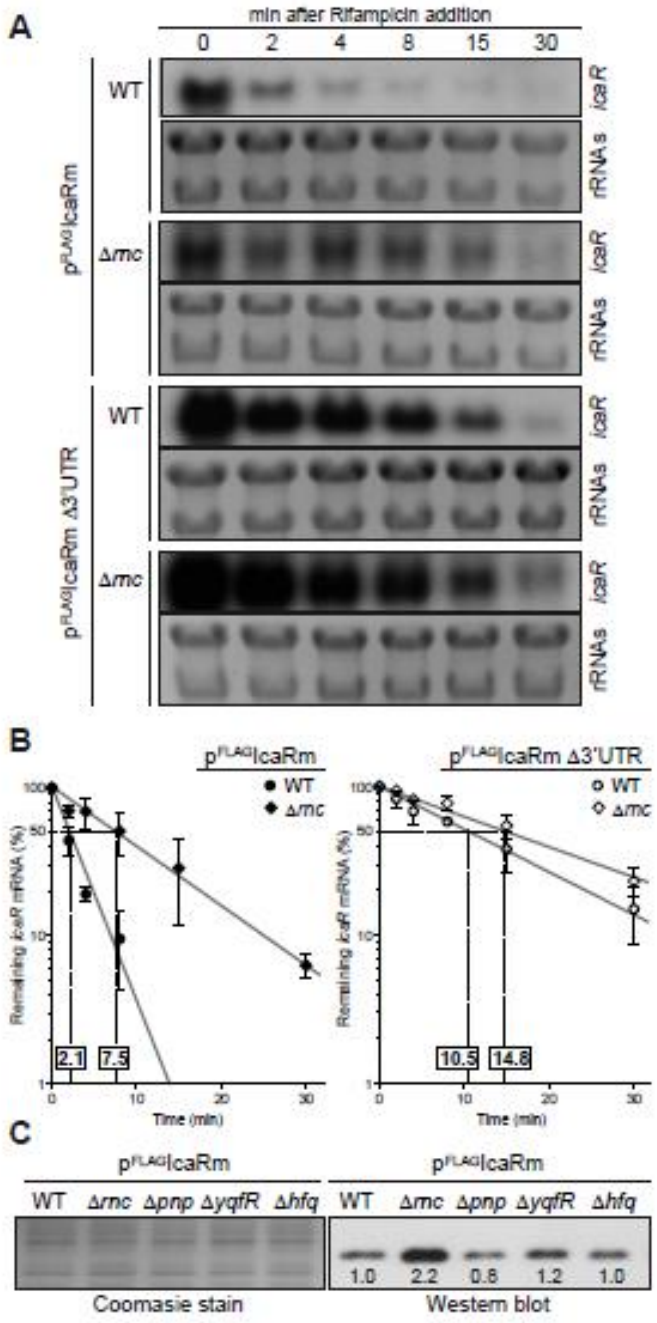
A
min after Rifampicin addition
0 2 4 8 15 30
WT
Δrnc
pFLAGIcaRm
WT
Δrnc
pFLAGIcaRm Δ3'UTR
icaR
rRNAs
B
pFLAGIcaRm
pFLAGIcaRm Δ3'UTR
WT
Δrnc
Remaining icaR mRNA (%)
Time (min)
2.1
7.5
10.5
14.8
C
pFLAGIcaRm
WT Δrnc Δpnp ΔyqfR Δhfq
1.0 2.2 0.8 1.2 1.0
Coomasie stain
Western blot

Figure 4 - Deletion of *rnc* gene, which encodes the double stranded endoribonuclease RNase III, affects *icaR* mRNA stability and IcaR protein levels. (A) Half-life measurement of *icaR* wild-type and Δ3′-UTR mRNAs constitutively expressed in the wild-type and Δ*rnc* mutant strains. These strains were grown in TSB-gluc at 37°C until exponential phase (OD_{600nm}=0.8) and then rifampicin (300 µg/ml) was added. Samples for RNA extraction were taken at the indicated time points (min). The experiment was repeated three times and representative images are shown. **(B)** Levels of *icaR* mRNA were quantified by densitometry of Northern blot autoradiographies using ImageJ (http://rsbweb.nih.gov/ij/). Each of mRNA levels was relativized to mRNA levels at time 0. The logarithm values of relative mRNA levels were subjected to linear regression analysis and plotted as a function of time. Error bar indicates the standard deviation of mRNA levels from three independent experiments. The dashed line indicates the time at which 50% of mRNA remained. The half-life of mRNAs is shown above of X-axis. **(C)** Representative Western blot showing IcaR protein levels in different mutant strains constitutively expressing the 3XFLAG tagged IcaR from the P*blaZ* promoter. Tagged IcaR protein was detected with commercial anti-3XFLAG antibodies. On the left, a Coomassie stained gel portion is shown as loading control. *rnc*, double-stranded endoribonuclease RNase III; *pnp*, polynucleotide phosphorylase PNPase; *yqfR*, (SAOUHSC_01659), ATP-dependent RNA helicase containing a DEAD box domain; *hfq*, RNA chaperone, host factor-1 protein.

Base-pairing interaction between 3′- and 5′-UTR of icaR mRNA

RNA secondary structures play key roles in posttranscriptional regulatory mechanisms including RNA decay (Arraiano *et al.*, 2010), recruitment of RNA-binding proteins (Babitzke *et al.*, 2009) and riboswitches (Serganov and Nudler, 2013; Winkler and Breaker, 2005). To gain insight into the 3′-UTR mediated *icaR* mRNA decay, the secondary structure of *icaR* mRNA was predicted using the Mfold program (http://mfold.rit.albany.edu/) [36]. Surprisingly, the prediction showing the lowest energy (initial DG= -230.50 Kcal mol-1) revealed a pairing between the 3′-UTR region (from 890 to 982-nt) and the 5′-UTR SD region (from 4 to 67-nt) of *icaR* mRNA (Figure S4). The predicted 3′-5′-UTR interacting region comprised around 40 base-paired nucleotides (including G-U interactions).

Because the interaction between the 3′-UTR and the 5′-UTR can be formed either in *cis* or *trans*, we analysed if the full-length *icaR* mRNA was able to

fold into various conformations *in vitro*. As expected the mRNA, which was renatured in the TE buffer, migrated as a single band on an agarose gel. In contrast, the *icaR* mRNA which was renatured at 37°C in a buffer containing KCl and $MgCl_2$, presented two distinct bands (Figure S5). The slower migrating band corresponded to a molecular mass consistent with a dimeric form of *icaR* mRNA (Figure S5).

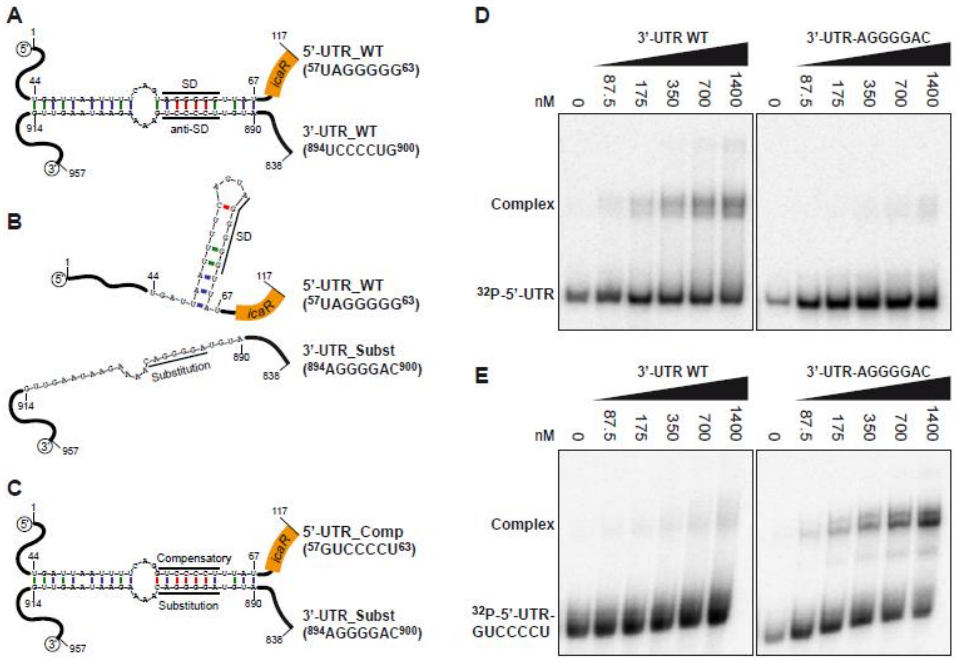

Figure 5 - A UCCCCUG motif is necessary for the interaction between the 3′-UTR and the Shine-Dalgarno region of *icaR* mRNA *in vitro*. (A) Schematic representation of the 3′-5′-UTR interaction. A UCCCCUG motif located at the 3′-UTR pairs the UAGGGGG Shine-Dalgarno region located at the 5′-UTR. The numbers indicate the relative position of the nucleotides in the full-length *icaR* mRNA. **(B)** Substitution of the ^{894}UCCCCUG^{900} motif by ^{894}AGGGGAC^{900}, disrupts the pairing predicted by Mfold program. **(C)** Introduction of a compensatory mutation sequence (^{57}GUCCCCU^{63}) in the 5′-UTR, complementary to the substituted ^{894}AGGGGAC^{900} motif, restores complex formation. **(D)** Gel shift analysis of the 5′ and 3′-UTR *icaR* mRNA interaction. The ^{32}P-labeled 5′-UTR fragment (1-117-nt) was incubated with increasing concentrations of unlabeled 3′-UTR (3′-UTR WT) or substituted 3′-UTR (3′-UTR-AGGGGAC) (838-957-nt). **(E)** Similarly, the ^{32}P-labeled compensatory-5′-UTR fragment (^{32}P-5′-UTR-GUCCCCU) was incubated with increasing concentrations of unlabeled 3′-UTR (3′-UTR WT) or substituted 3′-UTR (3′-UTR-AGGGGAC). After 30 min

of incubation at 37°C, the mixture was analysed by electrophoresis in a native 5% polyacrylamide gel and autoradiography.

A more detailed analysis of the predicted secondary structure revealed that the pairing region includes a ^{894}UCCCCUG^{900} motif located 260-nt downstream of the IcaR stop codon complementary to the SD region (^{57}UAGGGGG^{63}) (Figure 5A and S4). This UCCCC sequence motif has been previously described in several sRNAs of *S. aureus* where it promotes fast binding to target mRNAs and prevents the formation of the ribosomal initiation complex (Boisset *et al.*, 2007; Geissmann *et al.*, 2009a). To experimentally monitor the interaction between the ^{57}UAGGGGG^{63} and ^{894}UCCCCUG^{900} motifs, we performed RNA gel shift assays using a ^{32}P-labeled 5′-UTR fragment (117-nt) including the SD sequence and increasing concentrations of a 3′-UTR fragment (120-nt) containing either the wild-type ^{894}UCCCCUG^{900} or a substituted ^{894}AGGGGAC^{900} motif, which disrupts sequence pairing predicted by Mfold program (Figure 5B). The data showed that the 3′-UTR fragment binds to the 5′-UTR fragment carrying the SD with rather low affinity binding (>700 nM). However this interaction is specific because substitution of the ^{894}UCCCCUG^{900} motif by ^{894}AGGGGAC^{900} severely decreased binding with the 5′-UTR fragment (Figure 5D). Introduction of a compensatory mutation (^{57}GUCCCCU^{63}) in the SD sequence complementary to the substituted ^{894}AGGGGAC^{900} motif restored complex formation (Figure 5C and 5E). Together, these data show that the *icaR* mRNA 3′-UTR specifically anneals to the 5′-UTR in a region that overlaps with the ribosome-binding site.

The 3′-5′-UTRs pairing provides a substrate for RNase III cleavage

Because pairing between the 3′ and 5′-UTRs creates a double stranded region, we sought to determine whether RNase III was capable of cleaving *icaR* mRNA at the pairing region. We performed *in vitro* cleavage assays using a uniformly ^{32}P-labelled 5′-UTR fragment mixed with the 3′-UTR fragment in the

presence of the purified recombinant *S. aureus* RNase III. Results showed that RNase III is able to cleave the 5′-UTR fragment, only in the presence of the 3′-UTR, generating two bands. Thus, we could not detect processed bands either in the absence or in the presence of a 3′-UTR with the AGGGGAC substituted motif (Figure 6A).

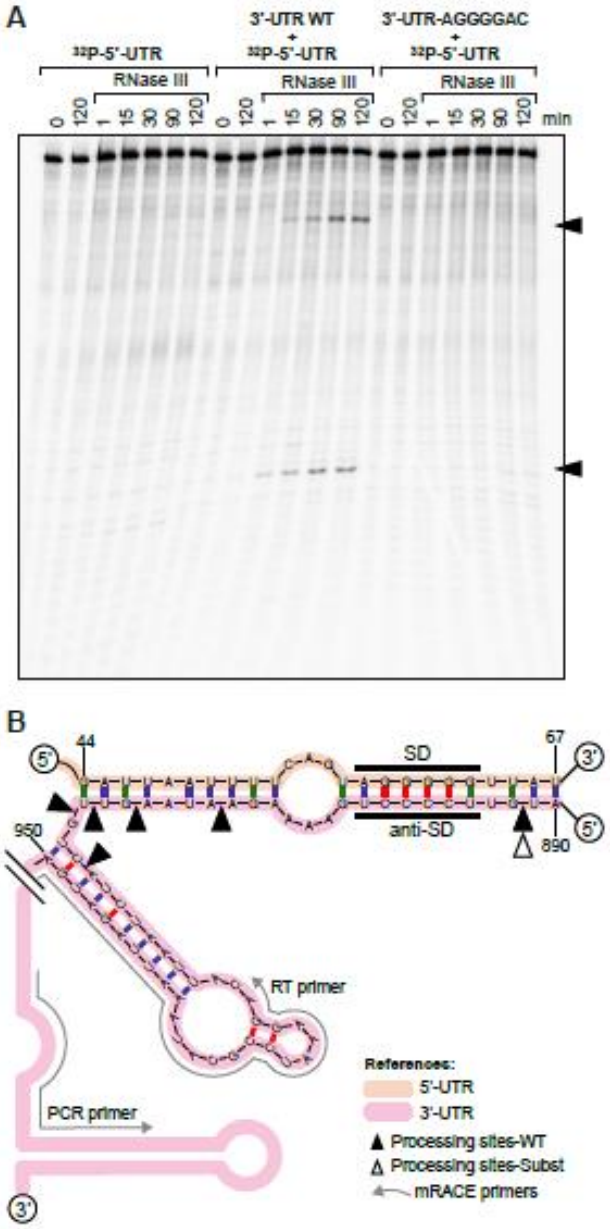

Figure 6 - *In vitro* and *in vivo* RNase III-mediated processing of the double stranded region generated by *icaR* mRNA 5′ and 3′-UTR regions pairing. (A) *In vitro* RNase III activity assay. A ^{32}P-labelled 5′-UTR fragment was incubated with purified recombinant *S. aureus* RNase III during different times in the absence or presence of either the 3′-UTR fragment or the substituted 3′-UTR fragment. The two RNA bands that are generated by

the presence of the wild-type 3′-UTR are indicated with arrows. **(B)** Schematic representation showing *in vivo* mRACE results. Mapping of *icaR* mRNA fragments naturally generated *in vivo* was carried out with circularized RNAs and two outward primers (RT and PCR) that pair next to the transcriptional terminator. Black and white triangles indicate *in vivo* processing sites identified in the *icaR* mRNA wild-type and the *icaR* mRNA with the UCCCC substitution respectively.

To test whether our *in vitro* assay mimicked RNase III capacity to cleave the 3′-5′-UTR duplex of *icaR* mRNA *in vivo*, we performed mRACE analysis with circularized RNA from extracts purified from the wild-type, the 3′-UTR *icaR*-SUBST and *rnc* mutant strains. Results showed several processing sites located at the double stranded region of the UCCCC motif when wild-type RNA was used (Figure 6B). In contrast, we were able to detect only one processing site at the UCCCC region in the 3′-UTR *icaR*-SUBST strain. In agreement with the *in vitro* results, no processing sites could be detected in the assay performed with the RNA extract purified from the Δ*rnc* mutant. These results are consistent with the conclusion that RNase III directs the processing of a double stranded region formed by the pairing between *icaR* 3′-UTR and 5′-UTR both *in vitro* and *in vivo*.

Interaction between icaR 3′-UTR and SD regions prevents the formation of the translational initiation complex

Because the interaction of the 3′-UTR with the 5′-UTR of *icaR* mRNA coincides with the ribosome binding site (RBS), we expected that the 3′-UTR should prevent ribosome loading on the *icaR* mRNA. Toeprint assays were performed to analyze the formation of the ternary ribosomal initiation complexes including purified *S. aureus* 30S ribosomes, initiator $tRNA^{Met}$ and various fragments of *icaR* mRNA. The experiment was first done on a truncated version of *icaR* mRNA containing the whole 5′-UTR and 75 nts from the coding sequence (Figure 7A). As expected, the formation of the ternary complex was able to block the elongation of a cDNA primer by reverse transcriptase (RT) to produce a

toeprint signal at 16 nt downstream of the initiation codon (Figure 7A). The addition of increasing concentrations of the 3′-UTR significantly reduced ribosome loading onto the *icaR* mRNA in a concentration-dependent manner. In contrast, increasing amounts of the mutated 3′-UTR *icaR*-SUBST, that cannot form a complex with the *icaR* mRNA (Figure 5), did not prevent ribosome loading onto the mRNA (Figure 7A and 7B). We then compared the ability of the *S. aureus* 30S to recognize the 5′-UTR and the whole mRNA (Figure 7C). Quantification of the data showed that the 5′-UTR fragment of *icaR* is recognized by the 30S more efficiently than the full-length mRNA (Figure 7D). In addition, a RT pause at the SD sequence was slightly stronger with the full-length mRNA than with the 5′-UTR (Figure 7C). We also have performed toeprinting assays on *S. aureus spa* mRNA which carries a short 5′-UTR, an unstructured ribosome binding site, and a similar SD and initiation codon as found in *icaR* mRNA (Figure S6A). The data showed that a large proportion of *spa* mRNA was able to form an active initiation complex, and that the 30S recognized *spa* mRNA better than the 5′-UTR and the full-length *icaR* mRNA (Figure S6B and C). All in all, these results indicate that pairing between the 3′-UTR and the SD region specifically hinders ribosome binding to the *icaR* transcript and that the 5′-UTR is weakly recognized by *S. aureus* 30S.

To demonstrate that the ^{894}UCCCCUG^{900} motif is able to regulate IcaR synthesis *in vivo*, we evaluated IcaR protein levels of wild-type and RNase III mutant strains harbouring plasmids that constitutively expressed *icaR* mRNA derivatives with a deletion of the ^{894}UCCCCUG^{900} motif (p^{FLAG}IcaRm Δanti-SD) or carrying the substitution of this motif by ^{894}AGGGGAC^{900} (p^{FLAG}IcaRm SUBST) (Figure 7E). Strains expressing *icaR* mRNA derivatives with a deletion or substitution of the UCCCCUG motif accumulated higher levels of IcaR protein, compared to the strain producing wild-type *icaR* transcript (Figure 7F). Interestingly, accumulation of IcaR protein was the highest in the Δ*rnc* mutant

strain expressing the *icaR* mRNA with the UCCCCUG substitution (Figure S6). These results strongly suggest that both processes, inhibition of ribosome loading and cleavage by RNase III, regulate the IcaR levels.

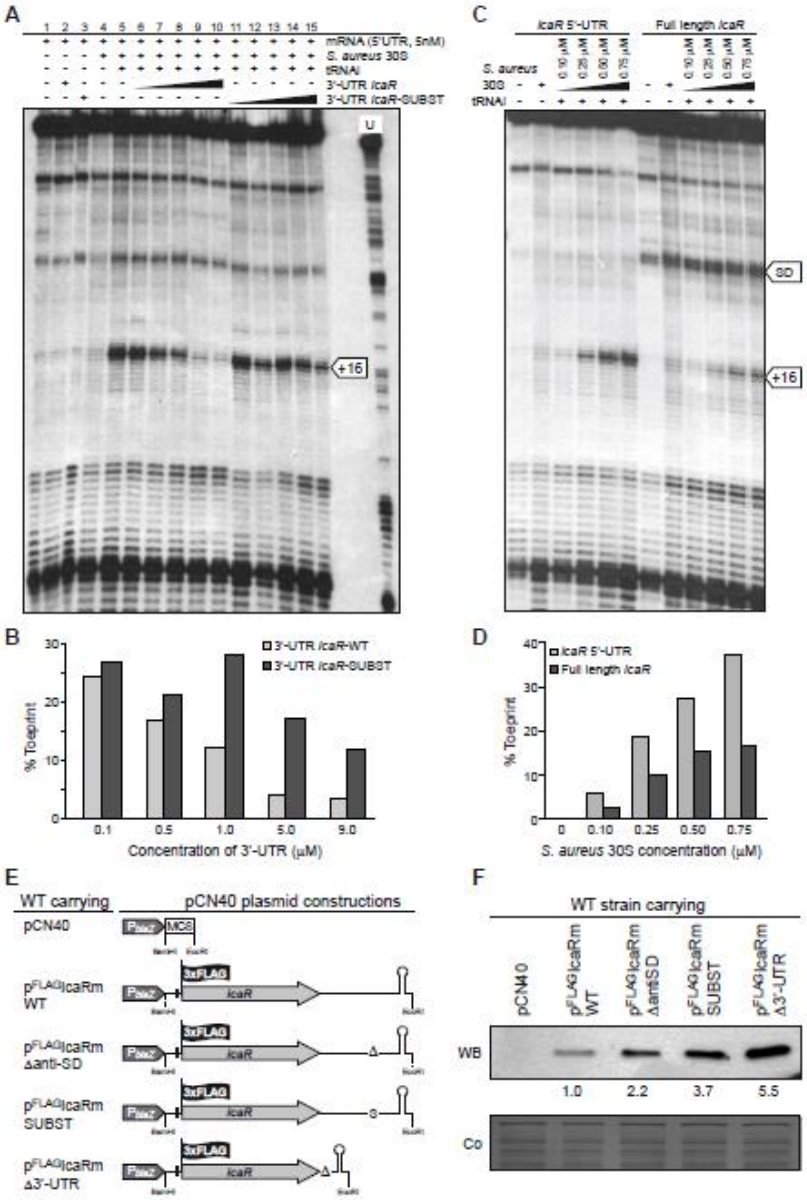

Figure 7 - The 3′-5′-UTRs interaction interferes with the translational initiation complex. **(A, B)** Formation of the ternary complex between *icaR* 5′-UTR fragment (5 nM), *S. aureus* 30S ribosomal subunit, and initiator tRNA was monitored in the absence or in the presence

of increasing concentrations of wild-type 3′-UTR fragment and substituted 3′-UTR fragment. The toeprint at position +16 is indicated. The quantification of the toeprint (B) was first normalized according to the full-length extension product bands using the SAFA software (Laederach *et al.*, 2008), and the toeprint signal (given in %) represents the yield of the toeprint obtained in the presence of the competitor RNA versus the yield of the toeprint obtained in the absence of the competitor RNA. **(C, D)** Formation of the ternary complex with the 5′-UTR fragment and the full-length *icaR* mRNA molecule was monitored using different *S. aureus* 30S concentrations. A reverse transcriptase pause at the Shine-Dalgarno (SD) sequence occurring in the full-length *icaR* mRNA molecule is indicated with an arrow. The quantification of toeprint experiment (D) is described above in B. **(E)** Schematic representation of plasmid constructions constitutively expressing the 3XFLAG tagged IcaR protein from the different *icaR* mRNA alleles. **(F)** A representative Western blot showing IcaR protein levels in strains shown in panel E. The 3XFLAG tagged IcaR protein was detected with commercial anti-3XFLAG antibodies. Band quantification according to densitometry analysis is shown. A Coomasie stained gel portion is shown as loading control.

Biological relevance of icaR mRNA 3′-UTR regulation

IcaR represents the checkpoint of *S. aureus* biofilm formation since it binds to a 42-bp region located just upstream of the *icaA* gene to directly inhibit *icaADBC* transcription (Jefferson *et al.*, 2003). To examine the biological relevance of the *icaR* mRNA 3′-UTR in regulating *in vivo* multicellular behaviour, we first checked if the high IcaR levels observed in the Δ3′-UTR mutant strain were able to affect *icaADBC* operon transcription. For that, we compared *icaADBC* promoter activity in the wild-type strain and its corresponding Δ3′-UTR mutant using a transcriptional reporter plasmid comprising the *lacZ* gene fused to the *ica* promoter (P*ica*). As expected, β-galactosidase assays revealed that the activity of the P*ica* promoter was ~7-fold lower in the Δ3′-UTR mutant than in the wild-type strain (Figure 8A). Then, we determined the effect of the 3′-UTR deletion on the capacity of two genetically unrelated *S. aureus* strains (*S. aureus* 15981 and *S. aureus* 132) to synthesize PIA-PNAG exopolysaccharide and develop a biofilm. Dot-blot assays using anti PIA-PNAG specific antibodies showed that the synthesis of PIA-PNAG was completely inhibited in both Δ3′-UTR mutant strains (Figure 8B). Accordingly, Δ3′-UTR mutant strains lost the capacity to develop a

biofilm under continuous-flow conditions in microfermenters (Figure 8D). Then, to assess specifically the relevance of ^{894}UCCCCUG^{900} motif for the regulation of PIA-PNAG synthesis and biofilm development, we tested PIA-PNAG levels and biofilm formation capacity in *S. aureus* 15981 wild-type strain transformed with plasmids carrying either full length *icaR* mRNA (pIcaRm_WT) or derivatives with deletion or substitution of the UCCCCUG motif (pIcaRm_Δanti-SD and pIcaRm_SUBST respectively). Strains producing *icaR* mRNA derivatives accumulated lower levels of PIA/PNAG (Figure 8C), and displayed a significant reduction in the capacity to produce biofilm compared to the strain expressing full length *icaR* mRNA (Figure 8E). These experiments demonstrate the biological relevance of the *icaR* 3′-UTR and the UCCCCUG motif in controlling PIA-PNAG production and biofilm development by adjusting IcaR repressor protein levels through a post-transcriptional mechanism involving the interaction of a 3′-UTR and a 5′-UTR of the same mRNA.

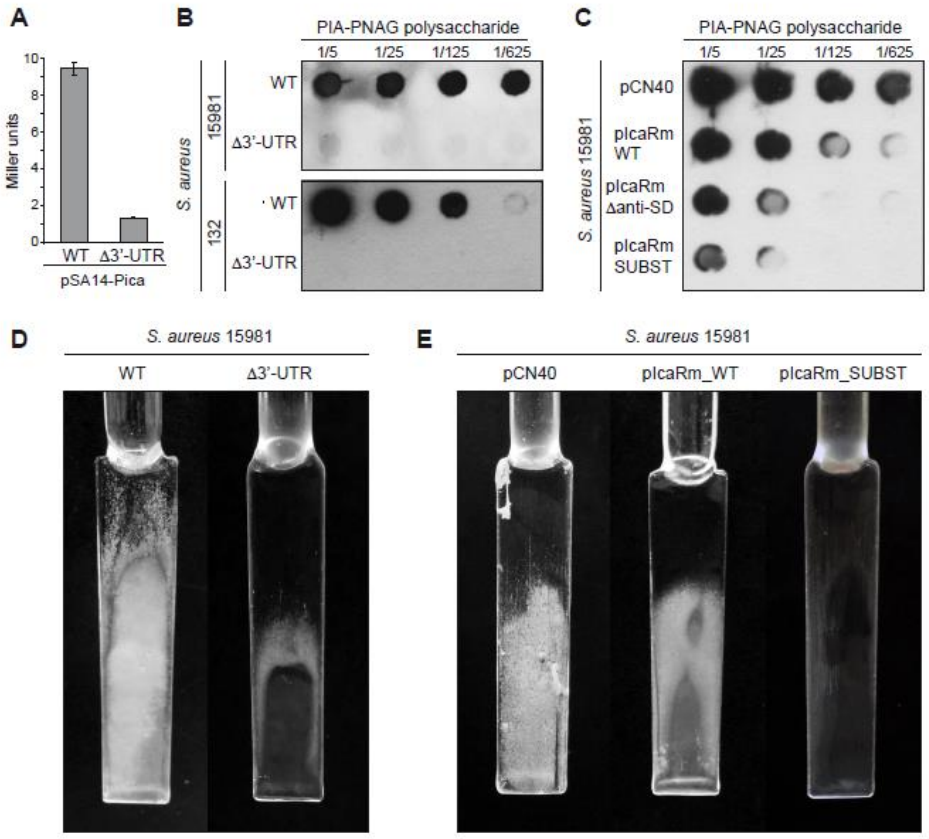

Figure 8 - *In vivo* relevance of the interaction between the 3′-UTR and the Shine-Dalgarno region of *icaR* mRNA. (A) β-galatosidase assays measuring *icaA* promoter activity in the wild-type and Δ3′-UTR strains grown in TSB-gluc at 37°C until exponential phase (OD_{600nm}=0.8). Each bar represents the average of three independent assays. **(B)** Consequences of *icaR* mRNA 3′-UTR deletion on PIA-PNAG exopolysaccharide synthesis and biofilm production of *S. aureus* 15981 and 132 strains. **(C)** *In vivo* effects of either the mutation or the substitution of the ^{894}UCCCCUG^{900} motif on PIA-PNAG synthesis. Quantification of PIA-PNAG exopolysaccharide biosynthesis by dot-blot. Serial dilutions (1/5) of the samples were spotted onto nitrocellulose membranes and PIA-PNAG production was detected with specific anti-PIA-PNAG antibodies. **(D)** Biofilm development of the wild-type and Δ3′-UTR strains grown in microfermentors under continuous flow for 8 h at 37°C. The glass slides where bacteria form the biofilm are shown. **(E)** Biofilm development of the *S. aureus* 15981 with the pCN40, pIcaRm_WT and pIcaRm_SUBST plasmids grown in microfermentors under continuous flow for 8 h at 37°C.

DISCUSSION

3′-5′-UTR base-pairing to control mRNA translation in bacteria

Our genetic and biochemical analysis revealed that regulation of IcaR translation depends on the ability of the long 3′-UTR of *icaR* to interact with a 40 nt complementary region of the 5′-UTR. Thus, inhibition of this interaction by either deleting or substituting few complementary nucleotides in the 3′-UTR causes the accumulation of IcaR protein *in vivo*. Because both 5′- and 3′-interacting motifs are encoded in the same mRNA molecule, the question arises as to whether the interaction occurs intramolecularly (3′- and 5′-UTRs of the same molecule) or intermolecularly (3′- and 5′-UTRs of different molecules). With respect to the first possibility, that is circularization of the mRNA, meaning the formation of a physical bridging of 5′- and 3′-ends, it is a widely accepted mechanism of translational regulation in eukaryotes and virus. Proteins associated with the 5′-cap- and 3′-poly(A) tail are usually required to mediate UTRs interaction and depending on the proteins involved, the interaction can stimulate or repress mRNA translation (Jackson *et al.*, 2010; Mazumder *et al.*, 2003; Tomek and Wollenhaupt, 2012). Transcript circularization can also be initiated by simpler RNA interactions in some viruses. For example, during the translation process of several RNA viruses such as *Barley yellow dwarf luteovirus* and dengue virus, the positive-strand RNA genome forms a closed loop by direct base-paring between complementary regions located at the 3′-UTR and the 5′-UTR to confer translation initiation at the 5′-proximal AUG (Alvarez *et al.*, 2005; Guo *et al.*, 2001). Transposition of this scenario to the 3′-5′-UTR interaction described here, needs to reconcile the widely established concept that transcription and translation processes are coupled in bacteria. If ribosomes started translation of *icaR* mRNA before the RNA polymerase synthetized the UCCCC regulatory element, the 3′-UTR would not be able to, regulate the initial rounds of *icaR* translation.

Comparative toeprinting assays showed that the 5′-UTR of *icaR* is recognized by the ribosome less well than *spa* mRNA which is characterized by an unstructured RBS. This data suggested that the 5′-UTR would adopt a structural fold to impair efficient 30S binding during transcription but sufficiently unstable to be displaced by the 3′-UTR. In such model, the 3′ end of *icaR* would trigger a refolding of the 5′-UTR to promote the access of RNase III and to fully impair ribosome loading. Such a step-wise mechanism would be reminiscent to the temporal translational control of *E. coli hok* mRNA involved in programmed cell death (Moller-Jensen *et al.*, 2001). We cannot exclude that translation initiation might be delayed by an unknown mechanism, i.e. involvement of trans-acting factors, while *icaR* mRNA is fully transcribed.

Alternatively, intermolecular interactions between identical RNA molecules through complementary sequences have been shown to be essential for retroviral RNAs (Paillart *et al.*, 2004), formation of ribonucleoprotein particles for transport and localization of *bcd* mRNA (bicoid) during *Drosophila* development (Ferrandon *et al.*, 1997; Wagner *et al.*, 2001) and the formation of the cyclic hexamer pRNA needed for efficient *in vitro* packaging of the *Bacillus subtilis* bacteriophage phi29 genome (Gan *et al.*, 2008; Guo, 2005; Guo *et al.*, 1998). In these examples, the intermolecular interaction provides a mechanism to recruit the mRNA molecules in specific structural complexes.

The finding that *icaR* mRNA can form dimers *in vitro* but not the 5′-UTR is consistent with an interaction between the 3′-UTR of one *icaR* mRNA molecule and the 5′-UTR of another *icaR* mRNA molecule in *trans* (Figure S5). However, ectopic expression of either the 3′-UTR or the full-length *icaR* mRNA was unable to modify the expression of the chromosomal copy of IcaR questioning the relevance of the intermolecular interaction *in vivo* (data not shown). Furthermore, results of toeprint and RNase III cleavage assays could be explained considering that the interaction occurs either in *cis* or *trans*. Therefore, more detailed studies

examining the structure of *icaR* mRNA and the environmental signals that modulate the 3′-5′-UTRs interaction are required before conclusively establishing the intra- or intermolecular mechanisms by which the 3′-UTR regulates IcaR translation and biofilm formation.

Another question that remains to be addressed is whether 3′-5′ interaction requires the participation of *trans*-acting factors that could use molecular mimicry to sequester the 3′-UTR away from the 5′-UTR and change the SD region from an open to a closed strucuture. Although we have shown that neither Hfq nor RNA helicase (YqfR) affect IcaR expression, we cannot exclude that other RNA binding proteins or unknown sRNAs might participate in *icaR* 5′-3′ mRNA interaction in response to environmental signals.

Biological relevance of bacterial 3′-5′-UTR-mediated regulation

Whatever the detailed interaction mechanisms involved, our results indicated that the ability of the 3′-UTR to interact with the 5′-UTR has profound consequences on the synthesis of IcaR and biofilm development (Figure 9). On one hand, pairing of 3′- and 5′-UTR regions provides a double stranded RNA substrate for RNase III activity, which accelerates *icaR* mRNA decay. On the other hand, 3′-5′-UTRs pairing also hinders the formation of the translational complex. There are examples in the literature in which pairing between 3′- and 5′-UTRs modulates translation in bacteria (Balaban and Novick, 1995; Thisted *et al.*, 1995). As regards, the *hok/sok* toxin-antitoxin system of plasmid R1, the 3'-end of the full-length *hok* mRNA folds back onto the translational initiation region inhibiting translation (Thisted *et al.*, 1995). Consequently, the full-length *hok* mRNA was found to be translationally silent whereas a truncated version with a deletion of the 3'-end was active. Novick and co-workers proposed a fold back interaction between the 5′-end and the 3′-end of RNAIII (Novick *et al.*, 1993). Although much shorter than the initial computational prediction, this interaction was later

confirmed through the analysis of the secondary structure of RNAIII using enzymes and chemical probes (Benito *et al.*, 2000). It is worth noting that RNAIII (514 nt), the most studied regulatory RNA in *S. aureus*, is actually an mRNA encoding a small peptide (δ–hemolysin) of 26 amino acids. This implies that the main regulatory region of RNAIII corresponds to a long 3'-UTR of 354-nt that folds in several loops to enable pairing with different target mRNAs to repress their translation (Felden *et al.*, 2011). Less known is the capacity of RNAIII to modulate the expression of its own gene, δ–hemolysin (Balaban and Novick, 1995). It has been shown that deletion of the 3'-end of RNAIII abolishes a temporal delay between the transcription of RNAIII and its translation. Although the mechanism was not clarified, it was proposed that the 3'-end might fold back to block translation and that a specific cellular factor would be required to unfold the molecule to allow δ–hemolysin translation (Balaban and Novick, 1995), anticipating the results described in this study.

A common feature between RNAIII and *icaR* mRNA is the presence of UCCCC motifs at the 3'-UTRs (Huntzinger *et al.*, 2005). Interestingly, this motif has also been found in several *S. aureus* regulatory sRNAs (Geissmann *et al.*, 2009a). In the case of RNAIII and RsaE, the UCCCC motif pairs with mRNA targets in *trans* whereas the UCCCC of *icaR* pairs the SD encoded in the same mRNA molecule. Nevertheless, we cannot exclude that the UCCCC motif of *icaR* 3'-UTR pairs other mRNA targets. Indeed, mRNA target predictions using the *RNA*Predator web server (Eggenhofer *et al.*, 2011) identified several mRNAs whose SD regions might pair with *icaR*-UCCCC region. Interestingly, some of this putative mRNA targets encode for proteins involved in biofilm development such as N-acetylglucosaminyl transferase, teichoic acid biosynthesis protein B, spermidine/putrescine ATP binding ABC transporter protein and the iron transcriptional regulator *fur*. Further studies will be needed to elucidate whether the *icaR* UCCCC motif interacts with other mRNAs.

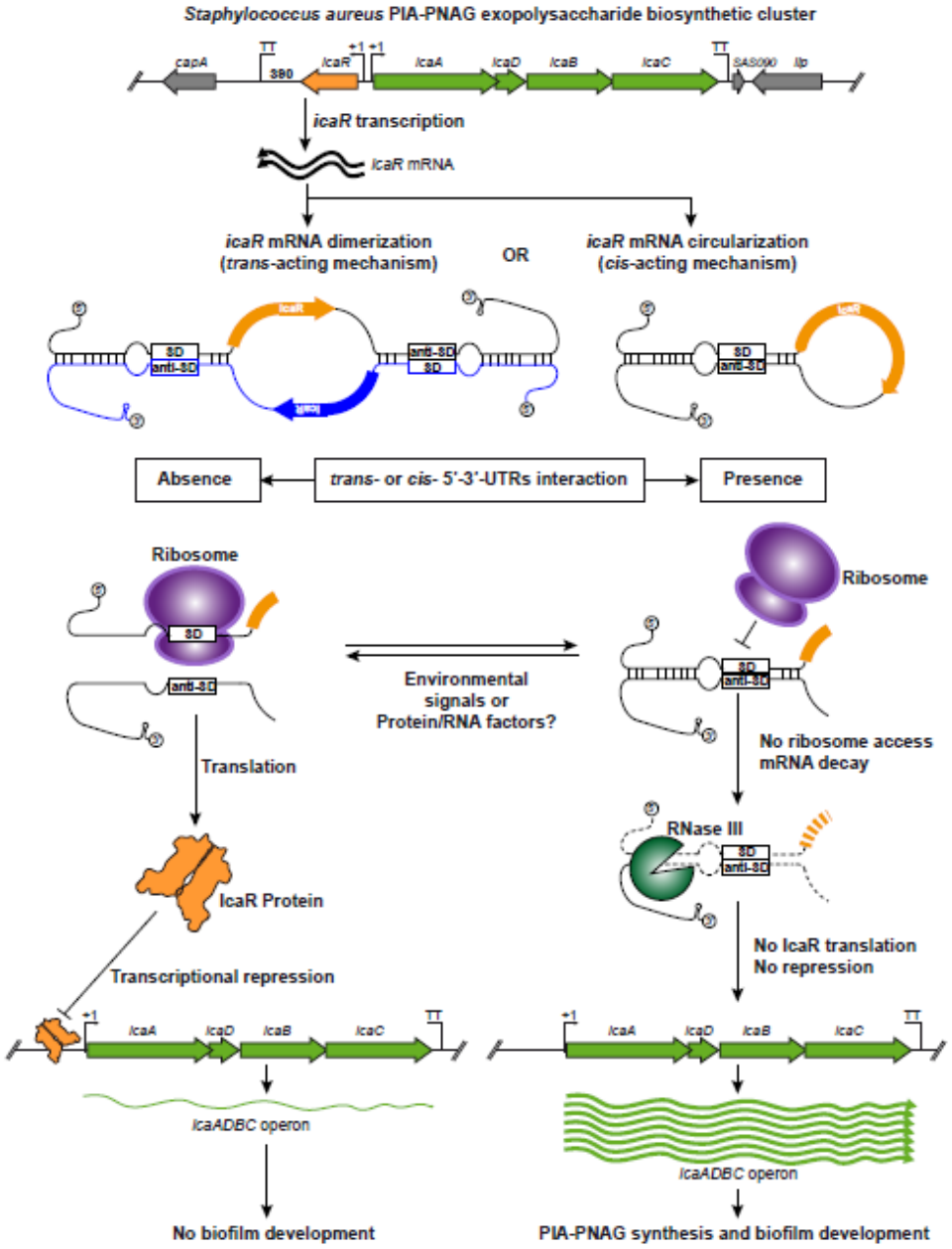
Staphylococcus aureus PIA-PNAG exopolysaccharide biosynthetic cluster
capA
TT
380
+1
icaR
+1
icaA
icaD
icaB
icaC
TT
SAS090
lip
icaR transcription
icaR mRNA
icaR mRNA dimerization
(trans-acting mechanism)
OR
icaR mRNA circularization
(cis-acting mechanism)
SD
anti-SD
Absence
trans- or cis- 5′-3′-UTRs interaction
Presence
Ribosome
Translation
Environmental
signals or
Protein/RNA factors?
No ribosome access
mRNA decay
RNase III
IcaR Protein
Transcriptional repression
No IcaR translation
No repression
icaADBC operon
No biofilm development
PIA-PNAG synthesis and biofilm development

Figure 9 - Model for 3′-UTR mediated regulation of IcaR expression. A model of post-transcriptional regulation of IcaR expression mediated by the 3′-UTR interaction with the Shine-Dalgarno region is shown. Once *icaR* gene is transcribed, the 3′-UTR interacts with the 5′-UTR through the anti-SD UCCCCUG motif. This interaction has two main consequences: i) it interferes with ribosome access to the SD region to inhibit the formation of the translational initiation complex and ii) it promotes RNase III-dependent mRNA decay. In consequence, IcaR repressor is less expressed and thus *icaADBC* transcription occurs, favouring PIA-PNAG biosynthesis and biofilm development. When the interaction between *icaR* mRNA 3′- and 5′-UTR regions does not happen, ribosome binds the SD and proceeds with IcaR protein translation. The resulting IcaR protein binds to *icaADBC* operon promoter inhibiting its transcription and consequently biofilm formation.

Functional regulatory 3′-UTRs will be broadly distributed in bacteria

Why have bacterial 3′-UTRs gone unnoticed? One possible explanation is that, up to now, bacterial transcriptome analyses have provided very limited knowledge about 3′-UTRs structural features because they have been focused on primary 5′ boundary identification (Albrecht *et al.*, 2010; Dornenburg *et al.*, 2010; Mitschke *et al.*, 2011; Schmidtke *et al.*, 2012; Sharma and Vogel, 2009; Wurtzel *et al.*, 2012a; Wurtzel *et al.*, 2012b). Also, the fact that bacterial genomes are very compact and the notion that long 3′-UTRs are restricted to complex organisms (Mazumder *et al.*, 2003; Pesole *et al.*, 2002) has created the feeling that bacterial genomes do not have room to allocate more than few small non-coding RNAs within their short IGRs. However, here, we anticipate that bacterial 3′-UTRs will control gene expression by different mechanisms, probably including similar ones to the 3′-5′ interaction described in this study. Our transcriptome analysis revealed that at least 35% of the *S. aureus* mapped mRNAs contained 3′-UTRs longer than 100-nt and that 68% of the mRNAs had a 3′-UTR longer than their corresponding 5′-UTR. These results are in line with another study showing that large UTRs are more frequently found in the 3′- than in the 5′-end in *S. aureus* (ten Broeke-Smits *et al.*, 2010). Because the average size of the 1,059 intrinsic Rho-independent TTs predicted by TransTermHP in *S. aureus* (Kingsford *et al.*, 2007),

with a confidence higher than 90%, is 33±10-nt, around 40-50-nt should be a sufficient length to allocate the transcriptional terminator sequence. Therefore, the prevalent high length (>100 nt) is a strong evidence for the potential of 3′-UTRs for assuming regulatory functions apart from accommodating the transcriptional terminator sequence and preventing degradation by 3′ exonucleases. Localization of sensor mechanisms at the 3′-UTR compared with the 5′-UTR of the transcript may present some advantages, since RNA secondary structure in the 3′-UTR is not constrained by the translational process. In this respect, it is interesting to note that the *icaR* mRNA encoded in other staphylococcal species such as *S. epidermidis*, *S. simiae*, *S. caprae*, and *S. capitis* also carries a long 3′-UTR (365, 482, 369 and 380 nt respectively), though it is not conserved at the sequence level. Interestingly, the UCCCC motif is not present in the *icaR* 3′-UTR of these species. These differences could reflect species-specific regulatory differences that may allow adjusting the biofilm formation process to particular niches. Understanding how distinct 3′-UTRs of homologous genes control protein expression will be a promising strategy to uncover the regulatory potential of bacterial 3′-UTRs.

ACKNOWLEDGEMENTS

We thank M. Uzqueda, L. Ortiz and F. J. Corrales from the Genomics, Proteomics and Bioinformatics Unit at the Center for Applied Medical Research, University of Navarra, for tiling microarray hybridization and analysis; T. Maira-Litrán for providing us with the anti-PNAG antiserum; and S. Burgui, A. Aires and M. Cerciat for helpful technical assistance. The NRS594 (RN9594, *S. aureus* RN4220 carrying the pCN40 plasmid) and NRS123 (*S. aureus* MW2) strains were obtained through the Network on Antimicrobial Resistance in *S. aureus* (NARSA) Program that is supported under NIAID/ NIH Contract No. HHSN272200700055C. I. Ruiz de los Mozos and J. Valle were supported by F.P.I.

(BES-2009-017410) and Ramón y Cajal (RYC-2009-03948) contracts respectively from the Spanish Ministry of Economy and Competitiveness. M. Villanueva was supported by a JAE-Predoc research contract from the Spanish National Research Council (CSIC, Spain). Fundação para a Ciência e Tecnologia (FCT - Portugal) gave financial support to S. Domingues (Postdoctoral fellowship) and M. Saramago (Doctoral fellowship). P. Romby and P. Fechter are supported by the Centre National de la Recherche Scientifique (CNRS). This work was supported by Spanish Ministry of Economy and Competitiveness Grants BFU2011-23222, BIO2008-05284-C02-01 and ERA-NET Pathogenomics PIM2010EPA-00606 and Fundação para a Ciência e Tecnologia (FCT - Portugal) grants ERA-PTG/0002/2010 and PEst-OE/EQB/LA0004/2011. The funders had no role in study design, data collection and analysis, decision to publish, or preparation of the manuscript.

REFERENCES

Agaisse, H., and D. Lereclus. 1996. STAB-SD: a Shine-Dalgarno sequence in the 5' untranslated region is a determinant of mRNA stability. Mol Microbiol. 20:633-643.

Albrecht, M., C.M. Sharma, R. Reinhardt, J. Vogel, and T. Rudel. 2010. Deep sequencing-based discovery of the Chlamydia trachomatis transcriptome. Nucleic Acids Res. 38:868-877.

Alvarez, D.E., M.F. Lodeiro, S.J. Luduena, L.I. Pietrasanta, and A.V. Gamarnik. 2005. Long-range RNA-RNA interactions circularize the dengue virus genome. J Virol. 79:6631-6643.

Amarasinghe, A.K., I. Calin-Jageman, A. Harmouch, W. Sun, and A.W. Nicholson. 2001. Escherichia coli ribonuclease III: affinity purification of hexahistidine-tagged enzyme and assays for substrate binding and cleavage. Methods Enzymol. 342:143-158.

Arciola, C.R., D. Campoccia, P. Speziale, L. Montanaro, and J.W. Costerton. 2012. Biofilm formation in Staphylococcus implant infections. A review of molecular mechanisms and implications for biofilm-resistant materials. Biomaterials. 33:5967-5982.

Arnaud, M., A. Chastanet, and M. Debarbouille. 2004. New vector for efficient allelic replacement in naturally nontransformable, low-GC-content, gram-positive bacteria. Appl Environ Microbiol. 70:6887-6891.

Arraiano, C.M., J.M. Andrade, S. Domingues, I.B. Guinote, M. Malecki, R.G. Matos, R.N. Moreira, V. Pobre, F.P. Reis, M. Saramago, I.J. Silva, and S.C. Viegas. 2010. The critical role of RNA processing and degradation in the control of gene expression. FEMS Microbiol Rev. 34:883-923.

Babitzke, P., C.S. Baker, and T. Romeo. 2009. Regulation of translation initiation by RNA binding proteins. Annu Rev Microbiol. 63:27-44.

Balaban, N., and R.P. Novick. 1995. Translation of RNAIII, the Staphylococcus aureus agr regulatory RNA molecule, can be activated by a 3'-end deletion. FEMS Microbiol Lett. 133:155-161.

Belasco, J.G. 2010. All things must pass: contrasts and commonalities in eukaryotic and bacterial mRNA decay. Nat Rev Mol Cell Biol. 11:467-478.

Benito, Y., F.A. Kolb, P. Romby, G. Lina, J. Etienne, and F. Vandenesch. 2000. Probing the structure of RNAIII, the Staphylococcus aureus agr regulatory RNA, and identification of the RNA domain involved in repression of protein A expression. RNA. 6:668-679.

Beuzon, C.R., S. Marques, and J. Casadesus. 1999. Repression of IS200 transposase synthesis by RNA secondary structures. Nucleic Acids Res. 27:3690-3695.

Boisset, S., T. Geissmann, E. Huntzinger, P. Fechter, N. Bendridi, M. Possedko, C. Chevalier, A.C. Helfer, Y. Benito, A. Jacquier, C. Gaspin, F. Vandenesch, and P. Romby. 2007. Staphylococcus aureus RNAIII coordinately represses the synthesis of virulence factors and the transcription regulator Rot by an antisense mechanism. Genes Dev. 21:1353-1366.

Britton, R.A., T. Wen, L. Schaefer, O. Pellegrini, W.C. Uicker, N. Mathy, C. Tobin, R. Daou, J. Szyk, and C. Condon. 2007. Maturation of the 5' end of Bacillus subtilis 16S rRNA by the essential ribonuclease YkqC/RNase J1. Mol Microbiol. 63:127-138.

Brodersen, P., and O. Voinnet. 2009. Revisiting the principles of microRNA target recognition and mode of action. Nat Rev Mol Cell Biol. 10:141-148.

Chao, Y., K. Papenfort, R. Reinhardt, C.M. Sharma, and J. Vogel. 2012. An atlas of Hfq-bound transcripts reveals 3' UTRs as a genomic reservoir of regulatory small RNAs. EMBO J. 31:4005-4019.

Charpentier, E., A.I. Anton, P. Barry, B. Alfonso, Y. Fang, and R.P. Novick. 2004. Novel cassette-based shuttle vector system for gram-positive bacteria. Appl Environ Microbiol. 70:6076-6085.

Chelladurai, B.S., H. Li, and A.W. Nicholson. 1991. A conserved sequence element in ribonuclease III processing signals is not required for accurate in vitro enzymatic cleavage. Nucleic Acids Res. 19:1759-1766.

Chen, L.H., S.A. Emory, A.L. Bricker, P. Bouvet, and J.G. Belasco. 1991. Structure and function of a bacterial mRNA stabilizer: analysis of the 5' untranslated region of ompA mRNA. J Bacteriol. 173:4578-4586.

Cramton, S.E., C. Gerke, N.F. Schnell, W.W. Nichols, and F. Gotz. 1999. The intercellular adhesion (ica) locus is present in Staphylococcus aureus and is required for biofilm formation. Infect Immun. 67:5427-5433.

Dornenburg, J.E., A.M. Devita, M.J. Palumbo, and J.T. Wade. 2010. Widespread antisense transcription in Escherichia coli. MBio. 1.

Eggenhofer, F., H. Tafer, P.F. Stadler, and I.L. Hofacker. 2011. RNApredator: fast accessibility-based prediction of sRNA targets. Nucleic Acids Res. 39:W149-154.

Fechter, P., C. Chevalier, G. Yusupova, M. Yusupov, P. Romby, and S. Marzi. 2009. Ribosomal initiation complexes probed by toeprinting and effect of trans-acting translational regulators in bacteria. Methods Mol Biol. 540:247-263.

Felden, B., F. Vandenesch, P. Bouloc, and P. Romby. 2011. The Staphylococcus aureus RNome and its commitment to virulence. PLoS Pathog. 7:e1002006.

Ferrandon, D., I. Koch, E. Westhof, and C. Nusslein-Volhard. 1997. RNA-RNA interaction is required for the formation of specific bicoid mRNA 3' UTR-STAUFEN ribonucleoprotein particles. EMBO J. 16:1751-1758.

Gan, J., G. Shaw, J.E. Tropea, D.S. Waugh, D.L. Court, and X. Ji. 2008. A stepwise model for double-stranded RNA processing by ribonuclease III. Mol Microbiol. 67:143-154.

Garneau, N.L., J. Wilusz, and C.J. Wilusz. 2007. The highways and byways of mRNA decay. Nat Rev Mol Cell Biol. 8:113-126.

Geissmann, T., C. Chevalier, M.J. Cros, S. Boisset, P. Fechter, C. Noirot, J. Schrenzel, P. Francois, F. Vandenesch, C. Gaspin, and P. Romby. 2009a. A search for small noncoding RNAs in Staphylococcus aureus reveals a conserved sequence motif for regulation. Nucleic Acids Res. 37:7239-7257.

Geissmann, T., S. Marzi, and P. Romby. 2009b. The role of mRNA structure in translational control in bacteria. RNA Biol. 6:153-160.

Ghigo, J.M. 2001. Natural conjugative plasmids induce bacterial biofilm development. Nature. 412:442-445.

Gotz, F. 2002. Staphylococcus and biofilms. Mol Microbiol. 43:1367-1378.

Gripenland, J., S. Netterling, E. Loh, T. Tiensuu, A. Toledo-Arana, and J. Johansson. 2010. RNAs: regulators of bacterial virulence. Nat Rev Microbiol. 8:857-866.

Guo, L., E.M. Allen, and W.A. Miller. 2001. Base-pairing between untranslated regions facilitates translation of uncapped, nonpolyadenylated viral RNA. Mol Cell. 7:1103-1109.

Guo, P. 2005. RNA nanotechnology: engineering, assembly and applications in detection, gene delivery and therapy. J Nanosci Nanotechnol. 5:1964-1982.

Guo, P., C. Zhang, C. Chen, K. Garver, and M. Trottier. 1998. Inter-RNA interaction of phage phi29 pRNA to form a hexameric complex for viral DNA transportation. Mol Cell. 2:149-155.

Huntzinger, E., S. Boisset, C. Saveanu, Y. Benito, T. Geissmann, A. Namane, G. Lina, J. Etienne, B. Ehresmann, C. Ehresmann, A. Jacquier, F. Vandenesch, and P. Romby. 2005. Staphylococcus aureus RNAIII and the endoribonuclease III coordinately regulate spa gene expression. EMBO J. 24:824-835.

Jackson, R.J., C.U. Hellen, and T.V. Pestova. 2010. The mechanism of eukaryotic translation initiation and principles of its regulation. Nat Rev Mol Cell Biol. 11:113-127.

Jefferson, K.K., S.E. Cramton, F. Gotz, and G.B. Pier. 2003. Identification of a 5-nucleotide sequence that controls expression of the ica locus in Staphylococcus aureus and characterization of the DNA-binding properties of IcaR. Mol Microbiol. 48:889-899.

Joanne, P., M. Falord, O. Chesneau, C. Lacombe, S. Castano, B. Desbat, C. Auvynet, P. Nicolas, T. Msadek, and C. El Amri. 2009. Comparative study of two plasticins: specificity, interfacial behavior, and bactericidal activity. Biochemistry. 48:9372-9383.

Kawano, M., A.A. Reynolds, J. Miranda-Rios, and G. Storz. 2005. Detection of 5'- and 3'-UTR-derived small RNAs and cis-encoded antisense RNAs in Escherichia coli. Nucleic Acids Res. 33:1040-1050.

Kingsford, C.L., K. Ayanbule, and S.L. Salzberg. 2007. Rapid, accurate, computational discovery of Rho-independent transcription terminators illuminates their relationship to DNA uptake. Genome Biol. 8:R22.

Kortmann, J., and F. Narberhaus. 2012. Bacterial RNA thermometers: molecular zippers and switches. Nat Rev Microbiol. 10:255-265.

Laederach, A., R. Das, Q. Vicens, S.M. Pearlman, M. Brenowitz, D. Herschlag, and R.B. Altman. 2008. Semiautomated and rapid quantification of nucleic acid footprinting and structure mapping experiments. Nat Protoc. 3:1395-1401.

Lasa, I., A. Toledo-Arana, A. Dobin, M. Villanueva, I.R. de los Mozos, M. Vergara-Irigaray, V. Segura, D. Fagegaltier, J.R. Penades, J. Valle, C. Solano, and T.R. Gingeras. 2011. Genome-wide antisense transcription drives mRNA processing in bacteria. Proc Natl Acad Sci U S A. 108:20172-20177.

Lasa, I., A. Toledo-Arana, and T.R. Gingeras. 2012. An effort to make sense of antisense transcription in bacteria. RNA Biol. 9:1039-1044.

Lioliou, E., C.M. Sharma, I. Caldelari, A.C. Helfer, P. Fechter, F. Vandenesch, J. Vogel, and P. Romby. 2012. Global regulatory functions of the Staphylococcus aureus endoribonuclease III in gene expression. PLoS Genet. 8:e1002782.

Maira-Litran, T., A. Kropec, D.A. Goldmann, and G.B. Pier. 2005. Comparative opsonic and protective activities of Staphylococcus aureus conjugate vaccines containing native or deacetylated Staphylococcal Poly-N-acetyl-beta-(1-6)-glucosamine. Infect Immun. 73:6752-6762.

Mangus, D.A., M.C. Evans, and A. Jacobson. 2003. Poly(A)-binding proteins: multifunctional scaffolds for the post-transcriptional control of gene expression. Genome Biol. 4:223.

Matoulkova, E., E. Michalova, B. Vojtesek, and R. Hrstka. 2012. The role of the 3' untranslated region in post-transcriptional regulation of protein expression in mammalian cells. RNA Biol. 9:563-576.

Mazumder, B., V. Seshadri, and P.L. Fox. 2003. Translational control by the 3'-UTR: the ends specify the means. Trends Biochem Sci. 28:91-98.

Mitschke, J., A. Vioque, F. Haas, W.R. Hess, and A.M. Muro-Pastor. 2011. Dynamics of transcriptional start site selection during nitrogen stress-induced cell differentiation in Anabaena sp. PCC7120. Proc Natl Acad Sci U S A. 108:20130-20135.

Moller-Jensen, J., T. Franch, and K. Gerdes. 2001. Temporal translational control by a metastable RNA structure. J Biol Chem. 276:35707-35713.

Nakamoto, T. 2009. Evolution and the universality of the mechanism of initiation of protein synthesis. Gene. 432:1-6.

Narberhaus, F. 2010. Translational control of bacterial heat shock and virulence genes by temperature-sensing mRNAs. RNA Biol. 7:84-89.

Novick, R.P., H.F. Ross, S.J. Projan, J. Kornblum, B. Kreiswirth, and S. Moghazeh. 1993. Synthesis of staphylococcal virulence factors is controlled by a regulatory RNA molecule. EMBO J. 12:3967-3975.

Paillart, J.C., M. Shehu-Xhilaga, R. Marquet, and J. Mak. 2004. Dimerization of retroviral RNA genomes: an inseparable pair. Nat Rev Microbiol. 2:461-472.

Perocchi, F., Z. Xu, S. Clauder-Munster, and L.M. Steinmetz. 2007. Antisense artifacts in transcriptome microarray experiments are resolved by actinomycin D. Nucleic Acids Res. 35:e128.

Pesole, G., S. Liuni, G. Grillo, F. Licciulli, F. Mignone, C. Gissi, and C. Saccone. 2002. UTRdb and UTRsite: specialized databases of sequences and functional elements of 5' and 3' untranslated regions of eukaryotic mRNAs. Update 2002. Nucleic Acids Res. 30:335-340.

Rasmussen, S., H.B. Nielsen, and H. Jarmer. 2009. The transcriptionally active regions in the genome of Bacillus subtilis. Mol Microbiol. 73:1043-1057.

Schmidtke, C., S. Findeiss, C.M. Sharma, J. Kuhfuss, S. Hoffmann, J. Vogel, P.F. Stadler, and U. Bonas. 2012. Genome-wide transcriptome analysis of the plant pathogen Xanthomonas identifies sRNAs with putative virulence functions. Nucleic Acids Res. 40:2020-2031.

Segura, V., A. Toledo-Arana, M. Uzqueda, I. Lasa, and A. Munoz-Barrutia. 2012. Wavelet-based detection of transcriptional activity on a novel Staphylococcus aureus tiling microarray. BMC Bioinformatics. 13:222.

Serganov, A., and E. Nudler. 2013. A decade of riboswitches. Cell. 152:17-24.

Serganov, A., A. Rak, M. Garber, J. Reinbolt, B. Ehresmann, C. Ehresmann, M. Grunberg-Manago, and C. Portier. 1997. Ribosomal protein S15 from Thermus thermophilus--cloning, sequencing, overexpression of the gene and RNA-binding properties of the protein. Eur J Biochem. 246:291-300.

Sharma, C.M., and J. Vogel. 2009. Experimental approaches for the discovery and characterization of regulatory small RNA. Curr Opin Microbiol. 12:536-546.

Sittka, A., S. Lucchini, K. Papenfort, C.M. Sharma, K. Rolle, T.T. Binnewies, J.C. Hinton, and J. Vogel. 2008. Deep sequencing analysis of small noncoding RNA and mRNA targets of the global post-transcriptional regulator, Hfq. PLoS Genet. 4:e1000163.

ten Broeke-Smits, N.J., T.E. Pronk, I. Jongerius, O. Bruning, F.R. Wittink, T.M. Breit, J.A. van Strijp, A.C. Fluit, and C.H. Boel. 2010. Operon structure of Staphylococcus aureus. Nucleic Acids Res. 38:3263-3274.

Thisted, T., N.S. Sorensen, and K. Gerdes. 1995. Mechanism of post-segregational killing: secondary structure analysis of the entire Hok mRNA from plasmid R1 suggests a fold-back structure that prevents translation and antisense RNA binding. J Mol Biol. 247:859-873.

Toledo-Arana, A., O. Dussurget, G. Nikitas, N. Sesto, H. Guet-Revillet, D. Balestrino, E. Loh, J. Gripenland, T. Tiensuu, K. Vaitkevicius, M. Barthelemy, M. Vergassola, M.A. Nahori, G. Soubigou, B. Regnault, J.Y. Coppee, M. Lecuit, J. Johansson, and P. Cossart. 2009. The Listeria transcriptional landscape from saprophytism to virulence. Nature. 459:950-956.

Tomek, W., and K. Wollenhaupt. 2012. The "closed loop model" in controlling mRNA translation during development. Anim Reprod Sci. 134:2-8.

Udekwu, K.I., F. Darfeuille, J. Vogel, J. Reimegard, E. Holmqvist, and E.G. Wagner. 2005. Hfq-dependent regulation of OmpA synthesis is mediated by an antisense RNA. Genes Dev. 19:2355-2366.

Valle, J., A. Toledo-Arana, C. Berasain, J.M. Ghigo, B. Amorena, J.R. Penades, and I. Lasa. 2003. SarA and not sigmaB is essential for biofilm development by Staphylococcus aureus. Mol Microbiol. 48:1075-1087.

Vergara-Irigaray, M., J. Valle, N. Merino, C. Latasa, B. Garcia, I. Ruiz de Los Mozos, C. Solano, A. Toledo-Arana, J.R. Penades, and I. Lasa. 2009. Relevant role of fibronectin-binding proteins in Staphylococcus aureus biofilm-associated foreign-body infections. Infect Immun. 77:3978-3991.

Wagner, C., I. Palacios, L. Jaeger, D. St Johnston, B. Ehresmann, C. Ehresmann, and C. Brunel. 2001. Dimerization of the 3'-UTR of bicoid mRNA involves a two-step mechanism. J Mol Biol. 313:511-524.

Wassarman, K.M., F. Repoila, C. Rosenow, G. Storz, and S. Gottesman. 2001. Identification of novel small RNAs using comparative genomics and microarrays. Genes Dev. 15:1637-1651.

Waters, L.S., and G. Storz. 2009. Regulatory RNAs in bacteria. Cell. 136:615-628.

Winkler, W.C. 2005. Metabolic monitoring by bacterial mRNAs. Arch Microbiol. 183:151-159.

Winkler, W.C., and R.R. Breaker. 2005. Regulation of bacterial gene expression by riboswitches. Annu Rev Microbiol. 59:487-517.

Wurtzel, O., N. Sesto, J.R. Mellin, I. Karunker, S. Edelheit, C. Becavin, C. Archambaud, P. Cossart, and R. Sorek. 2012a. Comparative transcriptomics of pathogenic and non-pathogenic Listeria species. Mol Syst Biol. 8:583.

Wurtzel, O., D.R. Yoder-Himes, K. Han, A.A. Dandekar, S. Edelheit, E.P. Greenberg, R. Sorek, and S. Lory. 2012b. The single-nucleotide resolution transcriptome of Pseudomonas aeruginosa grown in body temperature. PLoS Pathog. 8:e1002945.

Zuker, M. 2003. Mfold web server for nucleic acid folding and hybridization prediction. Nucleic Acids Res. 31:3406-3415.

SUPPLEMENTARY INFORMATION

Table S1 - Strains used in this study.

Strains	Relevant characteristic(s)	MIC[a]	Source or reference
Staphylococcus aureus			
15981	Clinical strain. Biofilm positive in TSBg	532	(Mazumder *et al.*, 2003)
MW2	Typical community-acquired strain of MRSA, which was isolated in 1998 in North Dakota, USA.	3566	NRS123, (Brodersen and Voinnet, 2009)
RN10359	RN450 lysogenic for 80α phage	3337	(Mangus *et al.*, 2003)
ISP479r	ISP479c with *rsbU* gene restored	1680	(Garneau *et al.*, 2007)
132	MRSA clinical strain with the capacity to form proteinaceous biofilm in TSB-glucose and PIA-PNAG-dependent biofilm in TSB-NaCl	29	(Matoulkova *et al.*, 2012)
15981 Δ3′-UTR	15981 strain with deletion in the *icaR* 3′ UTR	2695	This study
132 Δ3′-UTR	132 strain with deletion in the *icaR* 3′ UTR	3161	This study
15981 ^{FLAG}IcaR	15981 strain expressing the 3XFLAG tagged IcaR protein from the chromosome	2653	This study
15981 ^{FLAG}IcaR Δ3′-UTR	15981 Δ3′-UTR strain expressing the 3XFLAG tagged IcaR protein from the chromosome	2649	This study
RN9594	RN4220 strain carrying the pCN40 plasmid	2534	NRS594
15981 pCN40	15981 strain harbouring the pCN40 plasmid	1014	This study
15981 p^{FLAG}IcaRm	15981 strain harbouring the p^{FLAG}IcaRm plasmid	2683	This study
15981 p^{FLAG}IcaRmΔ3′-UTR	15981 strain harbouring the p^{FLAG}IcaRmΔ3′-UTR plasmid	2684	This study
15981 p^{FLAG}IcaRmΔanti-SD	15981 strain harbouring the p^{FLAG}IcaRmΔanti-SD plasmid	4392	This study
15981 p^{FLAG}IcaRm_SUBST	15981 strain harbouring the p^{FLAG}IcaRm-SUBST-anti-SD plasmid	4395	This study
15981 pIcaRm	15981 strain harbouring the pIcaRm plasmid	1011	This study
15981 pIcaRmΔ3′-UTR	15981 strain harbouring the pIcaRmΔ3′-UTR plasmid	1012	This study
15981 pIcaRmΔanti-SD	15981 strain harbouring the pIcaRmΔanti-SD plasmid	4391	This study
15981 pIcaRm_SUBST	15981 strain harbouring the pIcaRm-SUBST-anti-SD plasmid	4394	This study
15981 Δ*rnc::cat86*	15981 strain with deletion in the *rnc* gene	1327	(Nakamoto, 2009)
15981 Δ*pnp*	15981 strain with deletion in the *pnp* gene	1100	(Nakamoto, 2009)

Strains	Relevant characteristic(s)	MIC[a]	Source or reference
Staphylococcus aureus			
15981 Δ*yqfR*	15981 strain with deletion in the *SA1387* gene which encodes a DEAD-box RNA helicase	1394	This study
15981 Δ*hfq::cat86*	15981 strain with deletion in the *hfq* gene	1055	This study
15981 Δ*rnc* p^{FLAG}IcaRm	15981 Δ*rnc::cat86* strain harbouring the p^{FLAG}IcaRm plasmid	2706	This study
15981 Δ*rnc* p^{FLAG}IcaRmΔ3'-UTR	15981 Δ*rnc::cat86* strain harbouring the p^{FLAG}IcaRmΔ3'-UTR plasmid	2707	This study
15981 Δ*rnc* p^{FLAG}IcaRm_SUBST	15981 Δ*rnc::cat86* strain harbouring the p^{FLAG}IcaRm-SUBST-anti-SD plasmid	4970	This study
15981 Δ*yqfR*p^{FLAG}IcaRm	15981 Δ*yqfR*strain harbouring the p^{FLAG}IcaRm plasmid	2704	This study
15981 Δ*hfq* p^{FLAG}IcaRm	15981 Δ*hfq::cat86* strain harbouring the p^{FLAG}IcaRm plasmid	2708	This study
15981 pSA14-PicaA53	15981 strain harbouring the pSA14-PicaA53 plasmid	1449	This study
Escherichia coli strains			
XL1 Blue	Used for cloning experiments		Stratagene
BL21(DE3) rnc105	BL21(DE3) *rnc105 recA*	4848	(Beuzon *et al.*, 1999)
BL21 pET-15b RNase III	BL21(DE3) *rnc105 recA* strain carrying the pET-15b expressing the *S. aureus* RNase III fused to His-tag	4867	This study

[a]Microbial Biofilm Laboratory strain collection number

Table S2 - Plasmids used in this study.

Plasmids	Relevant characteristic(s)	Source or reference
pMAD	*E. coli - S. aureus* shuttle vector with a thermosensitive origin of replication for Gram-positive bacteria. The vector contains the *bgaB* gene encoding a β- galactosidase under the control of a constitutive promoter as reporter of plasmid presence. Ap^{R}, Em^{R}.	(Chen *et al.*, 1991)
pMAD Δ3'-UTR	pMAD plasmid containing the mutant allele for deletion of the long 3'-UTR of the *icaR* mRNA	This study
pMAD 3xFLAG-icaR	pMAD plasmid containing the allele for insertion of the 3xFLAG at the N-terminus of the IcaR protein	This study
pMAD Δ*SA1387*	pMAD plasmid containing the allele for deletion of the DEAD-box RNA helicase (*S. aureus* N315 ID: SA1387)	This study
pLUG533	pMAD derivative for deletion/replacement of *S. aureus hfq* gene	(Agaisse and Lereclus, 1996)

Plasmids	Relevant characteristic(s)	Source or reference
pSA14	*E. coli - S. aureus* shuttle vector for transcriptional LacZ reporter fusions. The plasmid carries the promoterless *Escherichia colilacZ* gene downstream from the *Bacillus subtilis spoVG* ribosome binding site.	(Waters and Storz, 2009)
pSA14-P*ica*	pSA14 plasmid carrying the *ica* operon promoter region from –422 to +1, where +1 corresponds to the mapped transcriptional start site of *icaADBC* mRNA	This study
pCN40	*E. coli - S. aureus* shuttle vector to express genes under the control of the P_{blaZ} constitutive promoter. Low copy number (20 to 25 copies/cell). Em^R	(Babitzke *et al.*, 2009)
p^{FLAG}IcaRm	pCN40 plasmid constitutively expressing the N-terminal 3XFLAG tagged IcaR protein from the entire mRNA	This study
p^{FLAG}IcaRmΔ3′-UTR	pCN40 plasmid constitutively expressing the N-terminal 3XFLAG tagged IcaR protein from the mRNA carrying a deletion of 331 nt downstream of the stop codon	This study
p^{FLAG}IcaRmΔanti-SD	pCN40 plasmid constitutively expressing the N-terminal 3XFLAG tagged IcaR protein from the mRNA carrying the UCCCCUG deletion	This study
p^{FLAG}IcaRm-SUBST	pCN40 plasmid constitutively expressing the N-terminal 3XFLAG tagged IcaR protein from the mRNA carrying the substitution of the UCCCCUG motif by AGGGGAC	This study
pIcaRm	pCN40 plasmid constitutively expressing the entire *icaR* mRNA molecule	This study
pIcaRmΔ3′-UTR	pCN40 plasmid constitutively expressing the *icaR* mRNA carrying a deletion of 331 nt downstream of the stop codon	This study
pIcaRmΔanti-SD	pCN40 plasmid constitutively expressing the entire *icaR* mRNA carrying the UCCCCUG deletion	This study
pIcaRm-SUBST	pCN40 plasmid constitutively expressing the *icaR* mRNA carrying the substitution of the UCCCCUG motif by AGGGGAC	This study
pIcaRm-Compensatory	pCN40 plasmid constitutively expressing the *icaR* mRNA carrying the substitution of the UCCCCUG motif by AGGGGAC and the substitution of the SD region (CAGGGGG) by GTCCCCT	This study
pET-15b RNase III	pET-15b expressing the *S. aureus* rnc gene which encodes the double stranded endoribonuclease RNase III fused to His-tag.	This study

Table S3 - Oligonucleotides used in this study.

Oligonucleotide	Sequence
mRACE for simultaneous mapping of transcriptional start and stop sites	
RACE-IcaR-1	TATCATCAAGTGTTGTACCGTCAT
RACE-IcaR-2	TCAAAGATGAAGTGTATTCGCTAC
Northern blot probes	
NB-IcaR-Sense	AGCTATATCATCAAGTGTTGTACCGTCATACCCCTTCTCTG
400-Sense	TGTAATTAGATGACAACTTATTCTTTTCAGGGGAAC
RP-T7-Sentido-IcaR	TAATACGACTCACTATAGGGTACTTTCTTCCACTGCTCCA
IcaR+1 (BamHI)	*GGATCC*GAAATATTTGTAATTGCA
Deletion of *icaR* 3′-UTR	
IcaR-A (EcoRI)	*GAATTC*TTTCAGAGAAGGGGTATGACG
IcaR-B (SalI)	*GTCGAC*CAAAAATTATTTCTTCAAAAATAT
IcaR-C (SalI)	*GTCGAC*TAATTTATTGATAAGCGCCTA
IcaR-D (BamHI)	*GGATCC*AACGACCACAAAACATACACAA
IcaR-E	GAGTAGAAGCAGTATATTTGT
IcaR-F	AAATAGAGTGAAGACACCC
Deletion of *dbpA* gene	
SA1387-A (BamHI)	*GGATCC*TCTTATCTTCACCAACATAA
SA1387-B (HindIII)	*AAGCTT*GTGTGTTTTATGTTATTAGG
SA1387-C (HindIII)	*AAGCTT*ATTTGGCCTCCTTATATGT
SA1387-D (BamHI)	*GGATCC*CTTTGAAAGTGAAGGAAGA
SA1387-E	ACAGTAATGTTTACGACTCA
SA1387-F	GTAGTGTATAAGCGACATTA
mRNA levels quantification by qRT-PCR	
icaC2.SG-5	TGCGTTAGCAAATGGAGACTATTG
icaC2.SG-3	TGAGAAAGCACTAATCATTTGAATGC
icaR.SG-5	TTCTTATTTGAGTTTATTTTCGACATCG
icaR.SG-3	CATAGAATTTTGCTATCTCTTTACTTAATGATTG
gyrB.SG-5	ACGTATGAAGGTGGTACGCATG
gyrB.SG-3	ACGCGTTAATGCACGTTTGA
Transcriptional fusions for *icaR* and *icaADBC* promoters	
icaA-pSA14-Fw (PstI)	*CTGCAG*CGTACATTCTAATATACCT
icaA-pSA14-Rv (BamHI)	*GGATCC*TAAGCCATATGGTAATTGATAG

Constitutive expression of *icaR* and icaRmΔ3′-UTR mRNAs

IcaR+1 (BamHI)	*GGATCC*GAAATATTTGTAATTGCA
IcaR-Term (EcoRI)	*GAATTC*CCTTTTAAAAAGATGTGGGTA

Constitutive expression of *icaR* 3′-UTR

400sinIcaR (BamHI)	*GGATCC*TTTTTGTTACTAGTTTGTAATAATTAAC
IcaR-Term (EcoRI)	*GAATTC*CCTTTTAAAAAGATGTGGGTA

Constitutive expression of 3XFLAG IcaR protein

IcaR+1 (BamHI)	*GGATCC*GAAATATTTGTAATTGCA
IcaR-3XFLAG-DCHA	GACTACAAAGACCATGACGGTGATTATAAAGATCATGATATCGACTACAAA GATGACGACGATAAAAAGGATAAGATTATTGATAACGCA
IcaR-3XFLAG-IZDA	ATGATCTTTATAATCACCGTCATGGTCTTTGTAGTCCAATTTTTATAACCCCCT ACT
IcaR-Term (EcoRI)	*GAATTC*CCTTTTAAAAAGATGTGGGTA

Constitutive expression of *icaR* mRNA carrying the UCCCCUG motif deletion

DEL-AntiRBS-IZDA-2	TGACAACTTATTCTTTTACATTACACTTTTATAATATGTTCAA
DEL-AntiRBS-DCHA	ATGTAAAAGAATAAGTTGTCATCTAATTACA

Constitutive expression of *icaR* mRNA carrying the UCCCCUG motif substitution

SUBST-AntiRBS-IZDA-2	TGACAACTTATTCTTTTGTCCCCTACATTACACTTTTATAATATGTTCAA
SUBST-AntiRBS-DCHA	ATGTAGGGGACAAAAGAATAAGTTGTCATCTAATTACA

Constitutive expression of *icaR* mRNA carrying the compensatory mutation at the SD region

SUBST-RBS-DCHA	CAGGTCCCCTTTATAAAAATTGAAGGATAAG
SUBST-RBS-IZDA	CAATTTTTATAAAGGGGACCTGAAAATTAATCACACTATGTTAC

Synthesis of the substrates for in vitro assays

RNA T7 icaR +1 RP 5′UTR icaR RV	TAATACGACTCACTATAGGGGAAATATTTGTAATTGCAACTTAATTT CTCTGAAAATAAGGTTATTGCG
RNA T7 3′UTR ucccc Fw	TAATACGACTCACTATAGGGCTTTATATTTGTGAATGGTTAAGT
RP3′UTR ucccc Rv	TTCCATTTCATCTAATTTATGCGG

Producction of Recombinat RNAse III

RNAse III Fw (NdeI)	*GGAATT*CCATATGTCTAAACAAAAGAAAAGTGAG
RNAse III Rv (BamHI)	*CGCGGA*TCCCTATTTAATTTGTTTTAATTGCTTATAG

mRACE for mapping of processing sites at the 3′-UTR

RACE-Frag-400-RT	TTCATCTAATTTATGCGGATTTCCTG
icaR-C (SalI)	*GTCGAC*TAATTTATTGATAAGCGCCTA

Toeprint

IcaR Forward	GGGAAATATTTGTAATTGCAACTTAATTTTCC
IcaR Reverse	TCCATGGATCCAAAAAAGCGCCTATGTCATGATTTAC
T7 5′-UTR	TAATACGACTCACTATAGGGAAATATTTGTAATTGCCAACTTAATTT
IcaR 5′ rev	ATCATCAAGTGTTGTACCGTCATACCCCTT
T7 3′-UTR	TAATACGACTCACTATAGGGCTTTATATTTGTGAATGGTTAAGTTTGTCTTT GAAC
IcaR 3′ term	AAAAAGCGCCTATGTCATGATTTACCATCA

Italic, restriction enzyme site included in the oligonucleotide. Underlined, T7 promoter

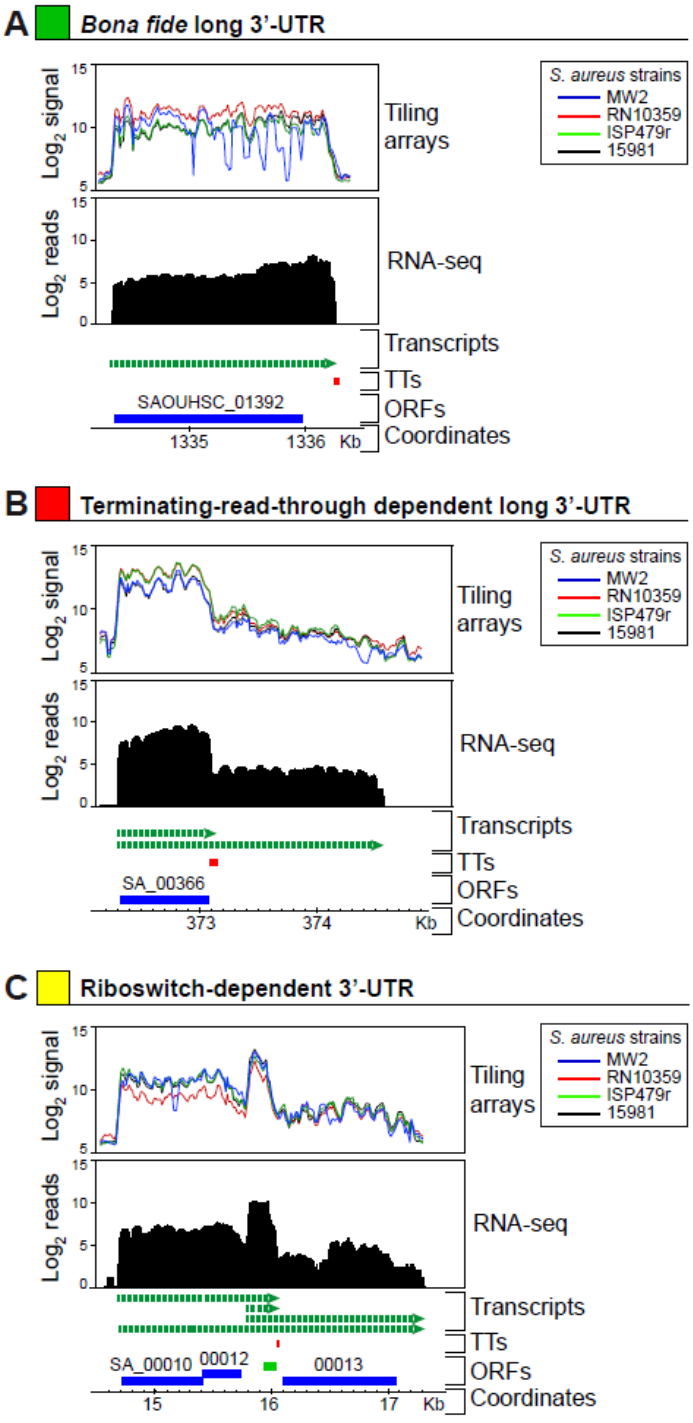
A
Bona fide long 3'-UTR
Log2 signal
Tiling arrays
S. aureus strains
MW2
RN10359
ISP479r
15981
Log2 reads
RNA-seq
Transcripts
TTs
SAOUHSC_01392
ORFs
1335
1336
Kb
Coordinates
B
Terminating-read-through dependent long 3'-UTR
SA_00366
373
374
C
Riboswitch-dependent 3'-UTR
SA_00010
00012
00013
15
16
17

Figure S1 - Examples of *S. aureus* transcripts carrying long 3'-UTRs. Drawings are IGB software images showing tiling array signals and RNA-seq mapped reads. The exterior tracks correspond to the tiling signals of four unrelated staphylococcal strains, 15981 (black line), ISP479r (green line), RN10359 (red line) and MW2 (blue line) while the interior tracks (black) correspond to the mapped reads from *S. aureus* 15981 strain. Blue boxes, ORFs; red boxes, intrinsic transcriptional terminators; Green dash lines, transcript. One representative example of a **(A)** bona fide long 3'-UTR; **(B)** a terminating-read-through dependent long 3'-UTR; **(C)** a riboswitch-dependent long 3'-UTR.

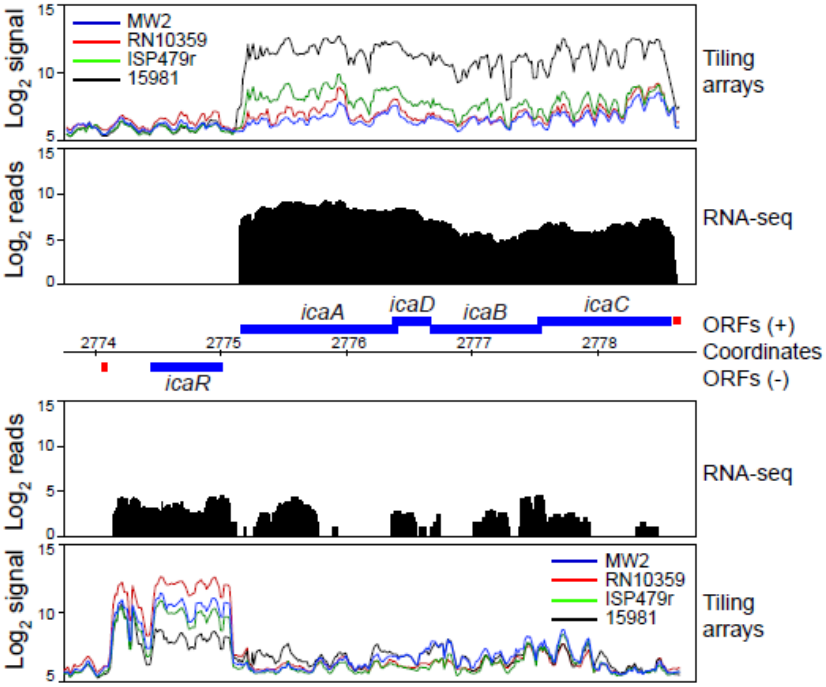

Figure S2 - IGB software image showing tiling arrays signals and RNA-seq mapped reads distribution in the *icaRADBC locus*. The exterior tracks correspond to tiling signals of four unrelated staphylococcal strains, 15981 (black line), ISP479r (green line), RN10359 (red line) and MW2 (blue line) while the interior tracks (black) correspond to the mapped reads from *S. aureus* 15981 strain. Blue boxes, ORFs; red boxes, intrinsic transcriptional terminators.

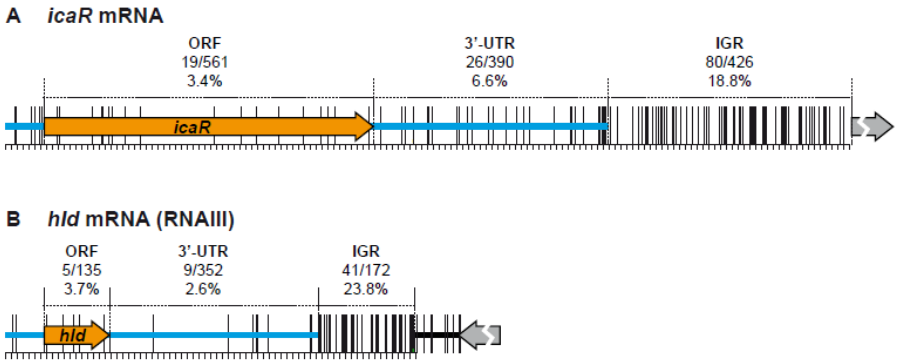

Figure S3 - *icaR* as well as *hld* 3′-UTRs are highly conserved in *S. aureus*. Nucleotide variation rate was calculated using the 176 *S. aureus* genomic sequences available at NCBI web page. Vertical lines represent a nucleotide change in at least one *S. aureus* genome. **(A)** *icaR* mRNA region. **(B)** *hld* mRNA (RNAIII) region. ORF, open reading frame; IGR, intergenic region comprised between the corresponding 3′-end and the end of the next known transcript.

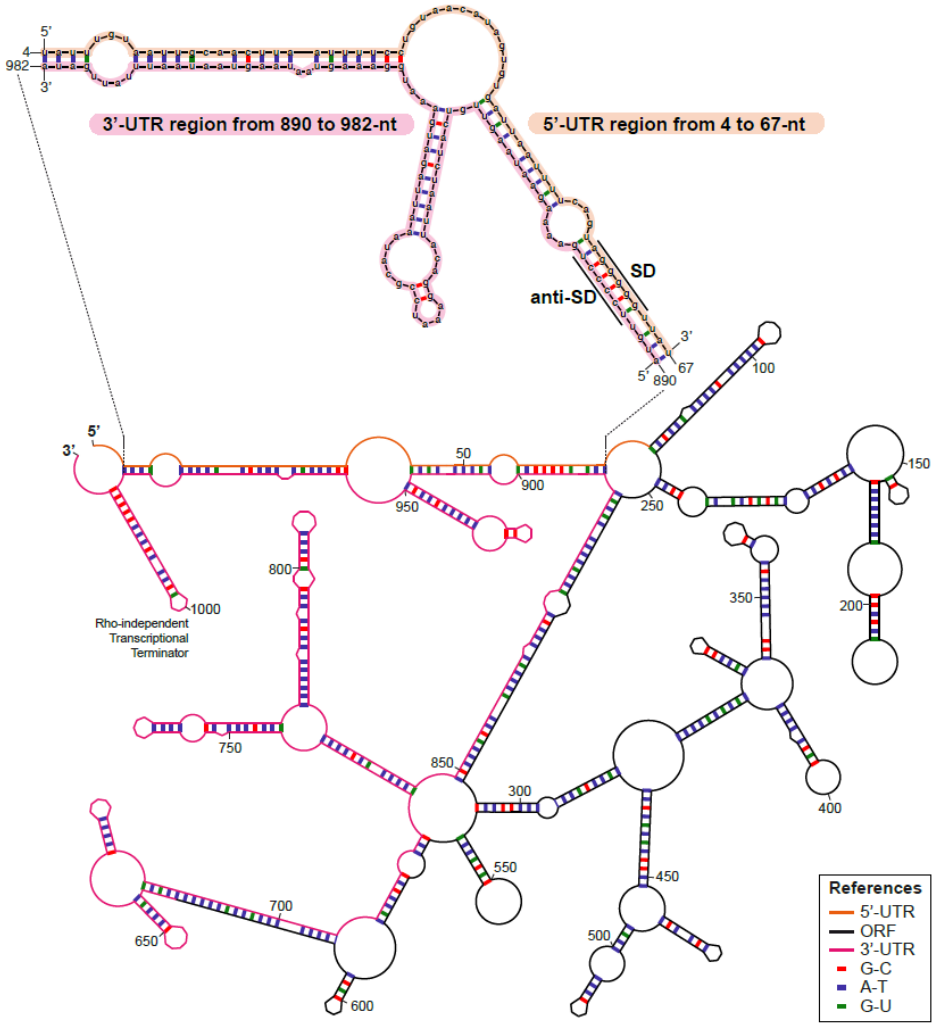

Figure S4 - Schematic representation of the RNA secondary structure prediction of the whole *icaR* mRNA molecule generated by Mfold program (http://mfold.rit.albany.edu/)(Zuker, 2003). G-U paring was allowed. The 5′-UTR/3′-UTR interaction region is amplified to show pairing nucleotides. The lowest-energy secondary-structural prediction is shown. RNA stem-loops were organized to avoid image superposition.

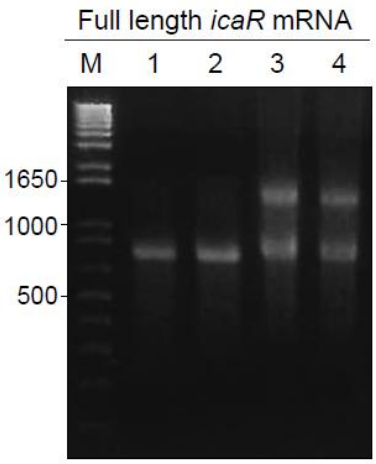

Figure S5 - Interaction of two *icaR* mRNA molecules in *trans*. Native agarose gel electrophoresis of the full-length *icaR* mRNA synthetized *in vitro*. Line 1, RNA in water; line 2, RNA in TE buffer (Tris-HCl 20 mM p 7.5, 1 mM EDTA) incubated 3 min at 90°C, chilled on ice and incubated 15 min at 37°C; line 3, RNA renatured in a buffer containing 20 mM Tris HCl pH 7.5, 50 mM KCl at 37°C for 15 min; line 4, RNA in a buffer containing 20 mM Tris HCl pH 7.5, 50 mM KCl, 10 mM $MgCl_2$ renatured at 37°C for 15 min. Sizes of some bands of the molecular weight marker (M) are indicated.

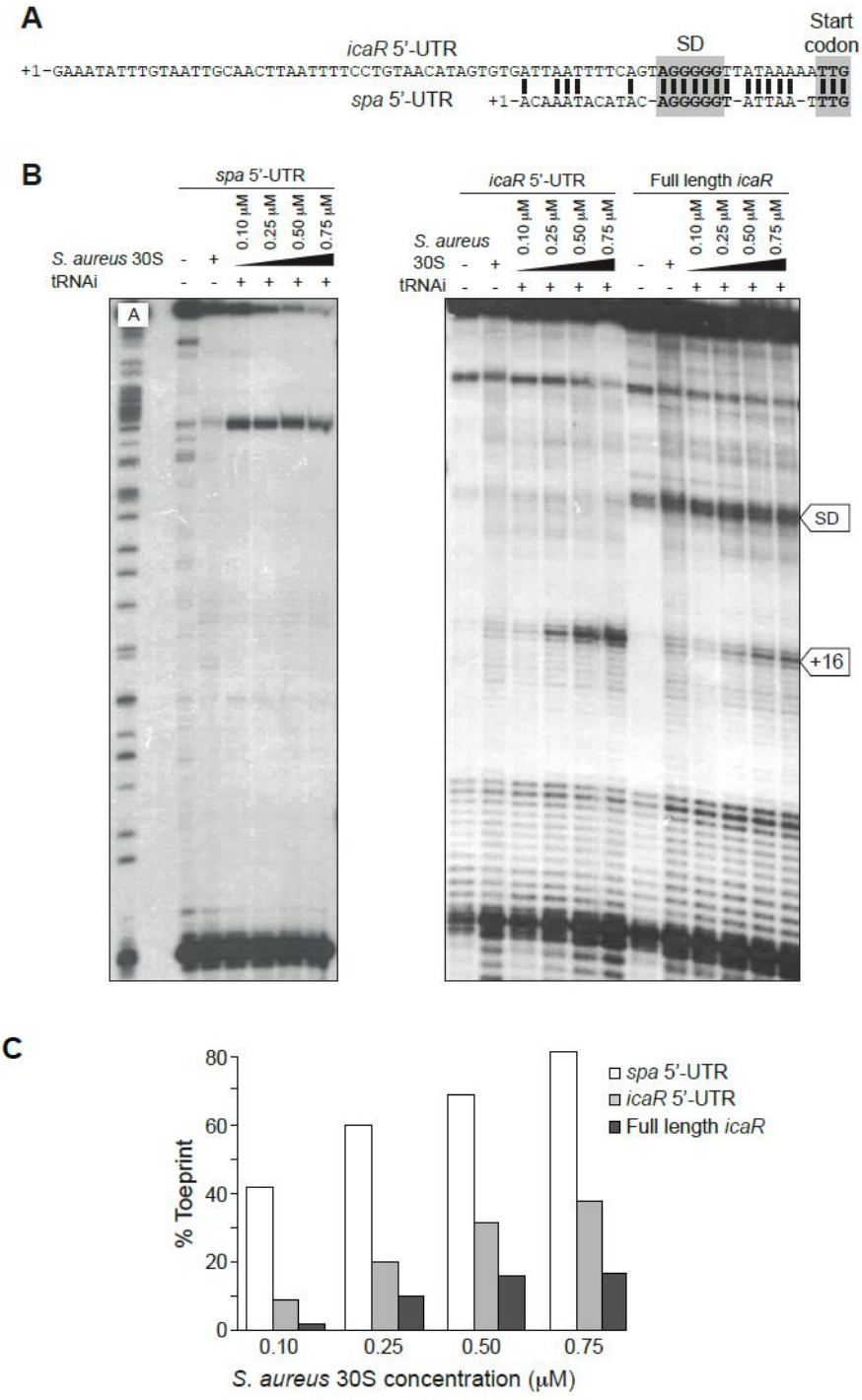
A
icaR 5'-UTR
SD
Start codon
+1-GAAATATTTGTAATTGCAACTTAATTTTCCTGTAACATAGTGTGATTAATTTTCAGTAGGGGGTTATAAAAATTG
spa 5'-UTR
+1-ACAAATACATAC-AGGGGGT-ATTAA-TTTG
B
spa 5'-UTR
icaR 5'-UTR
Full length icaR
0.10 µM
0.25 µM
0.50 µM
0.75 µM
S. aureus 30S
tRNAi
A
SD
+16
C
% Toeprint
80
60
40
20
0
0.10
0.25
0.50
0.75
S. aureus 30S concentration (µM)
spa 5'-UTR
icaR 5'-UTR
Full length icaR

Figure S6 - Toeprinting assays performed with *S. aureus spa* mRNA, the 5′-UTR of *icaR* mRNA and the full-length *icaR* mRNA. (A) Sequence of the 5′-UTR of *spa* and *icaR* mRNA are given for comparison. The Shine-Dalgarno (SD) sequence is in bold letter as well as the initiation codon UUG. **(B)** Autoradiographies showing the toeprinting assays performed on either *spa* mRNA, the 5′-UTR of *icaR*, and the full-length *icaR* mRNA. The toeprint at position +16, representing the formation of ternary initiation complex formed by *S. aureus* 30S ribosomal subunit, mRNA and the initiator $tRNA_f^{Met}$, is indicated. **(C)** Quantification of the toeprint was first normalized according to the full-length extension product bands using the SAFA software (Laederach *et al.*, 2008), and the toeprint signal is given in %.

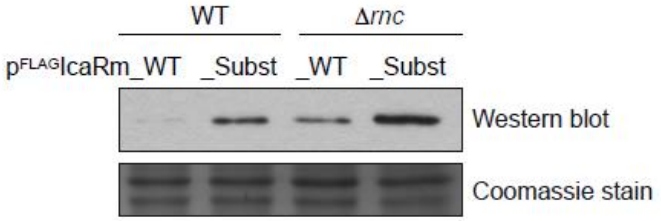

Figure S7 - IcaR protein levels expressed from wild-type and UCCCC substituted mRNAs in wild-type and RNase III mutant strains. A representative Western blot showing IcaR protein levels in wild-type and *rnc* deleted strains constitutively expressing the *icaR* mRNA wild-type or the mRNA carrying the UCCCCUG substitution. The 3XFLAG tagged IcaR protein was detected with commercial anti-3XFLAG antibodies. A Coomasie stained gel portion is shown as loading control.

REFERENCES

Amarasinghe AK, Calin-Jageman I, Harmouch A, Sun W, Nicholson AW. 2001. *Escherichia coli* ribonuclease III: affinity purification of hexahistidine-tagged enzyme and assays for substrate binding and cleavage. Meth Enzymol 342: 143–158.

Arnaud M, Chastanet A, Débarbouillé M. 2004. New vector for efficient allelic replacement in naturally nontransformable, low-GC-content, Gram-

positive bacteria. Applied and Environmental Microbiology 70: 6887–6891. doi:10.1128/AEM.70.11.6887-6891.2004.

Baba T, Takeuchi F, Kuroda M, Yuzawa H, Aoki K-I, *et al.* 2002. Genome and virulence determinants of high virulence community-acquired MRSA. Lancet 359: 1819–1827.

Boisset S, Geissmann T, Huntzinger E, Fechter P, Bendridi N, *et al.* 2007. *Staphylococcus aureus* RNAIII coordinately represses the synthesis of virulence factors and the transcription regulator Rot by an antisense mechanism. Genes & Development 21: 1353–1366. doi:10.1101/gad.423507.

Charpentier E, Anton AI, Barry P, Alfonso B, Fang Y, *et al.* 2004. Novel cassette-based shuttle vector system for Gram-positive bacteria. Applied and Environmental Microbiology 70: 6076–6085. doi:10.1128/AEM.70.10.6076-6085.2004.

Joanne P, Falord M, Chesneau O, Lacombe C, Castano S, *et al.* 2009. Comparative study of two plasticins: specificity, interfacial behavior, and bactericidal activity. Biochemistry 48: 9372–9383. doi:10.1021/bi901222p.

Lasa I, Toledo-Arana A, Dobin A, Villanueva M, de los Mozos IR, *et al.* 2011. Genome-wide antisense transcription drives mRNA processing in bacteria. Proceedings of the National Academy of Sciences 108: 20172–20177. doi:10.1073/pnas.1113521108.

Toledo-Arana A, Merino N, Vergara-Irigaray M, Débarbouillé M, Penadés JR, *et al.* 2005. *Staphylococcus aureus* develops an alternative, *ica*-independent biofilm in the absence of the *arlRS* two-component system. Journal of Bacteriology 187: 5318–5329. doi:10.1128/JB.187.15.5318-5329.2005.

Ubeda C, Barry P, Penadés JR, Novick RP. 2007. A pathogenicity island replicon in *Staphylococcus aureus* replicates as an unstable plasmid. Proc Natl Acad Sci USA 104: 14182–14188. doi:10.1073/pnas.0705994104.

Valle J, Toledo-Arana A, Berasain C, Ghigo J-M, Amorena B, *et al.* 2003. SarA and not sigma B is essential for biofilm development by *Staphylococcus aureus*. Mol Microbiol 48: 1075–1087.

Vergara-Irigaray M, Valle J, Merino N, Latasa C, García B, *et al.* 2009. Relevant role of fibronectin-binding proteins in *Staphylococcus aureus* biofilm-associated foreign-body infections. Infection and Immunity 77: 3978–3991. doi:10.1128/IAI.00616-09.

Chapter 5

THE FINE-TUNED CONTROL OF BIOFILM RESPONSE IN STAPHYLOCOCCUS AUREUS

This chapter contains unpublished data in which the author of this dissertation had a major contribution in the planning of the experimental work and in the performance of the experiments. The author (together with S. Domingues and IR de los Mozos) performed purification of RNase III and PNPase proteins, mapping of the cleavage sites generated by RNase III on the *5'*-3'UTR hybrid, RNA structure mapping, *in vitro* RNA interaction studies, and *in vitro* study of PNPase influence on 3'-UTR decay.

ABSTRACT

Biofilm development is a highly complex process, and constitutes one of the major medical concerns within *S. aureus* pathogenesis. Thus, the understanding of how it is regulated would help medical developments. *icaR* encodes for a key transcriptional regulator controlling biofilm formation in *Staphylococcus aureus*.

In a previous report, we have demonstrated that the 3'-UTR of *icaR* mRNA affects the expression level of the IcaR protein by controlling the stability of its own transcript. This modulation is performed through RNA base-pairing between *icaR 5'*-3'UTR. The RNA duplex formed traps the Shine-Dalgarno sequence and impairs the entry of the ribosomes, triggering degradation by RNase III and rendering the process irreversible.

Some questions remained unanswered, namely how the *5'*-3'UTR interaction is modulated by environmental signals. We show that temperature is one of the factors that modulate the *5'*-3'UTR base-pairing. At 23°C, the interaction was not efficient, and consequently RNase III lost its ability to cleave *icaR* mRNA. Structure probing of the *5'*-UTR showed a secondary structure more rigid at 23°C, which would explain the inability to interact with the 3'-UTR. Our findings indicate the presence of an RNA thermometer that appears to adjust IcaR protein levels according to the temperature sensed in the surrounding environment. To our knowledge, this is the first bacterial RNA thermometer whose regulation controls the accessibility of RNase III, and is also the first thermosensor reported in *S. aureus*.

This mechanism provides a rapid and efficient activation/inactivation of IcaR production in response to a sudden change in environmental conditions, allowing a fine-tuned adjustment of biofilm production in *S. aureus.*

INTRODUCTION

All living organisms have evolved rapid regulatory circuits to control gene expression in response to several stimuli. Ribonucleases (RNases) are key players in posttranscriptional control of gene expression by controlling RNA degradation. The degradation rate of an RNA molecule determines how long it is available as template for translation, directly modulating the levels of proteins with important cellular functions. Therefore, the decay of a given RNA is controlled by complex mechanisms (Silva *et al.*, 2011). RNases can be sensitive to specific sequence and/or structural features of the RNA molecule. RNA binding proteins or antisense RNA binding molecules can also modulate the activity of RNases (Silva *et al.*, 2011). These enzymes have been involved in the control of several important processes in the cell (Jester *et al.*, 2012; Silva *et al.*, 2011). RNase III is an ubiquitous enzyme specific for double-stranded RNA that has recently emerged as a global regulator. In *Staphylococcus aureus*, this enzyme was shown to cleave sense/antisense transcripts that arise from genome-wide antisense transcription (Lasa *et al.*, 2011; Lioliou *et al.*, 2012). RNase III has been shown to control the expression of transcripts directly involved in biofilm formation (Andrade and Arraiano, 2008; Carzaniga *et al.*, 2012; Rouf *et al.*, 2011; Sim *et al.*, 2010; Viegas *et al.*, 2011). However, its role in *S. aureus* biofilm development has not been explored.

Biofilm production is a main factor of *S. aureus* virulence, being critical for the progression of infections caused by this bacterium. Due to its ability to colonize implants as a biofilm, it is the etiological agent of persistent and recurrent infections in patients with indwelling medical devices (Arciola *et al.*, 2012). The main exopolysaccharide of *S. aureus* biofilm is a polymer of N-acetylglucosamine (PIA-PNGA), which is synthesized by the genes of the *icaADBC* operon (Cramton *et al.*, 1999; Gotz, 2002). In a previous report, we have

demonstrated that IcaR, the main repressor of this operon, posttranscriptionally regulates its own expression through a *cis*-acting element. This regulation is performed through RNA base-pairing between the 3'-UTR of *icaR* mRNA and the Shine-Dalgarno (SD) region at the *5'*-UTR. This RNA interaction inhibits ribosome loading and triggers mRNA degradation by RNase III, leading to low IcaR levels and thus reducing biofilm production.

It is known that biofilm development in *S. aureus* is regulated by temperature (Archer *et al.*, 2011). *Cis*-acting elements located at *5'*-UTRs may include temperature regulators so-called thermosensors. These RNA thermometers undergo conformational changes that modulate ribosome accessibility upon temperature shift (Kortmann and Narberhaus, 2012). For instance, increase in temperature by a melting process, destabilizes their secondary structure and releases the ribosome binding site (RBS). On the other hand, at low temperatures, ribosome loading is blocked by complementary base-pairing (Bohme *et al.*, 2012; Jorgensen *et al.*, 2012; Kortmann and Narberhaus, 2012; Narberhaus *et al.*, 2006).

In the present work, we have indications that *icaR* expression levels are regulated through an RNA thermometer. This thermosensor modulates the access of the 3'-UTR to the *5'*-UTR region to adjust IcaR levels according to the temperature sensed in the surrounding environment. This further regulates the access of RNase III to the *5'*-3'UTR duplex.

EXPERIMENTAL PROCEDURES

Bacterial strains and culture conditions

The oligonucleotides, plasmids and strains used in this study are listed in Table 1, Table 2 and Table 3, respectively. *S. aureus* wild-type strains, its isogenic mutants and transformants were grown in Trypticase Soy Broth supplemented with 0.25% glucose (TSB-gluc) (Pronadisa). *Escherichia coli* transformants were grown in Lysogeny Broth (Pronadisa). When required for selective growth, medium was supplemented with appropriated antibiotics at the following concentrations: erythromycin (Em), 1.5 μg/ml and 20 μg/ml, and ampicillin (Amp), 100 μg/ml.

Western blot analysis

Overnight cultures of the strains tested were diluted 1:100 in TSB-gluc, and 20 ml of this cell suspension were grown in 125 ml flasks until OD_{600nm} reached 0.8. Ten ml of bacterial cultures were centrifuged and pellets were resuspended in 100 μl PBS. Then, 2 μl of Lysostaphin 1 mg/ml (Sigma) and 3 μl of DNase I 1mg/ml (Sigma) were added. After 2 h of incubation at 37°C cell lysates were centrifuged and supernatants were collected. Protein concentration was determined with the Bio-Rad protein assay (Bio-Rad). Samples were adjusted to 5-10 μg/μl of total protein and one volume of Laemmli buffer was added. Total protein extracts were denatured by boiling at 100°C for 5 min. Proteins were separated on 12% SDS-polyacrylamide gels and stained with 0.25% Coomassie brilliant blue R250 (Sigma) as loading controls. For Western blotting, proteins were transferred onto Hybond-ECL nitrocellulose membranes (Amersham Biosciences) by semi-dry electroblotting. Membranes were blocked overnight with 5% skimmed milk in phosphate-buffered saline (PBS) with 0.1% Tween 20, and incubated with anti-FLAG antibodies labelled with phosphatase alkaline

(Sigma) diluted 1:500 for 2 h at room temperature. 3XFLAG labelled IcaR protein was detected with the SuperSignal West Pico Chemiluminescent Substrate (Thermo Scientific).

Biofilm formation assay

Biofilm formation assay in microtiter plates was performed as described (Heilmann *et al.*, 1996). Briefly, strains were grown overnight at 37°C and were diluted 1:40 in TSB-gluc and TSB-NaCl for *S. aureus* 15981 and *S. aureus* 132 strains respectively. 200 μL of cell suspension was used to inoculate sterile 96-well polystyrene microtiter plates (Iwaki). After 24 hours at 37°C, wells were gently rinsed by immersion in a water bath three times. Bacteria adhered at the bottom of the well was developed by staining with 0.1% of crystal violet for 5 min. Biofilm formation assay in 10-ml glass test tubes after 18 hours of growth at 37°C in TSB-gluc medium with shaking (180 rpm).

In vitro transcription

Synthetic RNA molecules used as substrates were obtained by *in vitro* transcription using "Riboprobe *in vitro* Transcription System" (Promega). DNA templates were generated by PCR and carried a T7 promoter sequence. *5'*-UTR and 3'-UTR wild-type *icaR* fragments were amplified using chromosomal DNA from *S. aur*eus 132 strain, while *5'*-UTR-compensatory and 3'-UTR-substituted fragments were amplified from the corresponding plasmids (see Table 2) (de los Mozos IR, 2013) using the oligonucleotides pairs RNA T7 IcaR+1/ RP *5'*-UTR IcaR RV and RNA T7 3'-UTR UCCCC Fw / RP 3'-UTR UCCCC Rv, respectively (Table 1).

For the synthesis of the internally labelled RNA substrates, *in vitro* transcription was carried out using the purified PCR product as template in the presence of an excess of [^{32}P]-α-UTP over unlabeled UTP with 'Riboprobe *in vitro*

Transcription System' (Promega) and T7 RNA polymerase. Non-radioactive molecules were transcribed in the same conditions but using equimolar concentrations of all four ribonucleotides.

All the substrates were purified by electrophoresis on an 8.3M urea/ 6% polyacrylamide gel to separate full length transcripts from prematurely terminated transcription products. The corresponding bands were excised from the gel, the sliced gel fragment was crushed and the RNA eluted with elution buffer [3 M ammonium acetate pH 5.2, 1mM EDTA, 2.5% (v/v) phenol pH 4.3], overnight at room temperature. The RNA was ethanol precipitated, resuspended in RNase free water and quantified using the Biophotometer Plus (Eppendorf). The yield of the labelled substrates (cpm/µl) was determined by scintillation counting.

For 5'-end labeling of RNA, the *5'*-triphosphates of the purified cold transcripts were replaced by *5'*-monophosphates and phosphorylated with [^{32}P]-γ-ATP, using the KinaseMax *5'*-End-Labeling Kit (Ambion), according to manufacturer's recommendations. Reactions were electrophoresed again on an 8.3M urea/6% polyacrylamide gel, and the RNA was purified as described above.

Gel shift assays

Binding assays were performed in 1X TMN buffer (20 mM Tris acetate pH 7.6, 100 mM sodium acetate, 5 mM magnesium acetate) as previously described (Udekwu *et al.*, 2005). Briefly, 0.025 pmol of labelled *5'*-UTR-wt was incubated with increasing concentrations of unlabelled 3'-UTR-wt in a total volume of 10 µl, at 37°C or 23°C for 30 min. The binding reactions were then mixed with 2 µL of loading buffer (48% glycerol, 0.01% bromophenol blue) and electrophoresed on native 5% polyacrylamide gels in 0.5X TBE buffer at 200V in a cold room for 3 h. Gels were analyzed using PhosphorImaging technology (FLA-2000, Fuji, Stamford, CT).

TABLE 1 - List of oligonucleotides used in this work. The restriction and T7 sequences in the primers used for cloning procedures and for riboprobe synthesis, respectively, are shown in bold and underlined.

Oligo	Sequence *5'- to 3'*
RNA T7 IcaR +1	TAATACGACTCACTATAGGGGAAATATTTGTAATTGCAACTTAATTT
RP *5'*-UTR IcaR RV	CTCTGAAAATAAGGTTATTGCG
RNA T7 3'-UTR UCCC FW	TAATACGACTCACTATAGGGCTTTATATTTGTGAATGGTTAAGT
RP 3'-UTR UCCC FW	TTCCATTTCATCTAATTTATGCGG
RNase III Fw	**GGAATTC**CATATGTCTAAACAAAAGAAAAGTGAG
RNase III Rv	**CGCGGA**TCCCTATTTAATTTGTTTTAATTGCTTATAG
ams020 FW	AAACCATGGATGTCTCAAGAAAAGAAAG
ams021 RV	TTCTCGAGTTCTTCTAATGCTCTATGTG

TABLE 2 - List of plasmids used in this work.

Plasmid	Relevant Characteristics	Source/Reference
pET-15b	Inducible expression vector, N-terminal HisTag	Novagen
pET-15b RNase III	pET-15b expressing an N-terminal His-tag fusion of the S. aureus *rnc* gene.	(de los Mozos IR, 2013)
pET-28b	Inducible expression vector, C-terminal HisTag	Novagen
pET-28b PNPase	pET-28b expressing a C-terminal His-tag fusion of the *S. aureus pnp* gene.	This study
p^{FLAG}IcaRm	pCN40 plasmid constitutively expressing the N-terminal 3XFLAG tagged IcaR protein from the entire mRNA	(de los Mozos IR, 2013)
p^{FLAG}IcaRmΔ3'UTR	pCN40 plasmid constitutively expressing the N-terminal 3XFLAG tagged IcaR protein from the mRNA carrying a deletion of 331 nt downstream of the stop codon	(de los Mozos IR, 2013)
p^{FLAG}IcaRm3'UTR	pCN40 plasmid constitutively expressing the N-terminal 3XFLAG tagged IcaR protein from the mRNA carrying only the 3'UTR	(de los Mozos IR, 2013)

TABLE 3 - List of strains used in this work

Strain	Relevant Characteristics	Source or Reference
S. aureus 132	MRSA clinical strain with the capacity to form proteinaceous biofilm in TSB-glucose and PIA-PNAG-dependent biofilm in TSB-NaCl	(Vergara-Irigaray *et al.*, 2009)
S. aureus 15981	Clinical strain. Biofilm positive in TSB.	(Valle *et al.*, 2003)
S. aureus 15981 pIcaRm	15981 strain harbouring the pIcaRm plasmid	(de los Mozos IR, 2013)
S. aureus 15981 pIcaRmΔ3'UTR	15981 strain harbouring the pIcaRm Δ3'UTR plasmid	(de los Mozos IR, 2013)
S. aureus 15091 + p*pnp* + pIcaRΔ3'UTR	15981 strain with deletion in the *pnp* gene harbouring pCU1-*pnp* and pCN40-*icaR* Δ3'UTR plasmids	This study
S. aureus 15981 Δ*pnp*	15981 strain with deletion in the *pnp* gene	This study
S. aureus 15091 + p*pnp* + pIcaR	15981 strain with deletion in the *pnp* gene harbouring pCU1-*pnp* and pCN40-*icaR* plasmids	This study
S. aureus 15091 + p*pnp* + pIcaRΔ3'UTR	15981 strain with deletion in the *pnp* gene harbouring pCU1-*pnp* and pCN40-*icaR* Δ3'UTR plasmids	This study
E. coli DH5α	*rec*A1 *end*A1 *gyr*A96 thi-*hsd*R17 *sup*E44 *rel*A1 Δ*lac*ZYA-*arg* FU169 f80dLacZDM15	(Studier and Moffatt, 1986)
E. coli BL21(DE3)	*sup*E44 *rel*A1 Δ*lac*ZYA-*arg* FU169 f80dLacZDM15	(Studier and Moffatt, 1986)
BL21(DE3)*rnc*105*recA*	F^- *omp*T *hsd* S_B(rb^-mb^-) gal dcm (DE3) *rec*A *rnc*105	(Amarasinghe *et al.*, 2001)

Cloning of Recombinant S. aureus RNase III and PNPase

S. aureus RNase III was cloned and purified as described in (de los Mozos IR, 2013). Briefly, *S. aureus* RNase III coding sequence (*rnc*) was amplified with primer pairs RNAse III Fw and RNAse III Rv. The forward primer includes the NdeI restriction site and the reverse primer contains the BamHI restriction site. The purified PCR products were double digested with BamHI and NdeI and ligated to the pET-15b vector (Promega) previously digested with the same enzymes, generating the plasmid pET-15b-*rnc*. This plasmid was first cloned into *E. coli* DH5α and subsequently transformed into BL21(DE3) *rnc*105 *rec*A (Amarasinghe *et al.*, 2001). This derivative of BL21(DE3), carrying an RNase III mutation, was used because it blocks the regulation of *S. aureus* RNase III by the

endogenous *E. coli* homologue, resulting in a higher yield of the enzyme upon overexpression.

S. aureus PNPase coding sequence (*pnp*) was amplified with primer pairs ams020 Fw and ams021 Rv. The forward primer includes the *Nco*I restriction site and the reverse contains the *Xho*I restriction site. The purified PCR product and pET-28b vector (Novagen) were digested with *Nco*I, and further treated with 0.1U of MungBean Nuclease (New England Biolabs) for 30 min at 30°C. After incubation, the reactions were stopped with 0.1% SDS. Afterwards, the purified PCR product and pET-28b vector were digested with *Xho*I and further ligated. The plasmid obtained (pET-28b-*pnp*) was first cloned into *E. coli* DH5α and subsequently transformed into BL21(DE3) competent cells.

All constructs were confirmed by DNA sequencing.

Purification of Recombinant S. aureus RNase III and PNPase

The recombinant RNase III was overexpressed and purified according with de los Mozos *et al.* (de los Mozos IR, 2013). Briefly, to overexpress the protein, the BL21(DE3) *rnc*105 *rec*A strain containing pET-15b-*rnc* was grown in 200 ml of LB medium supplemented with ampicillin (100 μg/ml) to an optical density at 600 nm of 1.5. At this point, protein expression was induced by addition of 1 mM of IPTG and the culture was further incubated over-night at 15°C. Cells were then harvested by centrifugation and the pellet stored at -80°C. Briefly, the histidine tagged recombinant RNase III was purified by affinity chromatography, using the ÄKTA FPLCTM System (GE Healthcare). The purity of the enzyme was analysed by sodium dodecyl sulphate-polyacrylamide gel electrophoresis (SDS-PAGE) and revealed >90% homogeneity.

To overexpress the recombinant PNPase, BL21(DE3) strain containing pET-28b-*pnp* was grown in 200 ml of LB medium supplemented with kanamycin (50 μg/ml) to an optical density at 600 nm of 0.5. At this point, protein expression

was induced by addition of 0.4 mM of IPTG and the culture was further incubated for 4h at 30℃. Cells were then harvested by centrifugation, and the pellet was resuspended in 6 ml of cold buffer (PBS 1X pH 7.4, 10 mM Imidazole). Cells were lysed using a French Press at 900 psi in the presence of 0.1 mM of PMSF. After lysis, the crude extract was treated with 125 U of Benzonase (Sigma) and incubated on ice for 30 min. Protein extract was then clarified by centrifugation, 30 min, 27.000xg at 4℃. The histidine tagged recombinant PNPase was purified by affinity chromatography, using the ÄKTA FPLC™ System (GE Healthcare). Clarified extracts were loaded onto a HisTrap HP Sepharose 1 ml column. Protein elution was achieved in elution buffer (PBS 1X, 500 mM Imidazole) (0-100% in 20min – flow 1ml/min). The fractions containing the protein of interest, free of contaminants, were pooled. The sample was desalted in amicon 50 KDa protein and by dialysis against desalting buffer (PBS 1X, 1mM DTT). Protein samples were quantified using Bio-Rad protein assay (Bio-Rad). Samples were were stored at -20℃ in 50% of glycerol. The purity of the enzyme was analysed by SDS-PAGE and revealed >90% homogeneity.

RNase III and PNPase Activity Assays

The activity of purified RNase III was tested over internally labelled or *5′*-end labelled *5′*-UTR *icaR* fragment in the presence or absence of unlabeled 3′-UTR-wt or 3′-UTR-substituted *icaR* fragments. Hybridization between labelled and unlabelled substrates was always performed in a 1:50 ratio in the Tris component of the activity buffer by incubation for 10 minutes at 80℃, followed by 45 minutes at 37℃. The same treatment was applied to free *5′*--UTR-wt or free 3′-UTR-wt. The activity assays were done in a final volume of 40µl containing the activity buffer (30 mM Tris-HCl pH 8, 160 mM NaCl and 0.1 mM DTT) and approximately 0.14 pmol of the substrate mix. 10 mM of $MgCl_2$ was added to the reaction mixture. As a control, prior to the beginning of each assay an aliquot

(without the enzyme) was taken and was incubated in the same conditions until the end of the assay. The reactions were started by the addition of RNase III at a concentration of 500 nM, and were further incubated at 37°C or 23°C.

PNPase was tested over internally labelled free 3'-UTR-wt or before or after RNase III cleavage, at 37°C. Likewise, 60 nM of PNPase was added to the ongoing reactions with 500 nM of RNase III, at the time points indicated on the top of the figures. The activity assays were performed in a final volume of 40µl containing the activity buffer (150mM Tris-HCl pH 8, 50mM Na_2PO_4, 150mM KCl, 500mM NaCl, 0.5mM DTT). 10 mM of $MgCl_2$ was added to the reaction mixture. The reactions were stopped by the addition of formamide-containing dye supplemented with 10 mM EDTA. Reaction products were resolved in a 7M urea/10% polyacrylamide gel as indicated in the respective figure legends. Gels were analyzed using PhosphorImaging technology (FLA-2000, Fuji, Stamford, CT).

M13 sequencing reactions

M13 sequencing reactions were performed with the Sequenase Version 2.0 sequencing kit according to the instructions manual.

RNA Structure Mapping

0.2 µg of *5'*-end labelled *5'*-UTR-wt *icaR* was probed with RNase A, RNase T1 and RNase V1 using the RNA structure probing kit from Ambion according to the instructions of the manufacturer. The RNA substrate was heated at 50°C for 5 minutes in the presence of RNA Structure buffer (Ambion) and 4 µg of yeast RNA (Ambion), and then allowed to refold by incubation at 23°C or 37°C for 30 min. 10µl of refolded substrate was then probed separately with different concentrations (indicated on the top of the figures) of RNase A, RNase T1 and RNase V1 at 23°C and 37°C for 15 min. A control RNA sample was processed

simultaneously without enzymes. Sequencing reactions were performed in RNA Sequencing Buffer using RNase A and RNase T1 after denaturation of the substrate at 50°C for 5 min according to the manufactures' suppliers. All reactions were analyzed in a 8.3M urea polyacrylamide gel at different polyacrylamide concentrations in order to resolve the whole RNA molecule. Gels were analyzed using PhosphorImaging technology (FLA-2000, Fuji, Stamford, CT).

RESULTS

icaR mRNA is thermoregulated

It is well established that temperature is an important modulator of biofilm development (Archer *et al.*, 2011). We decided to check if *icaR* expression levels and biofilm formation are modulated by temperature in a 3'-UTR-dependent manner. Therefore, we started by analysing the ability of strains harbouring different *icaR* constructions (Figure 1A) to form biofilm at different temperatures. The most remarkable effects were detectable at 23°C and 37°C (Figure 1B). The strain overexpressing *icaR* wt revealed incapacity to form biofilm at 23°C, contrary to what was observed at 37°C (Figure 1B). However, when Δ3'-UTR *icaR* was overexpressed, the strain lost its ability to develop biofilm even at 37°C. We have also analysed IcaR protein levels in the same conditions by Western blot. As shown in Figure 1C, upon overexpression of *icaR* wt, higher levels of IcaR repressor were observed at 23°C, as compared to those observed at 37°C. This observation is in agreement with the incapacity of this strain to form biofilm only at 23°C. In contrast, when *icaR* lacks the 3'-UTR, the amount of repressor is always high and the ability to form biofilm is compromised.

Taken together, *icaR* expression levels seem to be thermo-regulated in a 3'-UTR dependent manner with consequences for biofilm development.

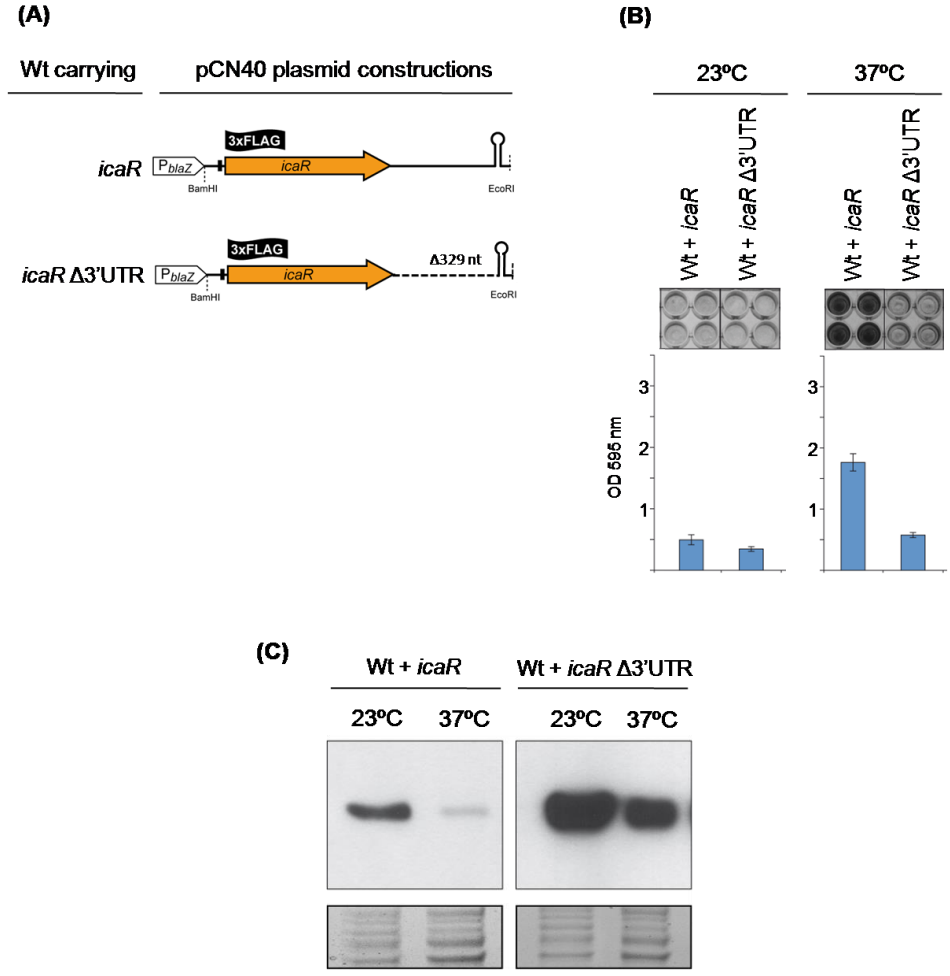

Figure 1 - Influence of temperature on the 3′-UTR mediated regulation of IcaR levels. **(A)** Schematic representation of the plasmid constructions harboring the whole *icaR* mRNA (*icaR*) and a 329 nt *icaR* 3′-UTR deletion (*icaR* Δ3′-UTR). The constructions constitutively express 3XFLAG tagged genes from a P*blaZ* promoter. **(B)** Biofilm formation capacity of the strains wt harboring the constructions shown on panel A, as indicated on the top of the figure, on polystyrene microtiter plates after 24 hours of growth at 37ºC in TSB-gluc medium. **(C)** Western blot showing the IcaR protein levels of the strains wt+*icaR* and wt+*icaR* Δ3′-UTR. The 3XFLAG tagged IcaR protein was detected by commercial anti-3XFLAG antibodies. A Comassie stained gel portion is shown as loading control. Experiment performed by IR de los Mozos.

We have previously demonstrated that binding of *icaR* 3'-UTR to the SD region, at 37ºC, inhibits IcaR synthesis by competitively blocking ribosome loading (de los Mozos IR, 2013). Taking the results above, we wondered if the binding of *icaR* 3'-UTR to the *5'*-UTR region could be affected at 23ºC. We compared the interaction between 3'-UTR and *5'*-UTR at 23ºC and 37ºC by RNA gel shift assays. The assays are shown in Figure 2. By lowering the temperature we would expect a stronger hybridization through complementary base pairing. However, the data obtained show that the binding between *5'*-UTR and 3'-UTR is less efficient at 23ºC, indicating that this interaction is not thermodynamically favoured at this temperature. Hence, we hypothesized that *icaR 5'*-UTR may form a secondary structure that is unable to interact with the 3'-UTR at 23ºC.

Taken together, these results suggest that *5'*-3'UTR base pairing is modulated by temperature. The different interaction between *5'*-UTR and 3'-UTR observed at 37ºC and 23ºC could explain the results displayed on Figure 2. The lack of *5'*-3'UTR interaction at 23ºC would permit the synthesis of IcaR repressor and consequently abolishes biofilm formation.

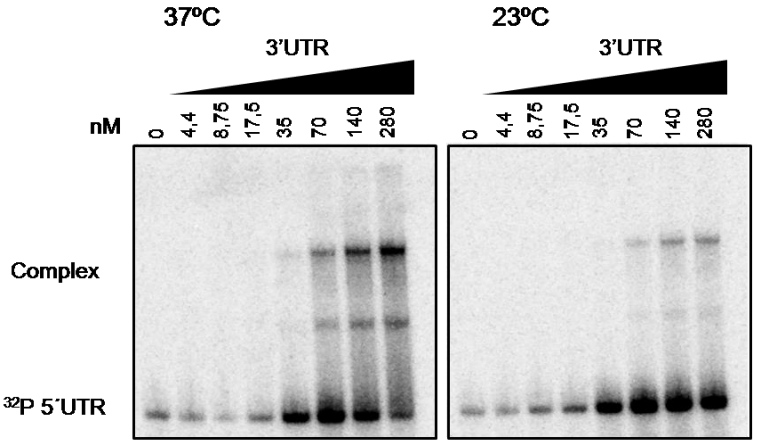

Figure 2 – Influence of temperature on *5′-3′*UTR interaction. (A) Gel shift analysis of the *5′-* and 3′-UTR interaction at 37℃ and 23℃. The internally labeled *5′*-UTR fragment was incubated with various concentrations of unlabeled 3′-UTR. After 30 min of incubation at 37℃/23℃, the mixture was analyzed by electrophoresis in a 5% native polyacrylamide gel and visualized by phosphorimaging.

RNase III activity on icaR 5′-UTR is affected by temperature

Given that the formation of the complex *5′*-UTR-3′UTR promotes RNase III cleavage at 37℃, and that this interaction is not favoured at 23℃, we wanted to compare the activity of RNase III over the *5′*-UTR at both temperatures. The activity assays were carried out with *5′*-UTR alone or in combination with 3′-UTR wt. A 3′-UTR with substitutions on the UCCCCUG motif (3′-UTR substituted) was used as a control. As we can observe in Figure 3B, the enzyme was indeed less efficient in cleaving the *icaR 5′*-UTR at 23℃, and was less sensitive to the presence of the *icaR* 3′-UTR. Taking into consideration that at 37℃ RNase III is only efficient in cleaving the hybrid *5′-3′*UTR, we infer that the inefficiency of the enzyme at 23℃ is probably due to poor hybridization at this temperature. This hypothesis was verified by accurate determination of the RNase III cleavage positions. Since *5′*-UTR was labeled in the *5′*-end, the size of the fragments generated by RNase III indicates the distance from the cleavage site to the *5′*-end of the *icaR 5′*-UTR. Several degradation products with a size comprised between 38 and 44 nts were generated by RNase III cleavage. As expected, these corresponds to cuts in the double stranded region, upstream the Shine-Dalgarno (Figure 3C). However, a main degradation product of 38 nts, indicates a preferential cleavage site in the *icaR 5′*-UTR (Figure 3A). Nevertheless, although within the same region, the cleavage sites determined *in vitro* do not completely match the ones previously found *in vivo* by mRACE analysis (de los Mozos IR, 2013). This difference is most likely related with the presence of additional players *in vivo*. In fact, RNase J enzymes may rapidly degrade *icaR* in the *5′*-3′ direction following the initial cut by RNase III. Our results confirmed that *5′*-UTR

is cleaved by RNase III inside the duplex region created upon base pairing with the 3′-UTR. Since this interaction is governed by temperature, RNase III cleavage is also temperature-dependent.

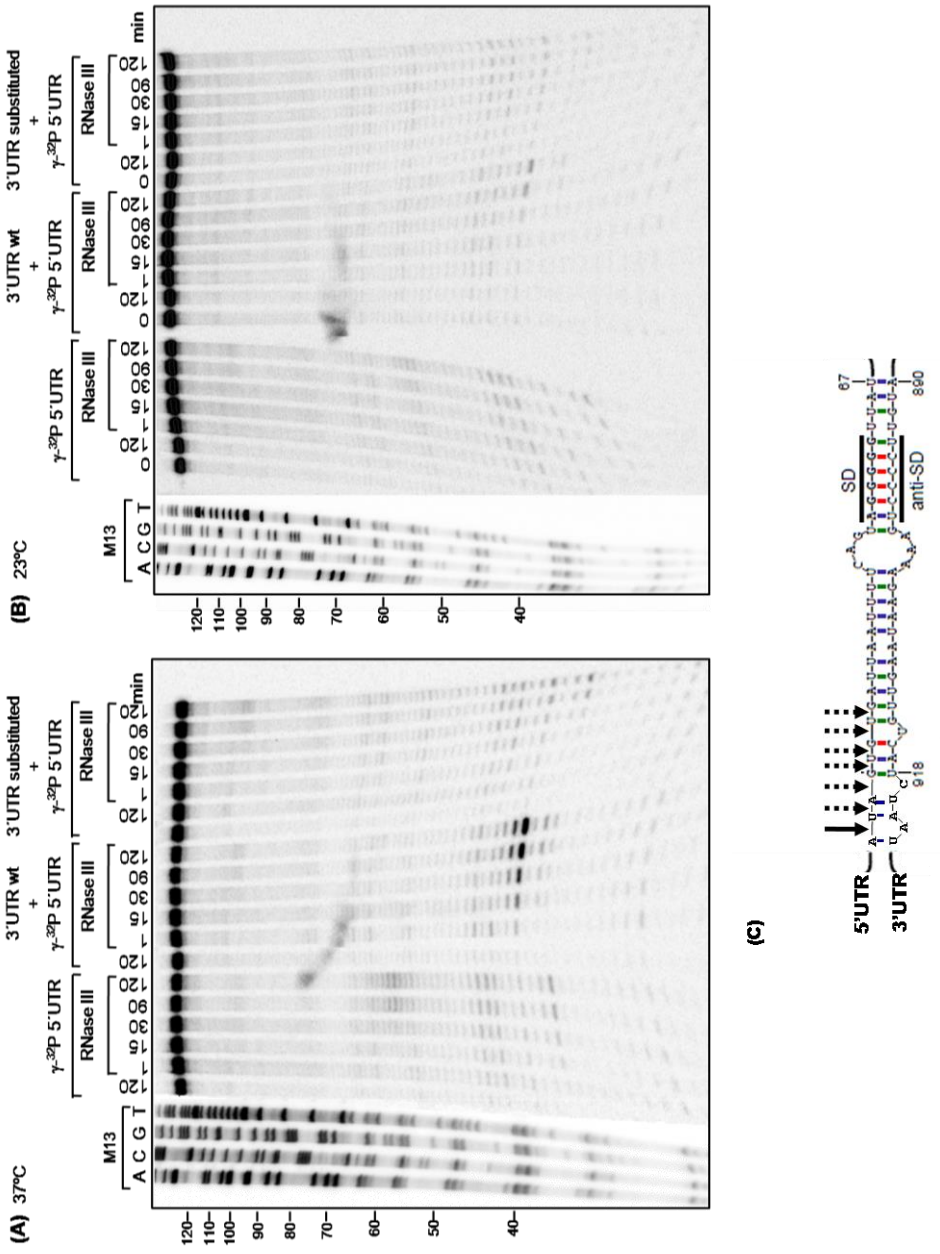

Figure 3 – Influence of temperature on RNase III activity. Activity assays showing the *in vitro* cleavage of *icaR 5′*-UTR by 500 nM of *S. aureus* RNase III at 37°C **(A)** and 23°C **(B)**. The assays were performed with *5′*-end labeled *5′*-UTR in the absence or presence of a molar excess of 3′-UTR wt or 3′-UTR substituted unlabeled transcripts. Aliquots were withdrawn at the time-points (minutes) as indicated above each lane. The first lanes of each reaction correspond to the control without the protein at time zero (0 min) and at the end of the reaction time (120 min). Reactions were electrophoresed in a 10% (w/v) polyacrylamide gel containing 8.3M urea and visualized by phosphorimaging. The lanes labeled with A, T, C and G represent M13 sequencing reactions that were used as molecular size marker. **(C)** Proposed interaction region between *icaR 5′*-UTR and 3′-UTR generated by Mfold [adapted from {de los Mozos IR, 2013 #1077}]. The Shine-Dalgarno region is indicated. The Anti Shine-Dalgarno at 3′-UTR is also identified. The black arrow indicates the major RNase III cleavage site on *5′*-UTR as determined on (A).

icaR 5′-UTR secondary structure is more loosely at 37°C

Changes in temperature usually alter RNA structure. The inability of *icaR* 3′-UTR to interact with the *5′*-UTR at 23°C suggests that the *5′*-UTR could be thermoregulated by changes in its RNA secondary structure. At 23°C, the *5′*-UTR might fold into a secondary structure that impairs hybridization with 3′-UTR, while at 37°C its structure may be melted, allowing 3′-UTR interaction. Thereby, we have analyzed the structural conformation of *5′*-UTR at 37°C and 23°C. For this purpose, *5′*-end labelled *5′*-UTR was probed with RNase A (cleaves 3′ of unpaired cytosines and adenines), RNAse T1 (cleaves 3′ of unpaired guanines), and RNase V1 (specific for double-stranded sequences) (Figure 4A and B). In figure 4C is represented the *icaR 5′*-UTR secondary structure as inferred from analysis of structure probing results at 37°C. This molecule seems to fold in a stem-loop structure interrupted by two internal loops separated by double stranded regions. The Shine-Dalgarno (red) is located in a single-stranded region of the loop II. This is in agreement with our toeprint results, which showed that at 37°C the *5′*-UTR fragment of *icaR* is able to form the ternary ribosomal initiation complex (de los Mozos IR, 2013). Some bases of the region comprised between -60 and -20 (relative to the AUG start codon) are weakly cleaved both by single and

double-stranded specific enzymes. This suggests that the secondary structure in this region might be relatively unstable at 37°C, suffering oscillations between single and double-stranded. On the contrary, at 23°C although we could not observe striking variations in the general *5′*-UTR structure, the -60/-20 region is less accessible to RNA single-stranded specific enzymes. This fact indicates that the structure of this region is more rigid at 23°C. Since this is the region that hybridizes with the 3′-UTR, the closer conformation might inhibit the formation of the *5′*-3′UTR duplex. This is in agreement with our binding shift results that revealed pour hybridization between the *5′*-UTR and 3′-UTR at 23°C (Figure 2).

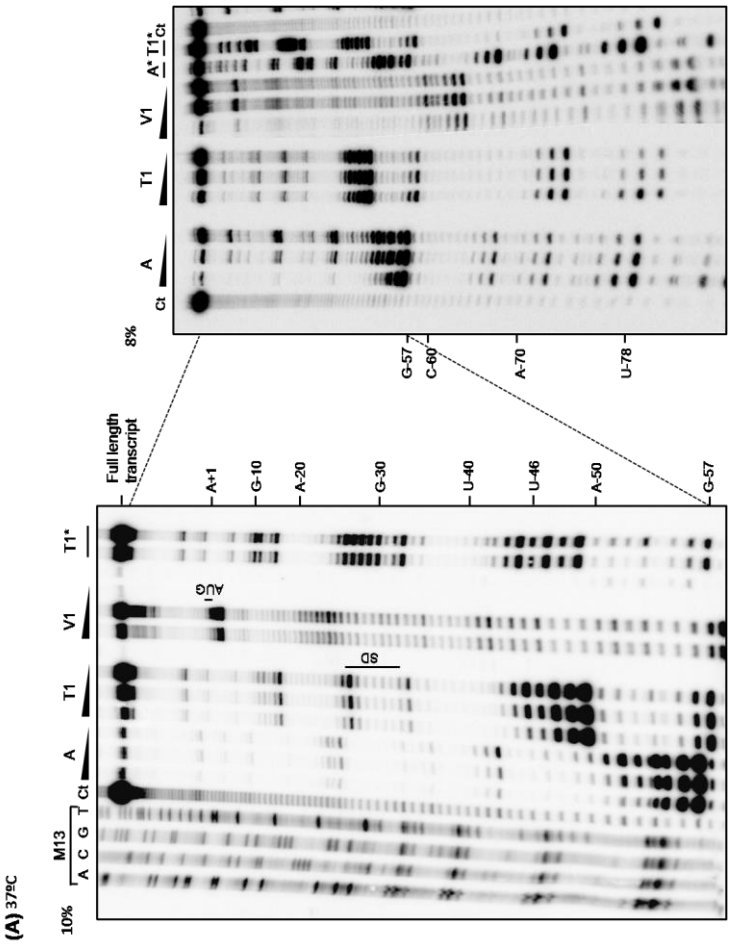

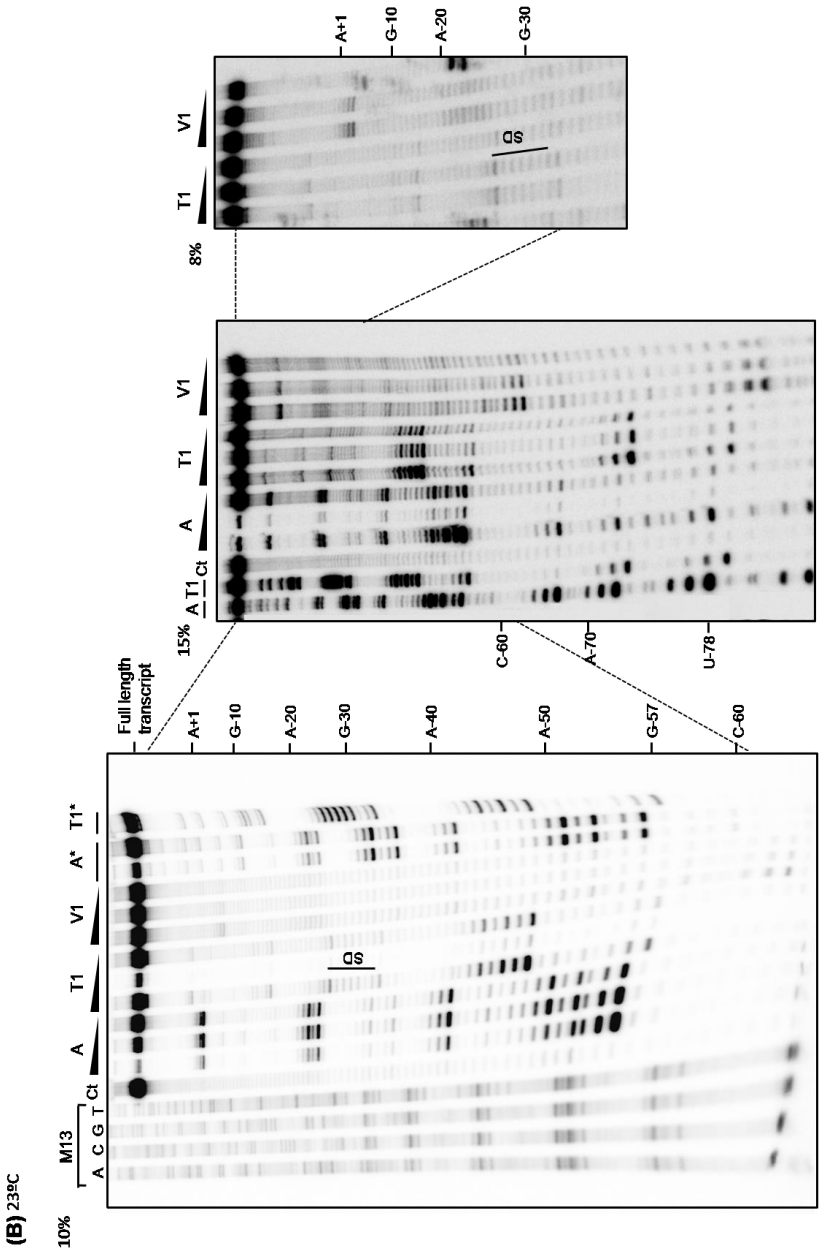
(B) 23ºC
10%
M13
A C G T Ct
A
T1
V1
A*
T1*
SD
Full length transcript
A+1
G-10
A-20
G-30
A-40
A-50
G-57
C-60
15%
A T1 Ct
A
T1
V1
C-60
A-70
U-78
8%
A+1
G-10
A-20
G-30
T1
V1
SD

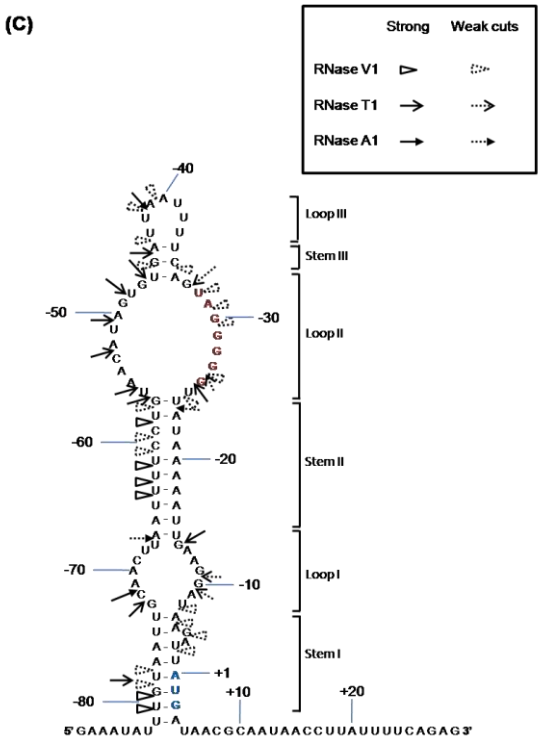

Figure 4 – *icaR 5′*-UTR secondary structure. Migration of the fragments generated by RNase A (A), RNase T1 (T1) and RNase V1 (V1) digestion of *5′*-end ^{32}P-labelled *icaR 5′*-UTR mRNA at 37°C **(A)** and 23°C **(B)**. Lane Ct corresponds to the control without RNase. Lanes A* and T1* correspond to cleavage with RNase A1 and RNase T1, respectively, under denaturing conditions. Lanes A, C, G and T correspond to M13 sequencing ladders. Further details are given in the Materials and Methods. The percentages of polyacrylamide gels used to separate the RNA fragments are indicated in the respective figures. The AUG start codon and the Shine-Dalgarno sequence are also indicated. **(C)** *icaR 5′*-UTR secondary structure inferred from the probing data. The positions of the RNase cleavage sites, as determined by RNase digestion are highlighted on the predicted structure for the *icaR 5′*-UTR. The SD sequence (red) and the start codon (blue) are indicated. Probing data were obtained from at least two independent experiments.

DISCUSSION

In recent years different classes of regulatory RNAs have been recognized as mediators of intricate networks that enable bacteria to survive and proliferate under environmental pressures. *S. aureus* is an important human pathogen, and several studies have identified regulatory RNAs involved in its pathogenicity and adaptation to external stresses (Romilly *et al.*, 2012). The role of RNases in the regulation of these players has just started to be explored in Gram positive bacteria, namely in *S. aureus* (Jester *et al.*, 2012; Lasa *et al.*, 2011; Liu *et al.*, 2011; Roux *et al.*, 2011).

We have previously shown that *icaR*, a gene encoding a key transcription repressor of biofilm development is posttranscriptionally regulated by its own 3'-UTR. This finding highlights the importance of bacterial 3'-UTRs as regulators of gene expression. The long 3'-UTR of *icaR* mRNA base-pairs with the Shine-Dalgarno region, interfering with the translation initiation complex, and promoting RNase III-dependent *icaR* mRNA decay. Accordingly, the RNase III cleavage sites were determined *in vitro* on the *5'*-UTR-3'-UTR hybrid, and were located in the double-stranded region formed upstream the Shine-Dalgarno (Figure 1C). RNase III has frequently been involved in the posttranscriptional control mediated by small regulatory RNAs that elicit cleavage in a target-coupled way, that is after sRNA-mRNA interaction (Boisset *et al.*, 2007; Huntzinger *et al.*, 2005; Viegas *et al.*, 2011). For instance, RNAIII, the main effector of quorum sensing system in *S. aureus* controls the expression of virulence factors by pairing with target mRNAs, creating suitable substrates for RNase III cleavage (Boisset *et al.*, 2007; Huntzinger *et al.*, 2005). Posttranscriptional regulation by sRNAs assures a fast fine-tuned control of mRNAs in the cell, and RNA degradation makes the process irreversible.

Many genes in bacteria are regulated by temperature (Shapiro and Cowen, 2012). In this study, we found evidences that the *5′-* leader sequence of the *ica*R transcript together with the 3′-UTR may be important in setting the expression level of IcaR protein depending on the temperature sensed. Accordingly, *5′*-3′UTR base pairing seems to be modulated in a temperature dependent mechanism. We found that, at 23°C the leader sequence from *icaR* may fold in a closed conformation, which prevents the interaction with the 3′-UTR. Melting of this structure at 37°C allows the 3′-UTR binding and further degradation of the hybrid duplex by RNase III (Figure 5). In fact, we have demonstrated that RNase III is less efficient at 23°C.

To our knowledge, this is the first report of a bacterial RNA thermosensor that controls *5′*-3′UTR base-pairing, and the first described in the pathogenic microorganism *S. aureus*.

Interestingly, *icaR 5′*-UTR seems to bear some resemblance with the fourU thermometer class (Waldminghaus *et al.*, 2007). It contains a four consecutive uracil residues that were predicted to pair with an upstream sequence of the *icaR* 3′-UTR (UUUU pairing with AAGA) (Figure 3C). The four-U thermometers reported until now contain a stretch of Us that pair with the SD sequence (UUUU pairing with AGGA) in order to repress translation at low temperatures (Waldminghaus *et al.*, 2007). At increasing temperatures, melting of the structure permits ribosome access (Narberhaus *et al.*, 2006). By contrast, in our example we have demonstrated that translation is blocked by 3′-UTR hybridization at high temperature, and we are tempted to speculate that translation is allowed at low temperature (Figure 5). *icaR* RNA thermometer does not fold to hybridize with the SD, but rather melts at high temperatures to allow the entry of the 3′-UTR, which in turn inhibits translation. Recent work has unveiled *cspA*, a thermosensor that adopts an active structure following a cold shock treatment (Giuliodori *et al.*, 2010).

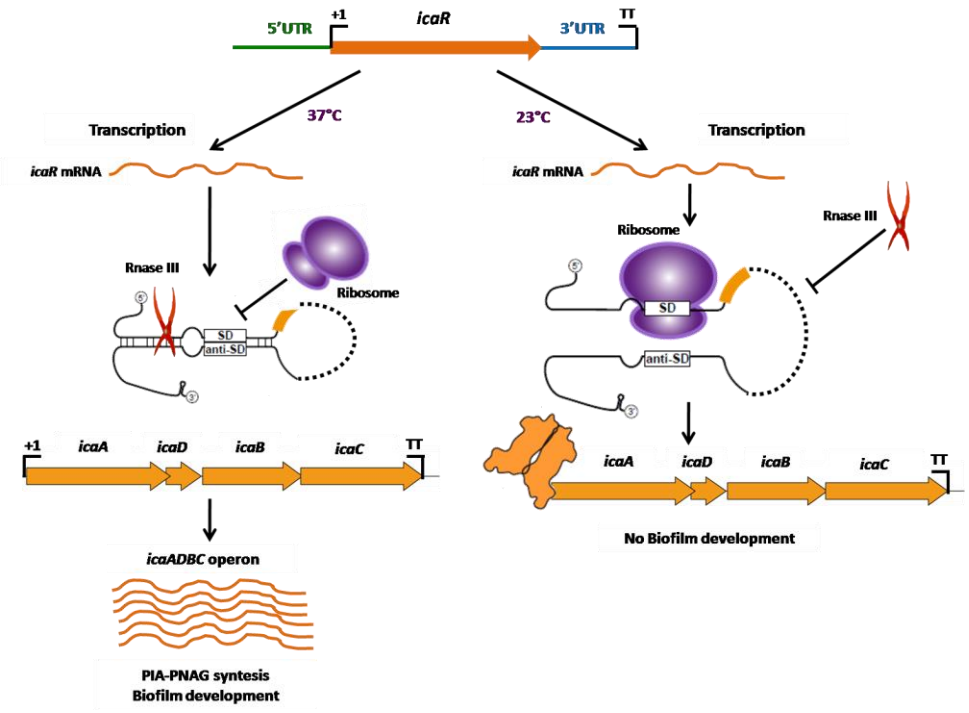

Figure 5 – Model for posttranscriptional regulation of IcaR expression by the 3'-UTR interacting with the Shine-Dalgarno region. Once *icaR* gene is transcribed, the 3'-UTR may interact with the *5'*-UTR trough the anti-SD UCCCUG motif. This interaction interferes with the ribosome access to the SD, inhibiting the formation of the translational initiation complex, and promotes an RNase III-dependent mRNA decay. Thus, IcaR repressor is less expressed and consequently *icaADBC* transcription could occur, favoring PIA-PNAG biosynthesis and biofilm development. If this interaction does not occur, ribosome could bind to the SD and proceed to IcaR translation. The IcaR protein could bind to IcaR promoter inhibiting the *icaADBC* transcription and biofilm formation. Temperature is one of the factors that would influence the UTRs interaction. As shown in the model at 37°C the binding of *5'*-3'UTR is promoted, leading to *icaR* mRNA degradation. Contrarily to this, at 23°C, the interaction is prevented and translation takes place.

icaR 5'-UTR structure is somehow similar to the structure adopted by an RNA thermosensor found in the *pfrA* gene, a transcriptional activator of virulence genes in *Listeria monocytogenes* (Johansson *et al.*, 2002). The listerial RNA thermometer is positioned within the *5'*-UTR of the *pfrA* mRNA and forms an

extended stem loop structure (130 nt) in which the ribosome binding site and the start codon locate in two small bulges within the long hairpin structure. However, contrarily to *icaR 5'*-UTR in this case the translation is promoted at 37°C through melting of the loops facilitating the access of ribosomes. In *icaR* the SD is available in the closed conformation and melting allows hybridization with the 3'-UTR, leading to translation blocking. Interestingly, *prfA* mRNA is targeted in its *5'*-UTR region at 37°C by SreA sRNA. It was hypothesized by Loh *et al.* (Loh *et al.*, 2009) that opening of the secondary structure allows a possible interaction with SreA, leading to the repression of translation (Loh *et al.*, 2009). Absence of SreA increases the level of PrfA and virulence gene expression in *L. monocytogenes*. This could resemble the regulation of IcaR. However, in the case of PrfA the regulation involves a *trans*-acting regulatory element (SreA sRNA), contrarily to IcaR regulation, which implicates a *cis*-acting element (its own 3'-UTR).

We have seen that at 37°C, the interaction between *icaR 5'*-UTR with 3'-UTR triggers RNase III cleavage and since 3'-UTR hybridization is controlled by temperature, accessibility of RNase III to *icaR* mRNA is controlled by the *5'*-UTR thermosensor. To our knowledge this is the first bacterial thermosensor, whose regulation by temperature controls the accessibility of an RNase. Curiously, in *cIII*, the first RNA thermosensor studied, RNase III action was shown to expose the occluded ribosome binding site, leading to translation activation (Altuvia *et al.*, 1989; Altuvia *et al.*, 1987). However the role of RNase III needs further clarification.

This work opens new perspectives to the thermoregulation of RNA molecules.

ACKNOWLEDGEMENTS

We thank Andreia Aires for technical assistance. Fundação para a Ciência e Tecnologia (FCT-Portugal) gave financial support to M. Saramago (Doctoral fellowship) and S. Domingues (Postdoctoral fellowship). I. Ruiz de los Mozos was supported by F.P.I. (BES-2009-017410 associated to BIO2008-05284-C02-01 grant). This work was supported by Fundação para a Ciência e Tecnologia (FCT-Portugal) grants including Grant ERA-PTG/0002/2010 and Pest-OE/EQB/LA0004/2011 and also by Spanish Ministry of Economy and Competitiveness Grants BFU2011-23222 and ERA-NET Pathogenomics PIM2010EPA-00606

.

REFERENCES

Altuvia, S., D. Kornitzer, D. Teff, and A.B. Oppenheim. 1989. Alternative mRNA structures of the cIII gene of bacteriophage lambda determine the rate of its translation initiation. *J Mol Biol*. 210:265-280.

Altuvia, S., H. Locker-Giladi, S. Koby, O. Ben-Nun, and A.B. Oppenheim. 1987. RNase III stimulates the translation of the cIII gene of bacteriophage lambda. *Proc Natl Acad Sci U S A*. 84:6511-6515.

Amarasinghe, A.K., I. Calin-Jageman, A. Harmouch, W. Sun, and A.W. Nicholson. 2001. Escherichia coli ribonuclease III: affinity purification of hexahistidine-tagged enzyme and assays for substrate binding and cleavage. *Methods Enzymol*. 342:143-158.

Andrade, J.M., and C.M. Arraiano. 2008. PNPase is a key player in the regulation of small RNAs that control the expression of outer membrane proteins. *RNA*. 14:543-551.

Archer, N.K., M.J. Mazaitis, J.W. Costerton, J.G. Leid, M.E. Powers, and M.E. Shirtliff. 2011. Staphylococcus aureus biofilms: properties, regulation, and roles in human disease. *Virulence*. 2:445-459.

Arciola, C.R., D. Campoccia, P. Speziale, L. Montanaro, and J.W. Costerton. 2012. Biofilm formation in Staphylococcus implant infections. A review of molecular mechanisms and implications for biofilm-resistant materials. *Biomaterials*. 33:5967-5982.

Bohme, K., R. Steinmann, J. Kortmann, S. Seekircher, A.K. Heroven, E. Berger, F. Pisano, T. Thiermann, H. Wolf-Watz, F. Narberhaus, and P. Dersch. 2012. Concerted actions of a thermo-labile regulator and a unique intergenic RNA thermosensor control Yersinia virulence. *PLoS Pathog*. 8:e1002518.

Boisset, S., T. Geissmann, E. Huntzinger, P. Fechter, N. Bendridi, M. Possedko, C. Chevalier, A.C. Helfer, Y. Benito, A. Jacquier, C. Gaspin, F. Vandenesch, and P. Romby. 2007. Staphylococcus aureus RNAIII coordinately represses the synthesis of virulence factors and the transcription regulator Rot by an antisense mechanism. *Genes Dev*. 21:1353-1366.

Carzaniga, T., D. Antoniani, G. Deho, F. Briani, and P. Landini. 2012. The RNA processing enzyme polynucleotide phosphorylase negatively controls biofilm formation by repressing poly-N-acetylglucosamine (PNAG) production in Escherichia coli C. *BMC Microbiol*. 12:270.

Celesnik, H., A. Deana, and J.G. Belasco. 2007. Initiation of RNA decay in Escherichia coli by *5′-* pyrophosphate removal. *Mol Cell*. 27:79-90.

Cramton, S.E., C. Gerke, N.F. Schnell, W.W. Nichols, and F. Gotz. 1999. The intercellular adhesion (ica) locus is present in Staphylococcus aureus and is required for biofilm formation. *Infect Immun*. 67:5427-5433.

de los Mozos IR, V.-I.M., Segura V, Villanueva M, Bitarte N, Saramago M, Domingues S, Arraiano CM, Fechter P, Romby P, Valle J, Solano C, Lasa I, Toledo-Arana A. 2013. Base Pairing Interaction Between *5′-* and 3′-UTRs Controls icaR mRNA Translation in Staphylococcus aureus. *In* PLoS Genet.

Giuliodori, A.M., F. Di Pietro, S. Marzi, B. Masquida, R. Wagner, P. Romby, C.O. Gualerzi, and C.L. Pon. 2010. The cspA mRNA is a thermosensor that modulates translation of the cold-shock protein CspA. *Mol Cell*. 37:21-33.

Gotz, F. 2002. Staphylococcus and biofilms. *Mol Microbiol*. 43:1367-1378.

Heilmann, C., O. Schweitzer, C. Gerke, N. Vanittanakom, D. Mack, and F. Gotz. 1996. Molecular basis of intercellular adhesion in the biofilm-forming Staphylococcus epidermidis. *Mol Microbiol*. 20:1083-1091.

Huntzinger, E., S. Boisset, C. Saveanu, Y. Benito, T. Geissmann, A. Namane, G. Lina, J. Etienne, B. Ehresmann, C. Ehresmann, A. Jacquier, F. Vandenesch, and P. Romby. 2005. Staphylococcus aureus RNAIII and the endoribonuclease III coordinately regulate spa gene expression. *EMBO J*. 24:824-835.

Jarrige, A.C., N. Mathy, and C. Portier. 2001. PNPase autocontrols its expression by degrading a double-stranded structure in the pnp mRNA leader. *EMBO J*. 20:6845-6855.

Jester, B.C., P. Romby, and E. Lioliou. 2012. When ribonucleases come into play in pathogens: a survey of gram-positive bacteria. *Int J Microbiol*. 2012:592196.

Johansson, J., P. Mandin, A. Renzoni, C. Chiaruttini, M. Springer, and P. Cossart. 2002. An RNA thermosensor controls expression of virulence genes in Listeria monocytogenes. *Cell*. 110:551-561.

Jorgensen, M.G., J.S. Nielsen, A. Boysen, T. Franch, J. Moller-Jensen, and P. Valentin-Hansen. 2012. Small regulatory RNAs control the multi-cellular adhesive lifestyle of Escherichia coli. *Mol Microbiol*. 84:36-50.

Kaberdin, V.R., A.P. Walsh, T. Jakobsen, K.J. McDowall, and A. von Gabain. 2000. Enhanced cleavage of RNA mediated by an interaction between substrates and the arginine-rich domain of E. coli ribonuclease E. *J Mol Biol*. 301:257-264.

Kime, L., S.S. Jourdan, J.A. Stead, A. Hidalgo-Sastre, and K.J. McDowall. 2010. Rapid cleavage of RNA by RNase E in the absence of *5′*- monophosphate stimulation. *Mol Microbiol*. 76:590-604.

Kint, G., D. De Coster, K. Marchal, J. Vanderleyden, and S.C. De Keersmaecker. 2010. The small regulatory RNA molecule MicA is involved in Salmonella enterica serovar Typhimurium biofilm formation. *BMC Microbiol*. 10:276.

Kortmann, J., and F. Narberhaus. 2012. Bacterial RNA thermometers: molecular zippers and switches. *Nat Rev Microbiol*. 10:255-265.

Lasa, I., A. Toledo-Arana, A. Dobin, M. Villanueva, I.R. de los Mozos, M. Vergara-Irigaray, V. Segura, D. Fagegaltier, J.R. Penades, J. Valle, C. Solano, and T.R. Gingeras. 2011. Genome-wide antisense transcription drives mRNA processing in bacteria. *Proc Natl Acad Sci U S A*. 108:20172-20177.

Lin-Chao, S., and S.N. Cohen. 1991. The rate of processing and degradation of antisense RNAI regulates the replication of ColE1-type plasmids in vivo. *Cell*. 65:1233-1242.

Lioliou, E., C.M. Sharma, I. Caldelari, A.C. Helfer, P. Fechter, F. Vandenesch, J. Vogel, and P. Romby. 2012. Global regulatory functions of the Staphylococcus aureus endoribonuclease III in gene expression. *PLoS Genet*. 8:e1002782.

Liu, Y., J. Dong, N. Wu, Y. Gao, X. Zhang, C. Mu, N. Shao, M. Fan, and G. Yang. 2011. The production of extracellular proteins is regulated by ribonuclease III via two different pathways in Staphylococcus aureus. *PLoS One*. 6:e20554.

Loh, E., O. Dussurget, J. Gripenland, K. Vaitkevicius, T. Tiensuu, P. Mandin, F. Repoila, C. Buchrieser, P. Cossart, and J. Johansson. 2009. A trans-acting riboswitch controls expression of the virulence regulator PrfA in Listeria monocytogenes. *Cell*. 139:770-779.

Mackie, G.A. 1998. Ribonuclease E is a *5′*-end-dependent endonuclease. *Nature*. 395:720-723.

Mackie, G.A. 2000. Stabilization of circular rpsT mRNA demonstrates the *5′*-end dependence of RNase E action in vivo. *J Biol Chem*. 275:25069-25072.

McDowall, K.J., and S.N. Cohen. 1996. The N-terminal domain of the rne gene product has RNase E activity and is non-overlapping with the arginine-rich RNA-binding site. *J Mol Biol*. 255:349-355.

Narberhaus, F., T. Waldminghaus, and S. Chowdhury. 2006. RNA thermometers. *FEMS Microbiol Rev*. 30:3-16.

Romilly, C., C. Chevalier, S. Marzi, B. Masquida, T. Geissmann, F. Vandenesch, E. Westhof, and P. Romby. 2012. Loop-loop interactions involved in antisense regulation are processed by the endoribonuclease III in Staphylococcus aureus. *RNA Biol*. 9:1461-1472.

Rouf, S.F., I. Ahmad, N. Anwar, S.K. Vodnala, A. Kader, U. Romling, and M. Rhen. 2011. Opposing contributions of polynucleotide phosphorylase and the membrane protein NlpI to biofilm formation by Salmonella enterica serovar Typhimurium. *J Bacteriol*. 193:580-582.

Roux, C.M., J.P. DeMuth, and P.M. Dunman. 2011. Characterization of components of the Staphylococcus aureus mRNA degradosome holoenzyme-like complex. *J Bacteriol*. 193:5520-5526.

Saramago, M., Domingues, S., Viegas, SC and Arraiano C.M. 2013. Ribonucleases promote biofilm formation and antibiotic resistance in Salmonella Typhimurium. *Submitted in Appl Environ Microbiol*

Shapiro, R.S., and L.E. Cowen. 2012. Thermal control of microbial development and virulence: molecular mechanisms of microbial temperature sensing. *MBio*. 3.

Silva, I.J., M. Saramago, C. Dressaire, S. Domingues, S.C. Viegas, and C.M. Arraiano. 2011. Importance and key events of prokaryotic RNA decay: the ultimate fate of an RNA molecule. *Wiley Interdiscip Rev RNA*. 2:818-836.

Sim, S.H., J.H. Yeom, C. Shin, W.S. Song, E. Shin, H.M. Kim, C.J. Cha, S.H. Han, N.C. Ha, S.W. Kim, Y. Hahn, J. Bae, and K. Lee. 2010. Escherichia coli ribonuclease III activity is downregulated by osmotic stress: consequences for the degradation of bdm mRNA in biofilm formation. *Mol Microbiol*. 75:413-425.

Studier, F.W., and B.A. Moffatt. 1986. Use of bacteriophage T7 RNA polymerase to direct selective high-level expression of cloned genes. *J Mol Biol*. 189:113-130.

Udekwu, K.I., F. Darfeuille, J. Vogel, J. Reimegard, E. Holmqvist, and E.G. Wagner. 2005. Hfq-dependent regulation of OmpA synthesis is mediated by an antisense RNA. *Genes Dev*. 19:2355-2366.

Valle, J., A. Toledo-Arana, C. Berasain, J.M. Ghigo, B. Amorena, J.R. Penades, and I. Lasa. 2003. SarA and not sigmaB is essential for biofilm development by Staphylococcus aureus. *Mol Microbiol*. 48:1075-1087.

Vergara-Irigaray, M., J. Valle, N. Merino, C. Latasa, B. Garcia, I. Ruiz de Los Mozos, C. Solano, A. Toledo-Arana, J.R. Penades, and I. Lasa. 2009. Relevant role of fibronectin-binding proteins in Staphylococcus aureus biofilm-associated foreign-body infections. *Infect Immun*. 77:3978-3991.

Viegas, S.C., and C.M. Arraiano. 2008. Regulating the regulators: How ribonucleases dictate the rules in the control of small non-coding RNAs. *RNA Biol*. 5:230-243.

Viegas, S.C., V. Pfeiffer, A. Sittka, I.J. Silva, J. Vogel, and C.M. Arraiano. 2007. Characterization of the role of ribonucleases in Salmonella small RNA decay. *Nucleic Acids Res*. 35:7651-7664.

Viegas, S.C., I.J. Silva, M. Saramago, S. Domingues, and C.M. Arraiano. 2011. Regulation of the small regulatory RNA MicA by ribonuclease III: a target-dependent pathway. *Nucleic Acids Res*. 39:2918-2930.

Waldminghaus, T., N. Heidrich, S. Brantl, and F. Narberhaus. 2007. FourU: a novel type of RNA thermometer in Salmonella. *Mol Microbiol*. 65:413-424.

ADDENDUM

Although PNPase is a key regulator of several important processes, its role on *S. aureus* main cellular mechanisms is yet unexplored. In *E. coli* and *Salmonella* PNPase has been involved in biofilm formation (Carzaniga *et al.*, 2012; Rouf *et al.*, 2011). We decided to investigate the enzyme's involvement in the development of *S. aureus* biofilm. We constructed an isogenic PNPase mutant strain and tested its biofilm-forming ability. Our results show that the absence of PNPase completely abolished biofilm formation (Figure 1A and B). We wondered if this enzyme would be involved in the modulation of IcaR levels. Thus, we measured by Western blot the influence of overexpressing PNPase in strains ectopically expressing *icaR* tagged with a 3XFLAG. A considerable decrease of IcaR protein levels in the cell was observed (Figure 1C). Since we have seen in the previous chapter that IcaR levels depend on the presence of *icaR* 3'-UTR, we did the same experiment using a Δ3'-UTR *icaR* expressing strain. As shown in Figure 1C, deletion of 3'-UTR from *icaR* mRNA restored IcaR wild-type levels. This demonstrates that PNPase controls IcaR levels in a 3'-UTR-dependent fashion. Given the above evidences, and that PNPase is a 3'-*5'*- exoribonuclease, we wanted to test the ability of this enzyme to cleave the 3'-UTR of *icaR* transcript. To this purpose PNPase from *S. aureus* was cloned and purified as described in Materials and Methods section, and the purified protein was tested *in vitro* over uniformly labelled *icaR* 3'-UTR transcript. Surprisingly, PNPase was not able to cleave efficiently the 3'-UTR from *icaR* (Figure 2A). Since RNase III cleaves the *icaR* hybrid *5'*-3'UTR, we decided to test if it would be able to cut free 3'-UTR. This could create suitable substrates for subsequent PNPase degradation. We started by confirming the activity of purified RNase III over 3'-UTR of *icaR*. As we can see in Figure 2B, RNase III efficiently cleaves this substrate. In this view, we could see that 60 seconds after RNase III digestion, PNPase was highly active on

the products generated. Thereby, it seems that *icaR* mRNA degradation/processing is triggered by RNase III endonucleolytic cleavage, and the resulting intermediate products are further digested by PNPase.

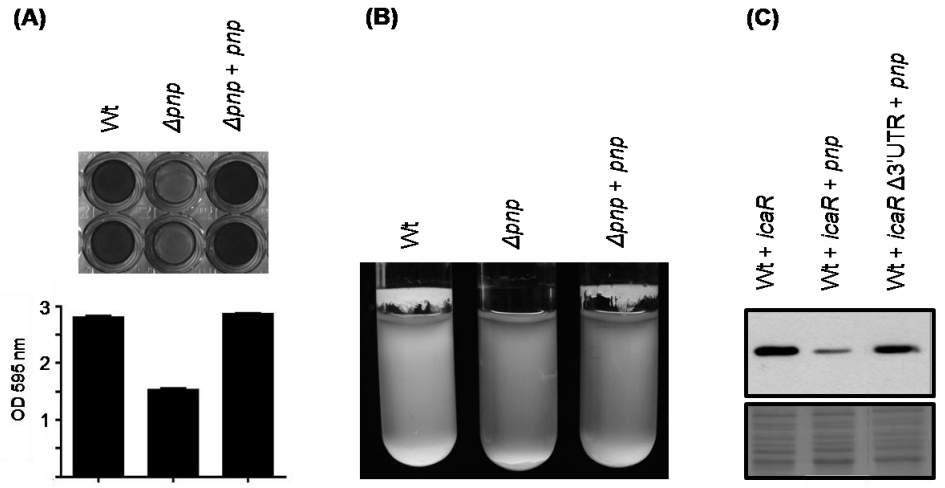

Figure 1 - Influence of PNPase in the regulation of IcaR levels. (A) Biofilm formation capacity of *S. aureus* 15981 strains harboring the empty plasmid pCU1 (wt), PNPase mutant harboring the empty plasmid pCU1 (*ΔpnpA*+pCU1), and the complementation strain (*ΔpnpA*+pCU1-*pnpA*), on polystyrene microtiter plates after 24 hours of growth at 37ºC in TSB-gluc medium, **(B)** or in 10-ml glass test tubes after 18 hours of growth at 37ºC in TSB-gluc medium with shaking (180 rpm). **(C)** Western blot showing IcaR protein levels in the following derivative *S. aureus* 15981 strains harboring the pCN40-*icaR* plasmid (wt + *icaR*), the pCN40-*icaR* and pCU1-*pnp* (wt + *icaR* + *pnp*), and pCN40-icaR_Δ3'UTR and pCU1-*pnp* (wt + *pnp* + *icaR* Δ3'UTR). The 3XFLAG tagged IcaR protein was detected by commercial anti-3XFLAG antibodies. A Comassie stained gel portion is shown as loading control. These experiments were performed by IR de los Mozos.

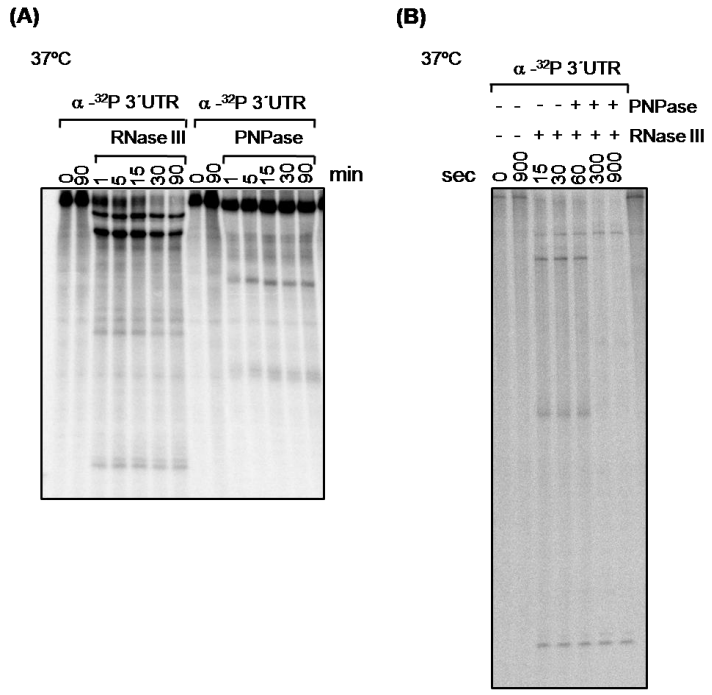

Figure 2 - (A) Activity assays showing the *in vitro* cleavage of *icaR* 3'UTR by RNase III or PNPase at 37°C. The radioactive labeled substrate was incubated with 500 nM of *S. aureus* RNase III or 60 nM of *S. aureus* PNPase. **(B)** Activity assay showing the *in vitro* cleavage of *icaR* 3'-UTR by RNase III and PNPase at 37°C, simultaneously. The radioactive labeled substrate was first incubated with 500 nM of *S. aureus* RNase III and after 60 seconds, 60nM of *S. aureus* PNPase were added to the reaction. Aliquots were withdrawn at the time-points (minutes) as indicated above each lane. The first two lanes of each reaction correspond to the controls without the protein at time zero (0 min) and at the end of the reaction time (90 min). Reactions were electrophoresed in a 10% (w/v) polyacrylamide gel containing 8.3M urea and visualized by phosphorimaging.

Our results strongly suggest that PNPase is a new player involved in the regulation of *S. aureus* biofilm formation. We have observed that the ability to form biofilm is severely compromised in a strain lacking PNPase. Moreover, IcaR levels significantly decreased upon PNPase overexpression, and this effect is dependent on the presence of 3'-UTR. This indicates that PNPase exerts its action on biofilm development by modulating IcaR levels. Hence, in addition to RNase III, PNPase may also be an important factor in modulating the amount of PIA-

PNAG and thus biofilm development in *S. aureus*. Indeed, PNPase was recently shown to affect PNAG production in *Escherichia coli* (Carzaniga *et al.*, 2012). In agreement with the *in vivo* observations, PNPase was shown to be active *in vitro* over the degradation products generated by RNase III cleavage of 3'-UTR. We demonstrate a direct interplay of an endo- and an exoribonuclease in which RNase III generates breakdown products suitable for further cleavage by 3'-exoribonuclease PNPase. This situation is reminiscent of the autoregulation mechanism of PNPase reported in *Escherichia coli* (Jarrige *et al.*, 2001). RNase III cleaves a long stem-loop in the *pnp* leader region, which triggers subsequent degradation by PNPase (Jarrige *et al.*, 2001). Both ribonucleases were also found to act in the regulation of MicA, a sRNA important for biofilm formation in *Salmonella* (Andrade and Arraiano, 2008; Kint *et al.*, 2010; Viegas *et al.*, 2007; Viegas *et al.*, 2011). Finally, we have also shown that RNase III and PNPase are implicated in biofilm development in *Salmonella* Typhimurium (Saramago, 2013).

This part of the work points out for the specific contribution of PNPase in the regulation of biofilm formation in *S. aureus*. However, further experiments are needed to clarify the role of this enzyme in this process.

REFERENCES

Andrade, J.M., and C.M. Arraiano. 2008. PNPase is a key player in the regulation of small RNAs that control the expression of outer membrane proteins. *RNA*. 14:543-551.

Carzaniga, T., D. Antoniani, G. Deho, F. Briani, and P. Landini. 2012. The RNA processing enzyme polynucleotide phosphorylase negatively controls biofilm formation by repressing poly-N-acetylglucosamine (PNAG) production in Escherichia coli C. *BMC Microbiol*. 12:270.

Jarrige, A.C., N. Mathy, and C. Portier. 2001. PNPase autocontrols its expression by degrading a double-stranded structure in the pnp mRNA leader. *EMBO J*. 20:6845-6855.

Kint, G., D. De Coster, K. Marchal, J. Vanderleyden, and S.C. De Keersmaecker. 2010. The small regulatory RNA molecule MicA is involved in Salmonella enterica serovar Typhimurium biofilm formation. *BMC Microbiol*. 10:276.

Rouf, S.F., I. Ahmad, N. Anwar, S.K. Vodnala, A. Kader, U. Romling, and M. Rhen. 2011. Opposing contributions of polynucleotide phosphorylase and the membrane protein NlpI to biofilm formation by Salmonella enterica serovar Typhimurium. *J Bacteriol*. 193:580-582.

Saramago, M., Domingues, S., Viegas, SC and Arraiano C.M. 2013. Ribonucleases promote biofilm formation and antibiotic resistance in Salmonella Typhimurium. *Submitted in Appl Environ Microbiol*

Viegas, S.C., and C.M. Arraiano. 2008. Regulating the regulators: How ribonucleases dictate the rules in the control of small non-coding RNAs. *RNA Biol*. 5:230-243.

Viegas, S.C., V. Pfeiffer, A. Sittka, I.J. Silva, J. Vogel, and C.M. Arraiano. 2007. Characterization of the role of ribonucleases in Salmonella small RNA decay. *Nucleic Acids Res*. 35:7651-7664.

Viegas, S.C., I.J. Silva, M. Saramago, S. Domingues, and C.M. Arraiano. 2011. Regulation of the small regulatory RNA MicA by ribonuclease III: a target-dependent pathway. *Nucleic Acids Res*. 39:2918-2930.

Waldminghaus, T., N. Heidrich, S. Brantl, and F. Narberhaus. 2007. FourU: a novel type of RNA thermometer in Salmonella. *Mol Microbiol*. 65:413-424.

Chapter 6

GENERAL DISCUSSION AND FUTURE PERSPECTIVES

Every living organism must be able to sense environmental stimuli and convert these input signals into appropriate cellular responses. Posttranscriptional regulation is a key step in the control of bacterial gene expression and provides a powerful way for bacteria to rapidly adjust to a changing environment. Bacteria can use several forms of posttranscriptional regulation encompassing different types of regulatory elements. These regulatory elements comprise RNA-binding proteins, *cis*- and *trans*-acting regulatory RNAs, RNA thermosensors, riboswitches, and RNases (Waters and Storz, 2009).

RNA processing and degradation reactions involve site-specific cleavages carried out by a diverse collection of RNases. These enzymes play very important roles in the control of gene expression by altering the stability of specific RNAs. For instance, after the response to a given stress, bacteria must degrade unnecessary stress responsive transcripts through RNA degradation. Thus, they are also important in cellular metabolism, recycling ribonucleotides in order to synthesize new RNA molecules (Silva *et al.*, 2011).

The conventional model for RNA decay in prokaryotes usually begins with an endonucleolytic cleavage at one or more internal sites on the RNA molecule, which is performed by endoribonucleases. Then, RNA degradation products generated are further degraded from one extremity by exoribonucleases.

This Dissertation is mainly focused on the contribution of RNase III endoribonuclease to the mechanisms of posttranscriptional regulation of three different pathogenic microorganisms: *Campylobacter jejuni*, *Salmonella* Typhimurium and *Staphylococcus aureus*.

Ribonucleases have been mainly studied in the Gram-negative model *Escherichia coli*, and in the Gram-positive *Bacillus subtilis* (Arraiano *et al.*, 2010), and there is little information regarding the importance of these enzymes on *Campylobacter jejuni*. To our knowledge there is only one published report about

the importance of PNPase for *C. jejuni* survival and pathogenicity. This exoribonuclease was shown to facilitate *Campylobacter* swimming, cell adhesion, colonization, invasion, and to contribute for survival in refrigerated temperatures (Haddad *et al.*, 2009; Haddad *et al.*, 2012).

In this part of the work we performed a biochemical and functional characterization of RNase III from *Campylobacter jejuni* (*Cj*-RNase III). Following ingestion by a human or animal host C. *jejuni* must adapt to higher temperatures and pass through the acidic environment of the stomach before reaching the intestine where invasion occurs (Holzer, 2007; Lee *et al.*, 1998; Rao *et al.*, 2004). We discovered that *Cj*-RNase III is highly active over a wide range of temperatures (4-42◦C). This range includes the physiologic temperatures encountered by this bacterium inside the avian and human hosts (42◦C and 37◦C, respectively), and also during food refrigeration (4◦C). Moreover, *Cj*-RNase III also demonstrated high activity at different pH values between 5.2 and 7.3. Following transit through the stomach, bacteria encounter a variety of environments within the intestine, ranging from mildly acidic (pH 5.5) to moderately alkaline (pH 7.4) (Holzer, 2007; Rao *et al.*, 2004). The pH tolerance of *Cj*-RNase III and its capability to cleave RNA over a broad range of temperatures, including 4◦C, highlights the importance of this enzyme for the survival and homeostasis maintenance of this bacterium over a broad range of conditions. Interestingly, RNase III from the hyperthermophilic bacterium *Thermotoga maritime* exhibits a broad optimal temperature range of ~40-70◦C, being still active at 95◦C (Nathania and Nicholson, 2010). By contrast, the *E. coli* counterpart contains a much narrow pH and temperature tolerance. In *E. coli* this enzyme is only active at temperatures ranging from 20◦C to 50◦C and at pH values between 6.9 and 7.4 (Nathania and Nicholson, 2010; Srivastava and Srivastava, 1996). This reinforces the idea that the activity of RNase III is consistent with the environments that bacteria faces, and this is likely to contribute to the success of

C. jejuni as pathogen, allowing it to infect diverse hosts and to survive through the food chain.

We have also demonstrated that Mn^{2+} seems to be the preferred co-factor of *Cj*-RNase III, contrarily to the consensus that Mg^{2+} is the physiologic relevant cofactor for RNase III family members. This is an evidence that RNase III would have an important contribution for the survival of *Campylobacter* under manganese-rich environments. Upon the entrance into the host, *C. jejuni* is confronted with host immune cells such as macrophages (Pogacar *et al.*, 2010). When it infects macrophages, it encounters an acidic media poor in magnesium (Papp-Wallace and Maguire, 2006). It is within the macrophages that Mn^{2+} homoeostasis is thought to be important for *C. jejuni* (Pogacar *et al.*, 2010). In fact, the availability of metal ions is restricted to the different environments, and bacterial proteins must be able to function according to the resources available. Interestingly, a recent study about RNase HII from *Pyrococcus furiosus* demonstrates that the presence of Mn^{2+}, and not Mg^{2+}, promotes dsRNA digestion (Kitamura *et al.*, 2010). This raises the question if a possible shift in metal cofactors could be related with the modulation of RNase activity according to the bacterial needs. Further investigations are required in this regard.

Despite the peculiarities found in the RNase III from *C. jejuni*, this enzyme was able to fully mature *E. coli* rRNA and to regulate the synthesis of *E. coli* PNPase. Similar results were previously obtained for the *Lactococcus lactis* RNase III (Amblar *et al.*, 2004). Moreover, mutations at conserved acidic residues in the catalytic domain affected the activity of *Cj*-RNase III as it was previously demonstrated for several RNase III family members (Gravenbeek and Jones, 2008; Li and Nicholson, 1996; Lioliou *et al.*, 2012; Sun *et al.*, 2004). This is consistent with the fact that this family of enzymes shows a high degree of sequence conservation in prokaryotes (see Figure 1 in chapter 2).

Very recent studies focused on genome-wide searches enabled the identification of a plethora of non-coding and antisense RNAs in *Campylobacter jejuni* (Dugar *et al.*, 2013; Porcelli *et al.*, 2013). Indeed, RNase III has been associated to complex posttranscriptional mechanisms involving regulatory RNAs. However, our knowledge of the mechanisms governing the regulation of gene expression in *Campylobacter* and their responses to the environment is still rather poor. Hence, it would be important to understand the action of this and other RNases on the riboregulation of this human foodborne pathogen. For instance, it would be interesting to obtain transcriptomic and proteomic profiles of *C. jejuni* RNase III mutant strain at refrigerated conditions, in a manganese-rich environment, and at physiologically relevant pH values. This approach will lead to the identification of RNase III targets involved in the survival of this bacterium.

We have already shown that RNase III has a high impact on antibiotic resistance and biofilm formation in *Salmonella* Typhimurium (Chapter 3). Antibiotics are essential in the fight against infectious diseases, and bacterial resistance to antibiotics is widely recognized as a health issue. Thus, it is critical to understand the mechanisms of antibiotic resistance both for maintaining the effectiveness of existing drugs and for developing new ones. RNases are already established as important components on virulence and in adaptation to stress (Silva *et al.*, 2011). To our knowledge, no information was available regarding the influence of these enzymes on antibiotic resistance mechanisms until now. Using the foodborne pathogen *Salmonella* Typhimurium as a model, we have evaluated the contribution of the main RNases on susceptibility to a panoply of known antimicrobial agents. We have seen that the RNase III mutant strain was more susceptible to ribosome-targeting agents, known to interfere with protein synthesis (Saramago, 2013). In addition, a *Salmonella* strain lacking the C-terminal domain of RNase E, which impairs the formation of the multiprotein complex degradosome, also displayed different susceptibilities to antibiotics that affect

protein synthesis. The involvement of these two endoribonucleases, RNase III and RNase E, in ribosomal biogenesis can be on the basis of the different susceptibilities to antibiotics that interfere with protein synthesis. Thus, endoribonucleolytic activity may constitute a previously uncharacterized regulatory pathway for adaptive resistance of *Salmonella* to these antibiotics. The use of ribosome-targeting agents has also been considered a powerful tool for capturing functional states of the ribosome and understanding the mechanism of the various steps of translation (Poehlsgaard and Douthwaite, 2005). More work is obviously needed for a complete understanding of RNases function on these cellular mechanisms.

Existence in a biofilm gives bacteria many advantages over planktonic cells including improved increased resistance to antimicrobial agents, and adaptation to nutrient deprivation. In chapter 3, the capacity of ribonucleases in promoting biofilm was also evaluated. Not surprisingly, both enzymes RNase III and RNase E also demonstrated to have a role on biofilm development. Biofilm production was deficient whether in the absence or upon overexpression of RNase III. This highlights the importance of RNase III in the formation of a proper biofilm matrix, such that a small variation in its levels has detrimental consequences. The ability of the strain lacking RNase III to adhere on plastic surface was compromised. Moreover, this strain was deficient in the production of cellulose, and the production of curli fimbriae could also be affected. We have indications that endoribonuclease E also modulates the amount of cellulose. Indeed, it was recently reported that *Salmonella* mutants on RNase E and RNase III exhibit a strong variation of the levels of CsgD, a master activator of biofilm development (Viegas *et al.*, 2013). In *Escherichia coli*, RNase III was also found to modulate *bdm* mRNA levels, whose product enhances biofilm formation in cells under high osmotic stress (Sim *et al.*, 2010). Also in *E. coli*, RNase E is recruited to

regulate the levels of two sRNAs, CsrB and CsrC, that are known to impact the ability of this bacterium to form and maintain biofilms (Suzuki *et al.*, 2006; Weilbacher *et al.*, 2003). Thus, the endoribonucleases E and III seem to control a diversity of targets related with the formation of multicellular, surface-adherent communities in *Enterobacteriaceae*. Indeed, we have shown that both endoribonucleases are involved in modulating the levels of MicA (chapter 3), a sRNA important for biofilm formation in *Salmonella* (Kint *et al.*, 2010).

MicA is a *trans*-encoded sRNA that is highly expressed in stationary phase and upon stress conditions that unbalance outer membrane porine (OMP) levels (Figueroa-Bossi *et al.*, 2006; Johansen *et al.*, 2006; Papenfort *et al.*, 2006). In *Salmonella*, MicA is known to down-regulate the expression of two OMPs, OmpA and LamB (Bossi and Figueroa-Bossi, 2007; Rasmussen *et al.*, 2005; Udekwu *et al.*, 2005). However, MicA role in biofilm formation is not yet studied, and it would be interesting to further elucidate the underlined molecular mechanism. *In vivo*, it was previously reported a large impact of *Salmonella* RNase E and RNase III mutant strains on the levels and stability of MicA (Viegas *et al.*, 2007). Hence, we intended to study *in vitro* the particular contribution of each endoribonuclease to the degradation of this sRNA. Although RNase III is specific for double-stranded RNA, it was not able to recognize and cut the double-stranded regions presented in MicA secondary structure. Actually, RNase III cleavage was dependent on hybridization with the mRNA targets, and the cleavage was mapped inside the predicted region of interaction. Our *in vitro* results also revealed that RNase E is the enzyme that cuts free MicA, *e.g.* in the absence of target base-pairing. In summary, in this part of this Doctoral work, we have demonstrated that RNase E and RNase III are involved in two independent pathways for MicA decay. Each pathway involves a distinct endoribonuclease. When MicA is alone, RNase E comes into play, and when MicA is coupled with its mRNA targets, RNase III takes the control in the simultaneous degradation of the sRNA and the target.

This cleavage is important since it makes the repression irreversible. Interestingly, there are indications that this sRNA is implicated in *Salmonella* virulence. A *Salmonella* strain lacking MicA was shown to be more virulent in the mouse model comparing to that of wild-type (Homerova *et al.*, 2011). More recently, RNase III and RNase E *Salmonella* mutant strains showed an attenuated virulence phenotype and reduced proliferation inside the insect model, *Galleria mellonella* (Viegas *et al.*, 2013). Taken together, both endoribonucleases appear to be main regulators of RNA degradation in *Salmonella*, controlling different cellular processes.

Biofilm formation is also of extreme relevance in *Staphylococcus aureus*, a major Gram-positive human pathogen that causes a wide spectrum of nosocomial and community-acquired infections (Arciola *et al.*, 2012). Staphylococcal biofilm-associated infections remain a major clinical concern, especially in patients with indwelling devices. The main exopolysaccharide of *S. aureus* biofilm is a polymer of N-acetylglucosamine (PIA-PNGA), which is synthesized by the genes of the *icaADBC* operon (Cramton *et al.*, 1999; Gotz, 2002). IcaR is the main repressor of this operon and strongly reduces *ica* genes expression, PIA-PNGA production and consequently lowers biofilm formation (Jefferson *et al.*, 2003). In this work we have studied the posttranscriptional control of *icaR* transcript. We have demonstrated that the 3'-UTR of *icaR* mRNA affects the expression level of the IcaR protein by modulating the stability of its own transcript. This important finding showed for the first time the regulatory capacity of a bacterial 3'-UTR, opening new perspectives for this kind of regulation in prokaryotes. Additional indications supporting the regulatory role of these regions have been recently published (Dugar *et al.*, 2013; Lioliou *et al.*, 2012; Sittka *et al.*, 2008). We have demonstrated *in vitro* and *in vivo* that modulation of *icaR* transcript is performed through an RNA-pairing between the *icaR* 3'-UTR and the 5'-UTR regions. This

interaction traps the Shine-Dalgarno sequence and impairs ribosome loading. The formation of the duplex further triggers the degradation of *icaR* mRNA by RNase III, which renders the process irreversible. Deletion or substitution of the UCCCUG motif located at the 3'-UTR strongly decreased the 3'-UTR/Shine-Dalgarno interaction. As a consequence, PIA-PNAG synthesis and biofilm formation was impaired, demonstrating the biological relevance of this regulatory mechanism.

The question arises as to whether the interaction occurs intramolecularly (3' and 5'-UTRs of the same molecule) or intermolecularly (3' and 5'-UTRs from different molecules). In fact, RNase III *in vitro* was shown to be highly efficient in cleaving the *icaR* 3'-UTR. Hence, we cannot discard the possibility that RNase III processing could release the 3'-UTR. This 3'-UTR would then be free to hybridize with the same or another molecule. The possibility that the released 3'-UTR could also act *in trans* over other cellular transcripts can neither be ruled out. Indeed, this region from *icaR* contains a UCCCC motif, which has also been found in several *S. aureus* regulatory sRNAs (Geissmann *et al.*, 2009).

In addition to RNase III, the 3'-5' exoribonuclease PNPase is also implicated in the control of IcaR levels, and it is dependent on the integrity of the 3'-UTR. Indeed, *in vitro* this enzyme is only able to degrade *icaR* 3'-UTR in a concerted fashion with RNase III (see Addendum in chapter 5). In agreement with these results, we have demonstrated that PNPase is crucial for biofilm production in *S. aureus*. Our hypothesis is that PNPase would also have a role in the control of PIA-PNAG levels. PNPase was recently reported to be involved in PNAG production in *E. coli* (Carzaniga *et al.*, 2012). Finally, in Chapter 3, we have demonstrated that both enzymes, RNase III and PNPase, are directly involved in biofilm formation in *S.* Typhimurium.

Although there are several reports in the literature concerning the function of RNase III in *S. aureus*, we could not find any study about PNPase in

this bacterium. We envisage that this exoribonuclease could have a main role in the control of several cellular processes. The importance of PNPase in this bacterium may be even strengthened by the fact that RNase II (another 3′-5′ exoribonuclease) is absent from *S. aureus* genome. Further experiments are still required to uncover the involvement of PNPase in staphylococcal biofilm formation. The half-life of *icaR* mRNA will be estimated in the isogenic mutant for PNPase. Additionally, purified PNPase will be tested *in vitro* in its ability to cut the 3′-UTR hybridized with the 5′-UTR. As inferred by the ability of RNase III to cleave the 5′-UTR only after 5′-3′-UTR base-pairing, this hybridization is likely to promote changes in the RNA structure, which in turn may generate a 3′end more suitable for the action of PNPase.

We have seen that temperature is another factor that modulates the 5′-3′-UTR base-pairing and thus the final levels of IcaR. *In vitro* at 23◦C, this interaction is less efficient than at 37◦C, and consequently RNase III is not able to cleave *icaR* mRNA. The influence of both temperatures in RNase III cleavage efficiency should be further confirmed *in vivo*. This can be done by estimating the half-life of *icaR* mRNA in the RNase III mutant, in the presence or absence of the 3′-UTR. Toeprint assays should also be carried out at 23◦C in the presence and absence of the 3′-UTR. These assays will confirm our hypothesis that the translation initiation complex is formed even in the presence of the 3′-UTR, at this temperature. This may be an explanation for the up-shift in the levels of IcaR at this temperature. Transcriptional inhibition of *icaADBC* operon, and consequently PIA-PNAG production is probably blocked, which might lead to the decreased levels of biofilm observed at 23◦C. Expression of *icaADBC* and PIA-PNAG production should be experimentally verified.

The inefficiency of the 3′-UTR base-pairing is likely explained by the presence of an RNA thermometer in the 5′-UTR. Structure probing results

indicate that this region adopts a closer conformation at 23◦C, which might inhibit the 3′-UTR interaction. On the contrary, at 37◦C the melting of 5′-UTR may allow the binding of 3′-UTR. This may be confirmed by enzymatic probing at 23◦C and 37◦C in the presence of the 3′-UTR. Another possibility would be the visualization of the electrophoretic behavior of 5′-3′-UTR duplex in a 23-37◦C temperature gradient gel electrophoresis (TGGE) (Riesner *et al.*, 1989). Since hybridization with 3′-UTR regulates the accessibility of RNase III, this is the first bacterial RNA thermometer whose regulation controls the accessibility of an RNase. There is only one example of a prokaryotic RNA thermosensor known to involve the action of a ribonuclease, however its precise role needs further clarification (Altuvia *et al.*, 1989; Altuvia *et al.*, 1987). There is more information available regarding the control of riboswitches (RNA transcripts that sense metabolites) by RNases (Caron *et al.*, 2012; Collins *et al.*, 2007; Shahbabian *et al.*, 2009). For example, a riboswitch in the *lysC* mRNA senses the amino acid lysine, and adopts an OFF conformation, blocking translation, and inducing degradosome-dependent mRNA degradation (Caron *et al.*, 2012). This work opens new perspectives for the study of ribonucleolytic regulation by bacterial RNA thermosensors.

Overall, throughout this Doctoral work we have clarified some mechanisms involving the cooperation of RNase III with several regulatory elements, namely a small non-coding RNA, a regulatory 3′-untranslated region, and an RNA thermometer. The plasticity of this double-stranded RNA specific enzyme may be relevant to the control of several important cellular processes such as antibiotic resistance and biofilm formation. Its role as a global regulator has just started to be unveiled.

REFERENCES

Altuvia, S., D. Kornitzer, D. Teff, and A.B. Oppenheim. 1989. Alternative mRNA structures of the cIII gene of bacteriophage lambda determine the rate of its translation initiation. *J Mol Biol*. 210:265-280.

Altuvia, S., H. Locker-Giladi, S. Koby, O. Ben-Nun, and A.B. Oppenheim. 1987. RNase III stimulates the translation of the cIII gene of bacteriophage lambda. *Proc Natl Acad Sci U S A*. 84:6511-6515.

Amblar, M., S.C. Viegas, P. Lopez, and C.M. Arraiano. 2004. Homologous and heterologous expression of RNase III from Lactococcus lactis. *Biochem Biophys Res Commun*. 323:884-890.

Arciola, C.R., D. Campoccia, P. Speziale, L. Montanaro, and J.W. Costerton. 2012. Biofilm formation in Staphylococcus implant infections. A review of molecular mechanisms and implications for biofilm-resistant materials. *Biomaterials*. 33:5967-5982.

Arraiano, C.M., J.M. Andrade, S. Domingues, I.B. Guinote, M. Malecki, R.G. Matos, R.N. Moreira, V. Pobre, F.P. Reis, M. Saramago, I.J. Silva, and S.C. Viegas. 2010. The critical role of RNA processing and degradation in the control of gene expression. *FEMS Microbiol Rev*. 34:883-923.

Bossi, L., and N. Figueroa-Bossi. 2007. A small RNA downregulates LamB maltoporin in Salmonella. *Mol Microbiol*. 65:799-810.

Caron, M.P., L. Bastet, A. Lussier, M. Simoneau-Roy, E. Masse, and D.A. Lafontaine. 2012. Dual-acting riboswitch control of translation initiation and mRNA decay. *Proc Natl Acad Sci U S A*. 109:E3444-3453.

Carzaniga, T., D. Antoniani, G. Deho, F. Briani, and P. Landini. 2012. The RNA processing enzyme polynucleotide phosphorylase negatively controls biofilm formation by repressing poly-N-acetylglucosamine (PNAG) production in Escherichia coli C. *BMC Microbiol*. 12:270.

Collins, J.A., I. Irnov, S. Baker, and W.C. Winkler. 2007. Mechanism of mRNA destabilization by the glmS ribozyme. *Genes Dev*. 21:3356-3368.

Cramton, S.E., C. Gerke, N.F. Schnell, W.W. Nichols, and F. Gotz. 1999. The intercellular adhesion (ica) locus is present in Staphylococcus aureus and is required for biofilm formation. *Infect Immun*. 67:5427-5433.

Dugar, G., A. Herbig, K.U. Forstner, N. Heidrich, R. Reinhardt, K. Nieselt, and C.M. Sharma. 2013. High-resolution transcriptome maps reveal strain-specific regulatory features of multiple Campylobacter jejuni isolates. *PLoS Genet*. 9:e1003495.

Figueroa-Bossi, N., S. Lemire, D. Maloriol, R. Balbontin, J. Casadesus, and L. Bossi. 2006. Loss of Hfq activates the sigmaE-dependent envelope stress response in Salmonella enterica. *Mol Microbiol*. 62:838-852.

Geissmann, T., C. Chevalier, M.J. Cros, S. Boisset, P. Fechter, C. Noirot, J. Schrenzel, P. Francois, F. Vandenesch, C. Gaspin, and P. Romby. 2009. A search for small noncoding RNAs in Staphylococcus aureus reveals a conserved sequence motif for regulation. *Nucleic Acids Res*. 37:7239-7257.

Gotz, F. 2002. Staphylococcus and biofilms. *Mol Microbiol*. 43:1367-1378.

Gravenbeek, M.L., and G.H. Jones. 2008. The endonuclease activity of RNase III is required for the regulation of antibiotic production by Streptomyces coelicolor. *Microbiology*. 154:3547-3555.

Haddad, N., C.M. Burns, J.M. Bolla, H. Prevost, M. Federighi, D. Drider, and J.M. Cappelier. 2009. Long-term survival of Campylobacter jejuni at low temperatures is dependent on polynucleotide phosphorylase activity. *Appl Environ Microbiol*. 75:7310-7318.

Haddad, N., O. Tresse, K. Rivoal, D. Chevret, Q. Nonglaton, C.M. Burns, H. Prevost, and J.M. Cappelier. 2012. Polynucleotide phosphorylase has an impact on cell biology of Campylobacter jejuni. *Front Cell Infect Microbiol*. 2:30.

Holzer, P. 2007. Taste receptors in the gastrointestinal tract. V. Acid sensing in the gastrointestinal tract. *Am J Physiol Gastrointest Liver Physiol*. 292:G699-705.

Homerova, D., B. Rezuchova, A. Stevenson, H. Skovierova, M. Roberts, and J. Kormanec. 2011. Characterization of the micA gene encoding a small regulatory sigmaE-dependent RNA in Salmonella enterica serovar Typhimurium. *Folia Microbiol (Praha)*. 56:59-65.

Jefferson, K.K., S.E. Cramton, F. Gotz, and G.B. Pier. 2003. Identification of a 5-nucleotide sequence that controls expression of the ica locus in Staphylococcus aureus and characterization of the DNA-binding properties of IcaR. *Mol Microbiol*. 48:889-899.

Johansen, J., A.A. Rasmussen, M. Overgaard, and P. Valentin-Hansen. 2006. Conserved small non-coding RNAs that belong to the sigmaE regulon: role in down-regulation of outer membrane proteins. *J Mol Biol*. 364:1-8.

Kint, G., D. De Coster, K. Marchal, J. Vanderleyden, and S.C. De Keersmaecker. 2010. The small regulatory RNA molecule MicA is involved in Salmonella enterica serovar Typhimurium biofilm formation. *BMC Microbiol*. 10:276.

Kitamura, S., K. Fujishima, A. Sato, D. Tsuchiya, M. Tomita, and A. Kanai. 2010. Characterization of RNase HII substrate recognition using RNase HII-argonaute chimaeric enzymes from Pyrococcus furiosus. *Biochem J*. 426:337-344.

Lee, A., S.C. Smith, and P.J. Coloe. 1998. Survival and growth of Campylobacter jejuni after artificial inoculation onto chicken skin as a function of temperature and packaging conditions. *J Food Prot*. 61:1609-1614.

Li, H., and A.W. Nicholson. 1996. Defining the enzyme binding domain of a ribonuclease III processing signal. Ethylation interference and hydroxyl

radical footprinting using catalytically inactive RNase III mutants. *EMBO J*. 15:1421-1433.

Lioliou, E., C.M. Sharma, I. Caldelari, A.C. Helfer, P. Fechter, F. Vandenesch, J. Vogel, and P. Romby. 2012. Global regulatory functions of the Staphylococcus aureus endoribonuclease III in gene expression. *PLoS Genet*. 8:e1002782.

Nathania, L., and A.W. Nicholson. 2010. Thermotoga maritima ribonuclease III. Characterization of thermostable biochemical behavior and analysis of conserved base pairs that function as reactivity epitopes for the Thermotoga 23S rRNA precursor. *Biochemistry*. 49:7164-7178.

Papenfort, K., V. Pfeiffer, F. Mika, S. Lucchini, J.C. Hinton, and J. Vogel. 2006. SigmaE-dependent small RNAs of Salmonella respond to membrane stress by accelerating global omp mRNA decay. *Mol Microbiol*. 62:1674-1688.

Papp-Wallace, K.M., and M.E. Maguire. 2006. Manganese transport and the role of manganese in virulence. *Annu Rev Microbiol*. 60:187-209.

Poehlsgaard, J., and S. Douthwaite. 2005. The bacterial ribosome as a target for antibiotics. *Nat Rev Microbiol*. 3:870-881.

Pogacar, M.S., A. Klancnik, S.S. Mozina, and A. Cencic. 2010. Attachment, invasion, and translocation of Campylobacter jejuni in pig small-intestinal epithelial cells. *Foodborne Pathog Dis*. 7:589-595.

Porcelli, I., M. Reuter, B.M. Pearson, T. Wilhelm, and A.H. van Vliet. 2013. Parallel evolution of genome structure and transcriptional landscape in the Epsilonproteobacteria. *BMC Genomics*. 14:616.

Rao, K.A., E. Yazaki, D.F. Evans, and R. Carbon. 2004. Objective evaluation of small bowel and colonic transit time using pH telemetry in athletes with gastrointestinal symptoms. *Br J Sports Med*. 38:482-487.

Rasmussen, A.A., M. Eriksen, K. Gilany, C. Udesen, T. Franch, C. Petersen, and P. Valentin-Hansen. 2005. Regulation of ompA mRNA stability: the role of a small regulatory RNA in growth phase-dependent control. *Mol Microbiol*. 58:1421-1429.

Riesner, D., G. Steger, R. Zimmat, R.A. Owens, M. Wagenhofer, W. Hillen, S. Vollbach, and K. Henco. 1989. Temperature-gradient gel electrophoresis of nucleic acids: analysis of conformational transitions, sequence variations, and protein-nucleic acid interactions. *Electrophoresis*. 10:377-389.

Saramago, M., Domingues, S., Viegas, SC and Arraiano C.M. 2013. Ribonucleases promote biofilm formation and antibiotic resistance in Salmonella Typhimurium. *Submitted in Appl Environ Microbiol*

Shahbabian, K., A. Jamalli, L. Zig, and H. Putzer. 2009. RNase Y, a novel endoribonuclease, initiates riboswitch turnover in Bacillus subtilis. *EMBO J*. 28:3523-3533.

Silva, I.J., M. Saramago, C. Dressaire, S. Domingues, S.C. Viegas, and C.M. Arraiano. 2011. Importance and key events of prokaryotic RNA decay: the ultimate fate of an RNA molecule. *Wiley Interdiscip Rev RNA*. 2:818-836.

Sim, S.H., J.H. Yeom, C. Shin, W.S. Song, E. Shin, H.M. Kim, C.J. Cha, S.H. Han, N.C. Ha, S.W. Kim, Y. Hahn, J. Bae, and K. Lee. 2010. Escherichia coli ribonuclease III activity is downregulated by osmotic stress: consequences for the degradation of bdm mRNA in biofilm formation. *Mol Microbiol*. 75:413-425.

Sittka, A., S. Lucchini, K. Papenfort, C.M. Sharma, K. Rolle, T.T. Binnewies, J.C. Hinton, and J. Vogel. 2008. Deep sequencing analysis of small noncoding RNA and mRNA targets of the global post-transcriptional regulator, Hfq. *PLoS Genet*. 4:e1000163.

Srivastava, N., and R.A. Srivastava. 1996. Expression, purification and properties of recombinant E. coli ribonuclease III. *Biochem Mol Biol Int*. 39:171-180.

Sun, W., G. Li, and A.W. Nicholson. 2004. Mutational analysis of the nuclease domain of Escherichia coli ribonuclease III. Identification of conserved acidic residues that are important for catalytic function in vitro. *Biochemistry*. 43:13054-13062.

Suzuki, K., P. Babitzke, S.R. Kushner, and T. Romeo. 2006. Identification of a novel regulatory protein (CsrD) that targets the global regulatory RNAs CsrB and CsrC for degradation by RNase E. *Genes Dev*. 20:2605-2617.

Udekwu, K.I., F. Darfeuille, J. Vogel, J. Reimegard, E. Holmqvist, and E.G. Wagner. 2005. Hfq-dependent regulation of OmpA synthesis is mediated by an antisense RNA. *Genes Dev*. 19:2355-2366.

Viegas, S.C., D. Mil-Homens, A.M. Fialho, and C.M. Arraiano. 2013. The Virulence of Salmonella enterica Serovar Typhimurium in the Insect Model Galleria mellonella Is Impaired by Mutations in RNase E and RNase III. *Appl Environ Microbiol*. 79:6124-6133.

Viegas, S.C., V. Pfeiffer, A. Sittka, I.J. Silva, J. Vogel, and C.M. Arraiano. 2007. Characterization of the role of ribonucleases in Salmonella small RNA decay. *Nucleic Acids Res*. 35:7651-7664.

Waters, L.S., and G. Storz. 2009. Regulatory RNAs in bacteria. *Cell*. 136:615-628.

Weilbacher, T., K. Suzuki, A.K. Dubey, X. Wang, S. Gudapaty, I. Morozov, C.S. Baker, D. Georgellis, P. Babitzke, and T. Romeo. 2003. A novel sRNA component of the carbon storage regulatory system of Escherichia coli. *Mol Microbiol*. 48:657-670.

Appendix

PUBLICATIONS